

Novel Biopharmaceutical Development Investigations Towards Drug and Formulation
Performance Optimization

by

Daniela Amaral Silva

A thesis submitted in partial fulfillment of the requirements for the degree of

Doctor of Philosophy

in

Pharmaceutical Sciences

Faculty of Pharmacy and Pharmaceutical Sciences
University of Alberta

© Daniela Amaral Silva, 2021

ABSTRACT

For a drug to exert pharmacological action after oral intake, it first needs to be released from the formulation, get into solution (dissolve), be absorbed, and reach the systemic circulation. Since only solubilized drugs can be absorbed, and thus have therapeutic effect, the understanding of the dissolution and drug release processes of a drug product is of primary importance. Such understanding allows a robust formulation development with an ideal *in vivo* performance.

In order to meet set standards, the performance assessment of oral drug products, such as dissolution testing, often applies conditions that are not reflective of the *in vivo* environment. The use of non-physiologically relevant dissolution method during the drug product development phase can be misleading and give poor mechanistic understanding of the *in vivo* dissolution process. Hence, we hypothesized that applying physiologically relevant conditions to the dissolution test would result in more accurate *in vivo* predictability for a robust and precise development process.

Since the buffering system in the intestinal lumen operates at low molarity values, phosphate buffer at low buffer capacity was used as a first approach to an *in vivo* relevant parameter. Furthermore, a biphasic system was used, that is, the low buffer capacity medium was paired with an organic layer (n-octanol) to mimic the concurrent drug absorption that happens with the *in vivo* dissolution. Both poorly and highly soluble drugs in immediate release formulations (ibuprofen and metronidazole, respectively) were tested in this set-up to assess the dissolution in the aqueous medium and the partitioning to the organic phase.

Additionally, enteric coated formulations were tested in bicarbonate buffer at the *in vivo* reported molarities values to assess the impact of buffer species on drug dissolution. The

evaluated parameters were the buffer system (bicarbonate buffer vs. phosphate buffer), buffer capacity and medium pH. In all approaches, dissolution was also carried out in compendial buffer for comparison purposes.

Our results demonstrate that the USP-recommended dissolution method greatly lacked discriminatory power, whereas low buffer capacity media discriminated between manufacturing methods. The use of an absorptive phase in the biphasic dissolution test assisted in controlling the medium pH due to the drug removal from the aqueous medium. Hence, the applied non-compendial methods were more discriminative to drug formulation differences and manufacturing methods than conventional dissolution conditions. In this study, it was demonstrated how biphasic dissolution and a low buffer capacity can be used to assess drug product performance differences. This can be a valuable approach during the early stages of drug product development for investigating drug release with improved physiological relevance.

Similarly, all the enteric coated formulations displayed a fast release in phosphate buffer and complied with the compendial performance specifications. On the other hand, they all had a much slower drug release in bicarbonate buffer and failed the USP acceptance criteria. Also, the nature of the drug (acid vs base) impacted the dissolution behavior in bicarbonate buffer. This study indicates that compendial dissolution test for enteric coated tablets lacks physiological relevance and it needs to be reevaluated. Thus, an *in vivo* relevant performance method for EC products is needed.

Overall, the findings of this thesis comprehensively demonstrates that meaningful differences in performance and accordance to clinical reports were only obtained when physiological relevant conditions were applied. Hence, our results indicate that the central hypothesis was answered positively.

PREFACE

This thesis is an original work completed by Daniela Amaral Silva under the supervision of Prof. Dr. Raimar Löbenberg at the University of Alberta and Prof. Dr. Nádia Bou-Chacra at the University of São Paulo.

Some sections of **Chapter 1** of this thesis are part of Chapter 13 “Disintegration, Dissolution and Drug release” of the next edition of Martin's Physical Pharmacy and Pharmaceutical Sciences book. This chapter has been revised and rewritten by Daniela and Dr. Löbenberg.

Chapter 2 “Update on biorelevant media and physiologically relevant dissolution conditions” is a review manuscript accepted for publication as: Amaral Silva D., Davies, N. M., Bou-chacra N., Ferraz H. G., Löbenberg R. *Dissolution Technol.* 2021. Manuscript number: DT-D-21-00013. I was responsible for the concept formation, literature search as well as the manuscript composition.

Chapter 3 “The significance of disintegration testing in pharmaceutical development” is a review article published as: Amaral Silva D., Webster G. K., Bou-chacra N., Löbenberg R. *Dissolution Technol.* 2018;25:30–38. I was responsible for the concept formation, literature search as well as the manuscript composition.

Chapter 4 “Biphasic dissolution as an exploratory method during early drug product development” has been published as: Amaral Silva D., Al-Gousous, J., Davies, N. M., Chacra, N. B., Webster, G. K., Lipka, E., Amidon, G. L., & Löbenberg, R. *Pharmaceutics*, 2020; 12(5), 420. I designed and performed the experiments and was responsible for the data collection, analysis, and composition of the manuscript.

Chapter 5 “A BCS-based biowaiver approach using biphasic dissolution test” has been accepted for publication as: Amaral Silva D., Curo Melo K., Bou-chacra N., Ferraz H. G., Davies, N. M.,

Löbenberg R. *Dissolution Technol.* 2021. I was responsible for the data analysis, and composition of the manuscript.

Chapter 6 “Simulated, biorelevant, clinically relevant or physiologically relevant dissolution media: The hidden role of bicarbonate buffer” is a review article published as: Amaral Silva D., Al-Gousous J., Davies N. M., Bou Chacra N., Webster G. K., Lipka E., Amidon G., Löbenberg R. *Eur. J. Pharm. Biopharm.* 2019;142:8–19. I was responsible for the concept formation, literature search as well as the manuscript composition.

Chapter 7 “Mechanistic understanding of underperforming enteric coated products: Opportunities to add clinical relevance to the dissolution test” has been published as: Amaral Silva D., Davies N. M., Doschak M. R., Al-Gousous J., Bou-Chacra N., Löbenberg R. *Journal of Controlled Release.* 2020;325:323-34. I designed and performed the experiments and was responsible for the data collection, analysis, and composition of the manuscript.

Chapter 8 “Physiologically relevant dissolution conditions towards improved *in vitro* - *in vivo* relationship – A case study with enteric coated pantoprazole tablets” has been accepted for publication as: Amaral Silva D., Gomes Davanço M., Davies N. M., Krämer J., de Oliveira Carvalho P., Löbenberg R. *International Journal of Pharmaceutics.* 2021;605:120857. I designed and performed the experiments and was responsible for the data collection, analysis, and composition of the manuscript.

Chapter 9 “Are Excipients Inert? Phenytoin Pharmaceutical Investigations with New Incompatibility Insights” has been published as: Amaral Silva D., Löbenberg R., Davies N. *Journal of Pharmacy & Pharmaceutical Sciences.* 2018;21(1s):19s-31s. I designed and performed the experiments and was responsible for the data collection, analysis, and composition of the manuscript.

Chapter 10 “Application of in Silico Tools in Clinical Practice using Ketoconazole as a Model Drug” has been published as: Amaral Silva D., Duque M. D., Davies N. M., Löbenberg R., Ferraz H. G. *Journal of Pharmacy & Pharmaceutical Sciences*. 2018;21(1s):242s-53s. I designed and performed the experiments and was responsible for the data collection, analysis, and composition of the manuscript.

Appendix 3 “Influences of phytocannabinoids on drug-drug interactions and their clinical implications” has been published as: Silva DA, Pate DW, Clark RD, Davies NM, El-Kadi A, Löbenberg R. *Pharmacology & Therapeutics*. 2020 Jun 30:107621. I was responsible for the concept formation, literature search as well as the manuscript composition.

DEDICATION

I dedicate this thesis with much love and appreciation to my family and friends.

“In everything give thanks;
for this is the will of God in Christ Jesus for you”.
1 Thessalonians 5:18

ACKNOWLEDGEMENTS

First and foremost, all thanks goes to God.

I would like to express my sincerest and deepest gratitude to my supervisors Dr. Raimar Löbenberg and Dr. Neal Davies for their continuous support, guidance, and encouragement throughout the years. I truly could not have asked for better mentors that led by example and are role models to me. I feel extremely fortunate to have had the chance to learn from them and to conduct sound research under their supervision. I am tremendously grateful for all the opportunities it was provided for me.

Sincere thanks are extended to my supervisory committee members Dr. Nádia Bou-Chacra, Dr. Lingyun Chen and Dr. Kevin Morin for their insight, valuable suggestions and professional supervision.

Moreover, I also would like to express my warm appreciation to my “academic mother” Dr. Vijay Somayaji for all her advice, support, mentorship, steadfast encouragement and friendship over the years.

I’m grateful to my colleagues and lab mates at the University of Alberta and University of Sao Paulo that have made this journey much more interesting and pleasant.

I would like to thank Dr. Jozef Al-Gousous, Dr. Gregory K. Webster, Dr. Marcelo Dutra Duque, Dr. Michele Georges Issa, Dr. Humberto Gomes Ferraz, Dr. David W. Pate, Dr. Robert D. Clark, Dr. Ayman El-Kadi, Dr. Michael R. Doschak and Dr. Vishwa Somayaji for all the great collaborative work. I truly appreciate how much I have learned from them.

I extend my gratitude to everyone in the Faculty of Pharmacy and Pharmaceutical Sciences and the Faculty of Graduate Studies. Special thanks to the administrative staff for always being available to assist me and give support in all matters.

Finally, I would like to recognize the support from the Office of the Assistant Secretary of Defense for Health Affairs, through the Breast Cancer Research program, under Award No. W81XWH-17-1-0470, Alberta Innovates Graduate Student Scholarship and all the University donors that allowed for institutional scholarships.

Table of Contents

SECTION ONE: INTRODUCTION AND OVERVIEW	1
CHAPTER ONE	1
INTRODUCTION.....	1
1.1 Disintegration.....	2
1.2 Drug release	3
1.3 Dissolution.....	4
1.3.1 Noyes–Whitney Equation	4
1.3.2 Sink Conditions.....	6
1.4 Dissolution Methods and Apparatus.....	6
1.5 Intrinsic dissolution.....	7
1.6 Non-Quality Control dissolution methods	8
1.7 Biopharmaceutics	9
1.7.1 The Biopharmaceutics Drug Classification System (BCS).....	10
1.7.2 BCS Sub-classes	10
1.7.3 Dose, Dissolution and Absorption Number	12
1.7.4 Regulatory aspects - Biowaiver	13
1.8 Thesis overview	14
1.8.1 Rationale and previous studies.....	14
1.8.2 Hypothesis.....	16
1.8.3 Objectives.....	16
CHAPTER TWO	17
UPDATE ON BIORELEVANT MEDIA AND PHYSIOLOGICALLY RELEVANT DISSOLUTION CONDITIONS	17
2.1 Introduction.....	18
2.2 Physiologically relevant media	21
2.2.1 Gastric Environment.....	21
2.2.2 Small Intestinal Environment	23
2.2.2.1 Biorelevant dissolution media	23
2.2.2.2 Bicarbonate buffer – Physiologically relevant dissolution media.....	29
2.3 Conclusion	42
CHAPTER THREE	43
THE SIGNIFICANCE OF DISINTEGRATION TESTING IN PHARMACEUTICAL DEVELOPMENT	43
3.1 Introduction.....	44
3.2 Apparatus specifications and procedures – USP <701> and <2040>	49
3.3 Disintegration as a Quality Control test.....	53
3.4 Disintegration in the real world.....	54
3.4.1 Early-stage development	54
3.4.2 Relationship between disintegration and dissolution	55
3.5 Conclusion	60
SECTION TWO: PHYSIOLOGICALLY RELEVANT <i>IN VITRO</i> TESTING:.....	61
BUFFER CAPACITY AND BIPHASIC DISSOLUTION TESTING.....	61
CHAPTER FOUR.....	61
BIPHASIC DISSOLUTION AS AN EXPLORATORY METHOD DURING EARLY DRUG PRODUCT DEVELOPMENT.....	61
4.1 Introduction.....	62
4.2 Materials.....	65

4.3 Methods.....	66
4.3.1 Ibuprofen Immediate Release Formulations.....	66
4.3.2 Dissolution Tests.....	68
4.3.3 Statistical Analysis.....	69
4.4 Results.....	70
4.4.1 Compendial Dissolution Tests.....	70
4.4.2 Non-Compendial Dissolution Tests—Physiologically Based Exploratory Methods.....	71
4.4.2.1 Monophasic Dissolution With Low Buffer Capacity Medium.....	71
4.4.2.2 Biphasic Dissolution Test with Low Buffer Capacity Medium.....	72
4.4.2.3 Dissolution Medium pH Recovery.....	75
4.4.3 Statistical Analysis.....	77
4.5 Discussion.....	77
4.6 Conclusions.....	85
4.7 Limitations of the Study.....	85
CHAPTER FIVE.....	86
A BCS-BASED BIOWAIVER APPROACH USING BIPHASIC DISSOLUTION TEST.....	86
5.1 Introduction.....	87
5.2 Materials.....	89
5.3 Methods.....	90
5.3.1 Analytical Quantitation.....	90
5.3.2 Disintegration test.....	90
5.3.3 Dissolution tests.....	90
5.3.4 Data analysis.....	91
5.4 Results.....	92
5.4.1 Assay and disintegration tests.....	92
5.4.2 Dissolution tests and data analysis.....	92
5.5 Discussion.....	96
5.6 Conclusion.....	100
SECTION THREE: PHYSIOLOGICALLY RELEVANT <i>IN VITRO</i> TESTING: BICARBONATE BUFFER.....	101
CHAPTER SIX.....	101
SIMULATED, BIORELEVANT, CLINICALLY RELEVANT OR PHYSIOLOGICALLY RELEVANT DISSOLUTION MEDIA: THE HIDDEN ROLE OF BICARBONATE BUFFER.....	101
6.1 Introduction.....	102
6.2 Intestinal lumen environment - What are we trying to reproduce in a dissolution vessel?.....	103
6.2.1 Physiology overview of gastrointestinal secretions.....	103
6.3 Buffer species - <i>In vitro</i> considerations.....	105
6.3.1 Peculiarities of the bicarbonate buffer.....	105
6.3.1.1 Automated systems.....	109
6.3.1.2 Understanding the Bicarbonate–CO ₂ equilibrium.....	111
6.3.2 Phosphate buffer.....	113
6.3.2.1 Biorelevant media.....	115
6.4 Buffer capacity.....	118
6.5 Dissolution tests in phosphate buffer versus bicarbonate buffer.....	122
6.6 Applicability in the industry.....	126
6.7 Clinical reports.....	127
6.8 Conclusion.....	131
CHAPTER SEVEN.....	132

MECHANISTIC UNDERSTANDING OF UNDERPERFORMING ENTERIC COATED PRODUCTS: OPPORTUNITIES TO ADD CLINICAL RELEVANCE TO THE DISSOLUTION TEST.....	132
7.1 Introduction.....	133
7.2 Materials.....	138
7.3 Methods.....	139
7.3.1 Micro-CT analysis	139
7.3.2 Performance tests	140
7.3.2.1 Phosphate-based dissolution medium.....	141
7.3.2.2 Bicarbonate-based dissolution medium.....	141
7.4 Results.....	142
7.4.1 Micro-CT analysis	142
7.4.2 Performance tests	144
7.5 Discussion.....	150
7.6 Conclusion.....	158
CHAPTER EIGHT.....	159
PHYSIOLOGICALLY RELEVANT DISSOLUTION CONDITIONS TOWARDS IMPROVED <i>IN VITRO</i> - <i>IN VIVO</i> RELATIONSHIP – A CASE STUDY WITH ENTERIC COATED PANTOPRAZOLE TABLETS.....	159
8.1 Introduction.....	160
8.2 Materials.....	162
8.3 Methods.....	163
8.3.1 <i>In vitro</i> dissolution testing.....	163
8.3.2 Statistical analysis.....	164
8.3.3 Bioequivalence study.....	164
8.3.4 Pharmacokinetic data	165
8.3.5 <i>In silico</i> studies	166
8.3.6 <i>In vitro</i> – <i>In vivo</i> Relationship	167
8.4 Results.....	167
8.4.1 <i>In vitro</i> dissolution testing.....	167
8.4.2 Pharmacokinetic data	169
8.4.3 Cohorts	170
8.4.4 <i>In silico</i> studies	172
8.5 Discussion.....	176
8.6 Conclusion.....	183
8.7 Shortfalls.....	184
SECTION FOUR: OTHER ASPECTS OF <i>IN VIVO</i> DRUG PRODUCT PERFORMANCE.....	185
THE IMPACT OF FORMULATION COMPOSITION AND PHYSIOLOGY STATE	185
CHAPTER NINE.....	185
ARE EXCIPIENTS INERT? PHENYTOIN PHARMACEUTICAL INVESTIGATIONS WITH NEW INCOMPATIBILITY INSIGHTS	185
9.1 Introduction.....	186
9.2 Materials.....	187
9.3 Methods.....	188
9.3.1 Titration.....	188
9.3.2 Calorimeters experiments.....	188
9.3.3 Dissolution tests.....	189
9.3.4 Statistical analysis.....	190
9.4 Results.....	190

9.4.1 Titration.....	190
9.4.2 Calorimeter experiments	191
9.4.3 Dissolution	196
9.5 Discussion.....	198
9.6 Conclusion.....	204
CHAPTER TEN.....	205
APPLICATION OF IN SILICO TOOLS IN CLINICAL PRACTICE USING KETOCONAZOLE AS A MODEL DRUG	205
10.1 Introduction.....	206
10.2 Materials.....	207
10.3 Methods.....	208
10.3.1 Systematic search for clinical studies reporting Ketoconazole malabsorption due to increased gastric pH	208
10.3.2 Chemical structure analysis.....	208
10.3.3 Computer simulations using GastroPlus™.....	208
10.3.3.1 Compound Tab	209
10.3.3.2 Pharmacokinetics Tab.....	210
10.3.3.3 Physiology Tab.....	211
10.3.3.4 Simulation and Graph Tab.....	213
10.3.4 Data analysis	214
10.3.5 Solubility test	215
10.4 Results.....	215
10.4.1 Chemical structure analysis.....	215
10.4.2 PBPK model.....	216
10.4.2.1 Human fasted - Normal intragastric pH - No hypochlorhydria	217
10.4.2.2 Human fasted - Co-administration with PPI - Hypochlorhydria	217
10.4.4 Solubility test	219
10.5 Discussion.....	220
10.6 Conclusion	223
SECTION FIVE: GENERAL DISCUSSION, CONCLUSION AND FUTURE DIRECTIONS	224
CHAPTER ELEVEN.....	224
GENERAL DISCUSSION AND CONCLUSION	224
11.1 General discussion	225
11.2 Conclusion	229
CHAPTER TWELVE.....	231
FUTURE DIRECTIONS	231
12.1 Bicarbonate buffer and biphasic dissolution	232
12.2 Simplification of in vitro tests for Quality Control application – Delayed release and Immediate release	232
REFERENCES.....	234
APPENDIX 1: FORMULATION OF INHALABLE NANOCRYSTALS TO BE USED AS A THERAPEUTIC STRATEGY AGAINST BREAST CANCER METASTASIS TO THE LUNGS.....	300
APPENDIX 2: DESIGN OF NANOSTRUCTURED LIPID CARRIERS FOR LYMPHATIC DELIVERY OF TERBINAFINE	310
APPENDIX 3: PHYTOCANNABINOID DRUG-DRUG INTERACTIONS AND THEIR CLINICAL IMPLICATIONS.....	316

LIST OF TABLES

Table 2.1. Composition of proposed media to simulate the gastric fluid.....	22
Table 2.2. Composition of the snapshot media to simulate the gastric fluid under fed condition	23
Table 2.3. Composition of proposed media to simulate the small intestine fluids in the fasted and fed state.....	28
Table 3.1. Disintegration Mechanisms	45
Table 3.2. USP Specifications for Basket-Rack Assembly and Disk for Apparatus A and B	51
Table 3.3. Disintegration Test Specified for Each Dosage Form According to USP Chapters <701> and <2040>	52
Table 4.1. Excipient composition of IR ibuprofen tablets prepared in-house. Formulations were named according to the diluent mixture used	67
Table 4.2. Statistical evaluation for the 90% confidence interval between different formulation compositions	77
Table 5.1. Amount partitioned (Q%) into the organic phase for each drug product after disintegration time.....	92
Table 5.2. Drug content and disintegration time of different commercially available metronidazole immediate release tablets.....	92

Table 5.3. In-vitro performance comparison between Metronidazole products	94
Table 6.1. Composition of different bicarbonate buffer systems.....	106
Table 6.2. Composition of Simulated Intestinal Fluids	117
Table 6.3. Delayed release drug products listed as Reference Listed Drug (RLD) by the FDA Orange book	128
Table 7.1. Historic table of <i>in vivo</i> studies with EC formulations	135
Table 7.2. API properties (BCS class and pKa) and coating polymer of the tested EC products	140
Table 7.3. Coat thickness measured prior to dissolution testing using Dataviewer Software (mean \pm SD).....	143
Table 7.4. USP tolerance specification for drug release in the buffer stage and percent released in PB and BCB.....	147
Table 7.5. Non sparged bicarbonate medium pH at time zero (mean \pm standard deviation)	148
Table 8.1. Number of subjects per Tmax cohort for both test and reference formulations.....	171
Table 8.2. Deconvolution statistical results for both Test and Reference	173
Table 8.3. Convolution validation statistics for Test and Reference.....	174
Table 9.1. Powder mixtures composition used in the calorimeter experiments	189

Table 9.2. Excipients composition of different approved products of extended release phenytoin sodium capsules 100 mg in Canada and in the USA, and colour change intensity for the tested products in Milk, lactose free milk (LFM) and water.....	203
Table 10.1. Drug properties used as input data in Compound Tab in GastroPlus™	209
Table 10.2. ACAT parameters used in Physiology Tab for human fasted – PBPK model, normal and hypochlorhydria physiologies	213
Table 10.3. Area under the curve ($AUC_{0-\infty}$), C_{max} and T_{max} and after oral administration of ketoconazole 200 mg suspension.....	217
Table 10.4. ($AUC_{0-\infty}$), C_{max} and T_{max} after oral administration of ketoconazole 200 mg tablet	220

LIST OF FIGURES

Figure 1.1. Dissolution of a drug particle, showing the stagnant diffusion layer between the dosage form surface and the bulk solution (solid-liquid interface).	5
Figure 2.1. Representation of the enclosure and gas delivery system proposed by Scott et al. ...	31
Figure 2.2. Representation of the floating lid device proposed by Sakamoto et al.	32
Figure 2.3. Representation of the solid-liquid interface of a dissolving enteric polymer. N: Neutral (Unionized carboxylic acid: -COOH); - : Negative charge (Ionized carboxylic acid: -COO-). From the gel layer to the bulk solution the pH increases and the viscosity.....	40
Figure 2.4. Decision tree for establishing a surrogate buffer for EC products. (Adapted from (79)).....	41
Figure 3.1. Immediate release tablet disintegration process. Adapted from (3).....	44
Figure 3.2. USP specifications for disintegration apparatus A (a) and apparatus B (b). Reprinted with permission. ©2017 The United States Pharmacopeial Convention.	50
Figure 4.1. Simplified approach for dissolution method development for immediate release (IR) formulations containing acidic and basic drugs (BCS I–IV).FaSSIF: Fasted State Simulated Intestinal Fluid; FeSSIF: Fed State Simulated Intestinal Fluid; BCS: Biopharmaceutics Classification System.	65
Figure 4.2. Dissolution profiles of all formulations in 900 mL of compendial buffer (50 mM phosphate buffer pH 7.2). Error bars represent the standard deviation.	70

Figure 4.3. Dissolution profiles in the 5 mM phosphate buffer (900 mL). (A) MCC formulations, (B) CaHPO₄ formulations, (C) CaSO₄ formulations, (D) Dextrose formulations, (E) D formulations, (F) G formulations. Error bars represent the standard deviation.72

Figure 4.4. Organic phase partition profiles in a biphasic dissolution with 200 mL of aqueous media for G formulations (A) and D formulations (B) and with 900 mL of aqueous media (C). Oct: Octanol. Error bars represent the standard deviation.73

Figure 4.5. Aqueous phase dissolution profiles in a biphasic dissolution with 900 mL of aqueous media (BP aq). (A) MCC formulation, (B) CaHPO₄ formulation, (C) CaSO₄ formulation, (D) Dextrose formulation, (E) D formulations, (F) G formulations. Error bars represent the standard deviation.75

Figure 4.6. pH measurements for dissolution tests in a low buffer capacity medium. Dashed line: monophasic setup. Solid black line: biphasic setup with an aqueous layer at 900 mL. Solid blue line: biphasic setup with an aqueous layer at 200 mL.76

Figure 5.1. Dissolution profiles of metronidazole formulations in SIF (solid lines) and low buffer capacity phosphate buffer (5mM – dashed lines).....93

Figure 5.2. Biphasic dissolution profiles of metronidazole formulations in the aqueous (Aq – dashed lines) and organic phases (Oct - solid lines).95

Figure 5.3. Correlation between the comparator pharmaceutical product (CPP) and generic products of the amount partitioned to the organic phase. Only data after full tablet disintegration were used.96

Figure 6.1. Schematic illustration of the pHysio-stat device. (Adapted from Garbacz et. al., 2013) 110

Figure 6.2. Schematic illustration of the pHysio-grad® device. (Adapted from Garbacz et. al., 2014) 110

Figure 6.3. Schematic illustration of the Auto pH System™ device. (Adapted from Goyanes et. al., 2015)..... 111

Figure 7.1. Cross-sectional micro-CT images of marketed EC tablets prior to dissolution testing. (A) Sulfasalazine (B) Diclofenac (C) Aspirin (D) Esomeprazole (E) Pantoprazole. The red line in each upper shadow projection indicates the location of each lower reconstructed micro-CT image slice (voxel resolution of 9 μm isotropic). Differences in enteric coating thickness can readily be seen, as can density differences in tablet excipient content. 143

Figure 7.2. Dissolution profiles of enteric coated formulations in 50mM phosphate buffer (orange line) and 5mM bicarbonate buffer (blue line); USP dissolution specification (when available): black dashed line. Esomeprazole magnesium (A), Pantoprazole sodium (B); Aspirin (C), Sulfasalazine (D) and Diclofenac sodium (E). 146

Figure 7.3. Comparison of dissolution profiles of enteric coated formulations in 50mM phosphate buffer (A) and 5mM bicarbonate buffer (B). 147

Figure 7.4. Dissolution of enteric coated diclofenac sodium tablets in various bicarbonate molarities and effect of sparging the medium. (A) Dissolution profiles of enteric coated diclofenac sodium tablets in bicarbonate buffer 2.5 – 30mM range. Blue line: fresh buffer;

orange line: a day old; grey line: a week old; t20%: time taken for 20% release. (B) Effect of sparging the media (5mM bicarbonate buffer) on the dissolution of enteric coated diclofenac sodium tablets. 149

Figure 7.5. Phosphate and bicarbonate buffer equilibrium reactions and pKa values taking place in the bulk solution and diffusion layer..... 155

Figure 8.1. Dissolution profile of pantoprazole EC formulations in the buffer stage (mean \pm SD; n=3). Orange: test; blue: reference; solid line: phosphate buffer (PB); dashed line: bicarbonate buffer (BCB); Dotted black line: USP dissolution specification..... 169

Figure 8.2. Schematic picture of the contrast between phosphate buffer and bicarbonate buffer. In phosphate buffer the coating material rapidly dissolved, leaving the tablet core exposed to the dissolution medium (Top), whereas in bicarbonate buffer the coating presented ruptures instead of completely dissolving (Bottom). 169

Figure 8.3. Plasma concentration-time curves of reference formulation after oral administration under fed condition (N = 70). Highlighted black line: mean curve..... 170

Figure 8.4. Plasma concentration-time curves of test formulation after oral administration under fed condition (N = 70). Highlighted black line: mean curve..... 170

Figure 8.5. Plasma concentration-time curves of test and reference formulations for Tmax Cohort 1. Data are shown as mean \pm SD..... 171

Figure 8.6. Plasma concentration-time curves of test and reference formulations for Tmax Cohort 2. Data are shown as mean \pm SD..... 172

Figure 8.7. IVIVR graph. The compendial buffer *in vitro* data was correlated with the *in vivo* data from Cohort 1 and the *in vitro* data from bicarbonate buffer was correlated with the *in vivo* data from Cohort 2.174

Figure 8.8. IVIVR model predicted (lines) vs. observed (circles, mean \pm SD) plasma concentration-time profiles for Cohort 1 (prediction using phosphate buffer dissolution data). 175

Figure 8.9. IVIVR model predicted (lines) vs. observed (circles, mean \pm SD) plasma concentration-time profiles for Cohort 2 (prediction using bicarbonate buffer dissolution data).
.....176

Figure 9.1. H^1 NMR spectrum for the precipitate obtained in the titration of phenytoin solution with $CaCl_2$191

Figure 9.2. Calorimeter experiments result for the dry powder mixtures.192

Figure 9.3. Calorimeter experiments result for the powder mixtures with water added.....193

Figure 9.4. Calorimeter experiments result for the mixtures: milk and phenytoin; milk and sodium phenytoin.....194

Figure 9.5. Calorimeter experiments result for commercially available extended release phenytoin sodium capsules (100 mg) in milk.....195

Figure 9.6. Calorimeter experiments result for commercially available extended release phenytoin sodium capsules (100 mg) in water and lactose free milk (LFM).....196

Figure 9.7. Dissolution profiles obtained for phenytoin sodium with lactose (dashed line), phenytoin sodium with CaSO₄ (solid line) and phenytoin with sorbitol (dotted line and open circles) capsules in water.....197

Figure 9.8. Phenytoin sodium and lactose capsules after the dissolution tests. After 30 minutes at body temperature (37.0°C) the capsules became yellow.198

Figure 10.1. Scheme of perfusion-limited tissue. *V_t*: tissue volume; *C_t*: tissue concentration, *f_{ut}*: fraction unbound in tissue, *CL_{int}*: tissue intrinsic clearance; *V_p*: plasma volume; *C_p*: plasma concentration; *f_{up}*: fraction unbound in plasma; *C_{bi}*: blood concentration in (arterial) tissue; *R_{bp}*: blood/plasma concentration ratio; *Q*: tissue blood flow; *C_{bo}*: blood concentration out (venous) of tissue; *K_p*: tissue/plasma partition coefficient. (Image adapted from GastroPlus™ Manual, 2015).211

Figure 10.2. Microspecies distribution throughout pH range 0-14. Green line corresponds to microspecies 1 (both basic groups protonated - highlighted in red circles), blue line corresponds to microspecies 2 (neutral microspecies) and orange line corresponds to microspecies 3 (imidazole group protonated -highlighted in red circle). Images taken from <http://www.chemicalize.org/>.....216

Figure 10.3. Plasma concentration-time profiles under different scenarios. (A) after administration of ketoconazole 200 mg suspension; (B) ketoconazole 200 mg tablet to subjects with normal intragastric pH under a fasted condition; (C) ketoconazole 200 mg tablet to subjects with increased intragastric pH with water (predicted: dashed line; and Observed - black squares) and with Coca-Cola® (predicted: solid line and observed: black circles).218

Figure 10.4. Parameters sensitivity analysis: influence of particle size on AUC_{0-∞}, (A) and T_{max} (B) of ketoconazole in normal (squares) and increased intragastric pH (triangle).....219

LIST OF ABBREVIATIONS

AGF	Artificial Gastric Fluid
ACAT	Advanced Compartmental Absorption and Transit
AIC	Akaike Information Criterion
An	Absorption number
ANDA	Abbreviated New Drug Application
API	Active Pharmaceutical Ingredient
Aq	Aqueous
ASD	Artificial Stomach-Duodenum
ASF	Absorption Scale Factor
AUC	Area Under the Curve
BA	Bioavailability
BCB	Bicarbonate Buffer
BCS	Biopharmaceutics Drug Classification System
BDM	Biorelevant Dissolution Media
BE	Bioequivalence
BP	Biphasic
CAI	Carbonic Acid Ionization
CAT	Compartmental Absorption and Transit
CI	Confidence Interval
CPP	Comparator pharmaceutical product
CS	Croscarmellose Sodium

D	Direct compression
Dex	Dextrose
DF	Dosage Form
Dn	Dissolution number
Do	Dose number
EC	Enteric Coated
EMA	European Medicines Agency
FaSSGF	Fasted State Simulating Gastric Fluid
FaSSIF	Fasted State Simulated Intestinal Fluid
FDA	Food and Drug Administration
FeSSGF	Fed State Simulating Gastric Fluid
FeSSIF	Fed State Simulated Intestinal Fluid
G	Wet granulation
GI	Gastrointestinal
GIS	Gastro Intestinal Simulator
GIT	Gastrointestinal Tract
HIF	Human Intestinal Fluid
HMT	Hierarchical Mass Transfer
H¹NMR	Proton Nuclear Magnetic Resonance
HPLC	High-Performance Liquid Chromatography
HPMC	Hydroxypropyl methylcellulose
ICH	International Council for Harmonisation

IDR	Intrinsic Dissolution Rate
IR	Immediate Release
IRR	Irreversible Reaction
IVIVC	- <i>in vivo</i> correlation
IVIVR	- <i>in vivo</i> relationship
ka	Absorption rate coefficient
kp	Partitioning rate coefficient
LFM	Lactose Free Milk
MAE	Mean Absolute Error
MCC	Microcrystalline Cellulose
Micro-CT	Computerized x-ray microtomography
NLT	Not Less Than
NMR	Nuclear Magnetic Resonance
NSAID	Non-Steroidal Anti-Inflammatory Drug
Oct	Octanol
PB	Phosphate Buffer
PBPK	Physiologically Based Pharmacokinetic
Ph. Int.	International Pharmacopoeia
PK	Pharmacokinetic
PPI	Proton Pump Inhibitor
PSA	Parameter Sensitivity Analysis
QbD	Quality by Design

QC	Quality Control
RLD	Reference Listed Drug
RMSE	Root Mean Squared Error
RNE	Reversible Non-Equilibrium
Rs_q (R²)	Correlation coefficient
SD	Standard Deviation
SEIF	Simulated Endogenous Intestinal Fluid
SGF	Simulated Gastric Fluid
SGF_{sp}	Simulated Gastric Fluid without pepsin
SIF	Simulated Intestinal Fluid
SLS/SDS	Sodium Lauryl Sulphate
SSE	Sum of Squared Errors
SUPAC	Scale Up and Post Approval Changes
USP	United States Pharmacopeia
WHO	World Health Organization

SECTION ONE: INTRODUCTION AND OVERVIEW

CHAPTER ONE

Introduction

For a drug to exert pharmacological action after being taken by mouth, it first needs to be released from the formulation, get into solution (dissolve), be absorbed, and reach systemic circulation. The processes of disintegration, drug release and dissolution may occur simultaneously.

Since only solubilized drugs can be absorbed, and thus have therapeutic effect, the understanding of the dissolution and drug release processes of a drug product is of primary importance to the pharmaceutical industry. Such understanding will allow a robust formulation development with an ideal *in vivo* performance.

Dissolution is the process by which a solid phase (e.g., a tablet or powder) goes into a solution phase, such as water. Although simple in concept, the rate of dissolution can be affected by a variety of factors which include, but are not limited to, the type of media in which the drug is dissolving, temperature, pH, viscosity, agitation rate, and dosage form coatings. Hence, a dissolution method should be carefully designed to avoid confounding factors. The processes of disintegration, drug release and dissolution are described below.

1.1 Disintegration

Disintegration is a physical process related to the mechanical breakdown of a tablet into smaller particles/granules, representing the breakage of inter-particle interactions generated during tablet compaction or granulation (1), given that the tablet is not a contiguous polymeric device. After the immersion liquid wets the particle surface and penetrates through the pores, disintegration takes place in two steps: first, disintegration into smaller granules, and second, disaggregation or granule disintegration into fine particles. The first step is important to increase surface area. The increase in surface area compared to the intact tablet or granulate yields a higher dissolution rate. In the second step, an even faster drug dissolution rate is achieved due to

the increased surface area in contact with the medium. If no disintegration would occur, only the Active Pharmaceutical Ingredient (API) near the surface of the compact or granulate would dissolve. A more in depth description of disintegration is given in Chapter 3.

In the case of immediate-release dosage forms, such as typical tablets or capsules, the materials are generally selected and utilized to allow the disintegration and deaggregation processes to proceed rapidly. Therefore, the dissolution rate of the solid drug is often the limiting or rate-controlling step in the absorption of drugs with low solubility. However, if disintegration is slower than dissolution e.g. hydrophilic matrix tablets, then disintegration/surface erosion is the rate limiting process.

1.2 Drug release

Drug release is the process by which a drug leaves a drug product and is described with reference to the rate at which drug is available from a particular dosage form. It can be classified as immediate release or modified release, which includes both delayed and extended-release. Drug release refers not only to oral drug products, but also to other dosage forms, such as transdermal and drug-device combinations.

Drug dissolution and release patterns commonly fall into two groups: zero- and first-order release. Typically in the pharmaceutical sciences, zero-order release is achieved from nondisintegrating dosage forms such as topical or transdermal delivery systems, implantable depot systems, or oral controlled-release delivery systems. Sustained-release systems often attempt to mimic zero-order release by providing drug in a slow first-order manner, that is, concentration dependent.

1.3 Dissolution

Drug dissolution is the process by which drug molecules are liberated from a solid phase and enter into a solution phase. In general, only drugs in solution can be absorbed, distributed, metabolized, excreted, and even to exert pharmacologic action. Thus, dissolution is an important process in the pharmaceutical sciences and is mostly used in the context of oral drug products. Differences in dissolution performance can cause products not to pass quality control tests and/or bioequivalence tests. Therefore, dissolution testing is an important performance test.

The quantitative analysis of dissolution rate was firstly introduced by Noyes and Whitney in the late 19th century (2). The Noyes-Whitney equation related the rate of dissolution of solids to both the properties of the solid and the dissolution medium.

1.3.1 Noyes–Whitney Equation

In dissolution or mass transfer theory, it is assumed that an aqueous diffusion layer or stagnant liquid film of thickness h exists at the surface of a solid undergoing dissolution, as observed in Figure 1.1. This thickness, h , represents a stationary layer of solvent in which the solute molecules exist in concentrations from C_s to C . Beyond the static diffusion layer, at a distance of x greater than h , mixing occurs in the solution, and the drug is found at a uniform concentration, C , throughout the bulk phase.

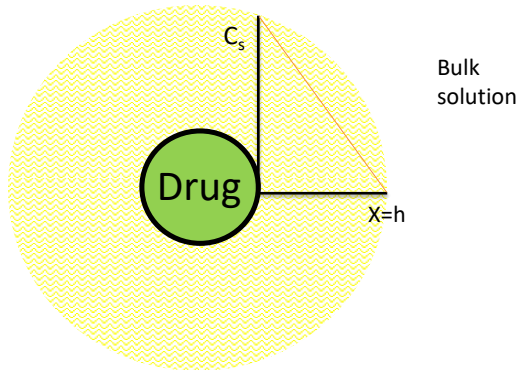


Figure 1.1. Dissolution of a drug particle, showing the stagnant diffusion layer between the dosage form surface and the bulk solution (solid-liquid interface).

At the solid surface–diffusion layer interface, $x = 0$, the drug in the solid is in equilibrium with drug in the diffusion layer. The gradient (or change in concentration) with distance across the diffusion layer, is constant, as shown by the straight downward-sloping line. The static diffusion layer thickness can be altered by the force of agitation at the surface of the dissolving drug particle.

The Noyes and Whitney equation can be written as

$$\frac{dM}{dt} = \frac{DS}{h}(C_s - C) \quad (\text{Equation 1-1})$$

or

$$\frac{dC}{dt} = \frac{DS}{Vh}(C_s - C) \quad (\text{Equation 1-2})$$

where M is the mass of solute dissolved in time t , dM/dt is the mass rate of dissolution (mass/time), D is the diffusion coefficient of the solute in solution, S is the surface area of the exposed solid, h is the thickness of the diffusion layer, C_s is the solubility of the solid (i.e., concentration of a saturated solution of the compound at the surface of the solid and at the temperature of the experiment), and C is the concentration of solute in the bulk solution and at time t . The quantity dC/dt is the dissolution rate, and V is the volume of solution.

1.3.2 Sink Conditions

The saturation solubility of a drug is a key factor in the Noyes–Whitney (2) equation. The driving force for dissolution is the concentration gradient across the boundary layer. Therefore, the driving force depends on the thickness of the boundary layer and the concentration of drug that is already dissolved. When the concentration of dissolved drug, C , is less than 10% of the saturation concentration, C_s , the system is said to operate under “sink conditions.” Another common rule for sink conditions is that the dissolution media is able to dissolve at least 3 times the amount of drug present in the dosage form.

1.4 Dissolution Methods and Apparatus

A dissolution test is performed to assess a drug product’s performance and to determine compliance with the dissolution requirements for dosage forms. The United States Pharmacopeia (USP) general chapter <711> Dissolution (3) lists four dissolution apparatuses, namely: Apparatus 1 (Basket), Apparatus 2 (Paddle), Apparatus 3 (Reciprocating Cylinder) and Apparatus 4 (Flow-Through Cell).

These methods for evaluating dissolution first appeared in the 13th edition of the USP in early 1970. The most commonly used pieces of dissolution equipment are the basket and the paddle apparatus. They are characterized as “stirred beaker” methods and are simple and well standardized. They are also “closed systems” because they use a fixed volume of dissolution medium (4,5). The basket method is generally preferred for capsules, whereas tablet dissolution is normally performed using the paddle method. Typically used media include (a) water, (b) 0.1 N HCl, (c) buffer solutions, (d) water or buffers with surfactants, and (e) low-content alcoholic aqueous solutions.

The USP Apparatus 3, a reciprocating cylinder, dips a transparent cylinder containing the dosage form at a rate determined by the operator (3). The tubes have a mesh base to allow the medium to drain into a sampling reservoir as the tube moves up and down, thus creating convective forces for dissolution. The cylinders can also be transferred to different media at specified times, automatically. It is suitable for sustained-/controlled-release dosage forms as it allows exposure of products to mechanical and physiochemical conditions which may influence the release of the products throughout the gastrointestinal (GI) tract.

The USP Apparatus 4 (3) is a flow-through cell containing the dosage form that is fed with dissolution medium from a reservoir. Directing the fluid through a porous glass plate or a bed of beads produces a dispersed flow of medium. Turbulent or laminar flow can be achieved by changing the bottom barrier. As with Apparatus 3, the medium can be changed to provide a pH gradient, surfactants, and other medium components. Limitations of volume and pH change associated with traditional rotating paddle and basket apparatus prompted the development of the flow-through cell apparatus. Because it can be run as an “open system” the volume of media in a dissolution test can be easily adapted to the solubility of the drug and release rate of the product. This system can be used for various dosage forms such as modified/extended-release tablets, medical devices, API’s or granules, suppositories, capsules, pellets, hydrogels, among others.

1.5 Intrinsic dissolution

All the aforementioned methods are used to assess the performance of a final drug product. Intrinsic dissolution testing, however, is used to characterize dissolution properties of a pure drug substance, not in a dosage form (6). Determining the rate of dissolution is important because it may allow the prediction of potential bioavailability problems. This method is described in the USP General Chapter <1087> Intrinsic Dissolution - Dissolution testing

procedures for rotating disk and stationary disk (7). A non-disintegrating compact of material is prepared. The compact and surrounding die assembly are placed in a suitable dissolution medium and subjected to the desired hydrodynamics near the compact surface. The amount of dissolved drug as a function of time is measured. The cumulative amount of drug dissolved is plotted against time and linear regression analysis is performed on data points in the initial linear region of the dissolution curve. The slope corresponds to the dissolution rate (mass s^{-1}). The dissolution rate is normalized for surface area to obtain the intrinsic dissolution rate (IDR) (units of $\text{mass cm}^{-2} \text{s}^{-1}$). This can be used to determine if a drug substance is highly or poorly soluble. IDR values above 0.0017 mg/s/cm^2 indicate a highly soluble drug. This method is independent of the particle size or shape and therefore ideal in early drug development when the crystal form, polymorph or particle size distribution requirements are not yet known. There are two types of apparatus specified in the USP for intrinsic dissolution testing, namely: rotating disk and stationary disk.

1.6 Non-Quality Control dissolution methods

In addition to USP listed devices, there are a large number of specially designed devices used in research applications. These methods were developed to attempt to replicate the environment that the dosage form encounters during its transit through the GI tract and to address the deficiencies of the traditional methods. The assessment of a drug's product performance under physiologically relevant conditions can give better insight of the dynamic aspects of *in vivo* dissolution. Some examples of physiologically adapted devices are the Artificial Stomach-Duodenum (ASD) model, the Gastro Intestinal Simulator (GIS), the TNO intestinal model System, the vibrating tube sensor and biphasic dissolution testing (8,9). An

overview of physiologically relevant dissolution media, such as bicarbonate based systems, is covered in Chapter 2.

1.7 Biopharmaceutics

Biopharmaceutics examines the relationship of the physicochemical properties of the API, dosage form and route of administration on the rate and extent of systemic drug absorption (10). After a solid dosage form such as a tablet is administered by mouth to a patient, it must in most cases first disintegrate. Then drug dissolution as a time-dependent process takes over and represents the final step of drug release, which is ultimately required before a drug can be absorbed or exert a pharmacologic effect. Several kinetic processes act simultaneously to determine the amount of drug ultimately absorbed. These include the rates of drug release, dissolution, transit through the intestine, and the permeability of the drug in the small intestine. There are two mechanistic cases which have to be differentiated when considering the bioavailability of a drug. A drug's bioavailability can be dissolution or absorption controlled. If drug dissolution is slow compared with drug absorption, the dose may not be totally absorbed before it has passed through the intestine, especially if the drug is absorbed preferentially in certain locations ("absorption windows") of the GI tract. Low absorption due to slower dissolution can also result in lower drug blood levels. At the same time, if dissolution controls the absorption process, then *-in vivo* correlation (IVIVC) can be established, and dissolution might be able to predict bioavailability (BA). In the case that absorption is slower than dissolution, dissolution might not be predictive for BA since the gut permeability is the absorption controlling factor.

1.7.1 The Biopharmaceutics Drug Classification System (BCS)

The BCS system was introduced by Amidon and colleagues in 1995 (11). This classification system is based on the two key physicochemical parameters for oral bioavailability: Solubility and Permeability. The BCS Classes are defined as: Class I - High solubility-high permeability drugs; Class II - Low solubility-high permeability drugs, Class III - High solubility-low permeability drugs, and Class IV - Low solubility-low permeability drugs.

High solubility was defined as the highest dose strength soluble in 250 mL of an aqueous medium with a pH range of 1–7.5 at $37 \pm 1^\circ\text{C}$ (SUPAC) (12). These pH ranges are slightly different in different guidance documents. High Permeability was defined as: “when the extent of absorption in humans is determined to be greater or equal to 90% of an administered dose based on a mass balance determination or in comparison to an intravenous reference dose”. This was reduced to 85% BA in 2017. The Food and Drug Administration (FDA) accepts *in vitro* data to establish permeability while most of the other regulatory agencies require human data only.

Only what is dissolved can get absorbed and reach its target organ, tissue or receptor triggering a pharmacological response. Since drug dissolution and gastrointestinal permeability are fundamental parameters in controlling the rate and extent of drug absorption, this system thus allows not only the correlation of the *in vitro* drug product dissolution and *in vivo* bioavailability but also allows to set standards for the *in vitro* drug dissolution method which will correlate with the *in vivo* process.

1.7.2 BCS Sub-classes

In 2014, Tsume and colleagues (13) proposed an extension of the BCS classes to include sub-classes of acid (a), base (b) and neutral (c) drugs, especially for classes II and IV. Since Classes I and III are high solubility drugs, although existent, such subclassification was not

emphasised - except for border line solubility cases. This BCS sub-classification is an important basis to develop *in vivo* predictive dissolution methods.

In terms of solubility and dissolution, BCS Classes IIa and IVa drugs (pKa values around 4 to 5) are insoluble at low pH values (e.g. fasted stomach) but soluble at higher pH values (e.g. intestinal pH). With the increase in solubility at intestinal pH values, the dissolution rate of acidic drugs is also likely to be increased upon entering the intestines. In such cases, dissolution would likely be faster than gastric emptying rate depending on dose and intrinsic solubility. Hence, BCS IIa drugs, for example, would behave as a Class I drug in the small intestine, where the absorption rate would likely reflect gastric emptying time. Due to their high permeability and high solubility and dissolution rate in the small and large intestine environment, BCS Class IIa (weak acids) may be completely absorbed, given a sufficient residence time throughout the whole intestines. Conversely, weak bases under BCS Class IIb exhibit high solubility and dissolution rates at acidic pH (stomach) and low solubility at higher pH values (intestines). This may lead to precipitation upon entering the intestines, a process that depends on many factors, such as formulation and the GI physiological environment at the time of dosing. Immediate release (IR) oral dosage forms containing basic drugs (~ pKa 3–6) may have sufficient time for dissolution in the stomach thus exhibiting good absorption in the proximal intestinal region. For BCS IIb drugs, the absorption rate would likely be impacted by the gastric emptying rate, the intestinal permeability and the precipitation time. In the case of BCS Class IIc drugs, the solubility would not be affected by the *in vivo* pH change, but on the *in vivo* environment such as surfactants and lipids.

In terms of absorption, BCS IIa drugs will present an initial lag in absorption because of the limited dissolution in the stomach. This lag time and variability are dependent on the dosing

time relative to the gastric motility phase. The succeeding absorption rate will be mainly dependent on the gastric emptying and dissolution rate. For BCS IIb drugs, the initial absorption rate will be dependent on the dissolution in the stomach as well as gastric emptying. Generally, since dissolution is expected to be rapid in the stomach, the absorption in the duodenum will be mostly dependent on gastric emptying. After the initial rapid phase, the absorption rate tends to decrease due to subsequent precipitation, solubilization, dissolution and absorption along the intestines. BCS Class IIc drugs generally presents a slow and prolonged absorption throughout the GI tract. Factors that will influence the absorption rate are the *in vivo* solubilization, dissolution and motility (transit). Similar generalizations can be made for BCS Class IV drugs but accounting for the low intestinal permeability, which may play a larger role.

1.7.3 Dose, Dissolution and Absorption Number

Based on the API's physicochemical properties and some GI physiological parameters, the BCS defined 3 distinct dimensionless numbers, namely: Dissolution number (D_n), Dose number (D_o) and Absorption number (A_n) (14). The parameters used to calculate each number are given in Equations (1-3 to 1-5). These numbers are useful for decision making process in drug development. If two potential drug candidates have differences in their D_n , D_o or A_n , the one with the better chances to get bioavailable might be chosen, however other factors such as stability, polymorphism, toxicology, and pharmacological potency have to be balanced to the BCS characteristics.

The dissolution number is the ratio between the small intestine transit time (T_{GI}) and the dissolution time (the longest time at pH 1, 4.5 or 6.8) (T_{DISS}). A $D_n < 1.0$ indicates that the whole dose may not be dissolved during transit through the small intestine. Hence, D_n values higher than 1.0 are desired for complete dissolution in the GI tract.

$$Dn = \left(\frac{3D}{r^2}\right)\left(\frac{Cs}{\rho}\right)(T_{GI}) = \left(\frac{T_{GI}}{T_{DISS}}\right) \quad (\text{Equation 1-3})$$

The dissolution time is calculated based on the solubility (C_s), diffusivity (D), density (ρ), and the initial particle radius (r) of a given compound.

The dose number is calculated as the ratio of dose concentration to drug solubility. $Do > 1.0$ indicates that the dose will not completely dissolve in the accompanying volume of water. This indicates that the drug presents solubility issues.

$$Do = \left(\frac{D/v_{water}}{Cs}\right) \quad (\text{Equation 1-4})$$

The drug concentration is calculated as the dose (D) divided by the accompanying volume of water (V_{water}) (usually 250 ml at the pH of lowest solubility between 1 and 8).

The absorption number is calculated as the ratio between the small intestine transit time (T_{GI}) and the estimated small intestine absorption time (T_{ABS}). An $A_n < 1.0$ indicates that all of the drug may not be absorbed during transit through the small intestine. Hence, A_n values higher than 1.0 are desired for complete absorption in the GI tract. The time required for complete absorption (T_{ABS}) is defined as the ratio of permeability (P_{eff}) and the gut radius (R).

$$An = \left(\frac{P_{eff}}{R}\right)(T_{GI}) = \left(\frac{T_{GI}}{T_{ABS}}\right) \quad (\text{Equation 1-5})$$

1.7.4 Regulatory aspects - Biowaiver

The BCS can be seen as the mechanistic foundation of modern drug development (e.g. Quality by Design (QbD) approaches) and regulatory guidance's. The system was mentioned for the first time in an FDA document in 1995 (12). The Scale Up and Post Approval Changes (SUPAC) guidance allowed to waive bioequivalence studies for formulation changes within specific ranges, if *in vitro* similarity for the before and after the change products can be documented via dissolution tests. This is called a Biowaiver.

In 1997 the FDA published another guidance (15) allowing dissolution testing as surrogate for bioequivalence testing for extended-release formulation if an IVIVC could be established. Since dissolution controls the absorption of such products, a graph plotting the fraction dose dissolved vs. fraction dose absorbed should result in a linear relationship. The Biowaiver for these products are not limited to any BCS class. This guidance was followed by the 2000 BCS based biowaiver guidance which allowed biowaivers for all BCS class I APIs. The FDA 2017 guideline changed the BA from 90% to 85% and allowed BCS III drugs.

An early BCS classification and the knowledge of the Do, Dn and An can be very valuable in drug development. For example, if different drug candidates derived from a lead molecule have differences in their properties, the biopharmaceutically “better” candidate can be chosen. On the other hand, biowaivers can be used in drug development to show that formulations are similar and avoid costly clinical studies and reduce the regulatory burden. Furthermore, generic drug approval can now be granted based on biowaivers.

1.8 Thesis overview

1.8.1 Rationale and previous studies

The mechanistic understanding of the *in vivo* drug product performance and API characteristics is of primary importance for a robust drug development process. This understanding is gained through the study of the physicochemical properties of the API (as outlined in the topic 1.7), as well as the study of the drug product in terms of disintegration, dissolution and drug release.

During the development process, different dissolution methods might be needed, which have different focuses, such as *in vivo* predictive dissolution methods and methods for quality control (QC) purposes. The information obtained in the physiologically based methods can be used to

establish appropriate discrimination of the QC method to be applied in late development stage toward critical quality attributes and process parameters. Hence, incorporating physiological features to the *in vitro* test is an excellent approach to understand the *in vivo* behavior of a drug/drug product hence gaining clinical insight for a QbD development.

Previous work in the literature has reported the lower buffer capacity of the intestinal fluids which results in a slower *in vivo* drug dissolution rate compared to compendial buffers. Additionally, the matter of absorption is not taken into consideration in a single-phase dissolution system. The approach of dissolution testing with low buffer capacity has been reported in the literature, as well as the use of an organic layer on the dissolution vessel to mimic absorption. However, to the best of our knowledge, the use of low buffer capacity together with an absorptive phase has not been investigated. Additionally, the application of this system to highly soluble drugs hasn't been explored yet. Similarly, it is well known that the intestinal lumen is buffered by bicarbonate. This has important implications for enteric coated formulations. Previous studies have reported the further delay on the onset of drug release in bicarbonate buffer, however, no approach has been taken to address this matter in a mechanistic way.

This thesis has been divided into three main sections covering aspects of physiologically relevant testing. Each section is built upon the knowledge gained in the previous one. Firstly, the matter of buffer capacity was investigated with immediate release formulations, as well as the use of an additional sink (organic phase). With the lessons learned from the theoretical and experimental assessment, more complex delivery systems (delayed release) were investigated addressing both the matter of buffer capacity and buffer species (bicarbonate buffer) on the drug product performance.

1.8.2 Hypothesis

Applying physiologically relevant conditions to the dissolution test results in more accurate *in vivo* predictability for a robust and precise development process.

1.8.3 Objectives

Overall objective:

To assess the impact and implications of buffer capacity, buffer species and alternative dissolution methods on drug dissolution of different dosage forms.

Specific objectives:

- 1) To investigate the influence of buffer capacity on a model poorly and highly soluble drugs.
- 2) To investigate the influence of having an organic layer on the dissolution system (to mimic the *in vivo* drug absorption) on the drug product performance.
- 3) To assess the discriminatory power and applicability of biphasic dissolution testing compared to standard conditions.
- 4) To mechanistically delineate the performance of enteric coated products in physiologically relevant bicarbonate buffer.
- 5) To investigate the impact of formulation composition in terms of drug-excipients interactions.

SECTION ONE: INTRODUCTION AND OVERVIEW

CHAPTER TWO

Update on biorelevant media and physiologically relevant dissolution conditions

A version of this chapter has been accepted to be published in:

Dissolution Technol. 2021. Manuscript number: DT-D-21-00013

2.1 Introduction

Dissolution testing constitutes one of the most widely used *in vitro* performance tests during the drug product development and routine quality control testing. It monitors the rate and extent of *in vitro* drug release (batch release test), and it is also often used to ensure consistent *in vivo* performance (16,17). The description of standard dissolution apparatus by the United States Pharmacopeia (USP) in the 1970s together with guidance's by the United States Food and Drug Administration (FDA) in the late 90's propelled its broad application during the various stages of drug development (17,18). Alongside that, the introduction of the Biopharmaceutics Classification System (BCS) (11), in 1995, provided a simple but robust way to mechanistically describe the biopharmaceutical behavior of a drug. Under this system, drugs are classified based on their solubility and permeability. These parameters can be used to predict the fraction dose absorbed and consequently its chances to become bioavailable (14,19).

At the time when USP apparatus 1 and 2 were introduced and FDA guidance's were published, most of the molecules under development presented good aqueous solubility (BCS classes 1 and 3) and conventional dosage forms were employed (capsule and tables). Hence, establishing *in vitro* dissolution conditions with presumed *in vivo* relevance was reasonably simple (17,20). However, the development scenario has changed to molecular entities that are more potent accompanied with lower aqueous solubility (BCS classes 2 and 4). While these drug substances have enhanced many therapies by acting on new molecular targets, they also present significant formulation and process development challenges (21), especially regarding the biopredictive power of the previous traditional *in vitro* performance methods. Hence, there was a need for advancement in the field of dissolution testing (e.g. development of biorelevant and

physiologically relevant dissolution methodologies) to address the shortfalls of traditional methods.

Accordingly, the use of dissolution testing has gained much space outside of the routinely end-product release application to a comprehensive analysis that can be implemented at the various stages of the product life cycle (17,19). Changes in the regulatory landscape, such as the introduction of quality by design (QbD) concept, have also contributed to the progression of dissolution methodology, linking quality tests to product performance in patients and ultimately therapeutic outcomes. Hence, there was a shift into developing dissolution media and apparatus that would mimic the human gastrointestinal (GI) tract to further understand the *in vivo* dissolution mechanisms. The innovation in this field has also evolved to the integration of *in vitro* dissolution data applying different methods and analytical techniques with modeling and simulation, correlating it to *in vivo* data (22–25). This approach is a robust way to select the best formulation with the desired *in vivo* performance.

The purpose of a particular dissolution test varies at the different stages of development (17). As first introduced by Azarmi et al. there might be a need for more than one dissolution test for the same product (26). For example, a quality control (QC) dissolution test is usually used to identify possible variations during product manufacturing and/or changes in product storage that could have an impact on the product's performance. This method needs to be simple in order to be used in a typical routine QC environment, such as conventional USP apparatus 1 or 2 and simple buffer media. At the same time, this method has to demonstrate an appropriate level of discriminatory power to confirm product consistency. On the other hand, a biorelevant/physiologically relevant dissolution method applies conditions that mimic the different physiological environments. These usually consist of non-compendial media and apparatus, such

as bicarbonate-based buffers, biphasic dissolution to assess the impact of concurrent drug absorption and multiple compartmental apparatuses (27–29). This methodology is mostly used to guide formulation selection and optimization. It typically starts during early development and may continue through clinical testing and beyond. Lastly, a clinically relevant dissolution method is any particular method in which a link between *in vitro* dissolution data with *in vivo* pharmacokinetic (PK) data can be established, creating an *in vitro* - *in vivo* correlation or relationship (IVIVC or IVIVR) which is important for lifecycle management.

The *in vivo* drug dissolution depends on the drug physicochemical properties as well as on the GI fluid environment. The current understanding of the human GI physiology allowed biorelevant dissolution media (BDM) to evolve, facilitating the *in vitro* prediction of *in vivo* dissolution performance (24,30–33). The many proposed BDM include various properties of the human GI tract, such as pH, buffer species, buffer concentration, osmolality, viscosity, surface tension, concentration and type of bile salts, lipolysis products, as well as physiological state, such as fasted and fed states (34–37). Evidently conventional dissolution media, such as simple USP buffers, fall short in mimicking the properties and composition of GI fluids, but at the same time are referenced in the majority of USP monographs (31). In the realm of *in vivo* predictability, compendial methods are most meaningful for the solubility and dissolution assessment of BCS class I drugs.

A more accurate prediction of the drug product's *in vivo* performance is expected the closer the *in vitro* conditions are to the *in vivo* environment. However, depending on the information one is seeking or on the physicochemical properties of the API (e.g. BCS class I), simulating all aspects of the GI tract may or may not be necessary to evaluate the drug product performance. Based on this, Markopoulos et al. (38) have suggested levels of simulation of

luminal composition, as follows: Level 0 (pH); Level I (pH and buffer capacity); Level II (pH, buffer capacity, bile components, dietary lipids, lipid digestion products and osmolarity) and Level III (pH, buffer capacity, bile components, dietary lipids, lipid digestion products, osmolarity, proteins, enzymes and viscosity effects).

The purpose of this review is to summarize and update the many physiologically adapted media and buffers proposed over the years focusing on the upper GI tract, since it is often where most drug absorption occurs. Emphasis will be given on the application of bicarbonate-based media, since this is the major buffering species in the human intestinal lumen.

2.2 Physiologically relevant media

2.2.1 Gastric Environment

The composition, pH, and surface tension are important aspects to be considered when simulating the gastric fluid. The composition of the stomach fluid is not merely hydrochloric acid; it also contains saliva, digestive enzymes (pepsin and gastric lipase), food and refluxed fluids from the duodenum (39). The pH of gastric fluids can vary greatly depending on the physiological state (fed vs fasted), health-related conditions (such as achlorhydria) and pharmacological treatments (such as anti-acid agents). The reported pH range of gastric fluids is 1.5–1.9 under fasted conditions (4,40,41) and 3.0 – 7.0 under fed conditions (the rate in which the pH changes is strongly related to the type and size of the meal) (42). The reported surface tension in gastric fluids ranges from 30 to 46 mN/m (40,43,44). This could be an indicative of the presence of surface-active agents, such as lecithin and lysolecithin (45).

One of the earliest proposed media to simulate the stomach in the fasted state was the artificial gastric fluid (AGF), described by Ruby et al. in 1996 (Table 2.1) (46). The compendial simulated gastric fluid (SGF) and its version without pepsin (SGFsp) described in the USP

presents a different composition than AGF, but a similar pH (pH 1.2) (7), as shown in Table 2.1. Many aspects of the gastric juice are addressed in these media, but qualities such as pH, surface tension and pepsin concentration could be more reflective of the *in vivo* values.

Table 2.1. Composition of proposed media to simulate the gastric fluid

	AGF	SGF	SGF _{sp}	SGF _{SLS}	SGF _{TritonX}	FaSSGF
Acetic acid (μL)	500	-	-	-	-	-
Lactic acid (μL)	420	-	-	-	-	-
Lecithin (μM)	-	-	-	-	-	20
Pepsin (g)	1.25	3.2				0.1
Sodium chloride (mM)	-	34.22	34.22	34.22	34.22	34.22
Sodium citrate (mM)	2.34	-	-		-	-
Sodium lauryl sulphate (mM)	-	-	-	8.57	-	-
Sodium malate (mM)	2.81	-	-		-	-
Sodium taurocholate (μM)	-	-	-	-	-	80
Triton X 100 (mM)		-	-	-	1.55	-
Hydrochloric acid	qs	qs	qs	qs	qs	qs
pH	1.2	1.2	1.2	1.2	1.2	1.6

In order to mimic the *in vivo* conditions as closely as possible, Vertozi et al. designed a fasted state simulating gastric fluid (FaSSGF) including compounds found in the intragastric environment, such as pepsin and sodium taurocholate (Table 2.1) (33). However, even though the use of physiologically relevant surfactants is desirable to mimic the *in vivo* conditions as closely as possible, these media can be unstable, difficult to prepare, and costly. Hence, synthetic surfactants, such as sodium lauryl sulphate (SLS) and Triton X 100 are often used as an alternative. These surfactants are added into compendial simulated gastric fluid without pepsin to form SGF_{SLS} and SGF_{Triton}, respectively (Table 2.1). This can be an interesting approach, but on the other hand it is important to be aware that different types of surfactants can impact the product's performance, leading to erroneous predictions of drug dissolution (33,47).

Another important aspect to consider is the difference of fasted vs. fed physiological states. Macheras et al. (48), proposed the use of milk as a medium that can simulate gastric components in the fed state because it contains similar ratios of fat, protein and carbohydrates present in the western diet (48,49). However, there are some drawbacks with the use of milk, such as batch- to-batch variability in the milk composition (contributing to variable dissolution data), the tendency of lipophilic compounds to bind to lipidic components of the milk, and the source of milk (goat vs. cow) (49).

Another approach was proposed by Jantratid et al. in 2008 (24). The authors proposed a “snapshot” approach to capture the changes in the composition of the gastric fluid associated with digestion and gastric emptying process (24). Table 2.2 describes the composition of early, middle, and late fed state gastric environment (FeSSGF). The early stage media corresponds to the first 75 min after meal ingestion, the middle stage to 75 - 165 min, and the late stage medium to 165 min on.

Table 2.2. Composition of the snapshot media to simulate the gastric fluid under fed condition

	FeSSGF Early	FeSSGF Middle	FeSSGF Late
Sodium chloride (mM)	148	237.02	122.6
Acetic acid (mM)	-	17.12	-
Sodium acetate (mM)	-	29.75	-
Ortho-phosphoric acid (mM)	-	-	5.5
Sodium dihydrogen phosphate (mM)	-	-	32
Milk/buffer	1:0	1:1	1:3
Hydrochloric acid/sodium hydroxide	qs pH 6.4	qs pH 5	qs pH 3
pH	6.4	5	3

2.2.2 Small Intestinal Environment

2.2.2.1 Biorelevant dissolution media

The bicarbonate ions secreted into the intestinal lumen neutralize the gastric fluid that is emptied in the intestines. The reported pH range under fasted conditions in the duodenum is 5.8

– 6.5, 5.3 – 8.1 in the jejunum and 6.8 – 8.0 in the ileum. Bile salts are also secreted into the intestines and the formation of micelles results in a much lower surface tension compared to the gastric fluids. The surface tension of the intestinal fluids is even lower under fed conditions due to the higher concentration of bile (50). Based on this, biorelevant media, e.g. USP simulated intestinal fluids, were developed to simulate the pH and include components present in the human GI tract, such as bile salts and lecithin. Osmolality, pH and surface tension were adjusted to physiological values. According to the FDA, simulated intestinal fluid with pancreatin (USP-SIF) and without enzyme (SIF-blank) reflect the physiologic conditions of the small intestine better than other simpler buffer systems (28,51,52).

Another example of biorelevant media is the fasted and fed simulated intestinal fluid (FaSSIF and FeSSIF) proposed by Dressman in 1998 and its many adaptations (42). The human intestinal lumen is buffer by bicarbonate, however, due to pragmatical reasons, other buffers are typically used to mimic the physiological pH of intestinal fluids (42). E.g., FeSSIF uses acetate buffer to adjust the pH to 5.0. Moreover, the prevalent bile salt in the human bile is cholic acid, but sodium taurocholate (conjugate of cholic acid with taurine) was chosen to be the most representative bile salt *in vitro*. Biorelevant media contain bile salts and phospholipids and when simulating the fed state also monoglycerides and free fatty acids. The composition of FaSSIF and FeSSIF are given in Table 2.3.

The revised version of FaSSIF and FeSSIF (FaSSIF-V2 and FeSSIF-V2, respectively) was developed in order to address some of the shortcomings of the initially proposed media. For example, Persson et al. (53) reported that cyclosporine, danazol, griseofulvin and felodipine presented between 2- to 5-times higher solubility values in fed Human Intestinal Fluid (HIF) compared to FeSSIF. This could be due to the lack of neutral lipids in the FeSSIF composition.

Additionally, the purity of bile salts can also have an impact on the solubility of poorly soluble drugs. Wei and Löbenberg (54) reported the solubility of glyburide in biorelevant media with crude bile salts to be over 2-fold higher than when pure bile salts were used in FaSSIF. Additionally, the reported *in vivo* bile salt concentration is lower than the concentration used previously (24,43).

Psachoulis et al. (55) proposed a methodology to predict the concentration and potential precipitation of lipophilic weak bases using an upgraded version of FaSSIF-V2 (FaSSIF-V2plus). The proposed *in vitro* methodology was composed of a gastric and duodenal compartment along with a reservoir. In the duodenal compartment FaSSIF-V2plus was used. The composition of FaSSIF-V2plus is very similar to FaSSIF-V2, but in addition to all FaSSIF-V2 components, the “plus” version also contains free fatty acid (sodium oleate, 0.5 mM) and cholesterol (0.2 mM). The authors concluded that for some weak bases, such as ketoconazole, FaSSIF-V2plus is a superior fluid for investigating the drug’s intraluminal precipitation.

Later, Fuchs et al. (32) further proposed an updated version of the fasted state biorelevant media based on the up to date physiological composition of fasted HIF at that time. The proposed media was named FaSSIF-V3. The surface tension was considered as a surrogate parameter in establishing the medium’s correctness. A number of prototypes were investigated containing five different bile salts (taurocholate, glycocholate, tauroursodeoxycholate, taurochenodeoxycholate and glycochenodeoxycholate), as well as replacing lecithin with its hydrolysis products (lysolecithin and sodium oleate). Additionally, a mixture of glycocholate and taurocholate, with or without 0.2 mM cholesterol, were investigated. The authors assessed the solubility of ten model compounds and observed that the amount and the type of phospholipids and bile salt significantly impacted the solubility and surface tension in the various prototypes.

Additionally, the authors reported that blank buffers tended to underestimate the physiological solubility of the investigated APIs whereas the SDS solutions overestimated solubility. Finally, the proposed FaSSIF-V3 composition was the one containing glycocholate and taurocholate with 0.2 mM cholesterol (32).

Cristofolletti and Dressman (56,57) used a FaSSIF-V3 with reduced phosphate buffer concentration (5.0 mM). The rationale behind this approach was to use a buffer system that would match the pH at the particle's surface utilizing physiologically relevant bicarbonate buffer. For this purpose, ibuprofen was used as the model drug. The authors reported that the proposed 5.0mM phosphate buffer FaSSIF-V3 was able to predict *in vivo* differences in peak and extent of exposure between test and reference ibuprofen formulations (57).

When analysing the fed state, as shown in Table 2.3, the main differences between FeSSIF and FeSSIF-V2 are the concentrations of bile salts and lecithin (43); the replacement of phosphate for maleate buffer resulting in lower osmolality and buffer capacity values; and the addition of glyceryl monooleate and sodium oleate to reflect the presence of lipolysis products. Similarly to SGF, Jantratid and Dressman also developed snapshot media to simulate the intestinal fluids in the fed state (Table 2.3). The authors proposed the inclusion of lipolysis products and changes in parameters such as bile salts concentration, osmolality, buffer capacity, and fluid pH according to the early, medium and late stages after food intake (24).

The use of biorelevant media has been shown to be very useful in assessing the *in vivo* solubility of compounds. Soderlind et al. studied the solubility of 24 molecules in FaSSIF, FaSSIF-V2 and HIF. FaSSIF-V2 solubilities correlated better with solubilities in HIF for neutral compounds, while for acidic and basic compounds the solubility in FaSSIF and FaSSIF-V2 were similar (58). A similar trend was observed by Fagerberg et al. (59). The authors reported that the

estimation of the *in vivo* solubility of poorly soluble compounds was more accurate in biorelevant media. This was particularly true for bases and neutral molecules, which display higher solubility in FeSSIF compared to FaSSIF. The opposite was observed for acidic drugs (59). Biorelevant media have also been widely used to forecast the *in vivo* performance drugs (60) (and references cited thereby), achieving good IVIVC in some cases (61–63), but not always (64). Other biorelevant media have also been proposed to simulate fluids in the fasted state small intestine, such as the Simulated Endogenous Intestinal Fluid (SEIF), described by Kossena et al. (65) (Table 2.3). Since the focus of this review is on the upper gastrointestinal tract, colonic fluids are not included in the table.

The use of bicarbonate based biorelevant media has been proposed in the literature (66,67). Litou and colleagues assessed a level II biorelevant media based on bicarbonate buffer to simulate the contents of upper small intestine under conditions of reduced acid secretion in the stomach. The authors reported that bicarbonates were not important in estimating drug precipitation and that level II biorelevant media underestimated the concentration of the given compounds in intestinal human aspirates. However, more data is needed to confirm this finding as the usefulness of bicarbonate in biorelevant dissolution testing may be compound specific (67). For example, two year later, Jede et al. (66) also investigated the supersaturation and precipitation kinetics of weak bases using a transfer model with biorelevant bicarbonate buffer. The authors compared FaSSIF_{bicarbonate} with the standard FaSSIF_{phosphate} and observed that bicarbonate-based FaSSIF had a better predictive power compared to phosphate-based. They concluded that the proposed model is a promising approach to increase the predictive power of *in vitro* tests thus contributing to a more biorelevant drug/ drug product development (66).

Even though biorelevant media have been extensively used, its preparation can be time-consuming, costly and it may present a short-shelf life for utility. Furthermore, the buffering species in the human intestinal lumen is bicarbonate, whereas FaSSIF uses phosphate, FeSSIF acetate, FaSSIF-V2 and FeSSIF-V2 maleate. Simpler and more physiologically relevant dissolution media is therefore desired.

Table 2.3. Composition of proposed media to simulate the small intestine fluids in the fasted and fed state

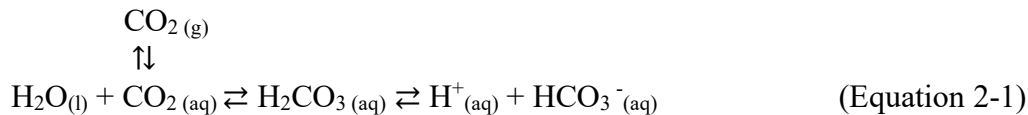
USP SIF	FaSSIF	FeSSIF	FaSSIF V2	FeSSIF V2	FeSSIF Early	FeSSIF Middle	FeSSIF Late	SEIF
NaOH (qs pH)	NaOH (qs pH)	NaOH (qs pH)	NaOH (34.8 mM)	NaOH (81.65 mM)	NaOH (52.5 mM)	NaOH (65.3 mM)	NaOH (72 mM)	NaN3 (6mM)
KH ₂ PO ₄ (6.8 g)	KCl (103.29 mM)	KCl (203.89mM)	NaCl (68.62 mM)	NaCl (125.5 mM)	NaCl (145.2 mM)	NaCl (125.8 mM)	NaCl (51 mM)	NaCl (98 mM)
Pancreatin (10.0 g)	Bile salt (Sodium taurocholate) (3 mM)	Bile salt (Sodium taurocholate) (15 mM)	Bile salt (Sodium taurocholate) (3 mM)	Bile salt (Sodium taurocholate) (10 mM)	Bile salt (Sodium taurocholate) (10 mM)	Bile salt (Sodium taurocholate) (7.5 mM)	Bile salt (Sodium taurocholate) (4.5 mM)	Bile salts* (4mM)
Deionized water qs 1L	Phospholipid (lecithin) (0.75 mM)	Phospholipid (lecithin) (3.75 mM)	Phospholipid (lecithin) (0.2 mM)	Phospholipid (lecithin) (2 mM)	Phospholipid (lecithin) (3 mM)	Phospholipid (lecithin) (2 mM)	Phospholipid (lecithin) (0.5 mM)	Phospholipid (Lyso-phosphatidylcholine) (1mM)
pH 6.8	Potassium dihydrogen orthophosphate (28.66 mM)	Acetic acid (144.05 mM)	Maleic acid (19.12 mM)	Maleic acid (55.02 mM)	Maleic acid (28.6 mM)	Maleic acid (44 mM)	Maleic acid (55.09 mM)	Cholesterol (0.25mM)
	Deionized water qs 1L	Deionized water qs 1L	Deionized water qs 1L	Glyceryl monooleate (5 mM)	Glyceryl monooleate (6.5 mM)	Glyceryl monooleate (5 mM)	Glyceryl monooleate (1 mM)	Sodium dihydrogen phosphate (18mM)
	pH 6.5	pH 5.0	pH 6.5	Sodium oleate (0.8 mM)	Sodium oleate (40 mM)	Sodium oleate (30 mM)	Sodium oleate (0.8 mM)	Sodium hydrogen phosphate (12mM)
				Deionized water qs 1L	Deionized water qs 1L	Deionized water qs 1L	Deionized water qs 1L	
				pH 5.8	pH 6.5	pH 5.8	pH 5.4	pH 6.5

*sodium salts of the following conjugates; glycocholate (1mM), glycodeoxycholate (0.7mM), glycochenodeoxycholate (1mM), taurocholate (0.5mM), taurodeoxycholate (0.3mM), taurochenodeoxycholate (0.5mM).

2.2.2.2 Bicarbonate buffer – Physiologically relevant dissolution media

At present, the most widely applied dissolution media are phosphate-based buffers (28,68). However, the concentration of phosphates in the intestinal luminal fluids is insignificant. This makes phosphate-based dissolution media poorly representative of the *in vivo* environment, failing to reflect *in vivo* characteristics such as ionic strength, buffer capacity, fluid volume and viscosity (28). The pH along the gastrointestinal tract is maintained by bicarbonate ions, which are present in the pancreatic, hepatic and intestinal secretions (69,70). Hence, the development of suitable *in vitro* dissolution media based on bicarbonate buffer (BCB) has gained much attention because it closely mimics the environment of the intestinal fluids and can thus improve *in vitro*-*in vivo* correlations compared to phosphate buffers (70).

In vivo, the pH is held stable by the constant supply of bicarbonate-containing secretions in the intestines. On the other hand, the application of BCB as an *in vitro* dissolution medium is challenging due to the evaporation of CO_{2(g)} from the aqueous phase causing the pH to rise. This can lead to changes in the buffer strength and poor reproducibility of the dissolution test. Hence, the first step in establishing a stable BCB is to maintain CO_{2(aq)} and CO_{2(g)} at equilibrium (Equation 2-1).



One of the ways to stabilise the bicarbonate buffer pH is to purge the medium with CO₂ gas, thus supplying CO_{2(g)} which compensates its loss from the aqueous medium. Automated systems have been developed to adjust the pH by sparging gas according to the pH shift and were reviewed by Amaral Silva et al. (28) (and references cited thereby). However, bubbling

gases into the dissolution medium can be problematic due to the hydrodynamic disturbances in the dissolution vessel. This can affect the dissolution rate of certain drugs leading to failure in meeting compendial requirements. Another concern is the possible foaming when surfactant containing media are used.

Preventing the escape of CO₂ instead of purging the medium has been proposed as an alternative to control the medium pH. Approaches such as sealing the dissolution vessel or using a liquid paraffin layer on top of the dissolution medium have been described (71,72) and were effective in stabilising the media pH. Nevertheless, since these were closed systems, a dynamic pH regulation was not possible. To circumvent this, Scott and colleagues (70) have recently studied the use of a novel bicarbonate-based dissolution system that supplies N₂ (pH increasing) and CO₂ (pH decreasing) gases above the dissolution medium without purging into the solution (Figure 2.1). The system is composed of an enclosure device with two inlets that supply N₂ and CO₂. The gases are distributed through a ring-shaped diffuser and released through outlets pointing towards the surface of the dissolution medium. The authors reported that this method regulated the pH of the bicarbonate buffer without substantial disruption to the surface of the media and that no foaming was observed when surfactant containing medium was used.

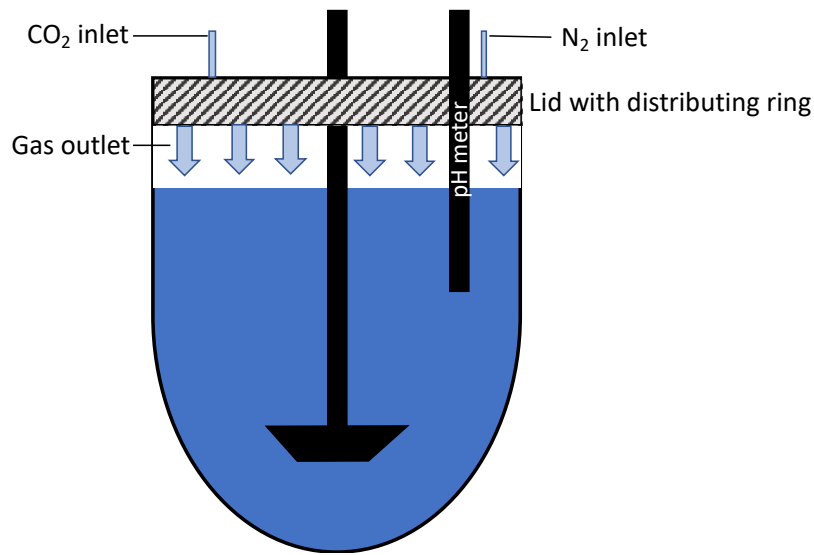


Figure 2.1. Representation of the enclosure and gas delivery system proposed by Scott et al. (Picture adapted from (70))

The approach taken by Scott et al. (70) is similar to the one reported by Boni et al. (68) in which the $\text{CO}_{2(g)}$ was supplied above the medium to maintain the pH throughout the dissolution test. However, the setup proposed by Boni et al. was not effective because the dissolution vessel only had a conventional lid on (open system) which didn't prevent the escape of the supplied gas. Hence, the enclosure method is a superior design in the sense that it prevents gas escape thus improving the efficiency of gas supply. The authors concluded that this novel system is a step towards the application of the physiological bicarbonate buffers as a dissolution media that meets compendial requirements.

Sakamoto et al. (73) proposed a simple and facile method that allows the use of bicarbonate buffer for dissolution testing (Figure 2.2). The authors developed a floating lid system that prevents the escape of CO_2 from the bicarbonate buffer solution. The lid is made of a 5mm thick foamed styrol that covers the surface of the medium almost completely but not in a tight-sealing configuration. The buffer is added to the dissolution vessel and the lid is placed on top of it. The medium pH was adjusted by adding HCl via a small hole. The authors investigated

the suitability of this method for a 6.0 - 7.5 pH range and 2 – 50mM bicarbonate buffer concentration. In all cases, the pH change was less than 0.1 pH unit after 3.5 h when the floating lid method was used whereas without the lid, the pH increased by more than one pH unit within 3.5 h. The authors concluded that the floating lid method would be useful for formulation development while covering the physiological intestinal and colonic conditions in terms of pH and buffer concentration.

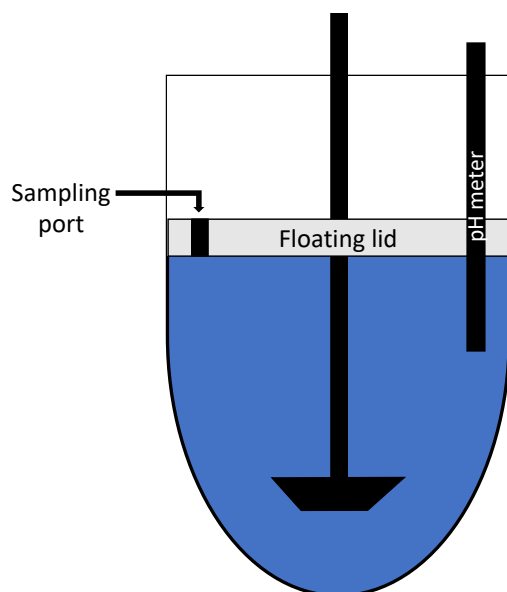


Figure 2.2. Representation of the floating lid device proposed by Sakamoto et al. (Picture adapted from (73))

It's interesting to note that the pH of the medium can be adjusted either by adding HCl/NaOH or by sparging gases or by a combination of both (70,73,74). In the case of sparging, when CO_2 gas is supplied and diffuses into the medium, the $\text{CO}_{2(\text{aq})}$ interacts with water generating carbonic acid, which in turn dissociates releasing hydrogen ion culminating in the pH decrease (equilibrium shown in Equation 2-1 is shifted to the right). Reversely, the sparging of a pH increasing gas (e.g. N_2 or He) has an indirect effect in increasing the medium pH (75,76). As the pH increasing gas is supplied, the partial pressure of CO_2 is reduced, decreasing the dissolved $\text{CO}_{2(\text{aq})}$ in the medium, thus increasing the pH (equilibrium shown in Equation 2-1 is shifted to

the left). Scott et al. (70) observed that the CO₂ supply was much more efficient in decreasing the medium pH than N₂ in increasing the pH. This is most likely due to the indirect effect of N₂ thus taking longer for the pH change to be observed.

Although BCB is physiologically relevant, because of the pragmatical hurdles, its application has been limited and some authors have doomed it as a medium with restricted suitability for dissolution testing (77). Matching the effective buffering pKa of bicarbonate at the solid-liquid surface (diffusion layer) of a dissolving solid with a surrogate buffer system is a way to simplify the dissolution conditions while maintaining physiologic relevance in terms of buffering capacity at the diffusion layer (78,79).

When the whole system is at equilibrium, the pKa of the BCB system (Equation 2-1) is 6.04, which is the situation in the bulk solution in a dissolution vessel (28,79). However, in the diffusion layer around dissolving solutes the interconversion $H_2O_{(l)} + CO_{2(aq)} \rightleftharpoons H_2CO_{3(aq)}$ does not equilibrate very rapidly compared to the fast diffusional processes. Therefore, bicarbonate buffer behaves as having an effective pKa in the diffusion layer that is different from that in bulk. This value is lower than 6.04 (bulk), but higher than the intrinsic pKa of 3.30 ($H_2CO_{3(aq)} \rightleftharpoons H^+_{(aq)} + HCO^-_{3(aq)}$). As a result, the ability of BCB in buffering the diffusion layer against incoming ionizable solute is weakened and the *in vivo* dissolution rate is slower than in highly concentrated compendial buffers.

Based on this, investigators have proposed the reduction in the molarity of non-bicarbonate based surrogate buffers as a possible approach to increase its biopredictability, thus matching the typically slower *in vivo* dissolution (27,78,79). For example, Tsume et al. showed that ibuprofen tablets had slower *in vitro* dissolution in phosphate 10 mM compared to 50 mM at a starting pH of 6.0 (80). This can be explained by Mooney's stagnant film-based dissolution

model, i.e. more diluted buffers have a reduced buffer capacity which is translated into a lower ability in countering the acidifying effect of the dissolving ibuprofen at the diffusion layer pH (81). In highly concentrated buffer systems, such as compendial buffers, an abundance of the buffer's conjugate base species surrounds the drug particle. This, in turn, leads to a prompt neutralization in the diffusion layer, that is, the buffer species readily consumes the ions formed on the dissolving drug surface. Hence, the pH in the diffusion layer is similar to the bulk, resulting in a higher dissolution rate (27,56,82,83). Conversely, when the buffer system is less concentrated (as *in vivo*) the neutralization is thus slower.

Different models have been proposed to predict the drug flux thus enabling calculation of the surrogate buffer molarity to determine a good match to physiological bicarbonate in terms of drug dissolution. This includes, but is not limited to the equilibrium model (which assumes that H_2CO_3 and CO_2 are at equilibrium), the carbonic acid ionization (CAI) model (hypothetical situation where neither hydration or dehydration is assumed), the irreversible reaction (IRR) transport model and the reversible non-equilibrium (RNE) model.

Krieg et. al. (84) proposed the IRR transport model to develop more physiologically relevant buffer systems for dissolution testing. This model assumes the dehydration process ($H_2CO_{3(aq)} \rightarrow H_2O_{(l)} + CO_{2(aq)}$) as an irreversible chemical reaction because it is approximately 500 times faster than the hydration rate. This approximate model yielded improved predictions for the intrinsic dissolution rates of Ibuprofen, Ketoprofen and Indomethacin in bicarbonate buffers. However, this assumption was shown by Al-Gousous et al. to not be as accurate (85). The authors then proposed the RNE model, which does not make any equilibrium assumptions. It not only includes both the hydration and dehydration rates ($H_2O_{(l)} + CO_{2(aq)} \rightleftharpoons H_2CO_{3(aq)}$) but also accounts for the fluxes of all species involved in the mass transfer process.

The authors reported that the RNE model predicted the flux values obtained in the intrinsic dissolution experiments more accurately compared to the other models. It is of crucial importance to understand the kinetics of bicarbonate at the diffusion layer of a dissolving particle. For example, in the equilibrium model, BCB would have a pKa close to the bulk pH, resulting in effective buffering at the surface of the dissolving drugs (overestimation). In the CAI model, the assumption that hydration and dehydration reactions do not happen means that the buffer pKa is much lower than the bulk pH, resulting in a very poor ability to buffer the surface of the dissolving drug, which is an underestimation. Similarly, the IRR transport model would also underestimate the drug flux, but not to the extent as of the CAI model because it includes an irreversible dehydration reaction. The RNE model represents an intermediate situation in which the reactions occur but do not reach equilibrium. In this case, as previously mentioned, this situation results in BCB not behaving as having a pKa exceeding 6 in terms of promoting the dissolution of ionizable solids. The RNE model has been shown to successfully estimate the pH on the surface of a solid particle in BCB, then the Mooney model can be used to estimate the phosphate concentration that would give the same surface pH (pH_0) (79,85). Thus, a proper surrogate buffer molarity can be used that would give good matches to physiological bicarbonate in terms of drug dissolution. This shows that in some cases it is feasible to develop surrogate buffers for bicarbonate.

Furthermore, Salehi et. al. (86) incorporated to the RNE model other properties such as medium hydrodynamics effect and drug particle size distribution. The authors described it as a hierarchical mass transfer (HMT) model that considers drug properties (intrinsic solubility, acid/base character, pKa, particle size, and particle polydispersity) as well as GI fluid properties and fluid hydrodynamics (bulk pH, buffer species concentration, fluid shear rate, and convection).

The findings reported by Álvarez et al. (87) further reinforces that the current compendial buffers concentrations seem to be too high to correlate with the *in vivo* carbonate concentration. The authors investigated the *in vitro* dissolution of ibuprofen tablets in different pharmacopeial media at both 50 rpm and 75 rpm rotation speed. The media investigated by the group included 130mM hydrochloric acid pH 1.2; 540mM acetate buffer pH 4.5; and 70mM phosphate buffer pH 6.8. In all media, the dissolution profiles showed similarity at both rotation speeds. However, the *in vivo* bioequivalence studies revealed that only one out of the three test formulations was bioequivalent to the reference. Hence, these *in vitro* tests were not able to detect differences regarding the rate of absorption. Based on this finding, the authors concluded that there remains a need to develop dissolution conditions that can predict bioequivalence outcomes and that the application of biowaivers to BCS class IIa drugs would not be feasible because the dissolution tests did not detect differences in absorption rate.

In contrast, Hofmann et. al. (79) studied the dissolution of Ibuprofen in physiologically relevant bicarbonate buffer and reported that the *in vitro* dissolution profiles in bicarbonate compared reasonably well with the *in vivo* intestinal dissolution of the tested suspensions. They concluded that this demonstrates the possible potential toward extending biowaivers to BCS class IIa compounds.

Amaral Silva et. al. (27) applied a 5mM phosphate buffer as the surrogate buffer for ibuprofen based on the IRR model described by Krieg et. al. The authors also observed a slower dissolution rate of Ibuprofen IR tablets in low buffer capacity (5mM) compared to compendial buffer (50mM) and that compendial buffer lacked discriminatory power (27,79,87). The authors pointed out that the rapid *in vitro* dissolution rate cannot be translated to the observed *in vivo* dissolution rate of ibuprofen. In contrast from the methodology used by Álvarez at al. (87), in

which different absorption rates could not be detected , Amaral Silva and colleagues utilized the low-capacity surrogate buffer in a biphasic dissolution system. This system is composed of an organic layer on top of the aqueous medium thus mimicking the concurrent *in vivo* processes of drug dissolution and absorption. The addition of the organic phase works as a sink to the aqueous layer, assisting the medium pH maintenance by the removal of the dissolved drug from the aqueous medium. Hence, the pH changes that are expected when a low buffer capacity medium is used are reduced. This is a valuable approach to investigate the drug product performance with improved physiological relevance (27).

Based on this, we herein suggest the use of a biphasic system with the aqueous layer composed of BCB. Adding paraffin on top of the buffer has been previously proposed (71) to prevent the CO₂ escape, however drugs do not partition to the liquid paraffin layer. We believe that the use of BCB coupled with an organic layer (octanol) would not only prevent the escape of CO₂ – thus taking away the need to sparge the medium – but it would also allow assessment of the drug partitioning (“absorption”). This would be a very robust physiologically relevant approach and we suggest that future *in vitro* studies along this line be conducted.

Oversimplification of the dissolution conditions, as for example using a surrogate buffer instead of BCB, may not be relevant or proper for certain formulations. This is the case for enteric coated (EC) drug products. Formulations coated with pH responsive polymers have been shown to have poor *in vivo* performance (88) (and references cited thereby). One of the reasons for this is the lack of biopredictability of the buffers used for *in vitro* performance testing, preventing suitable *in vitro* product evaluation (89). The great discrepancy in the performance of EC products in physiologically relevant BCB vs. phosphate buffer is well recognized in the literature, as highlighted by Amaral Silva et al. (88). This performance problem persists until

today, and recent reports by Scott et al. and Sakamoto et al. have corroborated these previous findings.

Scott and colleagues investigated the release of enteric coated prednisolone micro-particles, pellets and tablets (70). They observed that in phosphate buffer the drug release was immediate after the 2 h acid exposure for the all the tested dosage forms with no significant difference among the dissolution profiles. On the other hand, in BCB there was a long lag time for the onset of drug release. An interesting observation highlighted by the authors was a shorter lag time for the microparticle formulation compared to pellets and tablets which could be explained by the larger surface area available for polymer dissolution. Similarly, Sakamoto et al. reported a 30-minute disintegration time and similar release profiles for enteric coated 5-ASA tablets in a phosphate-based buffer, whereas in BCB the disintegration time was about 4–8 h with large variation (73).

With this in view, the ideal dissolution media for EC formulations would be a bicarbonate-based one. As highlighted before, the routine use of BCB is technically difficult and even unfeasible for disintegration testing and dissolution apparatuses such as reciprocal cylinder (89). Therefore, similarly to small drug molecules, developing a non-volatile surrogate buffer for EC products is of great interest. However, enteric polymers, being poly-acids with ionizable carboxylic groups, are much more complex than small molecules as its dissolution includes different phases as follows (44,88,90–93). In an environment with low pH values (such as the stomach) the carboxyl groups are not ionized, therefore the polymer is insoluble resisting disintegration and dissolution which prevents drug release. When the EC dosage form is exposed to the intestinal fluids (higher pH and buffered by bicarbonate) and when the pH_0 (surface pH) of the polymer is above its pK_a (dissolution pH threshold), its ionization is promoted (88). Due to

electrostatic repulsion, the polymer relaxes, swells, and undergoes chain disentanglement allowing further ionization of other polymer chains which diffuse away to the bulk solution (90,92). This consists of the dissolution phases of pH-responsive polymers ultimately leading to the disintegration and dissolution of the dosage form.

Recently, Blechar et al. (89) proposed a mechanistic approach to enable the development of surrogate buffers for EC products with little bench work. As described before, the effective pKa of BCB in the diffusion layer ($pK_{a\text{eff}}$) is different from other buffers such as phosphate and maleate (pKa's of 6.8 and 5.8, respectively) and different from the bulk where everything is at equilibrium. For small molecules under regular hydrodynamic conditions the $pK_{a\text{eff}}$ of bicarbonate lies between 4 and 5 (89,93). However, the complex behavior of enteric polymers makes it difficult for a direct calculation.

Besides the diffusion layer, a viscoelastic gel layer is formed on a polymer's surface (Figure 2.3), as opposed to only a diffusion layer on a particle's surface. The gel layer presents an increased diffusional resistance which reduces the diffusion rate of the buffer species. Consequently, the time available for the interconversion between CO_2 and H_2CO_3 is increased allowing " $\text{H}_2\text{O}_{(l)} + \text{CO}_{2(aq)} \rightleftharpoons \text{H}_2\text{CO}_{3(aq)}$ " to approach equilibrium. As a result, the pKa of bicarbonate in the gel layer is increased compared to the $pK_{a\text{eff}}$ in the diffusion layer. Finally, both the $pK_{a\text{eff}}$ (diffusion layer) and higher pKa in the gel layer will control the polymer's surface pH. Therefore, the gel layer increases the effective interfacial buffering pKa of bicarbonate.

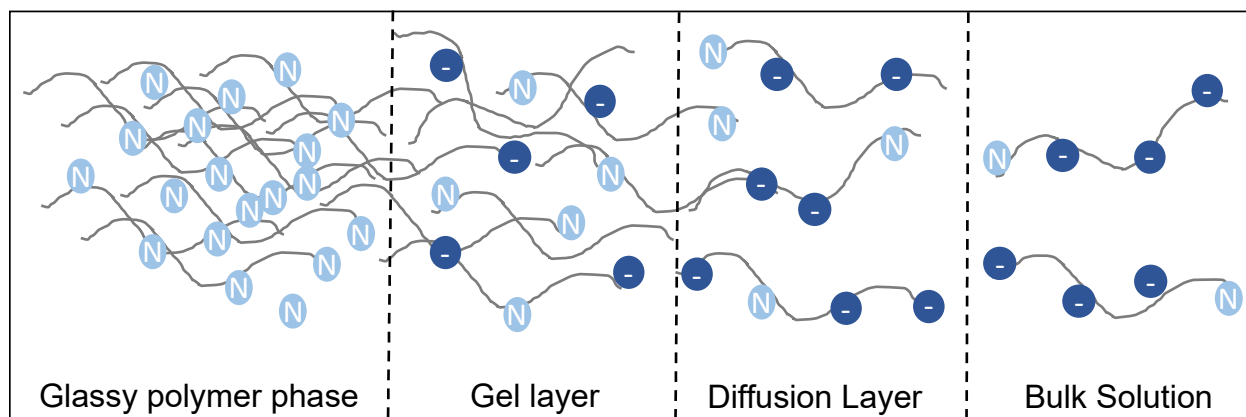


Figure 2.3. Representation of the solid-liquid interface of a dissolving enteric polymer. N: Neutral (Unionized carboxylic acid: $-\text{COOH}$); - : Negative charge (Ionized carboxylic acid: $-\text{COO}^-$). From the gel layer to the bulk solution the pH increases and the viscosity. Adapted from (89).

The authors performed dissolution experiments in maleate (pKa 5.8), citrate (pKa 5.7), succinate (pKa 5.2), and acetate (pKa 4.6) buffers to find a buffer species that would promote similar dissolution as bicarbonate. The time taken for 5% release ($t_{5\%}$) for comparison was used because it is most representative of the coat dissolution as opposed to the whole dissolution profile. The observed trend of dissolution based on $t_{5\%}$ was that succinate matched bicarbonate buffer well for relatively fast dissolving formulations while citrate would be a good estimate for relatively slow dissolving ones. These media could be used as good starting points. Based on these findings, the authors proposed a “decision tree” in establishing a surrogate buffer (Figure 2.4).

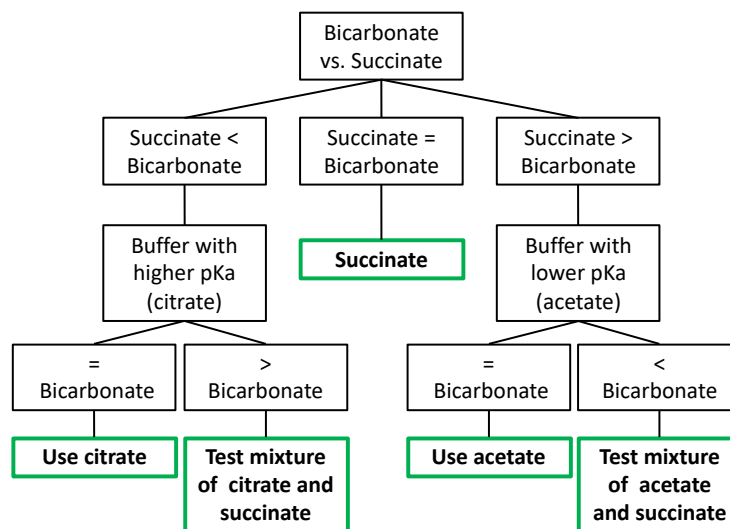


Figure 2.4. Decision tree for establishing a surrogate buffer for EC products. (Adapted from (89))

A physiologically relevant approach is of primary importance not only to predict the *in vivo* performance of a formulation under development, but also to assess the similarity of reference and test formulations in a bioequivalence (BE) study. Our group assessed clinical data of a failed BE study for EC pantoprazole tablets (submitted). The formulations used in the dissolution study were from the same batch as those used in the BE study. Both formulations complied with the USP specifications and had a somewhat similar performance in phosphate buffer, but when tested *in vivo* they did were not bioequivalent. Hence, solely satisfying the *in vitro* standard for drug dissolution does not guarantee similar *in vivo* behavior. On the other hand, when these formulations were tested in BCB, a great discrepancy was observed, where the test formulation had a much more delayed onset of dissolution than the reference. The use of non-physiologically relevant dissolution method during the drug product development phase can be misleading, causing poor selection of prototype formulations. Therefore, it was further evidenced that using BCB can de-risk the development of generic EC formulations, increasing the likelihood for a successful BE.

2.3 Conclusion

The evolution of media and buffers to be used in dissolution testing to achieve physiological relevance was herein presented. There are many important factors to be considered when developing a biorelevant dissolution method such as, pH, buffer species, buffer concentration, osmolality, viscosity, surface tension, concentration and type of bile salts, lipolysis products, as well as physiological state, such as fasted and fed states. Physiologically relevant methods usually don't apply compendial conditions and its use is most meaningful in the development phase, rather than in a QC environment for batch release, for example. One of the major disconnects between the *in vivo* environment and *in vitro* conditions is the buffer species and concentration. While the human intestinal lumen is buffered by bicarbonate at low molarities, highly concentrated phosphate buffers is often used in dissolution testing, which can give misleading results during the drug product development. This is especially true for enteric coated formulations. Hence, using BCB would be the most ideal in terms of physiological relevance. On the other hand, one has to keep in mind that a biorelevant test will not necessarily be a clinically relevant dissolution test, but the chances are higher to capture critical quality attributes. The pragmatical hurdles of using BCB makes it desirous to develop a surrogate method with simpler buffer systems. This can be achieved on a case-by-case study by comparing the drug flux in BCB and other buffer solutions (which are often more diluted systems compared to compendial buffers). Precise mechanistic understanding of the *in vivo* and *in vitro* dissolution processes is imperative to set physiological relevance to the dissolution methodology. Using such conditions can de-risk the drug product development which increases the likelihood to select formulations with improved *in vivo* performance.

SECTION ONE: INTRODUCTION AND OVERVIEW

CHAPTER THREE

The significance of disintegration testing in pharmaceutical development

A version of this chapter is published in:

Dissolution Technol. 2018;(August):30–8. [dx.doi.org/10.14227/DT250318P30](https://doi.org/10.14227/DT250318P30)
Reprinted from reference (1).

3.1 Introduction

Disintegration is a physical process related to the mechanical breakdown of a tablet into smaller particles/granules, representing the breakage of inter-particle interactions generated during tablet compaction of granulated particles of the active pharmaceutical ingredient (API) and excipients (94). Generally speaking, after the liquid wets the tablet surface and penetrates the pores, disintegration takes place in two steps: first, tablet disintegration into small granules, and second, disaggregation or granule disintegration (95). The first step is important for the rate of initial drug release from the tablet. Gelling of a disintegrant, however, slows this process down. If no disintegration would occur, only the API near the surface of the compact would dissolve. The increase in surface area compared to the intact tablet yields a higher dissolution rate. In the second step, an even faster drug dissolution rate is achieved due to the increased surface area in contact with the medium, as represented in the scheme shown in Figure 3.1 (96).

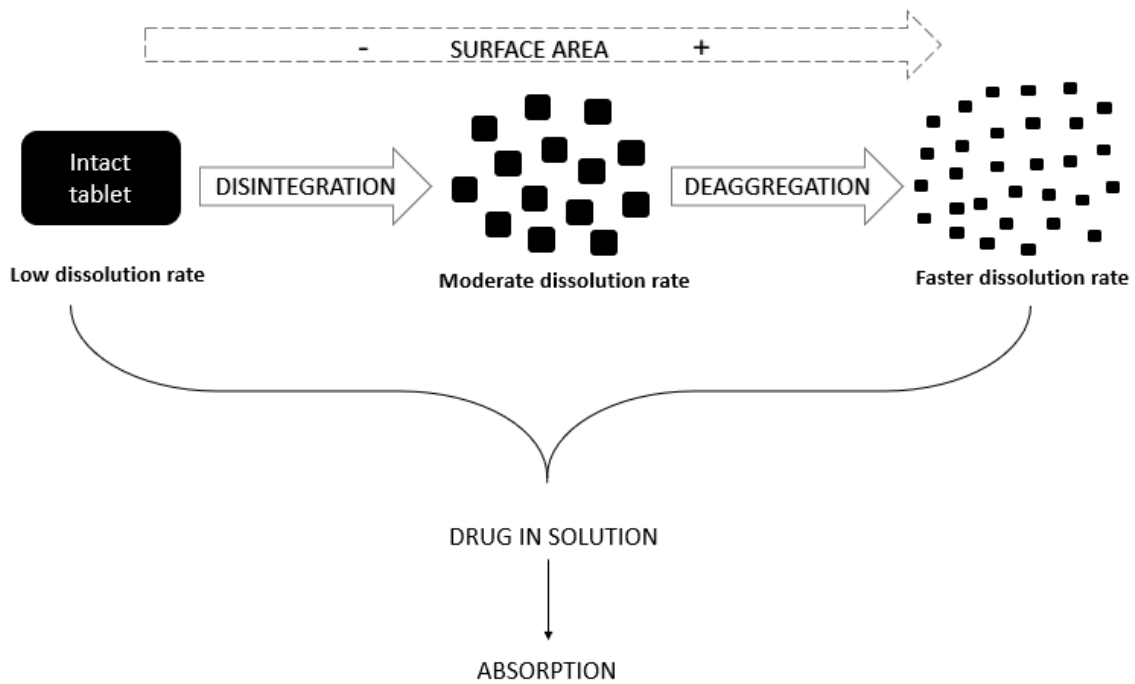


Figure 3.1. Immediate release tablet disintegration process. Adapted from (96).

Disintegrants can be added to the formulation to promote the dosage form (DF) disintegration when in contact with a fluid (97). Such excipients soften the DF matrix, allowing disintegration by different mechanisms (97–99). The different mechanisms of tablet disintegration are summarized in Table 3.1.

Table 3.1. Disintegration Mechanisms

Mechanism	Description	References
Wicking (capillary action)	<p>The liquid enters the DF compact through the pores by capillary action. Subsequently the interparticle bonds generated during tablet compression, such as intermolecular forces, solid bridges, and mechanical interlocking that hold the solid particles together to maintain the structural integrity of the DF are disrupted. Thus, wicking (liquid penetration) is one of the main steps in the disintegration of a DF.</p> <p>How much the liquid penetrates in the DF is closely related to the micro-pore structure (pore size) of the compact and also the hydrophilicity of excipients added in the compact, not just the disintegrants.</p> <p>The balance between capillary force and viscous forces also plays a role in disintegration. Viscous forces act in the opposite way of capillary forces. As the liquid goes into the DF, the viscous forces increase, decreasing the total penetration rate. Nevertheless, simultaneously to this, a breakage of the matrix can occur, increasing the penetration rate.</p>	(94,97–100)
Swelling	<p>One of the most accepted mechanisms in disintegration.</p> <p>Particles swell omni-directionally, pushing other components apart and resulting in matrix breakage. One of the most common methods for promoting tablet disintegration is the addition of a disintegrant. How much a disintegrant swells is directly related to its chemical structure and degree of crosslinking.</p> <p>Another factor that plays a role on the disintegrant performance is the compact porosity. On one hand, high porosity with large empty spaces can diminish the force of disintegrant swelling on the surrounding matrix, decreasing its efficiency. While on the other hand, low porosity and high compression force can hinder liquid penetration into the matrix, resulting in a</p>	(94,97–99,101)

longer disintegration time.

Substances that form gels when swelling are not effective disintegrants because the viscosity of the gel slows down the liquid penetration and increases the disintegration time. Therefore, swelling gums, such as agar, karaya, and tragacanth, are not very effective disintegrants.

Strain recovery	<p>Described as the reversible viscoelastic process of deformation. During tableting, the disintegrant particles are deformed. When in contact with water, the disintegrant tends to go back to its previous structure, recovering its original shape. The disintegration medium can also favor the polymer chains of the disintegrant to adopt the most energetically favorable position.</p> <p>The movements and volume expansion generated by the shape recovery process can cause the compact matrix to break up.</p> <p>This mechanism is less studied than swelling and wicking.</p>	(94,97–99,102)
Interruption of particle-particle bonds	<p>During tablet manufacture, bonding can occur by solid bridges, mechanical interlocking, or intermolecular forces. It is proposed that the interruption of these binding bonds is one of the disintegration mechanisms. An example of that is microcrystalline cellulose. When the tablet is in contact with the disintegration medium it disintegrates when the intermolecular forces between the cellulose fibers are disrupted by the imbedded water.</p> <p>Microcrystalline cellulose particles contribute to capillarity, i.e., liquid is drawn into the DF causing adhered particles to be separated.</p>	(99,103,104)
Expansion due to heating entrapped air	<p>There is a lot of controversy regarding this mechanism. Some authors report that exothermic interactions of materials with water generate heat, which can cause localized stress, resulting in expansion of the air entrapped in the compact, thus resulting in disintegration of the matrix.</p> <p>Other authors say that the heat generated by this process of wetting is too small to cause the entrapped air to expand. If that was the case, then break-up of the compact would occur during manufacturing, when compacting or ejecting the tablet.</p>	(97–99,103,105)

Release of gaseous materials	Effervescent tablets are made in such a way that when in contact with water they release CO ₂ , resulting in rapid disintegration. This is triggered by a reaction between an acid and carbonate or bicarbonate.	(97)
Enzymatic action	Enzymes which break down tablet components can be added to the product.	(97)

DF, dosage form.

In immediate release (IR) systems, drug release from the DF begins with the liquid wetting the solid and subsequent disintegration; thus, this step is of primary importance and a prerequisite for dissolution followed by absorption and bioavailability of the API (94). Although it cannot measure the amount of drug released, disintegration is, for IR tablets, the first process before dissolution can occur. The disintegration test basically consists of placing a DF in an immersion medium under defined experimental conditions and measuring the time taken for the DF to disintegrate (106). The time in which the tablet or capsule should disintegrate is defined in the applicable monograph. The United States Pharmacopoeia (USP) defines complete disintegration as the “state in which any residue of the unit, except fragments of insoluble coating or capsule shell, remaining on the screen of the test apparatus or adhering to the lower surface of the disk, if used, is a soft mass having no palpably firm core” (7). Nevertheless, complete disintegration does not necessarily imply complete API dissolution (107).

Disintegration testing goes back as far as 1907 when it was first mentioned in the Swiss Pharmacopoeia describing the test in water (108). It was then incorporated in the British Pharmacopoeia (BP) in 1948 which described the test using test tubes (109). In the 1950’s, the USP described the test using the basket-rack assembly apparatus, which is still used today to perform disintegration tests of DFs administered orally (110). In addition to the disintegration

test, a rupture test is used as a performance test of soft-shell capsules for dietary supplements, as directed in USP General Chapter <2040>, “*Disintegration and Dissolution of Dietary Supplements*”, first published in USP 30–NF 25 in 2017 (111).

The dimensions and measurements of the apparatus’ components used for the disintegration test were changed quite a few times in the USP in order to harmonize with the European Pharmacopoeia and Japanese Pharmacopoeia (106). The apparatus consists of a basket-rack assembly, a low-form beaker (1000 mL), a thermostatic arrangement for heating the fluid, and a device for raising and lowering the basket in the immersion fluid at a constant defined frequency rate. The basket-rack assembly moves vertically along its axis with no appreciable horizontal motion or movement of the axis from the vertical (112).

There are two types of basket-rack assemblies, which are denominated as apparatus A and apparatus B. The European Pharmacopoeia, USP general chapter <701>, and Japanese Pharmacopoeia describe apparatus A while only the European Pharmacopoeia and Dietary Supplements chapter <2040> of the USP describe apparatus B (112,113). According to USP chapter <2040>, apparatus A should be used for tablets or capsules that are not greater than 18 mm long. For larger tablets or capsules, apparatus B should be used.

As mentioned above, disintegration testing is described in two chapters in the USP, general chapter <701> and <2040> for dietary supplements. There are some differences between the two chapters. For example, for hard gelatin capsules, chapter <701> uses water as the immersion medium, whereas chapter <2040> uses acetate buffer pH 4.5. For soft gelatin capsules, chapter <701> recommends this DF to be tested like uncoated tablets while chapter <2040> uses a rupture test. In order to explore these differences and other parameters, Almukainzi et al. systematically investigated how the basket assembly (apparatus A and B) and

other parameters impact the disintegration of different commercially available dietary supplement products (114). After this thorough study, many of the products tested had the disintegration time impacted by the different test conditions. This led to the conclusion that “the current harmonized ICH specifications for the disintegration test are insufficient to make the disintegration test into reliable test for dietary supplements” (114).

3.2 Apparatus specifications and procedures – USP <701> and <2040>

The 1-L low-form beaker should have 138 to 160 mm in height and an inside diameter of 97 to 115 mm for the immersion fluid. The immersion fluid temperature should be between 35 °C and 39 °C, and the immersion frequency should be between 29 and 32 cycles per minute through a distance of not less than 53 mm and not more than 57 mm. The volume of the fluid in the vessel is such that at the highest point of the upward stroke of the wire mesh remains at least 15 mm below the surface of the fluid and descends to not less than 25 mm from the bottom of the vessel on the downward stroke. At no time should the top of the basket-rack assembly become submerged. The time required for the upward stroke is equal to the time required for the downward stroke, and the change in stroke direction is a smooth transition, rather than an abrupt reversal of motion. The specifications for each apparatus regarding the basket-rack assembly and disks are summarized in Table 3.2 and illustrated in Figure 3.2 (112,113).

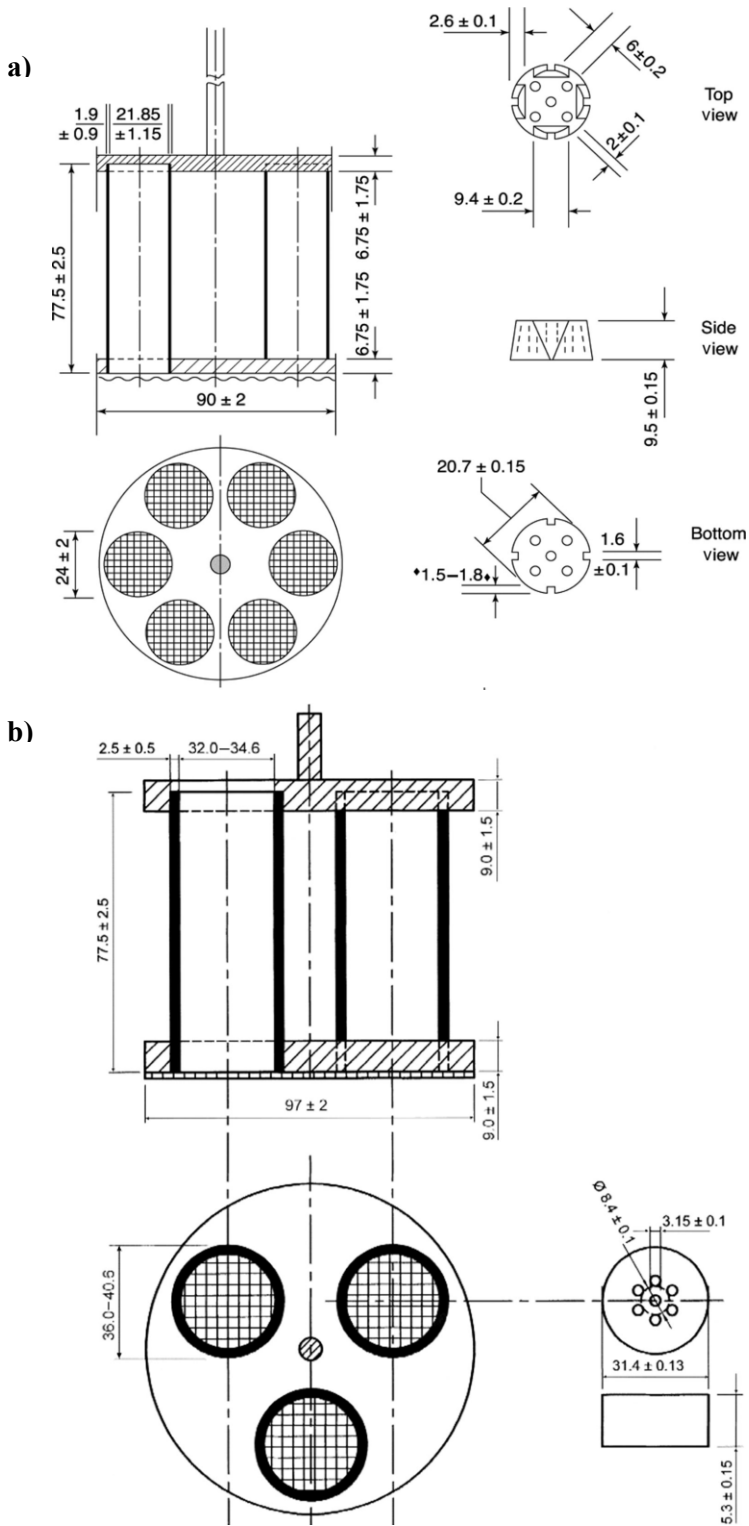


Figure 3.2. USP specifications for disintegration apparatus A (a) and apparatus B (b). Reprinted with permission. ©2017 The United States Pharmacopeial Convention.

Table 3.2. USP Specifications for Basket-Rack Assembly and Disk for Apparatus A and B

	Apparatus A	Apparatus B
Basket-rack assembly		
Tubes (n)	6	3
Tube length (mean ± SD) (mm)	77.5 ± 2.5	77.5 ± 2.5
Inside diameter range (mm)	20.7–23	32.0–34.6
Wall thickness range (mm)	1.0–2.8	2.0–3.0
Plates (n)	2	2
Plate diameter range (mm)	88–92	97 ± 2
Plate thickness range (mm)	5–8.5	7.5–10.5
Plate holes (n)	6	3
Hole diameter range (mm)	22–26	33–34
Wire weave gap range (mm)	1.8–2.2	Not specified
Wire diameter range	0.57–0.66 mm	0.025 in.
Disks		
Thickness (mean ± SD) (mm)	9.5 ± 0.15	15.3 ± 0.15
Diameter (mean ± SD) (mm)	20.7 ± 0.15	31.4 ± 0.13
Specific gravity range	1.18–1.20	1.18–1.20
Holes (n)	5	7
Hole diameter (mean ± SD)	2 ± 0.1	3.15 ± 0.1

The disintegration test might be performed differently for each DF as specified in USP chapter <701> (112). For example, when testing uncoated tablets in apparatus A, one dosage unit should be placed in each of the six tubes of the basket and, if prescribed, add a disk. The immersion fluid can be water or other specified medium, with temperature maintained at 37 ± 2 °C. Each monograph specifies the time the test should run for and that all tablets should have disintegrated completely at the end of the time limit. Interestingly, the disintegration test for uncoated tablets in general chapter USP <2040> specifies a 30-min time limit, showing that the specifications in <701> and <2040> are not identical(113). The specifications are described in each chapter for other DF's, such as plain coated tablets, delayed release tablets, buccal tablets, sublingual tablets, hard- and soft-gelatin capsules; details are listed in Table 3.3. There are not only differences between the two USP chapters as to how to conduct disintegration for the different DF, but there are also differences between the pharmacopeias of the different regions. These differences were summarized by Al-Gousous and Langguth (107). The problem with these

differences in the disintegration testing conditions is that it can lead to different test results. A study using enteric-coated soft gelatin capsules showed that the conditions specified by the USP and European Pharmacopoeia led to different test results (115).

Generally, when 1 or 2 tablets fail to disintegrate completely, the test should be repeated on 12 additional tablets. The requirement is met if at least 16 of the total of 18 tablets tested are disintegrated (112).

Table 3.3. Disintegration Test Specified for Each Dosage Form According to USP Chapters <701> and <2040>

Dosage Form	USP General Chapter <701>	USP Dietary Supplements Chapter <2040>
Uncoated Tablets	Immersion fluid: water or the specified medium; if prescribed, add a disk. Use the time specified in the individual monograph.	Immersion fluid: water or the specified medium for 30 min. If prescribed, add a disk.
Plain Coated Tablets	Same as uncoated tablets using the time specified in the individual monograph.	Immersion fluid: water or the specified medium for 30 min. If prescribed, add a disk. For tablets with external sugar coating: immerse in water at room temperature for 5 min.
Delayed-Release (enteric coated) Tablets	Immersion fluid: Start with simulated gastric fluid. After 1 h, no evidence of disintegration, cracking, or softening. Continue using simulated intestinal fluid for the time specified in the monograph. For tablets with external sugar coating: immerse in water at room temperature for 5 min.	Omit the use of a disk. Immersion fluid: Start with simulated gastric fluid. After 1 h, no evidence of disintegration, cracking, or softening. Continue using simulated intestinal fluid for the time specified in the monograph. For tablets with external sugar coating: immerse in water at room temperature for 5 min.

Delayed-Release (enteric coated) Soft Shell Capsules	Not specified	Immersion fluid: Start with simulated gastric fluid, omit the use of disks. After 1 h, no evidence of disintegration or rupture. Continue using simulated intestinal fluid with disks for no more than 60 min.
Hard Shell Capsules	Same as uncoated tablets using the time specified in the individual monograph. Attach a removable wire cloth to the surface of the upper plate of the basket-rack assembly.	Same as uncoated tablets for 30 min. Immersion fluid: pH 4.5 acetate buffer. Attach a removable wire cloth to the surface of the upper plate of the basket-rack assembly.
Soft Shell Capsules	Same as hard gelatin capsules	Rupture test for soft shell capsules: performed in dissolution Apparatus 2 (paddle) operated at 50 rpm with 500 mL of water as the immersion medium for 15 min.
Buccal Tablets	Same as uncoated tablets for 4 h	Not specified
Sublingual Tablets	Same as uncoated tablets using the time specified in the individual monograph.	Not specified

3.3 Disintegration as a Quality Control test

According to decision Tree #7 in the International Council for Harmonization (ICH) Tripartite Guideline Q6A, the use of disintegration testing instead of dissolution is allowed when the following criteria are met (116):

1. Immediate-release dosage form (i.e. no modified release);
 2. The drug product contains a drug that is highly soluble throughout the physiological range (dose/solubility volume < 250 mL from pH 1.2 to 6.8);
 3. Rapidly dissolving products (dissolution > 80% in 15 minutes at pH 1.2, 4.0, and 6.8);
- and

4. Establishment of a relationship between disintegration and dissolution or when disintegration is shown to be more discriminating than dissolution.

The FDA draft guideline on dissolution testing also allows replacement of dissolution by disintegration testing for BCS class I and III drug products using the same criterion of rapid dissolution specification (Q = 80% in 15 minutes). When this criterion is met, the product should completely disintegrate within 5 min in 0.01 M HCl (via USP apparatus) (117).

USP chapter <2>, *Oral drug products – Product quality test*, states that disintegration testing is used only as a quality control test and not as a product performance test following the ICH guidance criteria for tablets (118). Furthermore, it states that “only when disintegration has been correlated with dissolution of a dosage form can a disintegration test be used as a product performance test”, also following the ICH guidance criteria. Since disintegration tests are less complicated and less time consuming than dissolution tests, its use is desirable in a quality-by-design (QbD) approach. Due to its simplicity, concentrating more efforts and research on disintegration testing could result in time and resource saving for quality control (QC) departments in pharmaceutical industries throughout the product’s lifecycle (107). Nevertheless, when using disintegration as a quality control test, it must be reproducible within the set specifications (106).

3.4 Disintegration in the real world

3.4.1 Early-stage development

Commonly, at early stages of drug development, there are restricted or no pharmacokinetic data from the IR formulation under development. Not much data exist about the solubility in different media (19). For that reason, dissolution testing for quality control is unfeasible at this stage. Scientists from Pfizer name this first stage in the development process as

the “exploratory development” stage. The focus of this stage is to reach ‘proof-of-concept’ to decide “as to whether the candidate is suitable for further development” (119). As stated by Klute, at this point in early drug development, the “API characteristics such as particle size and disintegration are monitored to ensure batch quality for Pfizer immediate release solid oral dosage forms, therefore dissolution is no longer the default method of choice to ensure product performance” (119).

As shown in Figure 3.1, in order to have the API in solution for absorption, the tablet has to first disintegrate into primary particles, and then API particles can dissolve. Thus, the critical quality attributes for drug solubilization are the tablet disintegration rate and API dissolution rate. For Pfizer, if rapid disintegrating tablet formulation is used and the API particle size is small enough to completely dissolve, the disintegration test is a suitable surrogate for tablet performance and is adequate for early stage development (119). QC dissolution testing at this stage is negated. Instead, the key QC test to certify tablet performance is disintegration testing, which is included “as the key performance test on the drug product specification as part of clinical applications submitted in support of early clinical studies using IR tablets” (119). In the cases where the ‘proof-of-concept’ is positive, the drug candidate will undergo further development, where a QC dissolution test is more appropriate and is used as a tool to predict the formulation bioperformance (119).

3.4.2 Relationship between disintegration and dissolution

Drugs that have high solubility (BCS classes I and III) and high dissolution number dissolve within the gastrointestinal tract and may not have dissolution as the rate limiting step, as long as the DF disintegrates and releases the API particles (106). For BCS class I and III, it is expected that the drug’s highest dose dissolves within the physiological pH; BCS class II and IV

drugs might not dissolve within the small intestinal passage. Here, formulation approaches are often used to increase API dissolution. In all cases, dissolution will happen after disintegration, i.e., after liberation of the API from the DF (106,107). Hence, when facing the scenario where the API dissolution is not dependent on the formulation but is dependent on the drug particle properties, particle size or surface area disintegration might be the appropriate parameter to predict API dissolution (120).

The experiment set up, such as media composition and pH, may also play a role in the disintegration test result. Stamatakis et al. investigated the influence of the medium pH on the disintegration time of commercially available phosphate binder formulations (121). Tablet formulations of calcium carbonate, calcium acetate, and aluminum hydroxide, and capsule formulations of aluminum hydroxide were analyzed using three different media: simulated gastric fluid (pH 1.5), distilled water (pH 5.1), and simulated intestinal fluid (pH 7.5). The USP standard disintegration apparatus at the time (USP 23–NF 18) was used. Their results showed that nine out of the 15 products tested were sensitive to changes in pH, showing differences in disintegration time. They concluded that “the pH significantly affected *in vitro* disintegration in the majority of phosphate binders tested”. This study, thus, portrays how the disintegration time can vary depending on the immersion medium pH.

In a study done in 1971 by Alam and Parrott, the disintegration time of hydrochlorothiazide tablets (granulated with acacia, polyvinylpyrrolidone, or starch as binding agents) was measured in four different media: distilled water, 0.1 N HCl, simulated intestinal fluid, and borate buffer at pH 10 (122). The average disintegration time for the tablets granulated with all three binders was faster than the USP disintegration time, according to the available USP

at the time. Besides that, each formulation had significant differences on the disintegration time throughout the media tested.

Furthermore, Zuo et al. demonstrated how the media composition can affect the disintegration time (123). In their study, they used different beverages (alcoholic beverages, regular cola (Pepsi), and orange juice (Minute Maid)) as media and compared it to the pharmacopeial immersion medium water, which is the USP reference medium in <701> and for dietary supplements formulated as tablets (112,113). Four commercial tablet products, calcium citrate, Ester-C, *Boswellia serrata* extract, and cinnamon extract were analyzed in the cited media. Orange juice and high alcohol content in particular extended the disintegration times. For orange juice, the extension was attributed to the increased viscosity of the orange juice but could also be an effect of the low pH. For high alcoholic beverages the hydration of disintegrants could be impacted, which in turn impacts DF disintegration. The study concluded that “with the exception of 5% alcohol, all beverages had a significant effect on the disintegration time of calcium citrate and Ester-C. Only cola, orange juice, and 40% alcohol significantly influenced the disintegration time of the cinnamon extract. Therefore, the tested beverages should not be used to replace water when ingesting therapeutic products” (123). Taking these results into consideration, experimental conditions must be carefully chosen because they impact the test results (123,124).

Regarding the rupture test as a performance test for soft-shell capsules established in USP 30–NF 25 (2007) under the General Chapter <2040>, Bachour et al. evaluated the use of this test as a quality control tool for long-term stability samples using different enzymes (125). The rupture test for soft-shell capsules can fail for samples that were exposed to stability conditions, an aging problem that has already been reported by the nutraceutical industry. This may be due

to gelatin cross-linking, as stated in the USP General Chapter <711>, which states “Gelatin, in the presence of certain compounds and/or in certain storage conditions, including but not restricted to high humidity and temperature, may present cross-linking. A pellicle may form on the external and/or internal surface of the gelatin capsule shell or on the dosage form that prevents the drug from being released during dissolution testing” (3). With this in view, Bachour performed a rupture test and compared oil-based, oral multivitamin soft-shell capsules with stability samples of the same product. The immersion medium was water and enzyme-containing media (pepsin, pancreatin, papain, and bromelain) as used for rupture and dissolution testing of gelatin-based capsules. The stability sample capsules failed to pass the requirements in all tested media, while the commercial capsules passed. Nevertheless, the study also reports that “the cross-linked capsules ruptured readily when emptied out of the vessel, thus the capsules would likely rupture in the stomach, [...] even if cross-linked” (125). This indicates that the observed “fail to rupture” might not represent the in-vivo conditions where the capsule is exposed to motility forces. Therefore, *in vitro*, the rupture test can detect gelatin cross-linking in long-term stability samples but new or modified test methods are needed to assess the performance of aged soft-shell gelatin capsules when using the rupture test.

The requirements of ICH/FDA and USP to substitute dissolution testing with disintegration testing require the establishment of a relationship between disintegration and dissolution. This may not be an easy task to accomplish, given that the dissolution rate of IR solid formulations is not necessarily determined by disintegration, as shown by Radwan et al. (126). Nevertheless, Nickerson et al. was able to obtain a relationship between disintegration and dissolution for a rapidly dissolving immediate-release tablet with a highly soluble drug (BCS class I), thus justifying the use of disintegration in lieu of dissolution testing (127). In their work,

given the stated characteristics, drug release from the DF was shown to be limited by disintegration. The authors reported a linear relationship between disintegration and dissolution results for that particular drug product, concluding that disintegration would be an appropriate drug product quality control method to evaluate drug release from that DF.

Gupta et al., however, compared 12 different IR tablet formulations of Verapamil hydrochloride and no direct relationship was obtained between the disintegration and dissolution across all formulations (128). This was attributed to the interactions between different formulation components, which showed that the dissolution process depends not only on the disintegrating agent but also on formulation components. In this study, only one out of the 12 formulations met the ICH Q6A criteria, therefore being the only formulation suitable to use for the disintegration test instead of dissolution as the QC test (128). Thus, it becomes clear that the determination of a relationship between disintegration and dissolution test is not an easy task, and a systematic study is needed before using disintegration testing as part of the drug product specifications.

Uebbing et al. went further and demonstrated that if disintegration occurs first, and if dissolution is controlled by the drug particle properties based on API characteristics and not on formulation factors, then disintegration can be used as a performance test for rapidly disintegrating tablets beyond the current FDA criteria (120). Their mechanistic study differentiated between API controlled dissolution behavior and DF impacted/controlled dissolution. They concluded that if the formulation interferes with dissolution, then the dissolution test should be used as the QC test. Similar to this study, Han and Gallery described the use of disintegration instead of dissolution testing for liquid-filled gelatin capsules (129). Although it was an encapsulated poorly soluble drug, they argued that if the product was to be

administered in a spoon instead of a capsule, no dissolution test would be required. This case study also shows how a disintegration test can be used beyond ICH criteria as a surrogate for dissolution testing.

3.5 Conclusion

Further work is still needed to establish the scientific framework for using disintegration testing as a performance test for different DFs. Disintegration is an important quality control test today. In the future, disintegration testing could become a release test for formulations with API-controlled dissolution. Hence, in cases like this, disintegration is the critical quality attribute of the DF and determines the onset of dissolution, and dissolution is only determined by API properties.

With a proper understanding and demonstration or justification of the mechanistic details of drug dissolution from the DF, dissolution testing might be replaced by disintegration testing for certain DFs as a performance test. Disintegration testing can save time and cost for QC departments in the pharmaceutical industry due to its simplicity.

In order to harmonize the disintegration test throughout the different pharmacopeias, many specification changes have been made in the USP. These changes still need to be thoroughly investigated as to how much – especially the current beaker specifications – they might impact the disintegration time of dosage forms. To make this matter clearer, more research is needed to make disintegration test results less variable. This will improve the mechanistic understanding of the disintegration process and might lead to an *in vivo* predictive disintegration test.

**SECTION TWO: PHYSIOLOGICALLY RELEVANT *IN VITRO* TESTING:
BUFFER CAPACITY AND BIPHASIC DISSOLUTION TESTING**

CHAPTER FOUR

Biphasic Dissolution as an Exploratory Method during Early Drug Product
Development

A version of this chapter is published in:

Pharmaceutics. 2020;12(5):420. doi:10.3390/pharmaceutics12050420
Reprinted from reference (27).

4.1 Introduction

In the modern drug development process, a major tool used to assess a drug product's performance is dissolution testing. The test was developed in the late 1950s/early 1960s and accepted by the United States Pharmacopeia (USP) convention in 1970 (130). Ever since, *in vitro* dissolution testing has been used as a quality control (QC) test for solid oral dosage forms and it plays a critical role in enhanced product understanding (131). The different compendial dissolution equipment includes the basket (USP apparatus 1), the paddle (USP apparatus 2), the reciprocating cylinder (USP apparatus 3), and the flow-through cell (USP apparatus 4). The latter two are used for extended-release products, whereas apparatus 2 is the most widely applied method (130). However, compendial equipment and methods use conditions that may limit both the method's discriminatory power and its ability to emulate aspects of *in vivo* dissolution. Thus, the quality control aspects of the dissolution methodologies are mostly meaningful in a commercial environment of finished drug product release. Nevertheless, during the drug product development process, *in vivo* predictive methods are needed for the creation of products of predictable quality (131). In this realm, dissolution testing is a major tool used to assess a drug product's performance.

When testing poorly soluble drugs, conditions in which the medium is not saturated should be maintained to ensure the method robustness. These are later used to test the finished product to comply with regulatory guidance (132,133). Different strategies are often adopted to obtain such conditions throughout the dissolution test, such as the addition of solubility modifiers (e.g., surfactants) and the use of large volumes of dissolution medium among other strategies (134) that result in conditions with little physiologic resemblance. Within this context, the matter of buffer strength stands out (35).

In vivo studies demonstrate that the buffer capacity of gastrointestinal fluids is much lower than that of compendial buffers (35,36). Not only that, but the buffer species also differ; bicarbonate is the predominant buffer species in the human small intestine (28). This finding was linked to slower drug dissolution rates *in vivo*, which has important implications for the oral drug delivery of both acidic and basic drugs, and it should be considered in the *in vitro* dissolution studies during the drug product development process (35). Although the intestines are buffered by bicarbonate, when possible the use of simpler buffer systems, such as phosphate, is preferred for pragmatic reasons. According to Krieg et. al., the phosphate buffer concentration range needed to match ibuprofen dissolution in physiologically relevant bicarbonate buffers is 4–8 mM (83).

Furthermore, while the drug dissolves in the intestinal fluids, it is also absorbed through the gut wall. Biphasic dissolution is one of the possible approaches to assess the concurrent *in vivo* drug absorption process. It is composed of a two-phase system in which the simultaneous evaluation of drug dissolution and partitioning into an organic phase is studied, and it can be used as a non-compendial exploratory dissolution method. This approach was first described in the early 60s and its use has gained much attention in recent years (133–143).

The information obtained from the physiologically based dissolution test is used to identify what aspects of the drug substance, formulation composition, and process are most important to achieve the desired target release profile. In this way, variables that are likely to impact the drug dissolution can be identified early on in the development, allowing the ranking of formulation prototypes under physiologic-like conditions.

As suggested by Azarmi et al., two different dissolution methods might be needed, one for formulation predictive dissolution and the other for QC purposes, which is the current practice in pharmaceutical companies (26,131). The information obtained from early stage dissolution methods (exploratory and physiologically based) can be then used to establish appropriate discrimination of the QC method to be applied in the late development stage to critical dosage form attributes and other parameters (Figure 4.1).

In this exploratory study, the hypothesis was two-fold in order to evaluate both the influence of manufacturing methods and the excipient composition on the dissolution behavior of the tablets. Regarding the manufacturing process, we hypothesized that direct compression vs. wet granulation would result in different dissolution behavior, whereas excipients would create with the model drug a microclimate, also resulting in different profiles. Therefore, we screened the different tablets using compendial and physiologically based methods to identify which performance test method had the highest discriminatory power. Considering that the majority of molecules in the discovery pipeline are poorly water-soluble (144) and the knowledge gained with poorly soluble drug in previous work (35), ibuprofen (BCS IIa) was used as a model drug.

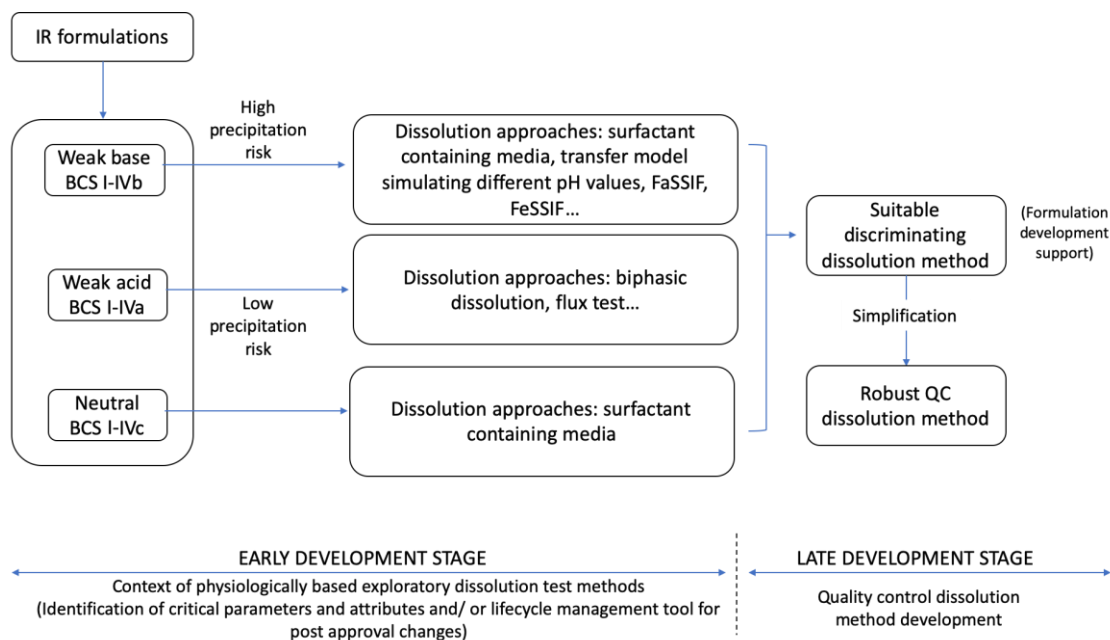


Figure 4.1. Simplified approach for dissolution method development for immediate release (IR) formulations containing acidic and basic drugs (BCS I–IV). FaSSIF: Fasted State Simulated Intestinal Fluid; FeSSIF: Fed State Simulated Intestinal Fluid; BCS: Biopharmaceutics Classification System.

4.2 Materials

The ibuprofen (USP grade) was purchased from Medisca (QC, Canada); the microcrystalline cellulose (Avicel[®] PH-102 NF) was purchased from FMC Biopolymer (Philadelphia, PA, USA); the dicalcium phosphate dihydrate and calcium sulfate NF were purchased from PCCA Canada (London, ON, Canada). The dextrose NF was purchased from Mallinckrodt chemical (USA); the croscarmellose sodium NF was from JRS Pharma (Rosenberg, Germany); the magnesium stearate was purchased from H.L. Blachford Ltd. (Mississauga, ON, Canada); and Starch 1500 was from Colorcon (Indianapolis, IN, USA). The 1-octanol 99% pure was purchased from Acros Organics (New Jersey, USA). The

buffer solutions were prepared with purified water (Elgastat Maxima UF and an Elgastat Option 3B water purifier by ELGA Laboratories Ltd. (Mississauga, ON, Canada)).

4.3 Methods

4.3.1 Ibuprofen Immediate Release Formulations

The formulations used in this study differed in their excipient composition and manufacturing process (Table 4.1). The selection of excipient was based on their chemical characteristics in terms of basicity and acidity. Granulating BCS IIa drugs (such as ibuprofen) with acidic excipients could create a microclimate with a lower pH, reducing the drug dissolution. On the other hand, basic excipients could create a higher microclimate pH, increasing the dissolution, whereas neutral excipients would not impact the microclimate pH. Dextrose was chosen as the acidic excipient, CaSO_4 and CaHPO_4 as basic excipients, and microcrystalline cellulose as neutral.

In order to analyze the manufacturing method, the tablets were prepared by direct compression and wet granulation. The direct compressed tablets (D) were prepared by mixing all the ingredients (except for the lubricant) for 6 min using a mortar and pestle until a homogenous mixture was obtained. The lubricant (magnesium stearate) was added last and mixed in for another minute to avoid the coating of the active pharmaceutical ingredient (API).

The tablets obtained by wet granulation (G) were prepared by mixing all the ingredients in the same manner as D. Ethanol 70% was used as the granulation solution and the wet powder mixture was granulated through a N60 sieve. The granules were dried for one hour in a 37 °C oven and sieved again through a N60 sieve. The lubricant (magnesium stearate)

was then added into the mixture (extragranular) and blended for another minute. All the tablets were pressed with a Carver Laboratory Press by Fred S Carver Inc. Hydraulic Equipment (Manomonee Falls, WI, USA) for 30 s at 1 metric ton.

Table 4.1. Excipient composition of IR ibuprofen tablets prepared in-house. Formulations were named according to the diluent mixture used

MCC D	MCC G	CaHPO ₄ D	CaHPO ₄ G	Dex D	Dex G1	Dex G2	CaSO ₄ D	CaSO ₄ G
Avicel PH102 (800 mg)	Avicel PH102 (800 mg)	Avicel PH102 (400 mg)	Avicel PH102 (400 mg)	Avicel PH102 (400 mg)	Avicel PH102 (400 mg)	Avicel PH102 (460 mg)	Avicel PH102 (400 mg)	Avicel PH102 (400 mg)
Ibuprofen (400 mg)	Ibuprofen (400 mg)	Ibuprofen (400 mg)	Ibuprofen (400 mg)	Ibuprofen (400 mg)	Ibuprofen (400 mg)	Ibuprofen (400 mg)	Ibuprofen (400 mg)	Ibuprofen (400 mg)
CS (3%)	CS (5%)	CS (3%)	CS (5%)	CS (3%)	CS (5%)	CS (5%)	CS (3%)	CS (5%)
Mg Stearate (1%)	Mg Stearate (1%)	Mg Stearate (1%)	Mg Stearate (1%)	Mg Stearate (1%)	Mg Stearate (1%)	Mg Stearate (1%)	Mg Stearate (1%)	Mg Stearate (1%)
		CaHPO ₄ (400 mg)	CaHPO ₄ (400 mg)	Dextrose (400 mg)	Dextrose (400 mg)	Dextrose (400 mg)	CaSO ₄ (400 mg)	CaSO ₄ (400 mg)
	Starch 1500 (210 mg)		Starch 1500 (210 mg)		Starch 1500 (210 mg)			Starch 1500 (210 mg)
Expected microclimate effect								
	-		↑		↓	↓↓		↑↑

MCC: microcrystalline cellulose (Avicel PH102); Dex: Dextrose; CaHPO₄: dicalcium phosphate dihydrate; CaSO₄: calcium sulfate; D: direct compression; G: wet granulation; CS: croscarmellose sodium; (↑ and ↑↑): increased dissolution; (↓ and ↓↓): decreased dissolution; (-): no effect.

4.3.2 Dissolution Tests

All the dissolution tests were performed in triplicate using a USP apparatus II (ERWEKA, GmbH) with a 75 rpm rotation speed at 37 °C. All buffer media were filtered by vacuum and degassed in an ultrasonic bath.

Compendial Dissolution Method

The USP-recommended method for ibuprofen immediate release (IR) tablets is 900 mL of phosphate buffer with a pH of 7.2 (50 mM) with not less than 80% of the labeled amount dissolved in 60 min (7).

Non-Compendial Dissolution Methods—Physiologically Based Exploratory Methods

Monophasic Dissolution with a Low Buffer Capacity Medium

The literature reports that a phosphate buffer with a pH of 6.5 at concentrations between 4–8 mM matches the ibuprofen dissolution in physiologically relevant bicarbonate buffer (83). Hence, 5 mM of phosphate buffer with a pH of 6.5 (900 mL) was used as a non-compendial and physiologically relevant dissolution medium for comparison reasons.

Samples (5 mL) were collected at specific time points (5, 10, 15, 20, 30, 45, 60 min) with media replacement after each sampling time. The amount of dissolved drug was determined by a UV-spectrophotometer at 221 nm. Since a low buffer capacity medium was being used, the pH was monitored throughout the dissolution test.

Biphasic Dissolution with Low Buffer Capacity Medium

Biphasic dissolution tests were performed in a 5 mM phosphate buffer with a pH of 6.5 with 100 mL of n-octanol on top. The aqueous layer mimicked the intestinal fluids and the organic layer mimicked the absorption compartment. A mini-paddle (kindly donated by Sotax AG) was mounted on the regular compendial paddle to obtain sufficient hydrodynamics in both phases.

The aqueous layer volume was also taken into consideration in order to increase the physiologic relevance. Considering the reported intestinal fluid volume of 77 mL (77 +/- 15 mL) (145), a lower volume of 200 mL was used in an attempt to better approximate that of the intestinal fluids. For comparison reasons, the dissolution experiments were also conducted at 900 mL.

Samples from the aqueous phase (5 mL) and the organic phase (1 mL) were collected at specific time points (5, 10, 15, 20, 30, 45, 60 min). The amount of the drug was determined by a UV-spectrophotometer at 221 nm for the aqueous phase and 272 nm for the organic phase. The pH of the aqueous phase was monitored throughout the dissolution test.

4.3.3 Statistical Analysis

The difference between the mean dissolution values at early exposure was measured through the 90% confidence interval (CI) of difference method using the Excel Add-In DDSolver (146,147). In order to compare the manufacturing methods, the % release at 15 min in the 5mM phosphate buffer was compared between the G and D formulations of the same composition. Furthermore, in order to compare the differences in the excipient composition, we analyzed both the early exposure (5 min) between the G formulations and

at 15 min between the D formulations. The 5 min selection was based on the fact that, even though the granular disintegration/deaggregation was still happening, the microclimate effect was most meaningful and expected to be strongest at this time point. The 15 min time point was selected to be able to analyze the early exposure, but was later than disintegration time.

4.4 Results

4.4.1 Compendial Dissolution Tests

All the profiles were similar in the compendial buffer, as >85% dissolved in 15 min (Figure 4.2). This method presented a low discriminatory power in differentiating between manufacturing methods as well as excipient compositions.

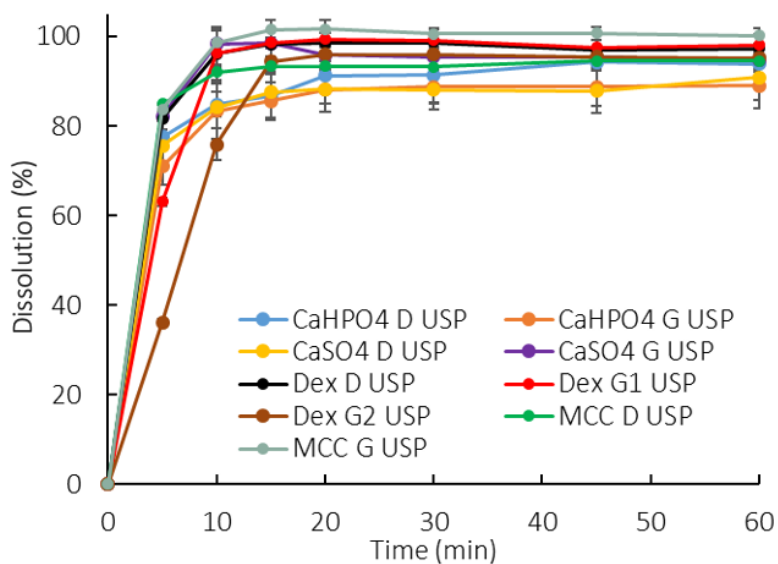


Figure 4.2. Dissolution profiles of all formulations in 900 mL of compendial buffer (50 mM phosphate buffer pH 7.2). Error bars represent the standard deviation. Ibuprofen was the active ingredient in all formulations.

4.4.2 Non-Compendial Dissolution Tests—Physiologically Based Exploratory Methods

4.4.2.1 Monophasic Dissolution With Low Buffer Capacity Medium

Overall, the dissolution rate of ibuprofen was much slower in the low buffer capacity medium compared to in the USP buffer (this observation is discussed in more detail in Section 4). The release pattern among the direct compressed formulations was very similar, which points out to a dissolution controlled by the API properties rather than a formulation-driven dissolution (Figure 4.3E). Interestingly enough, the G formulations presented a higher rate and extent of release compared to the D formulations (Figure 4.3A–D), which might have been due to a reduction in the drug particle size as a consequence of the granulating process itself. The higher level of disintegrant (crosscarmellose sodium) in the granulated formulations could also have contributed to the higher release. However, it is worth noticing that a higher level of disintegrant would primarily impact the dissolution rate (especially at early time points) rather than the extent. An additional factor was that the soluble fraction of Starch1500 could have enhanced the wettability of the ibuprofen particles.

The manufacturing methods were evaluated by granulating ibuprofen, with excipients that could modulate the drug dissolution in terms of a microclimate pH (Table 4.1). A pronounced effect was observed at early exposure (5–10 min), particularly for the DexG2 formulation, which presented a lower release compared to the other formulations (Figure 4.3F).

As expected, given that ibuprofen is a weak acid dissolving in a low buffer capacity medium, a drop in pH was observed.

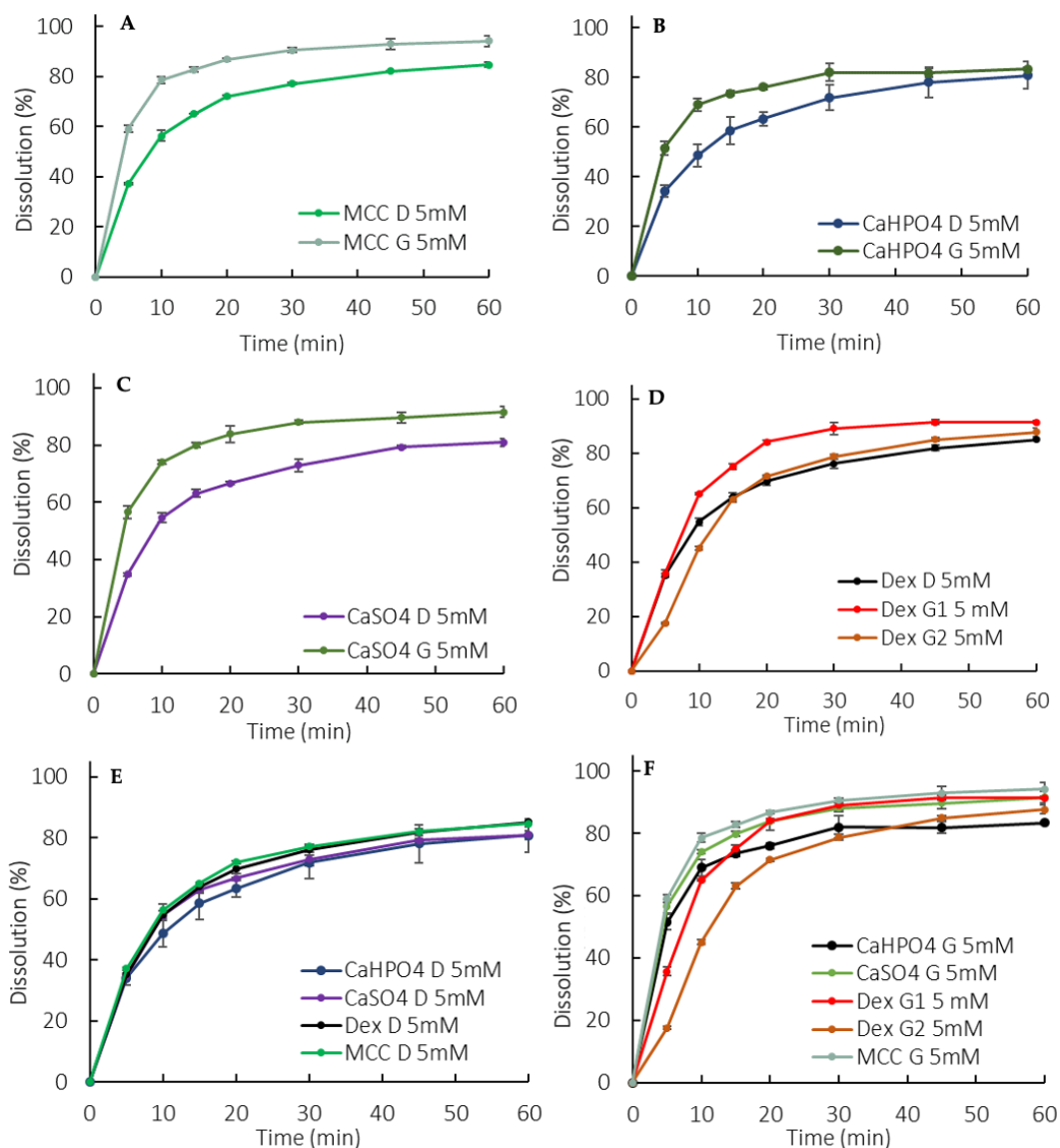


Figure 4.3. Dissolution profiles in the 5 mM phosphate buffer (900 mL). (A) MCC formulations, (B) CaHPO₄ formulations, (C) CaSO₄ formulations, (D) Dextrose formulations, (E) D formulations, (F) G formulations. Error bars represent the standard deviation. Ibuprofen was the active ingredient in all formulations.

4.4.2.2 Biphasic Dissolution Test with Low Buffer Capacity Medium

Biphasic Dissolution with 200 mL of Aqueous Phase

With a low aqueous volume, a high interfacial area to volume ratio was obtained and, as a consequence, a rapid drug partitioning into the organic phase was observed.

Manufacturing method and formulation composition differences were captured in the partition profiles of the drug to the organic phase (Figure 4.4A and B). A lower partitioning for dextrose containing G formulations was observed at early exposure (5–15 min). An overall lower partitioning for CaHPO₄-containing formulations (both D and G) was observed (Figure 4.4A and B).

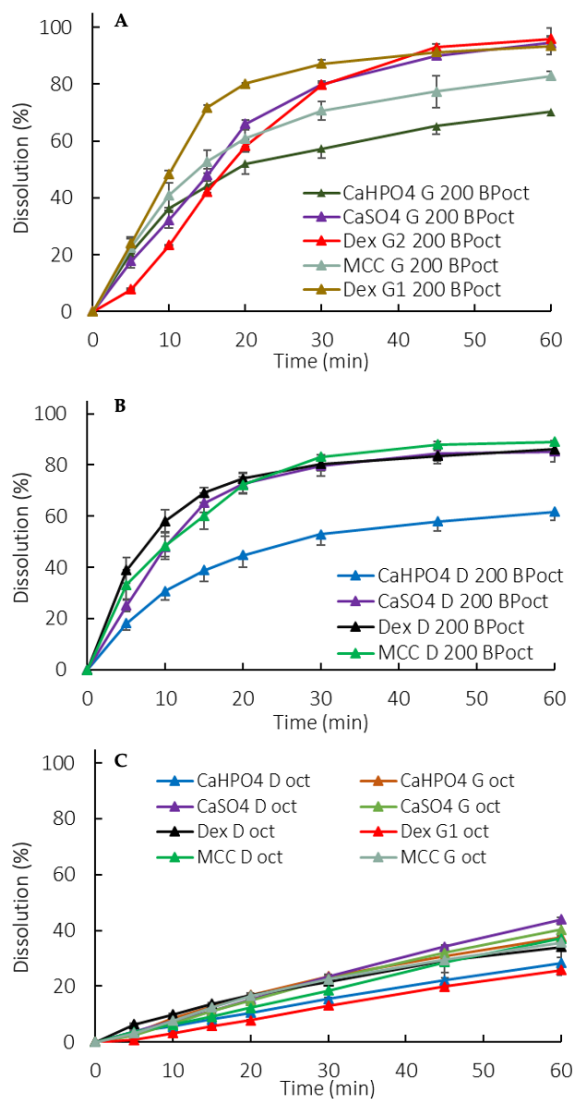


Figure 4.4. Organic phase partition profiles in a biphasic dissolution with 200 mL of aqueous media for G formulations (A) and D formulations (B) and with 900 mL of aqueous media (C). Oct: Octanol. Error bars represent the standard deviation. Ibuprofen was the active ingredient in all formulations.

Biphasic Dissolution with 900 mL of Aqueous Phase

Similarly to the monophasic dissolution, the G formulations presented a higher rate and extent of release compared to the D formulations (Figure 4.5 A–D). However, the higher release was not accompanied by an increased partitioning into the organic phase. Actually, the partitioning profiles of the organic phase were similar for all formulations (different excipients and manufacturing processes) (Figure 4.4C). Thus, in this setup, the organic phase didn't seem suitable for formulation differentiation purposes. Instead, the organic phase added a sink to the system through the removal of the dissolved drug from the aqueous phase, reducing the pH shift observed in the monophasic dissolution.

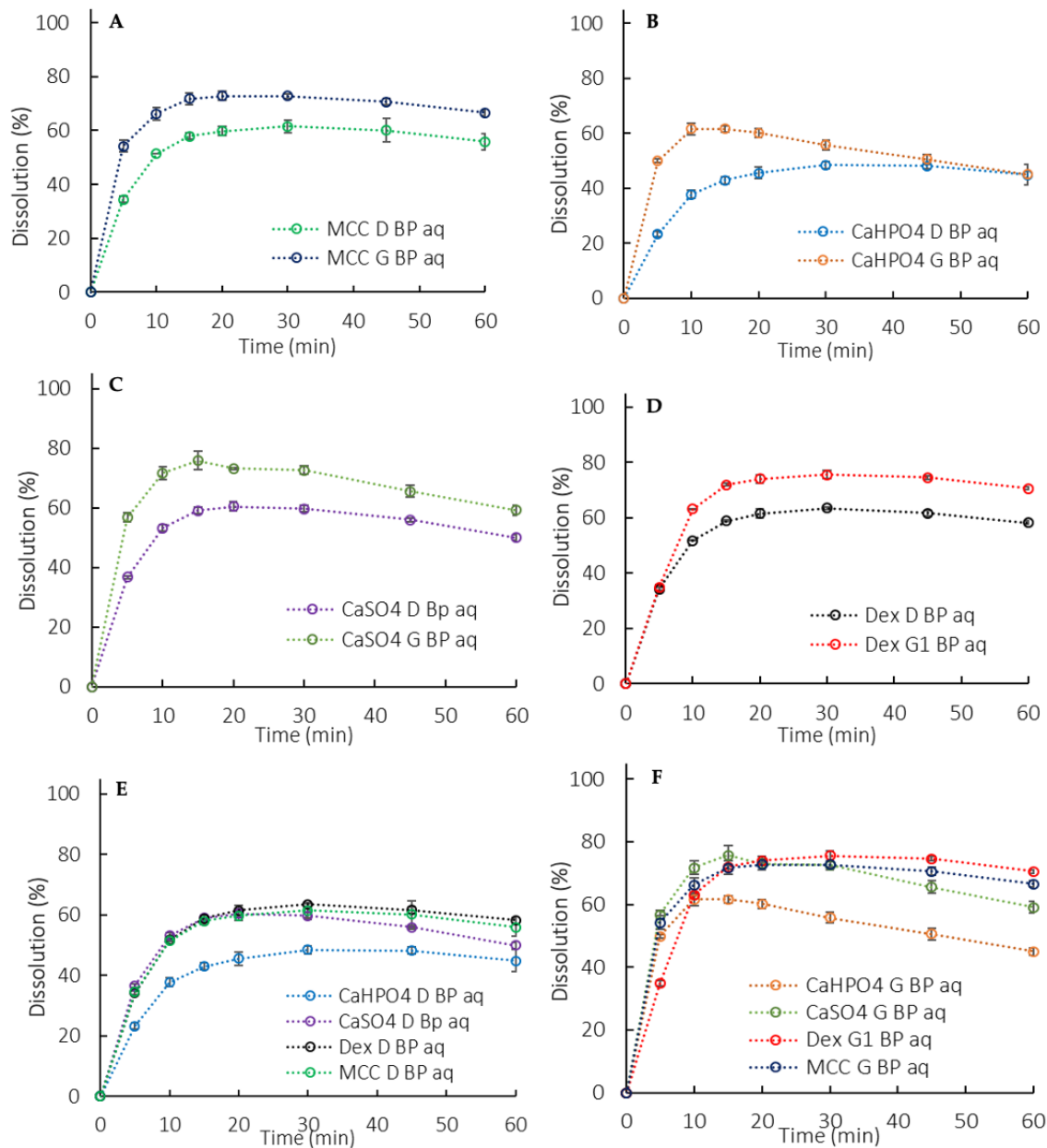


Figure 4.5. Aqueous phase dissolution profiles in a biphasic dissolution with 900 mL of aqueous media (BP aq). (A) MCC formulation, (B) CaHPO₄ formulation, (C) CaSO₄ formulation, (D) Dextrose formulation, (E) D formulations, (F) G formulations. Error bars represent the standard deviation. Ibuprofen was the active ingredient in all formulations.

4.4.2.3 Dissolution Medium pH Recovery

The use of an organic layer on top of the aqueous layer assisted in the medium pH maintenance by the removal the dissolved drug from the aqueous medium. In the case of an

acid, such as ibuprofen, the proton transfers to the organic phase with the drug. Hence, the pH changes that are expected when a low buffer capacity medium is used were reduced (Figure 4.6).

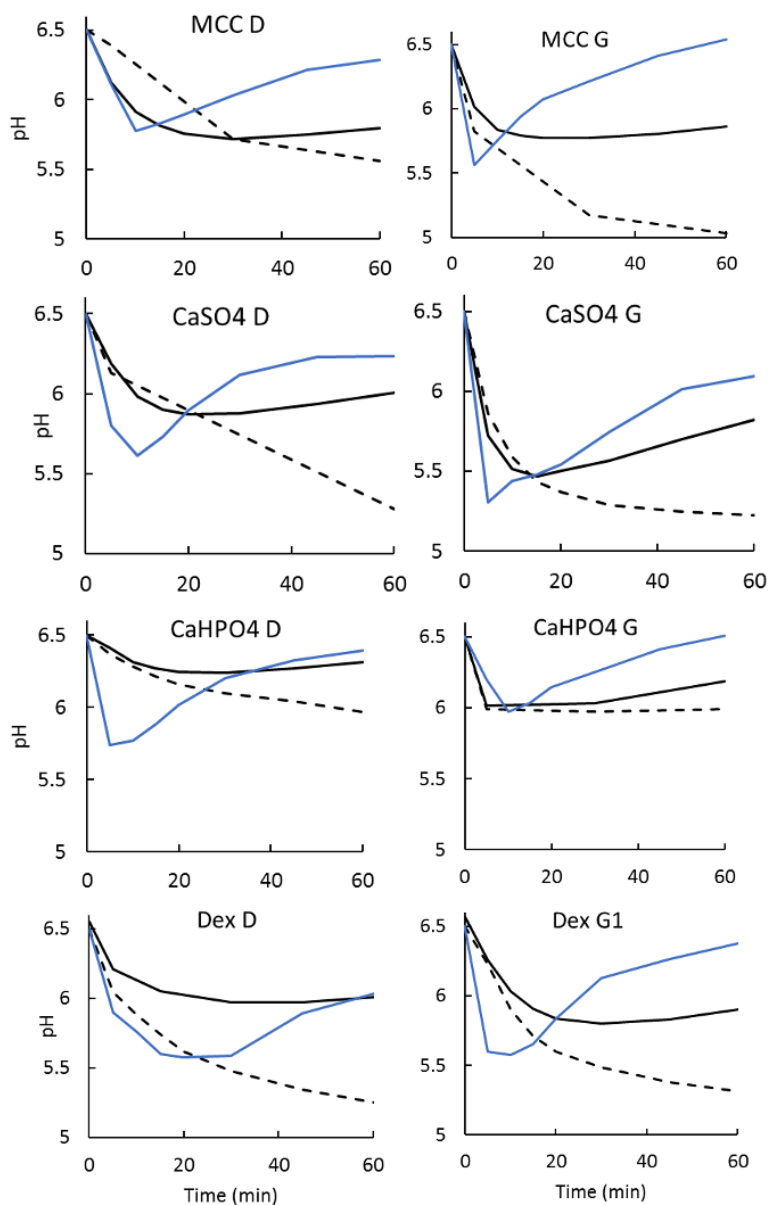


Figure 4.6. pH measurements for dissolution tests in a low buffer capacity medium. Dashed line: monophasic setup. Solid black line: biphasic setup with an aqueous layer at 900 mL. Solid blue line: biphasic setup with an aqueous layer at 200 mL.

4.4.3 Statistical Analysis

The higher percentage released for the granulated tablets compared to the direct compressed ones (Figure 4.3A–D) was statistically relevant, as the similarity between G and D using the 90% CI was rejected for all the formulations in the 5 mM phosphate buffer.

The consistent lower release for formulations containing calcium phosphate was statistically relevant, as shown in Table 4.2, pointing to a possible API-excipient interaction. The suspected microclimate effect for formulations containing dextrose was also statistically significant (Table 4.2).

Table 4.2. Statistical evaluation for the 90% confidence interval between different formulation compositions

D formulations						
	Dextrose		MCC		CaSO₄	
	Org 200	Aq 900	Org 200	Aq 900	Org 200	Aq 900
Dextrose	NA	NA	Fail	Pass	Pass	Pass
MCC	Fail	Pass	NA	NA	Fail	Pass
CaHPO ₄	Fail	Fail	Fail	Fail	Fail	Fail
G formulations						
	CaHPO₄		MCC		CaSO₄	
	Org 200	Aq 900	Org 200	Aq 900	Org 200	Aq 900
Dex G1	Pass	Fail	Pass	Fail	Pass	Fail
Dex G2	Fail	-	Fail	-	Fail	-
MCC	Pass	Pass	NA	NA	Fail	Pass
CaHPO ₄	NA	NA	Pass	Pass	Pass	Pass

Org 200: organic phase at 200 mL of aqueous phase; Aq 900: aqueous phase of biphasic test at 900 mL.

4.5 Discussion

A discriminating dissolution test is a method that can detect variations in the manufacturing process as well critical API or dosage from attributes that may have an impact on the *in vivo* performance of the final drug product. Physiologically based

exploratory dissolution methods used in early product development often follow a generic approach (17). Thus, in the absence of a link to *in vivo* drug product performance, the degree of discriminating power is often unknown. In such cases, risk assessments and prior knowledge, as well as modeling and simulation, may be helpful to guide the necessary adjustments to increase the method's sensitivity towards certain critical API attributes, manufacturing method, and/or formulation composition (17,131).

In contrast, the pharmacopoeial experimental conditions applied in a QC setting aim at the whole amount of drug being released from the dosage form. For such purposes, a high buffer concentration (50 mM) and capacity are used. Such conditions prevent pH shifts caused by the API dissolution that could hinder or increase the dissolution, resulting in a biased data interpretation caused by the dissolution method rather than due to poor drug product performance. In the compendial conditions used in this study, a similar release was obtained for the different ibuprofen formulations, achieving the “expected release” in a QC manner (Figure 4.2). Nevertheless, it showed a poor discriminatory power in identifying the possible effect of critical API attributes and manufacturing methods on drug dissolution.

Accordingly, Cristofolletti and Dressman have demonstrated that in the case of ionizable compounds, the pH at the solid–liquid interface is as a key parameter in predicting the dissolution rate. The authors showed that the *in vitro* dissolution of ibuprofen (weak acid) in phosphate buffer is a function of the pH in the diffusion layer, which is, in turn, affected by the properties of both the drug and the medium (56). The reported pH at the surface of the dissolving drug (ibuprofen) in a physiologically relevant bicarbonate buffer can be achieved by reducing the phosphate buffer concentration to 5 mM. Hence, using the appropriate

buffer concentration for *in vitro* experiments would likely increase the physiological relevance of this important biopharmaceutics performance test method (56).

A rapid *in vitro* dissolution rate cannot be translated to the *in vivo* dissolution rate of ibuprofen. An *in vivo* study, in which the gastrointestinal (GI) drug dissolution and systemic absorption of ibuprofen was evaluated, demonstrated that the drug could still be found in the GI tract fluids even after 7 h of aspiration, pointing out that BCS II drugs may undergo a slower dissolution in the GI tract due to their low water solubility (35,134,135). This slow dissolution rate was linked to the very low buffer capacity of luminal fluids.

This observation reflects what is going on in the drug particle diffusion layer. In highly concentrated buffer systems, the drug particle is surrounded by an abundance of the buffer's conjugate base species. This leads to a ready neutralization in the diffusion layer around the particle, that is, the H^+ ions formed on the dissolving drug surface are readily consumed by a buffer species. This causes the pH in the diffusion layer to be similar to the bulk solution pH, yielding a higher dissolution (56,81). However, in a less concentrated buffer (as in the human GI tract) the neutralization is slower, which is an important physiological aspect that should be taken into account in the drug development process. Selecting the right buffer system is, therefore, of primary importance (35), since the *in vitro* buffer system largely affects the surface pH of the drug particle, which in turn affects its dissolution (84,148).

As previously highlighted, it has been reported that a phosphate buffer pH of 6.5 at 5 mM matches ibuprofen dissolution in physiologically relevant bicarbonate buffer (83). The observed slower dissolution in 5 mM phosphate buffer (900 mL) compared to a USP-strength buffer (50 mM) (Figure 4.2 vs. Figure 4.3) is in line with the aforementioned *in vivo* findings (35). Thus, using a low buffer capacity is an alternative approach to bring

physiologically relevant components into the early stage exploratory dissolution tests. Clinically relevant specifications were not required at the time that ibuprofen was introduced to the market (late 60s/early 70s) and the developed dissolution method was a suitable test at the time.

On the other hand, as ibuprofen dissolves, the medium pH tends to decrease due to the acidic characteristics of the API (Figure 4.6). The pH drop observed in a low buffer capacity medium is unlikely to occur in the intestinal lumen due to neutralization mechanisms in the gut as well as the concurrent drug absorption (149). Attempts to maintain the pH by titrating the medium with NaOH have been made (56), however it can be experimentally difficult and impractical. In cases of dissolution methods based on other buffers systems, such as bicarbonate buffer, the medium pH can be regulated by sparging the medium (28).

Combining the low buffer capacity medium with an absorptive phase adds another aspect of the *in vivo* gastrointestinal environment, that is, drug absorption as it dissolves in the intraluminal fluids (and in the case of an acid, such as ibuprofen, the proton transfers to the organic phase with the drug). Thus, the organic phase serves as an additional sink for the pH recovery (Figure 4.6).

Ibuprofen dissolution in 5 mM phosphate buffer was characterized through the D formulations, since they presented an API-controlled dissolution (Figures 4.3E and 4.5E), as described by Uebbing (120). Considering that ibuprofen is a class II drug, a reduction in particle size may increase the drug dissolution, which could be the reason for the statistically relevant higher release observed in the G formulations (Figures 4.3A–D and 4.5A–D). The overall slower dissolution rate in 5 mM buffer enabled the characterization of a critical API attribute that affects *in vitro* dissolution.

The manufacturing method can also impact the dosage form performance. During a wet granulation process, the API and excipients come in close contact in such a way that the excipients can influence the API dissolution. After the tablet disintegrates, the drug dissolution depends also on the granules disintegration/deaggregation (1,150). As a result, a microclimate can be created around the granulate particle, which was seen in the dextrose formulations. Since dextrose is acidic (151), the pH around the dissolving drug particle could be lower than the bulk pH, impacting the API dissolution. This effect was observed primarily at early exposure, when the granules were being deaggregated (Table 4.2). A lower dissolution was observed during the first time points in both the 50 mM and 5 mM phosphate buffer, and the drug partitioning into the organic phase was also affected (Figures 4.2, 4.3D, 4.4D, and 4.5D). Early exposure is important and should be further explored in future studies. This is in accordance with Valizadeh et. al., who described the impact of the microclimate on the dissolution of solid dispersions of indomethacin with different excipients, such as PEG 6000, Myrj 52, Lactose, Sorbitol, Dextrin, and Eudragit1 E100 (150).

Overall, formulations containing calcium phosphate presented a statistically relevant lower release, regardless of the manufacturing process used. In this case, another excipient-API interaction might have occurred. Even though it behaves neutrally (pH 7.4), the surface of CaHPO_4 is alkaline (151). Since ibuprofen is a weak acid, drug particles could have adsorbed onto the CaHPO_4 particles due to their alkaline surface, resulting in the observed lower dissolution. It has been reported that various ions and molecules can be adsorbed onto the CaHPO_4 surface. Furthermore, ibuprofen adsorption onto calcium phosphate beads for bone substitutes in targeted drug delivery applications has been described (152).

Incompatibilities between CaHPO_4 and other acidic drugs, such as indomethacin and aspirin, have also been reported (151,153).

In the exploratory method used in the study, the sensitivity in discriminating dosage forms was seen in the octanol phase when applying 200 mL of the aqueous phase, whereas at 900 mL the differences were more pronounced in the aqueous phase. The low surface area to volume ratio at 900 mL and the hydrodynamics in the vessel with a paddle dissolution apparatus resulted in slower drug partitioning (drug removal) compared to at 200 mL (Figures 4.4A-B vs. 4.4C) (154,155). Consequently, in 900 mL partitioning is the rate-limiting step for the overall process of mass transfer between the solid, the aqueous and the octanol phases.

On the other hand, using a lower aqueous phase volume at the same rotational speed resulted in the aqueous phase experiencing a higher overall magnitude of shear stress. This might be a contributing factor to the 200 mL tending to be less discriminatory in comparing G vs. D formulations when compared on the basis of total dissolution (i.e., aqueous + organic).

Mudie et. al. described the drug transport phenomenon associated with the biphasic dissolution method, assuming first-order absorption kinetics (141). The *in vitro* partitioning rate coefficient (k_p) represents the drug partitioning rate into the organic phase. The physiological relevance of this is that the *in vitro* k_p approximates the *in vivo* absorption rate coefficient (k_a), as shown in Equation 4-1.

$$Kp = \left(\frac{Al}{va} PI \right)_{in vitro} = Ka = \left(\frac{A}{V} Peff \right)_{in vivo} \quad (\text{Equation 4-1})$$

PI: drug interfacial permeation rate across the aqueous and organic diffusion layers; AI: surface area of the aqueous–organic interface; Va: total volume of aqueous medium; Peff: permeation rate *in vivo*; A/V: area to volume ratio *in vivo*.

When k_a and PI are known (or can be estimated), AI/Va can be adjusted so that k_p and k_a become similar or equal when possible. For ibuprofen, the theoretical PI reported in the literature is 23.6×10^{-4} cm/s (141). Hence, the calculated k_p s for 900 mL (k_{p900}) and 200 mL (k_{p200}) are 2.1×10^{-4} s⁻¹ and 9.35×10^{-4} s⁻¹, respectively. In a recent human *in vivo* study, Hofmann and coworkers determined the real intestinal k_a for ibuprofen of 2.6×10^{-3} s⁻¹ (79). Thus, the 900 mL underestimates the k_a by a factor of 12.3, whereas the 200 mL underestimates it only by a factor of 2.8, making it much closer to the *in vivo* scenario. Not only that, but the pH recovery was much faster and better controlled in the 200 mL than in the 900 mL (Figure 4.6).

An effective drug development process aligns the best formulation strategies to obtain a suitable pharmaceutical dosage form with an adequate biopharmaceutical performance (156). Based on this study, for an ibuprofen IR dosage form, a granulation process would be chosen over direct compression and excipients such as dextrose and CaHPO₄ would be avoided.

The discriminatory power of biphasic dissolution is well acknowledged in the literature. Deng et. al. (2017) observed a high discriminatory power in the organic phase for minor formulation changes using racecadotril as a BCS II model drug (135). Three granule formulations of the lipophilic drug were prepared with equivalent compositions but using different manufacturing processes. The compendial tests lacked discrimination, whereas a remarkable discrimination between the granule formulations was observed in the octanol

phase of the biphasic dissolution system. The test was performed in a USP II apparatus with 400 mL of phosphate buffer (50mM, pH 6.8) as the aqueous layer and 100 mL of 1-octanol as the upper organic phase. The authors also correlated the organic phase profiles to *in vivo* pharmacokinetics data, which resulted in a good *in vitro-in vivo* correlation (IVIVC), and they concluded that “the release profiles from the organic phase could serve as an indicator for *in vivo* drug absorption” (135).

Several studies utilizing the biphasic system have reported its ability to obtain good IVIVCs and to be more discriminative than compendial methods (134,135,138,143,157–162). Vangani et al. investigated the formulation changes of several compounds using the flow through apparatus (USP IV) coupled with the USP paddle apparatus in a biphasic system. An excellent rank order correlation was obtained between the *in vitro* release and the *in vivo* absorption of the drugs (158). Al Durdunji et al. used a similar dissolution test method, i.e., USP IV coupled with USP II in a biphasic dissolution medium for a BCS II compound (Deferasirox). Similarly, the authors were able to differentiate between the formulations and establish an IVIVC (163).

Gao and coworkers reported the evaluation of several poorly soluble drugs also using a biphasic system combining USP apparatus IV (flow cell) with USP apparatus II (138–140,158,159,162). Using the biphasic dissolution-partition test method, an excellent IVIVC and IVIVR (*in vitro-in vivo* relationship) were obtained for a number of poorly soluble drugs, such as fenofibrate, celecoxib, and ritonavir. The authors also reported little relevance of the QC dissolution test results to pharmacokinetic observations in pre-clinical and clinical studies of the prototype formulations (162). This showcases how biphasic dissolution has the

potential to reflect the *in vivo* environment, linking the *in vitro* performance to clinical relevance.

4.6 Conclusions

In light of the up-to-date mechanistic understanding of *in vivo* dissolution, there is a current need to rethink how product specifications and performance can be linked through physiologically relevant parameters. This study revisited the rationale of using lower buffer capacity media to increase the physiological relevance of *in vitro* testing. This system was demonstrated to have a superior discriminatory power regarding the manufacturing method and excipient effects. The use of an absorptive phase added a sink to the low buffer capacity media, which decreased pH shifts while the test was performed.

Hence, biphasic dissolution systems using low buffer capacity dissolution media have the potential to be used as early stage discriminatory methods to investigate the impact of excipient effects and the manufacturing method on the *in vitro* drug release with improved physiological relevance.

4.7 Limitations of the Study

The authors recognize that whether the difference between formulations identified by the biphasic dissolution systems with a low buffering capacity translates to *in vivo* difference has yet to be assessed through IVIVC. However, the biphasic dissolution tests were clearly able to discriminate between the excipient and manufacturing methods under physiologically relevant conditions which may translate into different *in vivo* behavior, highlighting the importance of such method for drug performance verification.

**SECTION TWO: PHYSIOLOGICALLY RELEVANT *IN VITRO* TESTING:
BUFFER CAPACITY AND BIPHASIC DISSOLUTION TESTING**

CHAPTER FIVE

A BCS-based biowaiver approach using biphasic dissolution test

5.1 Introduction

The understanding of the physicochemical properties of drugs through the establishment of the Biopharmaceutics Classification system (BCS) (11) made a risk based *in vitro* assessment of bioequivalence for oral drug products possible. Biowaivers based on BCS class can be used to establish therapeutic equivalence. A biowaiver means that *in vivo* bioavailability and/or bioequivalence (BA/BE) studies may be waived based on *in vitro* dissolution testing (14,164). Here dissolution tests are used as a surrogate to determine if two pharmaceutical equivalent products are interchangeable/ bioequivalent instead of conducting expensive and time-consuming *in vivo* BE studies. Thus, the BCS-based biowaiver approach is intended to reduce *in vivo* BE studies and emphasises the importance of *in vitro* testing for predicting *in vivo* performance.

In 2000, the Food and Drug Administration (FDA) in the United States drafted the guidance document for industry “*Waiver of In Vivo Bioavailability and Bioequivalence Studies for Immediate-Release Solid Oral Dosage Forms Based on a Biopharmaceutics Classification System*”(165). The European Medicines Agency (EMA) and the World Health Organization (WHO) followed the FDA approach, implementing their own guidance documents in 2002 and 2006, respectively (166,167). These first guidance documents differed from each other, for example, while the FDA and EMA only allowed BCS-based biowaiver for BCS class I drugs, the WHO guidance also included BCS class III and BCS class IIA (168). However, the BCS class IIA was removed in the WHO guidance in 2015. Also, the different guidance documents define “highly soluble” differently by using either the highest available strength (i.e. highest dose available) or the highest single therapeutic dose (i.e. the administered dose, e.g. 2 tablets of 50mg, hence the therapeutic dose would be 100mg) (19). This can cause the same drug product

to be classified differently in different regions of the world, harmonization was recommended (19).

Even though they have been updated (165,169,170), in attempt to harmonize these various guidelines, the ICH published the “*ICH M9 Guideline on Biopharmaceutics Classification System-based Biowaivers*” for consultation in 2018 which has recently reached step 5 (implementation) of the ICH process (171). This guideline is applicable to immediate release solid oral dosage forms or suspensions containing BCS classes I and III drugs, i.e. drug products with highly soluble drug substance(s).

In 2012, Löbenberg et. al. (172) conducted a study to examine the *in vitro* performance of three widely used drug products marketed in different countries of the Americas, being them metronidazole, zidovudine and amoxicillin (all classified as BCS class I and WHO list of essential medicines). The generic products in the Americas were compared to the US comparator pharmaceutical product (CPP) and to each other to determine if they met *in vitro* bioequivalence criteria. The authors hypothesized that the different drug products would meet the criteria due to their BCS class. However, none of the tested metronidazole products were *in vitro* equivalent to the CPP or to other manufacturers. Thus, since the *in vitro* studies did not signal that bioequivalence criteria would be met, further clinical studies would be needed in order to confirm their interchangeability.

We hypothesized that whereas *in vitro* bioequivalence was not achieved in compendial methods (172), the partitioning profile to the organic phase in the biphasic system might signal *in vitro* equivalence among the drug products and CPP.

The objective of the present study was to replicate the aforementioned study using biphasic dissolution testing and metronidazole as the model drug. This is an innovative and more

physiologically relevant *in vitro* approach that has been developed to more effectively predict *in vivo* performance of drug products (27,133–135,138,141,143,158,159,163). The system is consisted of immiscible aqueous and organic phases in which the drug dissolves in the aqueous layer and partitions into the organic phase, thus maintaining sink conditions. The organic layer mimics the gastrointestinal (GI) membrane and the dissolution-partition process between the two phases resembles the *in vivo* drug dissolution and absorption process (27). Hence, the approach taken in this manuscript was to have scientific insight and mechanistic understanding rather than strict regulatory application.

5.2 Materials

Metronidazole (USP grade) was obtained from Medisca (Quebec, Canada). Commercial Metronidazole tablets were purchased: Flagyl 250 mg (Pfizer USA Inc, lot # C071094), Flagyl 500 mg (Sanofi Aventis Mexico Inc, lot # 888575), Flagenase 500 mg (Laboratorios Liomont, S.A. Mexico Inc, lot # 7009), Colpofilin 500 mg (Laboratorio Lazar Argentina Inc) and Metral 500 mg (Laboratorio Pablo Cassara Inc, lot # 77). Acetonitrile HPLC grade and 1-octanol 99% were purchased from Acros Organics (New Jersey, USA). The buffer solutions were prepared with purified water (Elgastat Maxima UF and an Elgastat Option 3B water purifier by ELGA Laboratories Ltd. Mississauga, ON, Canada).

The excipient composition of each drug product as listed in the package insert is as follows: Flagyl-USP (Cellulose, Fd&C Blue, Hydroxypropyl Cellulose, Hypromellose, PEG, Stearic Acid, Titanium Dioxide); Colpofilin (Lactose, MCC, DOSSNa, Povidone, Crosscarmellose Sodium, Talcum, Mg-Stearate); Flagyl-Mex, Flagenase and Colpofilin (Excipients).

5.3 Methods

5.3.1 Analytical Quantitation

The metronidazole content in the tablets was evaluated using liquid chromatograph Shimadzu LC-10AS (Tokyo, Japan) and Shimadzu SPD-M10AVP Diode Array Detector (Tokyo, Japan) UV-Vis detection at 254 nm using a LiChrospher® 60 RP-Select B 5µm (25 cmx 4,0mm) column (Merck - Darmstadt, Germany). The mobile phase consisted of acetonitrile and water (34:66), filtered and degassed. The flow rate used was 1.0 mL/min, the injection volume was 20 µL and the retention time was 6.83 min. A standard solution was prepared from an accurately weighed quantity of the reference chemical substance, using the methanol as diluent to obtain a solution of 1.00 mg/mL.

5.3.2 Disintegration test

The test was performed according to USP general chapter <701> (112). Disintegration time was measured in a disintegration tester (Eureka, Germany) using 900 mL of phosphate buffer pH 6.8 at 37 ± 2 °C as medium. Six tablets of each drug product were tested.

5.3.3 Dissolution tests

All dissolution tests were performed in triplicate using a USP apparatus II (ERWEKA, GmbH), 75 rpm rotation speed at 37 °C. All buffer media were filtered by vacuum and degassed in an ultrasonic bath.

The commercial metronidazole tablets were tested in compendial Simulated Intestinal Fluid (SIF) (50mM phosphate buffer at pH 6.8, 900 mL) without enzyme, as well as in physiological buffer capacity (5mM phosphate buffer at pH 6.8, 900 mL). The tablets were also

tested in a biphasic dissolution system in which the aqueous layer was composed of 200 mL of 5 mM phosphate buffer (pH 6.8) with 100 mL of n-octanol on top. A mini-paddle (kindly donated by Sotax AG) was mounted on the regular compendial paddle to obtain sufficient hydrodynamics in both phases. The volume of 200 mL was chosen in an attempt to better approximate that of the intestinal fluids (77 +/- 15 mL) while still being experimentally feasible (145).

For both compendial and biphasic dissolution tests, samples from the aqueous phase and the organic phase were collected at specific time points (5, 10, 15, 20, 30, 45, 60 min).

5.3.4 Data analysis

The Microsoft Excel™ add-in DDSolver was used to compare the dissolution profiles by f_2 statistics. The f_2 factor measures the closeness between two profiles and, according to the FDA criteria, f_2 values between 50-100 indicate similarity between two dissolution profiles.

The API has to be released from the formulation and dissolve in the aqueous medium in order to partition to the organic phase. Hence, formulation disintegration is of crucial importance for drug release, especially for immediate release tablets. With this in mind, the amount partitioned into the organic phase of the CPP was correlated to the amount partitioned of each one of the generic products after disintegration (see Table 5.2). The CPP (Flagyl-USP) had a 5.32 minutes disintegration time, hence the percent partitioned from 10 minutes on (next data point after 5.32 minutes) was considered. The same rationale was used for the other products: Flagyl-Mex: 20 minutes on; Colpofilin: 5 minutes on; Flagenase and Metral: 15 minutes on. Table 5.1 shows the amount partitioned for each drug product used in the correlation. The correlation was done by linear regression.

Table 5.1. Amount partitioned (Q%) into the organic phase for each drug product after disintegration time

Time point (min)	Flagyl-USP	Flagyl-Mex	Colpofilin	Flagenase	Metral
10	0.50	1.07	2.20	4.74	3.33
15	1.41	1.78	5.54	7.62	5.81
20	2.54	3.56	7.78	11.47	12.10
30	6.07	7.87	9.77	13.30	17.09
45	10.28		18.11	24.19	27.08

5.4 Results

5.4.1 Assay and disintegration tests

The assay and disintegration results are presented in Table 5.2. All tested drug products fell within the acceptance criteria of 90.0% – 110.0% of drug content (118). Among all the tested products, Flagyl-Mexico took the longest to disintegrate (around 18 minutes), followed by Metral, Flagenase, Flagyl-USP and finally Colpofilin.

Table 5.2. Drug content and disintegration time of different commercially available metronidazole immediate release tablets

Product	Assay		Disintegration	
	%	SD	Time (min)	SD
Flagyl-USP	104.88	7.61	5.32	0.43
Flagyl-Mexico	103.98	31.48	18.27	0.58
Flagenase	104.68	7.56	10.16	0.07
Colpofilin	102.02	62.61	0.60	0.22
Metral	98.02	29.89	13.32	0.78

5.4.2 Dissolution tests and data analysis

The dissolution results in the monophasic setup (900 mL) are presented in Figure 5.1, including both SIF and low buffer capacity phosphate buffer (5mM). All tested products presented a similar performance in both buffer systems, as seen in Figure 5.1 and evidenced by

the f_2 test results (Flagyl-USP: 49- border line; Flagyl-Mexico: 67; Flagenase: 54, Colpofilin: 82 and Metral: 82). Since metronidazole is a highly soluble drug its dissolution in a medium with lower buffer capacity is not expected to differ much from a highly concentrated buffer using a volume of 900 mL (Figure 5.1) (27).

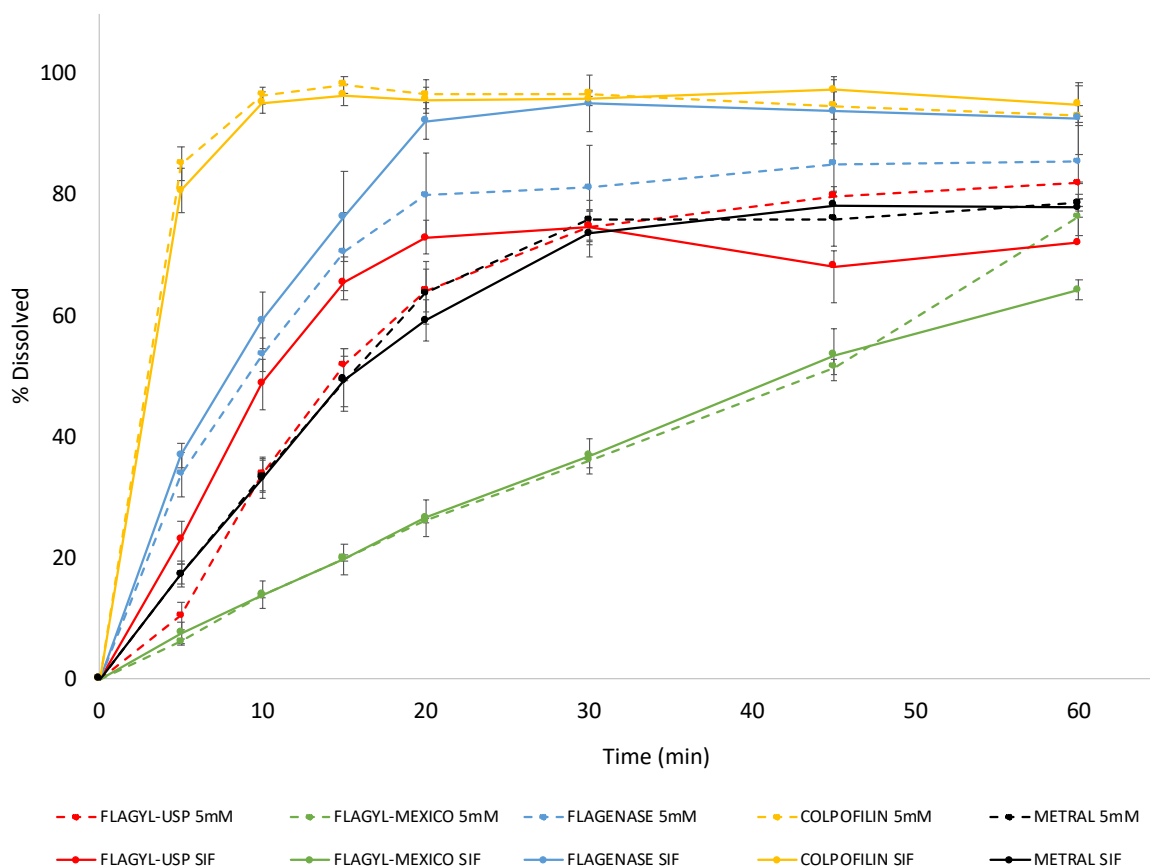


Figure 5.1. Dissolution profiles of metronidazole formulations in SIF (solid lines) and low buffer capacity phosphate buffer (5mM – dashed lines).

Except for Flagenase and Flagyl-USP, the dissolution rate followed the disintegration time, i.e., the fastest the disintegration, the higher was the release rate, even though all formulations were immediate release dosage forms. Table 5.3 presents the statistical analysis results for the comparison between the different metronidazole products. As observed by Löbenberg *et. al.* (172), none of the tested metronidazole products were *in vitro* equivalent to the

CPP or to other manufacturers in both monophasic dissolution experiments, with one exception of Flagyl-USP (CPP) and Metral in low buffer capacity ($f_2=73$).

Table 5.3. In-vitro performance comparison between Metronidazole products

USP SIF (f_2 test)				
	Flagyl-USP	Flagyl-Mexico	Flagenase	Colpofilin
Flagyl-USP	NA	-	-	-
Flagyl-Mexico	24	NA	-	-
Flagenase	37	16	NA	-
Colpofilin	23	10	32	NA
Metral	48	30	32	19
Low buffer capacity (f_2 test)				
Flagyl-USP	NA	-	-	-
Flagyl-Mexico	28	NA	-	-
Flagenase	41	20	NA	-
Colpofilin	18	09	27	NA
Metral	73	29	41	18

SIF: Simulated Intestinal Fluid; NA: Not applicable; -: repeated.

The biphasic dissolution test results are presented in Figure 5.2. A similar pattern to the monophasic dissolution test was observed in the aqueous phase, i.e., Colpofilin having the highest dissolution rate, followed by Flagenase, Flagyl-USP and Metral in the middle and finally, Flagyl-Mexico. Similarly, the partition profile followed the dissolution trend in aqueous phase and Metral was an exception.

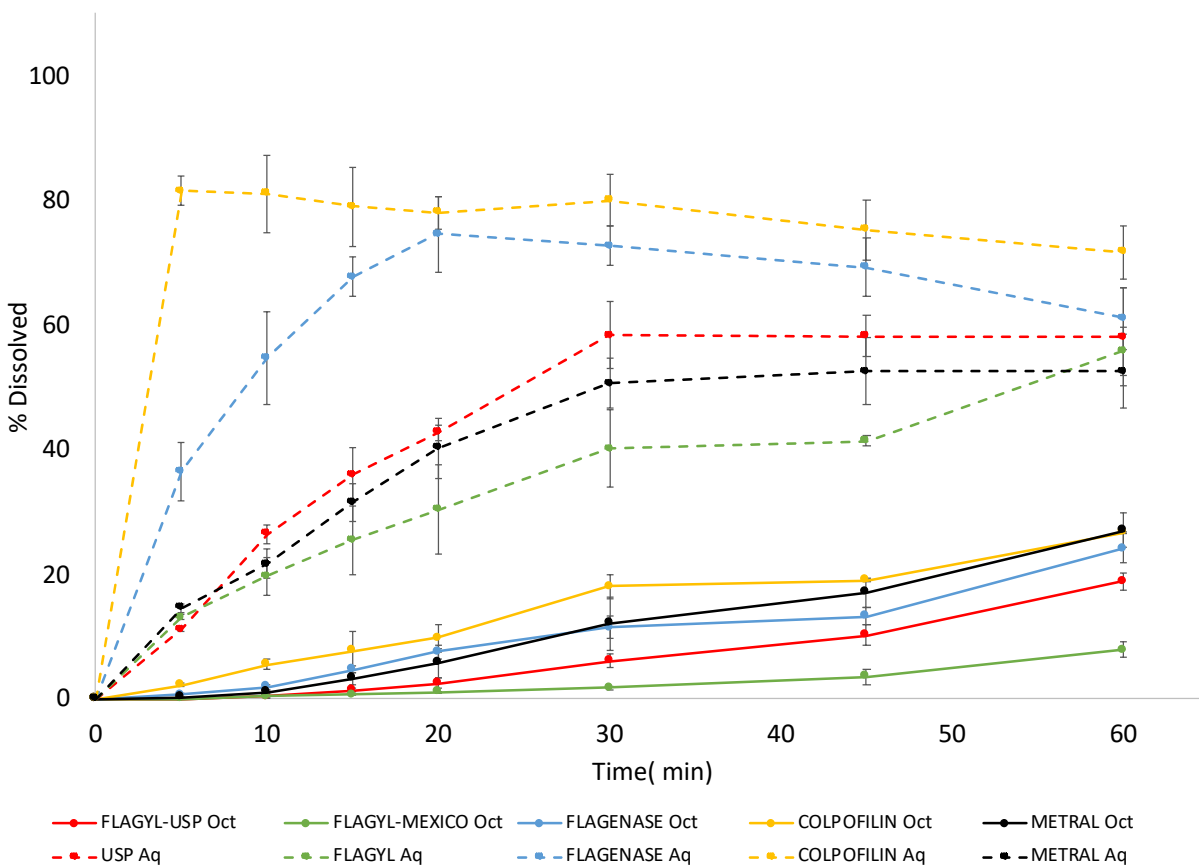


Figure 5.2. Biphasic dissolution profiles of metronidazole formulations in the aqueous (Aq – dashed lines) and organic phases (Oct - solid lines).

Figure 5.3 shows the correlation of drug partitioned to the organic phase between the CPP and the generic drug products after disintegration. Notably, a good correlation was obtained in all cases (R^2 values higher than 0.95), which could be an indicative of similar *in vivo* performance. Further clinical studies would be needed to confirm their interchangeability.

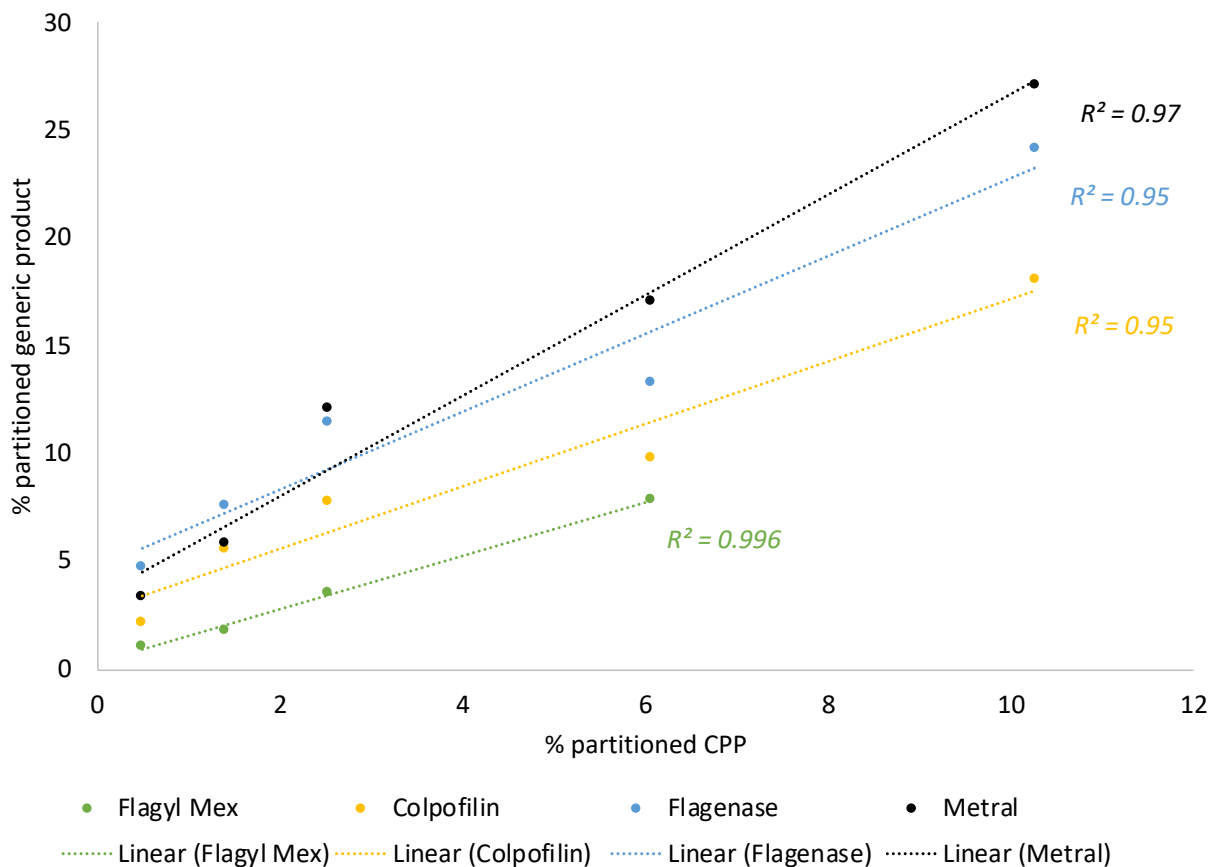


Figure 5.3. Correlation between the comparator pharmaceutical product (CPP) and generic products of the amount partitioned to the organic phase. Only data after full tablet disintegration were used.

5.5 Discussion

Metronidazole is classified as a BCS class I drug (high solubility and high permeability). According to the current regulatory guidances, an API is highly soluble if its *Dose/Solubility ratio* is 250 mL or less at the pH range of 1.0–6.8 (or 7.5) at 37°C. For all definitions of *Dose* (highest dose strength, highest dose recommended by WHO and the highest single dose administered) the ratio is below the 250 mL limit. The reported solubility of metronidazole in different aqueous

medium at 37°C is 30.6 mg/mL (pH 1.0); 14.1 mg/mL (pH 3.0); 12.8 mg/mL (pH 5.0); 11.6 mg/mL (pH 7.0). The reported log *P* value for metronidazole is 0.75 for *n*-octanol/water (173).

When applying the BCS based biowaiver approach to immediate release dosage forms containing highly soluble drugs, the *in vitro* dissolution tests are to be conducted in at least three pharmacopeial buffer systems of pH 1.2 (SGF), pH 4.5 (acetate buffer) and pH 6.8 (SIF). In all the aforementioned media, Löbenberg *et. al.* (172) reported that none of the tested metronidazole products were *in vitro* equivalent to the CPP.

According to the USP definition, an IR drug product is “a term for a dosage form in which no deliberate effort has been made to modify the drug substance release rate”. This definition lacks any mechanistic information, as pointed out by Uebbing *et. al.* (120). A mechanistic understanding of the drug release is of primary importance because in cases in which the drug release is controlled by the API properties, disintegration is the most important dosage form attribute. Hence, it could be used as a surrogate test for dissolution testing where the IR formulation (containing a highly soluble drug) presents a fast disintegration, such as Colpofilin (0.60 minutes). As shown in Table 5.2 and Figure 5.1, the disintegration time and release rate were quite different between the formulations. In this case, even though they were all identified/labelled as IR products, dissolution seems to be controlled by the formulation rather than the API itself, except for Colpofilin (120).

The similar performance of Colpofilin in both compendial buffer and 5mM phosphate buffer indicates that buffer capacity does not seem to affect the API’s dissolution, since metronidazole is freely soluble in aqueous medium. Additionally, the other products’ performance were also not affected by buffer capacity. These results clearly indicate that aqueous dissolution is overdiscriminating.

With this in mind, using a more physiologically relevant dissolution system could be an additional *in vitro* testing before rendering the formulations *in vitro* inequivalent based solely on the compendial methods. In this study we used a biphasic dissolution system as a physiological relevant test, applying 5mM phosphate buffer (low buffer capacity) as the aqueous phase and n-octanol as the organic phase (27). The free drug concentration in the aqueous phase dictates the amount of drug that partitions to the organic phase, which acts as an “absorptive compartment”, mimicking the *in vivo* dissolution-absorption process in the intestinal lumen (27,35,141). Since the drug is freely soluble in aqueous medium, the lipid dissolution could be the rate determining step for *in vivo* performance.

The stomach residence time value for half emptying under fasted state reported in the literature ranges from 11.5 – 17 minutes (174). The longest disintegration time among the products was 18 minutes for Flagyl-Mexico. This means that, for all products, most likely the disintegration will take place within the stomach and metronidazole will be released out of the formulation and dissolved by the time it gets to the intestines. Hence, in the intestinal lumen, absorption would be the most important aspect.

In the biphasic test, the organic phase profiles relate to the *in vivo* absorption. In the same way that only solubilized drug can be absorbed *in vivo*, only dissolved API molecules can partition to the organic phase. Disintegration and dissolution may occur simultaneously with the release of a drug from the dosage form. The drug particles that are on the surface of the tablet can be readily dissolved, however disintegration is of utmost importance to release the “bulk drug” that is in the tablet. Accordingly, as seen in Figure 5.2, even though drug dissolution and further partitioning can take place before complete disintegration of the dosage form (disintegration times presented in Table 5.2), the dissolution rate seems to follow disintegration

time. Hence, it's most meaningful to correlate the partition profiles after each formulation after disintegration time (Figure 5.3). When taking this mechanistic approach great correlation was obtained between the CPP and the other formulations, which could be an indicator of similar *in vivo* performance. However, in order to assess the therapeutic equivalence among these products, an *in vivo* BE study should be conducted to corroborate the *in vitro* similarity in terms of partitioning profile.

There are many studies reporting the application of biphasic dissolution for poorly soluble drugs in various dosage forms (e.g., capsule, tablet, solution, suspension, etc.) with higher discriminating capacity, as well as better *in vitro in vivo* relationships (135). However, there are not many studies using this model applied to BCS class I drugs, due to the good solubility of such drugs and the assumption that pharmacopeial methods might be sufficient to discriminate between biopharmaceutical properties. Hence, the results of the present study broaden the application of biphasic dissolution demonstrating that it is a plausible alternative for highly soluble drugs.

In the case of poorly soluble drugs, the organic phase acts as an additional sink as the drug is removed from the aqueous phase, preventing aqueous saturation. Since metronidazole is a highly soluble drug, the drug removal from the aqueous phase had low to neglectable effects on the aqueous dissolution. It was then further evidenced that for most products the formulation was the factor of pivotal importance in controlling the dissolution rate. After disintegration, metronidazole quickly dissolves, and permeability is then the most crucial aspect. A mechanistic formulation evaluation and understanding of the dissolution controlling factors together with the understanding of the *in vivo* events highlights that biphasic systems might be also used for highly soluble drugs. Our results delineate the potential *in vitro* equivalence between different

manufacturers and CPP, indicating that the compendial methods utilized previously might have been overdiscriminating and can be further optimized.

5.6 Conclusion

None of the tested metronidazole products demonstrated *in vitro* equivalence to the CPP in the monophasic dissolution methods, i.e. SIF and physiological buffer capacity. Hence, the monophasic aqueous systems seem to be overdiscriminating. On the other hand, the correlation of the organic phase of the biphasic system did present a similar partitioning pattern for all the different drug products and CPP, which could indicate *in vitro* equivalence. The application of biphasic dissolution to highly soluble drug and formulations has beneficial attributes to estimate the *in vitro* behavior and performance. Further *in vitro* studies with other products are needed to confirm and refine these findings. An *in vivo* BE study is needed to assess the therapeutic equivalence among these products.

**SECTION THREE: PHYSIOLOGICALLY RELEVANT *IN VITRO*
TESTING: BICARBONATE BUFFER**

CHAPTER SIX

Simulated, biorelevant, clinically relevant or physiologically relevant dissolution
media: The hidden role of bicarbonate buffer

A version of this chapter is published in:

Eur J Pharm Biopharm. 2019;142:8–19. <https://doi.org/10.1016/j.ejpb.2019.06.006>
Reprinted from reference (28).

6.1 Introduction

In-vitro dissolution testing of pharmaceutical formulations has been used as a quality control test for many years. During the drug development process, it is often used to optimize formulations according to a desired release profile (68). Additionally, dissolution experiments can also be used with a prognostic purpose of the dosage form's performance in the gastrointestinal tract, known as *in vivo* predictive dissolution testing (13). Drug dissolution in the gastrointestinal (GI) fluids is a prerequisite for drug absorption and subsequent pharmacokinetic and pharmacodynamic response. An *in vitro* dissolution test reflects the *in vivo* performance of a drug product when the *in vitro* dissolution rate is corresponding to the *in vivo* dissolution rate. This is the basis to establish an *in vitro-in vivo* relationship/ correlation (IVIVR/ IVIVC) (20).

At early drug product development, *in vivo* predictive dissolution testing can be used for guidance to rational selection of candidate formulations that best fit the desired *in vivo* dissolution characteristics. Such an approach can later serve as a surrogate for clinical studies by requesting a biowaiver.

In order to achieve this, *in vitro* dissolution test methods of oral products should be reflective of the *in vivo* situation, establishing conditions that closely reflect the physiological environment of the gastrointestinal tract (GIT) (20). Nevertheless, this is rather difficult to achieve in practice due to the inherent physiological complexity and variability of the GIT. Gastrointestinal transit time, unsteady hydrodynamics and changing fluid contents are a complex physiological system to attempt to experimentally mimic (20,43,53,175–177). It is important for the predictive *in vitro* dissolution test media to closely match the pH, buffer species and concentration, bile salts/ lipid content, electrolytes and enzymes of the GI fluids (20).

At present, the most widely applied dissolution media are phosphate-based buffers and, in some cases, the result of dissolution tests performed in such media have demonstrated reasonable/acceptable IVIVCs (19,20,68). This is true for dosage forms in which the choice of dissolution buffer is essential in achieving IVIVC. However, the concentration of phosphates in human GI luminal fluids is insignificant, which makes the use of such phosphate-containing media poorly representative of the *in vivo* environment. Thus, these media might fail to reflect *in vivo* characteristics including ionic strength, buffer capacity, fluid volume and viscosity (41,52,176,178).

The gastrointestinal lumen has long been shown to be buffered by bicarbonate, which maintains the pH gradient along the GIT (20,69). Hence, much interest has been drawn to the development of suitable biorelevant *in vitro* dissolution media (20,42,179–182). This review focuses on the use of bicarbonate-based buffer in clinically relevant dissolution tests and as a potentially biorelevant media as well as key determinants to *in vivo* predictive dissolution testing.

6.2 Intestinal lumen environment - What are we trying to reproduce in a dissolution vessel?

6.2.1 Physiology overview of gastrointestinal secretions

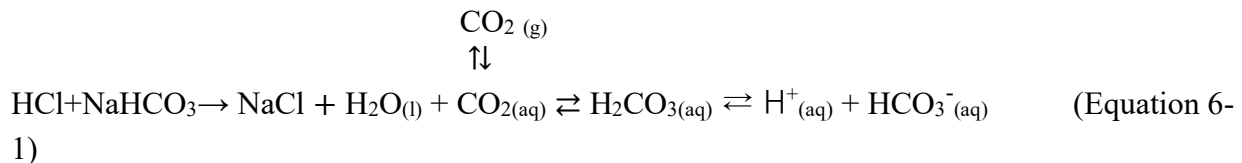
There are different anatomical components that make up the gastrointestinal tract with different functions, such as production of mucus and secretion of digestive enzymes. Complex glands and organs (salivary glands, pancreas and liver) assist with the digestion and emulsification of food. Secretions coming from the pancreas and the liver are emptied into the upper part of the small intestine (duodenum) through the pancreatic and hepatic duct. These two ducts join together immediately before the duodenum.

The pancreatic secretions are composed of various digestive enzymes and a large volume of sodium bicarbonate solution. The bicarbonate ions are important in neutralizing the acidity of

the content coming from the stomach (132). On the other hand, the hepatic secretions are primarily composed of bile. When secreted into the duodenum, the bile plays an important role in fat digestion and absorption. Similarly to the pancreatic secretion, a sodium bicarbonate solution is added to the initial bile (132). This solution is secreted by epithelial cells in the ducts. This additional quantity of bicarbonate ions supplement the bicarbonate ions in the pancreatic secretion for neutralizing the acid that empties into the duodenum from the stomach.

In addition to the hepatic and pancreatic secretion, the intestinal fluids are also composed of secretions by the epithelial cells of the duodenum. These secretions are an alkaline mucus to protect the duodenal wall from the highly acidic gastric juices. This mucus contains a large excess of bicarbonate ions, which adds to the bicarbonate ions from pancreatic and hepatic secretion in neutralizing the hydrochloric acid entering the duodenum from the stomach (69,149,183–188).

Consequently, the net result in the duodenum follows the neutralization equation (Equation 6-1):



The carbonic acid promptly dissociates into carbon dioxide (CO₂) and water. The CO₂ can be absorbed into the systemic circulation and released through the respiratory system. In this way, a neutral solution of sodium chloride is left in the duodenum and the acid contents from the stomach become neutralized (149). This results in an overall effect where the luminal fluids of the small intestine are predominantly buffered by bicarbonate (72).

6.3 Buffer species - *In vitro* considerations

Even though the human small intestinal fluid is buffered primarily by bicarbonate buffer, this buffer has been rarely used in dissolution studies (148,189). This is mainly due to the challenges involved with carrying dissolutions tests using bicarbonate buffer.

6.3.1 Peculiarities of the bicarbonate buffer

In a bicarbonate buffer system, carbon dioxide (CO_2) has an inherent tendency to leave the aqueous solution (Equation 6-1) and, consequently, the medium has to be continuously purged with CO_2 gas at a constant rate. This maintains the concentration of $\text{CO}_{2(\text{aq})}$ in solution in an equilibrium with HCO_3^- , avoiding a pH increase (148,189). Additionally, both the escape and sparging of $\text{CO}_{2(\text{g})}$ in the medium can potentially form bubbles in the medium, which can affect the dissolution process by building bubbles on the surface of the dosage form or powder particles and altering surface tension.

Different models of physiological bicarbonate buffers have been proposed, such as Hanks and Krebs buffers, varying in composition (Table 6.1) (19). Hanks buffer composition is similar to the proximal small intestine with respect to electrolyte composition. Nevertheless, modifications to the Hanks balanced salt solution (pH 7.4) is needed to match the physiological pH of 6.8 and to adjust its low buffer capacity (1 mmol/L/ ΔpH) to the human jejunal fluids (3.2mmol/L/ ΔpH) (72,190). This can be accomplished by following the Henderson–Hasselbalch equation (Equation 6-2), i.e. adjusting the concentration of the acid (H_2CO_3) and its conjugate base (HCO_3^-) by purging $\text{CO}_{2(\text{g})}$ into the medium, which shifts the equilibrium (Equation 6-1) towards formation of $\text{H}_2\text{CO}_{3(\text{aq})}$, thus decreasing the pH of the buffer system (71,72,76,190,191).

Table 6.1. Composition of different bicarbonate buffer systems

Buffer component (mM)	Hanks buffer (19)	Krebs buffer (190)
KH₂PO₄	1.18	0.441
Na₂HPO₄·2H₂O	-	0.337
NaHCO₃	24.97	4.17
NaCl	118.07	136.99
KCl	4.69	5.37
CaCl₂	2.52	1.26
MgSO₄·7H₂O	1.18	0.812
Ionic Strength	0.161	0.155
Buffer Capacity (mmol/L/ΔpH)	3.7	1.0

$$pH = pKa + \log \frac{[HCO_3^-]}{pCO_2} \quad (\text{Equation 6-2})$$

Another example of bicarbonate-based buffer is the Krebs buffer, which has a different salt composition and buffer capacity than Hanks buffer (Table 6.1) (190). Krebs buffer resembles the distal small intestine and approximates the ionic composition and buffer capacity of human small intestinal luminal fluids (19,71). Nevertheless, the system still has to be stabilized in terms of maintaining the pH and CO_{2(aq)}. Purging CO_{2(g)} into the medium is one way of accomplishing it. Garbacz et. al. investigated the pH shift caused by CO₂ loss in different bicarbonate buffer systems, including Krebs buffer. The authors reported that the evaporated CO₂ can be partly substituted by sparging the bicarbonate buffer with gas mixtures, such as 5% (vol/vol) CO₂ and N₂ (191). When appropriate partial pressure of CO₂ is applied, such purging maintains the bicarbonate equilibrium in the buffer solution, which, in turn, prevents the upward shift in pH. Another way to maintain the desired pH level is to prevent the CO₂ escape. Fadda et. al. (2009)

applied strategies such as the addition of liquid paraffin layer above the dissolution media and a completely sealed set-up made of a nylon lid that is impermeable to gas. The authors also investigated the approach of sparging the medium with $\text{CO}_{2(g)}$ and concluded that all the three approaches were successful.

However, the buffering capacity of the bicarbonate buffer in bulk is higher for a sparged system compared to a sealed or paraffin-covered system. This is because in a sparged system, mass transfer of CO_2 between gas and aqueous phases is allowed. As a result, for weak acid dissolution, accumulation of dissolved CO_2 is limited, and, for weak base dissolution, net loss of dissolved CO_2 is limited. Consequently, a sparged system is more capable of resisting changes in bulk pH resulting from drug dissolution, as was observed by Fadda et al (2009) (71). Taking into account that CO_2 is absorbed through intestinal mucosa, it would be recommended to use a sparged system for cases where significant shifts in bulk pH due to drug dissolution is expected. However, as explained later in the chapter, this enhanced buffer capacity in bulk does not typically translate into enhanced buffer capacity in the boundary diffusion layer.

Bicarbonate buffer can also be made by dissolving the appropriate amount of sodium carbonate and/or sodium bicarbonate in deionized water and sparging it with CO_2 (Equation 6-1) or a mixture of compressed air and carbon dioxide while monitoring the pH with a pH meter and CO_2 concentration with a suitable electrode (76,148). The ionic strength of the solution can be adjusted by adding sodium salts, such as NaCl and Na_2SO_4 (192).

Furthermore, bicarbonate buffer can also be made *in situ* by continuously sparging $\text{CO}_{2(g)}$ or a mixture of 100% dry compressed air and 100% CO_2 at a fixed partial pressure into a 0.9%(w/v) NaCl solution. The pH of the solution can be adjusted by addition of NaOH (74,84).

The sparging of gas into the medium can vary in many aspects, such as the rate in which the gas is purged, the position of the tube in the vessel and the gas(es) mixture composition sparged into the system (20,71,76,84,148,191,193). Different sparging rates have been reported and there is no consensus on what rate should be used for greatest efficiency. Simply purging the medium to equilibrate to the desired pH before commencing the experiment is not enough, due to the $\text{CO}_{2(\text{aq})}$ decrease (evaporation) the bicarbonate buffer is only stable if continuous sparging occurs. For instance, Boni et. al. (2007) used a sparging rate of 400mL/min until the desired pH was achieved and during the dissolution experiment the flow rate was adjusted appropriately for the surface area, buffer concentration, pH and volume of media (68).

McNamara et. al. (2003) used a sparging rate of 300ml/min to equilibrate the medium to the desired pH and a rate range of 250 - 500 ml/min during the dissolution itself (74). The authors also investigated different partial pressures of $\text{CO}_{2(\text{g})}$ in the sparging gas set at 5, 10, 15, and 20% CO_2 %atm which correspond to 6.4, 12.9, 19.3, and 25.8 mM HCO_3^- , respectively. Thus, higher partial pressures of $\text{CO}_{2(\text{g})}$ in the sparging gas lead to higher concentrations of $\text{CO}_{2(\text{aq})}$ and bicarbonate in the dissolution medium. It was observed that increasing bicarbonate concentration at pH 6.8 increased the dissolution rate and flux for a low-solubility acidic drug (indomethacin), whereas for a low-solubility basic drug (dipyridamole) no increase in dissolution was observed at pH 6.8. Nevertheless, at pH 5 dipyridamole dissolution was significantly impacted by increasing the concentration of $\text{CO}_{2(\text{g})}$ in the sparging gas.

Al-Gousous et.al. (2018) evaluated different setups in which the tube sparging the gas in the medium was either at a 5 cm depth in the medium or moved up so that its opening would only touch the surface of the liquid (148). The authors reported that buffer capacity enhancement is not only dependent upon the tube position, but also on sparging rate as well as

the titration rate. Accordingly, Boni et. al. (2007) conducted the dissolution experiments supplying the carbon dioxide above the liquid level to avoid noticeable bubble formation in the medium caused by inflow and evaporation of gas (68). Both authors reported that finer bubbles can be produced by using a gas inlet frit instead of direct sparging.

6.3.1.1 Automated systems

Different automated systems to monitor the pH and regulate bicarbonate buffers have been proposed in the literature. Garbacz et. al. (2013) developed a device called “pHysio-stat[®]” to adjust the bicarbonate buffer pH in a dissolution vessel (191). The system is composed of a pH electrode, a gas diffuser, a digital microcontroller and a valve system, as illustrated in Figure 6.1. In this setup the pH electrode and the gas diffuser remain at a 35mm depth in the medium during the dissolution test. Throughout the experiment, the potential of the electrode is measured and the CO₂ introduced into the dissolution medium via the diffuser is regulated accordingly.

The authors concluded that the pHysio-stat[®] system was able to monitor and adjust the pH in bicarbonate buffers, thus being a useful tool for routine applications in dissolution tests based on bicarbonate buffers.

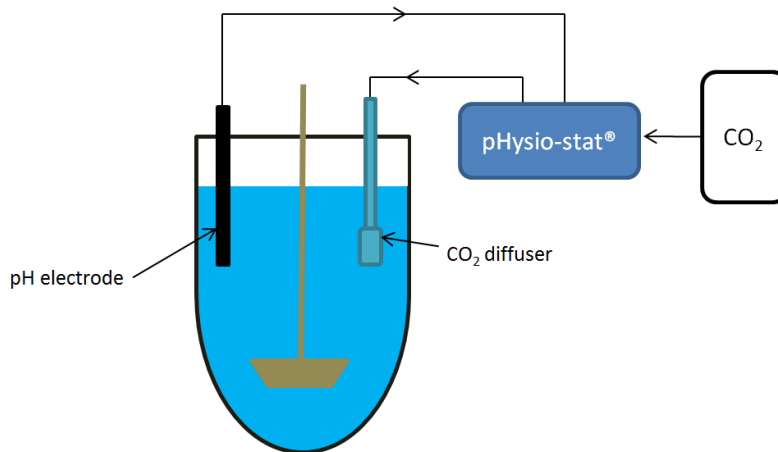


Figure 6.1. Schematic illustration of the pHysio-stat device. (Adapted from Garbacz et. al., 2013)

The pHysio-stat® system (Garbacz et al., 2013) was further developed to a system (pHysio-grad®) that enabled dynamic adjustment and media pH change by purging CO₂ or an inert gas into the dissolution medium (76). The system composition was similar to the previous one, but with an additional proportional valve, used for dosing N₂ or CO₂, as illustrated in Figure 6.2. In this setup the pH electrode and the gas diffuser remain at a 45mm depth in the medium during the dissolution test.

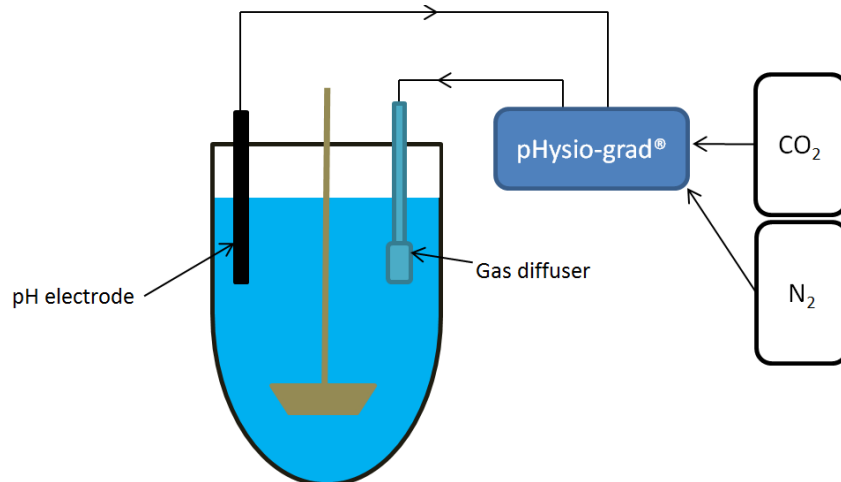


Figure 6.2. Schematic illustration of the pHysio-grad® device. (Adapted from Garbacz et. al., 2014)

Merchant et al. described a system (Auto pH System™) that is also triggered by a pH feedback from the dissolution vessel (Figure 6.3) (75,193). The pH probe is connected to a source of CO₂ gas (pH decreasing gas) and helium (pH increasing gas), and the system is controlled by a control unit. The sparged Helium displaces the dissolved CO₂ which will then result on an increased pH by shifting the equilibrium towards CO_{2(g)} (Equation 6-1). Changes in the bicarbonate buffer pH will cause the appropriate gas to be supplied into the dissolution vessel, providing a dynamic pH adjustment during testing.

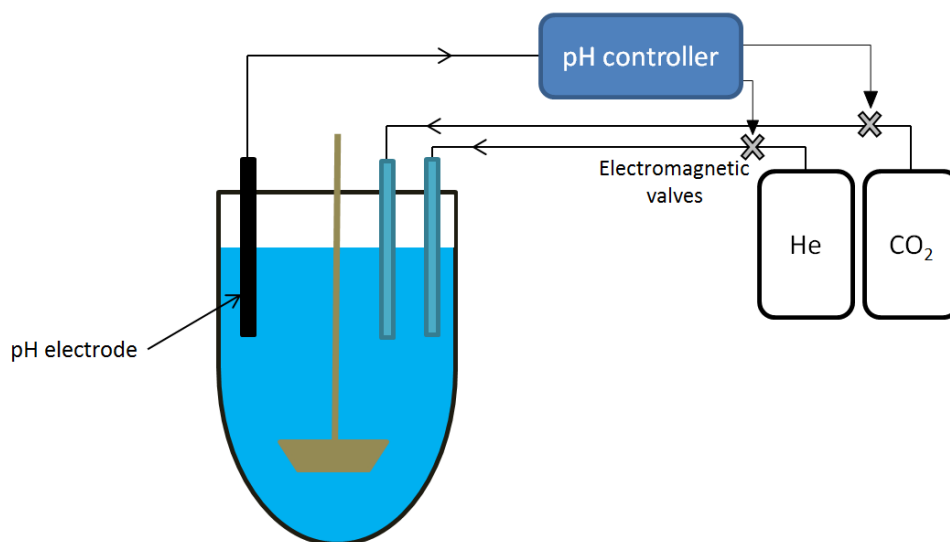


Figure 6.3. Schematic illustration of the Auto pH System™ device. (Adapted from Goyanes et. al., 2015).

6.3.1.2 Understanding the Bicarbonate–CO₂ equilibrium

The solubility of CO₂ in water depends on its partial pressure and medium temperature with Henry's constant being ~24 mM/atm at 37°C (84). When dissolved in water CO₂ reversibly hydrates to form carbonic acid (H₂CO₃) which deprotonates forming bicarbonate ion as follows in Equation 6-3:

Hydration



Dehydration

The intrinsic pKa for H₂CO₃ dissociation ($pK_a^{\text{H}_2\text{CO}_3}$) is ~3.5 (194). However, during potentiometric titration, the equilibrium that is established between H₂CO₃ and CO₂ results in the apparent pKa ($pK_a^{\text{potentiometric}}$) being equal to 6.35 since:

$$K_a^{\text{potentiometric}} = \frac{[\text{HCO}_3^-][\text{H}^+]}{([\text{CO}_2] + [\text{H}_2\text{CO}_3])} = \frac{[\text{HCO}_3^-][\text{H}^+]}{[\text{H}_2\text{CO}_3]} \times \frac{[\text{H}_2\text{CO}_3]}{([\text{CO}_2] + [\text{H}_2\text{CO}_3])} = K_a^{\text{H}_2\text{CO}_3} \times \frac{1}{1 + k_d/k_h} \quad (\text{Equation 6-4})$$

Where k_d is the rate constant for the dehydration reaction and k_h is the rate constant for the hydration reaction (Equation 6-4). This $pK_a^{\text{potentiometric}}$ will govern the pH of a bulk solution of the bicarbonate buffer, since the mixing processes limit the rate of neutralization processes in bulk, which in turn are slower than the interconversion between carbon dioxide and carbonic acid. Therefore, it would appear in bulk as if carbon dioxide were the conjugate acid with carbonic acid being merely a short-lived intermediate. However, in the diffusion layer at the solid-liquid interface of a tablet, the situation is different (85).

In contrast to the extremely rapid proton transfer reactions, the CO₂-H₂CO₃ interconversion is not faster than diffusional processes (under normal hydrodynamic conditions) to a degree that would allow it to reach equilibrium in this layer. As a result, the relative contribution of carbonic acid and carbon dioxide to the buffer flux and so to the buffering action in the boundary layer will not be reflective of the equilibrium situation present in bulk. Consequently, in the boundary layer, the buffering action of bicarbonate will not correspond to that of a pKa 6.35 buffer, and the buffer will act there as if its pKa were lower than that. In other

words, the apparent effective pKa governing the buffering action of bicarbonate in the diffusion layer will not be the potentiometrically determined value of 6.35 but lower. According to a recently published model this apparent effective pKa (at 37°C and ionic strength of 0.15 M) would be equal to (85):

$$\text{pKa} = 3.3 + \log \left(1 + \frac{D_{CO_2}}{D_{H_2CO_3}} \times \frac{k_d}{k_h + \left(\frac{2D_{CO_2}}{h^2} \right)} \right) \quad (\text{Equation 6-5})$$

Where D_{CO_2} and $D_{H_2CO_3}$ are the diffusion coefficients of carbon dioxide and carbonic acid respectively and h is the boundary layer thickness (Equation 6-5).

Accordingly, its buffering capacity in the diffusion layer against the dissolving drug/excipient will be lower, since the effective pKa values is shifted away from the intestinal pH range of 6-7.5. This means that while the buffer capacity of bicarbonate is enhanced in bulk, it is weakened in the diffusion layer, which further adds to the complexity of the system. This is of particular significance for enteric coated dosage forms. For, based on the equation above, in a 30 micron-thick diffusion layer, the apparent effective pKa of bicarbonate would be around 4.6, which will make it difficult for proximal intestinal bicarbonate molarities to maintain the surface of a dissolving enteric polymer at pH values exceeding 5.5. Therefore, obtaining prompt release from enteric-coated dosage forms at bicarbonate molarities present in the proximal small intestine is difficult as shown by data in literature (78).

6.3.2 Phosphate buffer

Dissolution testing for quality control (QC) as a performance test is used to ensure lot-to-lot consistency and batch compliance to the defined specifications for the drug product (26,195,196). For this purpose, compendial dissolution media (simple media), such as phosphate buffers, are used in most cases (195,197). Nevertheless, considering the concept of biorelevant

media, phosphate buffers are not physiologically relevant, since the buffering system in the human intestines is bicarbonate-based. Even though, many phosphate-based dissolution media have been proposed to be biorelevant, such as the USP simulated intestinal fluids (SIFs) (Table 6.2), which were developed to simulate the GI pH and bile salts concentration (discussed in the next section) (20,42,177,179–182). According to the FDA, simulated intestinal fluid with pancreatin (USP-SIF) and without enzyme (SIF-blank) better reflect the physiologic conditions of the small intestine than other buffers (19,51).

The different pharmacopoeias recommend different salts to make buffers. In the USP, SIF-blank and phosphate buffer pH 6.8 are made with the potassium salt, whereas the International Pharmacopoeia (Ph. Int.) recommends the use of sodium salt (195,198). Nevertheless, osmolality, ionic strength, and buffer capacity are similar between these buffers, as shown by Stippler et al. (198). The author considered the media to be interchangeable for the dissolution test of the tested drugs (ibuprofen, metronidazole, and indomethacin - immediate-release solid oral dosage form). Substitution of the two cations (Na^+ and K^+) is only necessary in cases where solubility is known to be affected by the cation. This is also true for surfactant containing media. Ropers et al. reported that surfactant precipitation can occur as a result of counter-ion interaction. The use of sodium buffer instead of a potassium buffer seems to avoid this issue (19,199). The counterion effect on surfactants has a lot to do with their micelle formation in aqueous media. The counterions of surfactant polar head groups have strong influence on their packing and thermodynamic behavior because each particular type of counterion possess different binding energy to the respective head group, causing structural changes which affect the surfactant self-assembly process.

The disintegration of HPMC (Hydroxypropyl methylcellulose) capsules containing carrageenan as gelling agent is also affected by the type of cation used in the buffer. Potassium ions are a gelling promoter for carrageenan, which causes delay in capsule opening along with increased variability of dissolution. Hence, the presence of potassium cations in the dissolution media hinders drug release from such capsules (200–203). This issue can be easily overcome by avoiding the use of potassium salt in the test media.

Almukainzi et.al. reported the impact on disintegration time of cellulose-based hard shell capsules based on the use of sodium and potassium buffers and SIF. Different salts caused different disintegration times of capsules, which will likely cause differences in dissolution behavior (114).

Furthermore, adding enzymes to the dissolution medium can be technically challenging when testing gelatin capsules. Gelatin can cross-link in the presence of aldehydes, or in high temperature and humidity conditions. Cross-linking is characterized by a covalent bonding between gelatin chains which creates water insoluble pellicles/ membranes on the internal or external surface of the capsule shell during the dissolution test. Cross-linking can cause slower drug release from the gelatin capsule or even no release altogether. Several examples of cross-linking are reported in the literature (125,204–206).

6.3.2.1 Biorelevant media

As mentioned before, biorelevant media were made to simulate the GI tract pH and components likely to be found in the human GI tract, such as bile salts and lecithin. Osmolality, pH and surface tension are adapted to physiological values (207). Food can have an impact on a drug's *in vivo* dissolution and further absorption. In the fed state the physiological environment

of the GIT differs in many ways, such as prolonged gastric emptying time, increased stomach pH, increased bile secretion into the small intestine, and increased hepatic blood flow, which can affect drug metabolism. In order to obtain meaningful *in vitro* dissolution results, the media used should reflect the *in vivo* dissolution environment and account for such factors and changes (208).

In 1998, Dressman et. al. proposed the first generation of biorelevant media known as fasted state simulated intestinal fluid and fed state simulated intestinal fluid (FaSSIF and FeSSIF, respectively) (Table 6.2). The dissolution tests performed using such media aimed to be an *in vitro* method that would serve as a surrogate for *in vivo* release (29,195). Later on FaSSIF and FeSSIF were updated and are now described as FaSSIF-V2 and FeSSIF-V2 (19,209)(Table 6.2). FaSSIF-V2 contains a reduced amount of lecithin (195,210) and FeSSIF-V2 contains two additional digestion components: glyceryl monooleate and sodium oleate.

Biorelevant media has been used both in solubility tests and dissolution experiments (19). Several studies have reported successful *in vitro/in vivo* correlations (IVIVC) using biorelevant media for poorly soluble drugs. Biorelevant media seems to be able to mimic the *in vivo* dissolution more effectively compared to other media (24,54,211,212). On the other hand, the purity of the surfactants present in biorelevant media highly impact the solubility and dissolution of certain drugs (213,214). Other factors such as the preparation methods can also impact the dissolution testing results. Kloefer et al. investigated different media preparation methods and observed that standard preparation methods resulted in reproducible dissolution profiles. However, the different methods yielded differences in the micelle sizes which may impact the dissolution behavior of other drugs (215). The current composition of biorelevant media falls deficient in some aspects, such as the fact that only taurocholic acid is present as the only bile

salt, when, in fact, it represents only 20% of the *in vivo* bile salt content. Moreover, lysolecithin, a naturally occurring phospholipid in the small intestine, is also not included in both FaSSIF and FeSSIF (52). Hence, due to their analytical properties, price, and variability in composition biorelevant media are not currently used as routine quality control media (19). In addition, such media may not be accepted by regulatory agencies based on the fact that a full release may not be achieved, even though it seems to be physiologically relevant. In such cases, addition of surfactant is needed to meet the requirements, causing the method to be no longer physiologically relevant.

Bicarbonate-containing biorelevant media for poorly soluble drugs is also technically challenging due to the foaming encountered when sparging the medium as a consequence of the surfactants present.

Table 6.2. Composition of Simulated Intestinal Fluids

Buffer component	USP PB	USP SIF	IntPh 3 PB	FaSSIF	FaSSIF V2	FeSSIF	FeSSIF V2
KH₂PO₄	50m M	6.8 g	3.4 g	-	-	-	-
Na₂HPO₄			3.53 g	-	-	-	-
NaH₂PO₄			-	3.438 g	-	-	-
NaOH	qs ad pH 6.8	15.4m M	-	qs ad pH 6.5	34.8 mM	4.04 g	81.65 mM
Pancreatin		10 g	-				
Bile salt (taurocholate)	-	-	-	3 mM	3 mM	15 mM	10 mM
Phospholipid (lecithin)	-	-	-	0.75 mM	0.2 mM	3.75 mM	2 mM
Acetic acid	-	-	-	-	-	8.65 g	-

NaCl	-	-	-	6.186 g	68.62 mM	11.874 g	125.5 mM
Maleic acid (mM)	-	-	-	-	19.12 mM	-	55.02 mM
Glyceryl monooleate (mM)	-	-	-	-	-	-	5 mM
Sodium oleate (mM)	-	-	-	-	-	-	0.8 mM
Deionized water		qs 1L	qs L	qs L	qs L	qs L	qs L
Buffer Capacity (mmol/L/ΔpH)	29 ⁺⁺	18.4 [#]	18.6	~12	10	~72	25
Osmolarity (mOsmol/kg)	-	113	115	~270	180 \pm 10	~670	390 \pm 10
pH	6.8	6.8	6.8	6.5	6.5	5	5.8

6.4 Buffer capacity

Buffer capacity is the efficiency of a buffer system to resist changes in pH (190). It is calculated as the amount of acid or base added per unit of buffer volume per unit of pH change (molar concentration/volume/ Δ pH) (148).

Buffer capacity (β) is usually calculated according to Equation 6-6:

$$\beta = \Delta AB / \Delta \text{pH} \quad (\text{Equation 6-6})$$

where AB is the mol/l increment of the amount of acid or base added to produce a pH change of Δ pH in the buffer (190).

The more concentrated a buffer is, the higher its buffer capacity. The buffer capacity of the human intestinal fluid ranges from 2.4 to 5.6 $\mu\text{mol/mL}/\Delta\text{pH}$ and conventional buffer systems such as FaSSIF and USP SIF fail to reproduce such characteristics. FaSSIF (pH 6.5) and USP

SIF (pH 6.8) have strong buffer capacities (Table 6.2), which is, respectively, 5 and 7.7 times higher than the buffer capacity of human intestinal fluids (24,35,80).

Due to such high buffer concentration (USP SIF: 50mM and FaSSIF: 29mM) it is likely to overestimate the dissolution of BCS II weak acids, particularly drugs with pKa values less than 6.5. Therefore, in spite of the fact that biorelevant media such as USP SIF buffer and FaSSIF may reflect the small intestine fluids pH, the buffer composition and concentration also significantly impacts the dissolution behaviour of BCS II weakly acidic drugs. Moreover, the discrepancy between the buffering capacity of bicarbonate in bulk and in the boundary layer (as explained in sections 3.1 and 3.1.2) also needs to be taken into account. Hence, not only the pH but, as importantly, the buffer species and concentrations should be carefully considered when making *in vivo* predictive dissolution media, especially in the case of poorly soluble and ionizable drugs. Sheng et. al. (2008) evaluated the difference between the phosphate buffers and the gastrointestinal bicarbonates in dissolution of ketoprofen and indomethacin and observed that even with FaSSIF (lower phosphate buffer concentration of 29 mM) the dissolution of ketoprofen and indomethacin demonstrated a higher rate than in the bicarbonate, that is, *in vitro* dissolution testing with either USP SIF or FaSSIF was overestimating the true dissolution rates of both drugs *in vivo* (20). There are many other reports in the literature about differences in dissolution rate when varying the buffer capacity (192,216–218). Ashford et al. compared the *in vitro* release characteristics of tablets coated with Eudragit S in different buffers varying the buffer's capacity and composition and observed that increasing phosphate concentration also causes a dissolution rate increase (219). Hamed et. al. (2016) tested carvedilol (BCS IIb - weak base) in phosphate buffer with varying capacities and observed that lowering the buffer capacity resulted in a decrease in carvedilol solubility and dissolution rate (220).

In a high buffer capacity medium there is an abundance of the buffer conjugate base species in the diffusion layer of a dissolving drug particle. In the case of BCS class IIa drugs (weak acids), a prompt neutralization of H^+ at the solid–liquid interface occurs, preventing a pH shift in the microclimate around the dissolving particle. As a result, the pH in the diffusion layer is similar to the bulk solution pH, which can lead to higher dissolution rates (56).

When considering *in vivo* predictive dissolution media both species and capacity are equally important. As already mentioned, the human intestine is chiefly buffered by a bicarbonate buffer system. The preparation of physiologically relevant bicarbonate buffer is complex, a generally slow process, and there is the potential formation of gas bubbles at the solid–liquid interface, which can affect the dissolution of drug product/particles. Hence, the use of a non-bicarbonate based surrogate buffer that produces equivalent buffer effect on drug dissolution may be preferable (83).

Phosphate is usually the buffer of choice and it is also the buffer proposed by US FDA to be used for *in vivo* biowaivers (83,221). Since its pKa of 6.8 falls right within the pH range of the small intestine, phosphate is a suitable buffer to be considered for physiologically relevant dissolution tests. Phosphate buffer is present in both USP SIF at pH 6.8, and FaSSIF at pH 6.5 with concentrations/buffer capacities of 50 mM/29 mM/ Δ pH and 29 mM/15 mM/ Δ pH, respectively (Table 6.2) (30,83).

On the other hand, the average concentrations/buffer capacity of bicarbonate buffer in the small intestine are approximately 6–20 mM/ 2.5–8.5 mM/ Δ pH at a pH of 6.5 (34,222–224). But, as discussed before, the buffer capacity of bicarbonate buffer at the diffusion layer does not correspond to that in bulk. As a result, lower buffer capacities would be necessary for the

surrogate phosphate buffer to be equivalent to bicarbonate buffer, and an additional external pH control may be needed to maintain the bulk solution pH (83).

Krieg et al. (2015) studied several different weak acid and weak base drugs and reported that it is possible to match the dissolution rate of weak acid/base drugs in bicarbonate buffer systems to phosphate buffer (83). This is a complex interdependence of buffer pH and pKa, drug pKa and solubility, and diffusion layer thickness. For weak acid drugs, the authors observed that phosphate buffer concentrations between 1– 25 mM are more physiologically relevant and may translate the impact of bicarbonate buffer on their dissolution. This means that the dissolution rate of the drug in phosphate buffer 1-25mM matches the drug dissolution rate in a physiologically relevant bicarbonate buffer. For weak base drugs, very low phosphate buffer concentrations of <2 mM would be necessary to match bicarbonate buffer. This study concluded that, in light of their findings, the current phosphate buffer concentrations used in dissolution testing (50 mM) does not seem to accurately reflect the dissolution media and conditions of the human intestine fluids that the drug is exposed to.

Sheng et. al. (2009) also evaluated the difference between phosphate buffer and bicarbonate buffer in the dissolution of ketoprofen and indomethacin (20). The author recommended the use of phosphate buffers of 13-15 mM and 3-4 mM for ketoprofen and indomethacin, respectively, to reflect the *in vivo* dissolution of both drugs in gastrointestinal bicarbonates, with special applications to the development of buffer systems for BCS II weak acids, which might allow later on the development of *in vitro* biowaiver dissolution methodology.

6.5 Dissolution tests in phosphate buffer *versus* bicarbonate buffer

There are many cases in the literature reporting differences in the dissolution profile of various drugs and dosage forms when tested in phosphate buffer *vs.* bicarbonate buffer (20,60,71,72,74,83,190,225,226).

McNamara et. al. investigated the use of stable bicarbonate buffer to characterize the dissolution of low-solubility ionizable drugs (74). The authors reported that dissolution of indomethacin in phosphate-based buffers (SIF and FaSSIF) with controlled pH yielded higher intrinsic dissolution rates than what can be expected at the same physiologic pH (pH 6.8), overestimating what occurs *in vivo* in a bicarbonate buffer system. Though SIF and FaSSIF may mimic the intestinal physiologic pH, the buffer composition and concentrations may not be physiologic, impacting the dissolution of ionizable compounds.

Karkossa and Klein assessed the drug release from commercial immediate-release (IR) and enteric-coated (EC) aspirin tablets in media with different composition and ionic strength (192). The authors conducted a systematic study in phosphate buffer pH 6.0 and 6.8 at three different ionic strengths of 75mM, 150mM and 300mM, and in bicarbonate buffer also pH 6.0 and 6.8 at three different ionic strengths of 10mM, 85mM and 235mM. For the IR tablets, dissolution was >85% within 15 min in all cases independent of the media composition and pH, indicating very rapid dissolution. The tested EC tablets presented a highly variable drug release performance and it was affected by both media pH and buffer species. In all cases, the release profile in a bicarbonate buffer system displayed longer lag times compared to phosphate-based buffers. After the coating had dissolved, the drug release was complete (100%) in bicarbonate buffer and at least >85% in phosphate buffers. In both buffer systems, higher ionic strength resulted higher release rate. The authors remarked that changes in the drug release behavior were

not attributed to the tablet core, but to the functional coating of the EC tablets. Hence, it was concluded that the dissolution behavior of enteric coating materials strongly depends not only on the pH but also on the dissolution medium composition (buffer species and ionic strength).

The impact of the buffer system utilized to test EC dosage forms has important implications. Rudolph et al. tested the release of 5-aminosalicylic acid formulations coated with Eudragit S in phosphate-based biorelevant media to simulate biological surfactants in intestinal fluids (30,190,225). No differences in drug release of Eudragit S coated formulations were observed, even with increasing ionic strength. Even though the prediction of *in vivo* dissolution processes of poorly soluble drugs can be enhanced in such media (49,190); it does not simulate the buffer composition of the GIT, failing to represent the *in vivo* performance of a given dosage form. Liu et al. tested the dissolution of prednisolone tablets coated with various enteric polymers in both pH 6.8 phosphate and modified Hanks bicarbonate buffer (72). The authors observed rapid and comparable dissolution profiles for the various polymers in pH 6.8 phosphate buffer. In the bicarbonate-based buffer, drug release was delayed and marked differences between the various coated tablets were observed. The *in vitro* bicarbonate dissolution results demonstrated a better fit with the *in vivo* observed data. Similarly, Ibekwe et al. 2006 tested the drug release of prednisolone tablets coated with different Eudragit polymer systems in phosphate buffer and Hanks buffer (227). The authors also observed similar drug release from the polymer coated tablets in the phosphate compendial media, whereas in the physiological buffer the drug release differed and was slower for all the coated tablets compared to the compendial buffer. Chan et al. also observed significantly faster drug release rate in phosphate buffer than in Hank's solution (bicarbonate-based) for EudragitS100 coated capsules (226).

Fadda and Basit investigated the drug release profiles of commercial Eudragit S coated mesalazine tablets (Asacol MR, Mesren MR and Ipocol) in different media: phosphate and physiological bicarbonate buffers (Hanks and Krebs) (190). Similarly to the above cited studies, the drug release profiles were substantially faster in phosphate buffer compared to physiological bicarbonate buffers. The buffer salts and concentrations in the two physiological buffers resulted in different dissolution profiles for the tested products.

Therefore, there is the need to adequately choose the ionic composition of dissolution media to match as closely as possible the intestinal fluid composition. The differences encountered in the dissolution profiles in phosphate vs. carbonate buffer can have relevant pharmaceutical implications. For instance, there are many reports in the literature of non-responsiveness or even "resistance" to aspirin when enteric coated (EC) products are administered (228–231). Studies have shown a decreased bioavailability (BA) of EC aspirin both in healthy volunteers and in patients and they do not recommend the use of EC aspirin in conditions requiring rapid onset of action (228,230). Failure of enteric coated formulations is a long known problem, dating back to 1964, where EC aspirin tablets did not pass the USP disintegration test, which was used to assess its physiologic availability (232). This problem has continued to persist with many cases of inadequate BA of EC products found in the literature: Wagner et. al. 1973, Maree et. al. 2005, Cox et. al. 2006, Grosser et. al. 2013, Bhatt et. al. 2017 (229,230,233–235). A particularly striking case was the report of slow release aspirin in the elderly(236). The study measured the plasma salicylate concentrations of a group of 77 elderly and no salicylate was detected in 26 of 77 patients. At the time, poor compliance was considered as one of the possible explanations for the undetected salicylate plasma level. However, the test was repeated in a subgroup to ensure compliance. In three of the six patients, absence of

detectable plasma salicylate was confirmed. Hence, there is strong evidence that this is a clinical drug product performance issue that has not yet been resolved.

The study conducted by Karkossa and Klein revealed that aspirin release from marketed EC products was strongly affected by the buffer species (192). The lag times before onset of drug release in phosphate-based buffers ranged from 10 to 20 min, whereas in bicarbonate-based buffers with the same pH, lag times of ~60 min were observed. Correlating the observations made in the above cited studies with in-vitro dissolution profiles obtained from standard tests using compendial buffers indicates that such in-vitro dissolution profiles are not predictive of the in-vivo release behavior of EC formulations. The poor outcome of the in-vitro experiments can be attributed to the buffer species and concentrations used in compendial dissolution tests (237–239). Hence, while resistance is claimed with EC aspirin formulations, the reduced BA could rather be linked to the dissolution behavior of the coating materials in the GI fluid.

In 1988 Bochner et. al. assessed the pharmacokinetics of Aspirin in man when administered in solution, modified release tablet (EC) and intravenously. The formulation and route of administration profoundly influenced several pharmacokinetic parameters of aspirin, with a 6-fold decrease in C_{max} , 1.8 fold decrease in AUC and 12-fold increase in T_{max} for the modified release tablet compared to the oral solution (240). Further on Bochner et. al. (1991) compared the pharmacokinetics of four commercially available oral aspirin formulations, in which two of the formulations were rapid release and the other two were EC formulations (241). The authors observed marked differences in the plasma concentration-time profiles between the rapid release compared to the EC formulations. Interestingly, a comparison between the rapid release formulations, demonstrated no significant differences in T_{max} were found, whereas

T_{max} was significantly prolonged for the EC formulations, and it presented great variability in the plasma concentration vs time profiles.

An additional factor that needs to be taken into account when comparing dissolution in bicarbonate to that in phosphate is that some drugs the possibility of CO_{2(g)} generation when bicarbonate reacts with a drug that has a combination of low pK_a and high intrinsic solubility. This could lead to the solid dosage form experiencing an additional disintegrating force in bicarbonate that is difficult to simulate using phosphate (242).

6.6 Applicability in the industry

A biorelevant dissolution method is the one that attempts to mimic the different physiological environments that the drug will encounter throughout its passage in the GI tract. The overall goal is guidance during formulation selection and optimization. Nevertheless, this does not necessarily mean that the method will be predictive of clinical outcomes. As the formulation development advances, a superior dissolution method can be development, which is able to model the *in vivo* performance more accurately yielding a good IVIVC/IVIVR. Hence, such a dissolution test is clinically relevant; i.e. it links the *in vitro* data with *in vivo* pharmacokinetic performance data, creating an IVIVC or IVIVR (17). When a level A IVIVC can be achieved then this method is predictive of the *in vivo* drug release in humans.

Bicarbonate buffer often falls under the biorelevant umbrella, contributing to an efficient design of drug formulations (243). Accordingly, the aforementioned studies demonstrate that bicarbonate buffer has its place and importance during the drug development process. Considering the differences and outcomes when using phosphate and bicarbonate buffers the role

and need of the latter should be revisited in a QC manner in cases in which it models *in vivo* performance more accurately, such as EC formulations (244).

6.7 Clinical reports

There are many different EC products from various classes of drugs that require further experimental scrutiny. A compilation of delayed release (enteric coated) products listed as Reference Listed Drug (RLD) by the FDA is shown in Table 6.3. According to the FDA, an RLD is “an approved drug product to which new generic versions are compared to show, among other things, that they are bioequivalent. A drug company seeking approval to market a generic equivalent must refer to the RLD in its Abbreviated New Drug Application (ANDA)”. Biowaivers are not applied to EC products. However, caution has to be taken as to which EC formulation is to be used in a bioequivalence study. Similar dissolution profiles in phosphate buffer may not render bioequivalence, as pointed out by Gelderen et. al., that compared the relative BA of four different diclofenac EC products (245). The authors reported that only one generic product was fully bioequivalent with the reference product Voltaren. The European Pharmacopeia test at the time did not detect any differences between the products. Elkoshi et. al., evaluated the bioequivalence of two enteric-coated formulations of omeprazole, Losec® (reference) and Omepradex® (test) (246). Surprisingly, the two products differed in both their rate and extent of absorption after a single dose and following multiple doses. The products failed the bioequivalence test for area under the plasma concentration-time curve (AUC) and maximum plasma drug concentration (C_{max}) after a single and multiple doses. The authors concluded that the two products may not be considered either therapeutically equivalent or interchangeable.

Table 6.3. Delayed release drug products listed as Reference Listed Drug (RLD) by the FDA
Orange book

Active ingredient	Proprietary name	Dosage form	Applicant Holder
Amoxicillin; clarithromycin; omeprazole	Omeprazole and clarithromycin and amoxicillin	Capsule, tablet, capsule, delayed release	Gastroentero Logic LLC
Aspirin; omeprazole	Yosprala	Tablet, delayed release	Genus Life Sciences Inc
Choline fenofibrate	Trilipix	Capsule, delayed release	Abbvie Inc
Crofelemer	Mytesi	Tablet, delayed release	Napo Pharmaceuticals Inc
Cysteamine bitartrate	Procysbi	Capsule, delayed release	Horizon Pharma USA Inc
Dexlansoprazole	Dexilant	Capsule, delayed release	Takeda Pharmaceuticals USA Inc
Diclofenac sodium; misoprostol	Arthrotec	Tablet, delayed release	Gd Searle LLC
Didanosine	Videx ec	Capsule, delayed rel pellets	Bristol Myers Squibb Co
Dimethyl fumarate	Tecfidera	Capsule, delayed release	Biogen Idec Inc
Divalproex sodium	Depakote	Capsule, delayed rel pellets	Abbvie Inc
Divalproex sodium	Depakote	Tablet, delayed release	Abbvie Inc
Doxycycline hyclate	Doryx	Tablet, delayed release	Mayne Pharma International Pty Ltd
Doxylamine succinate; pyridoxine hydrochloride	Diclegis	Tablet, delayed release	Duchesnay Inc
Duloxetine hydrochloride	Cymbalta	Capsule, delayed rel pellets	Eli Lilly And Co
Erythromycin	Eryc	Capsule, delayed rel pellets	Mayne Pharma International Pty Ltd
Esomeprazole magnesium	Nexium	Capsule, delayed rel pellets	Astrazeneca Pharmaceuticals Lp
Esomeprazole magnesium	Nexium	For suspension, delayed release	Astrazeneca Pharmaceuticals Lp
Esomeprazole magnesium; naproxen	Vimovo	Tablet, delayed release	Horizon Medicines LLC
Esomeprazole strontium	Esomeprazole strontium	Capsule, delayed release	R2 Pharma LLC
Fluoxetine hydrochloride	Prozac weekly	Capsule, delayed rel pellets	Eli Lilly And Co
Lansoprazole	Prevacid	Capsule, delayed rel pellets	Takeda Pharmaceuticals USA Inc

Lansoprazole	Prevacid	Tablet, orally disintegrating, delayed release	Takeda Pharmaceuticals USA Inc
Mesalamine	Delzicol	Capsule, delayed release	Allergan Pharmaceuticals International Ltd
Mesalamine	Asacol hd	Tablet, delayed release	Allergan Pharmaceuticals International Ltd
Mesalamine	Lialda	Tablet, delayed release	Shire Development Inc
Mycophenolic acid	Myfortic	Tablet, delayed release	Novartis Pharmaceuticals Corp
Naproxen	Ec-naprosyn	Tablet, delayed release	Atnahs Pharma US Ltd
Omeprazole magnesium	Prilosec	For suspension, delayed release	Covis Pharma Bv
Pancrelipase (amylase;lipase;protease)	Creon	Capsule, delayed release	Abbvie Inc
Pancrelipase (amylase;lipase;protease)	Pancreaze	Capsule, delayed release	Vivus Inc
Pancrelipase (amylase;lipase;protease)	Pertzye	Capsule, delayed release	Digestive Care Inc
Pancrelipase (amylase;lipase;protease)	Zenpep	Capsule, delayed release	Forest Laboratories Inc
Pantoprazole sodium	Protonix	For suspension, delayed release	Wyeth Pharmaceuticals LLC
Pantoprazole sodium	Protonix	Tablet, delayed release	Wyeth Pharmaceuticals LLC
Posaconazole	Noxafil	Tablet, delayed release	Merck Sharp And Dohme Corp
Prednisone	Rayos	Tablet, delayed release	Horizon Pharma Inc
Rabeprazole sodium	Aciphex sprinkle	Capsule, delayed release	Cerecor Inc
Rabeprazole sodium	Aciphex	Tablet, delayed release	Eisai Inc
Rifamycin	Aemcolo	Tablet, delayed release	Cosmo Technologies Ltd
Risedronate sodium	Atelvia	Tablet, delayed release	Allergan Pharmaceuticals International Ltd
Sulfasalazine	Azulfidine en-tabs	Tablet, delayed release	Pharmacia And Upjohn Co
Esomeprazole magnesium	Nexium 24hr	Capsule, delayed release	Astrazeneca Lp
Esomeprazole magnesium	Nexium 24hr	Tablet, delayed release	Astrazeneca Lp
Lansoprazole	Prevacid 24 hr	Capsule, delayed rel	Glaxosmithkline

		pellets	Consumer Healthcare
Omeprazole	Omeprazole	Tablet, delayed release	Dexcel Pharma Technologies Ltd
Omeprazole	Omeprazole	Tablet, orally disintegrating, delayed release	Dexcel Pharma Technologies Ltd
Omeprazole magnesium	Prilosec otc	Tablet, delayed release	Astrazeneca Pharmaceuticals Lp

Many other EC products drawbacks have been reported for various drugs. Inadequate BA due to delayed pharmacokinetics and poor absorption led to non-interpretable therapeutic drug monitoring results, for mycophenolate sodium, an antiproliferative agent used in kidney transplantation (245). Edaravone EC pellets, a drug used for acute ischemic stroke, had its BA 9 times lower than gastric retention pellets and almost 5 times lower than a solution preparation (245). Interestingly, >90% release was obtained in the *in vitro* release experiment with phosphate buffer pH 6.8. For some drugs, such as omeprazole and rasagiline, the delayed release and immediate-release formulations presented similar AUC, nevertheless, there were marked differences in C_{max} and T_{max}, which may delay the onset of action for such formulations (247,248). Studies done with drugs such as flurbiprofen and sulfapyridine presented much lower BA when administered in an enteric coated formulation and were not within the bioequivalence range (249,250).

Failure to dissolve the enteric coat may present disturbing outcomes as severe as fecal impaction. In many cases, ammonium chloride formulations caused gastrointestinal obstruction leading to patient hospitalization (251–253). Hence, the product safety in such cases may be a concern. Also, awareness of toxicological manifestations related to the use of non-steroidal anti-inflammatory drugs (NSAIDs) haven been raised, once it is possible that modified release formulations may increase the exposure of active drug to the distal GI regions (254,255).

6.8 Conclusion

Herein was presented an overview of promising trends in developing *in vivo* predictive dissolution media by means of using bicarbonate-based buffer systems. When assessing a dosage form's performance, the buffer media must be carefully considered. Currently, many studies are conducted in non-bicarbonate buffer systems, such as the so called "biorelevant" media. However, there have been many drawbacks related to these systems likely due to their sometimes limited *in vivo* predictability.

Bicarbonate-based buffers can be superior in predicting the *in vivo* behavior of certain dosage forms, like enteric coated formulations. This is possible owing to its composition, which resembles the intestinal fluids in terms of buffer species and buffer capacity. Nonetheless, the inherent difficulties associated with bicarbonate buffers make it difficult for routine dissolution testing. Hence, using simpler buffer systems as surrogate to produce equivalent buffer effects on drug dissolution remains preferred. Given inherent obstacles and drawbacks, each product has to be studied on a case-by-case basis.

Understanding the *in vivo* dissolution process may assist in setting clinically relevant *in vitro* dissolution testing methodologies. There is a major opportunity in utilizing bicarbonate-based buffers for *in vivo* predictive dissolution of EC dosage forms and further studies are still needed to assess its potential in a QC environment.

SECTION THREE: PHYSIOLOGICALLY RELEVANT *IN VITRO* TESTING:

BICARBONATE BUFFER

CHAPTER SEVEN

Mechanistic understanding of underperforming enteric coated products:
Opportunities to add clinical relevance to the dissolution test.

A version of this chapter is published in:

J Control Release. 2020;325:323–34. <https://doi.org/10.1016/j.jconrel.2020.06.031>
Reprinted from reference (88).

7.1 Introduction

Enteric coated (EC) products are modified release dosage forms used to delay the release of drug substances after oral administration (7). As such, they resist disintegration and dissolution in the gastric media, releasing the drug only after reaching the small intestine where the pH increases. Enteric coatings are generally used to maintain the stability of the active pharmaceutical ingredient (API) against the acidic gastric environment; or to protect the gastric mucosa against irritating effects of some APIs; or to target the drug release to a specific segment in the intestines (256).

Enteric coating polymers are poly-acids containing ionizable carboxylic groups. The theory behind how such polymers work is that in the low pH of the stomach the carboxyl groups are un-ionized, therefore insoluble, resisting dissolution and preventing drug release. As the dosage form travels through the gastrointestinal (GI) tract, it passes through the pylorus, reaching the duodenum, where the pH increases (44,91). When the fluid's pH is above the polymer's pKa, its ionization is promoted (256). Due to electrostatic repulsion, the polymer relaxes, undergoes chain disentanglement, which allows further ionization of polymer chains at its interface, and these chains diffuse away to the bulk solution. This process consists of the dissolution phases of pH-responsive polymers (90,92,257). Hence, according to this theory, the main factors influencing the enteric coat opening with further drug release are the polymer's pKa and the medium pH.

Based on this assumption, enteric polymers are designed with different ratios of carboxylic acid groups to set a dissolution pH threshold (usually reported by the manufacturer) enabling the development of dosage forms with targeted drug delivery (258). However, EC products are known to have unpredictable *in vivo* behaviour and several case reports of

therapeutic failure and other drawbacks involving such formulations have been reported in the literature throughout the years, dating back to 1946 and persist until the present (259) (Table 7.1).

The effect of the poor *in vivo* performance of EC products can range from patients having lower C_{max} and Area Under the Curve (AUC) to complete therapeutic failure with zero plasma concentration (Table 7.1). Completely undissolved tablets egested in the stool have also been reported which, in more severe cases, evolved to fecal impaction requiring medical intervention to resolve dangerous gut bleeding (251).

It is worth highlighting a study conducted in 2013 where the authors suspected that patients would have a phenotype that lead to pharmacological resistance to enteric coated aspirin, which would be explained by genetic causes (234). A total of 400 subjects participated in this study, however the authors failed to identify a single subject who satisfied the genetic criteria. On the other hand, they observed that variable absorption caused a high frequency of “apparent resistance” to a single dose of 325-mg enteric coated aspirin (up to 49%) but not to immediate release aspirin (0%). They state: “Delayed and reduced drug absorption was common after ingestion of enteric coated aspirin” (234).

Enteric coated formulations can also pose some challenges for acid-labile API's, such as omeprazole. The acidic groups present in the enteric coating can jeopardize omeprazole's stability, decreasing its content in the dosage form over time. To overcome this, AstraZeneca developed a formulation to enhance the stability of the API in the dosage form during storage. It was composed of a core containing the drug plus alkaline reacting compounds, a water-soluble subcoating (to prevent dissolution of the enteric coating), and the outer enteric coating. This formulation presented both good storage stability and sufficient gastric acid resistance. The

company held patents both on the API itself and the formulation. Anticipating the expiration of the API patents, eight generic drug manufacturers filed Abbreviated New Drug Applications (ANDA) with the Food and Drug Administration (FDA) seeking permission to manufacture and sell omeprazole. However, their applications infringed the formulation patents held by the innovator, which resulted in a major patent litigation case of AstraZeneca against the eight generic companies.

Table 7.1. Historic table of *in vivo* studies with EC formulations

Year	Clinical observation	API	Reference
1946	Enteric-coated ammonium chloride tablets passed unchanged through the GIT which lead to low effective absorption.	Ammonium chloride	(259)
1950	Tablets failed to disintegrate in the small intestine and became deposited in the large bowel, disturbing the normal fecal flow and causing fecal impaction.	Ammonium chloride	(251)
1963	Patients with myxedema frequently have relapses that are hazardous to them and puzzling to clinicians. In this study relapses were a result from impaired absorption of desiccated thyroid due to the use of enteric coated tablets.	Desiccated thyroid	(260)
1964	Enteric coated tablets were physiologically unavailable	Aspirin	(232)
1972	Enteric coated tablets had lower rate and extent of absorption	Aspirin	(261)
1973	Plasma samples of all eight subjects at each sampling time assayed “zero” for both drug and metabolite following oral administration of the enteric-coated tablet.	Aminosalicylic acid	(235)
1979	Enteric coated formulations presented 6 hours delay in Tmax and 50% lower Cmax	Sulfasalazine	(250)
1979	This case illustrates the necessity for awareness of possible drug malabsorption. The poor clinical response to prednisolone suggested poor prednisolone absorption. This study showed impaired bioavailability following the enteric coated preparation but normal bioavailability following the standard oral preparation. The	Prednisolone	(262)

enteric coated preparation showed biological inequivalence to the conventional oral preparation.

At the time this study was conducted the cause of the malabsorption of the enteric coated prednisolone was unknown.

1981	NSAID-Induced Toxicity in the large Intestine	Naproxen	(254,263)
1989	Patients responded poorly to enteric-coated ferrous sulfate preparations	Iron	(264)
1991	Enteric coated formulations presented significant prolonged Tmax and much lower AUC compared to immediate release tablets. The greatest variability in plasma aspirin concentration vs. time profiles was observed after administration of enteric coated formulations.	Aspirin	(265)
1991	NSAID-Induced Toxicity in the large Intestine	Diclofenac and naproxen	(266)
1992	NSAID-Induced Toxicity in the small Intestine	Diclofenac	(267)
1992	NSAID-Induced Toxicity in the large Intestine	Diclofenac, acetylsalicylic acid and naproxen	(268)
1994	Plasma salicylate concentrations were measured administration of aspirin to a group of 77 elderly patients for 7 days. The great variability on plasma concentration was not explained by differences in age, weight or serum creatinine. No salicylate was detected in 33.8% of the subjects. A second study was conducted with 6 patients to verify non-compliance issues. In 3 of these 6 patients, absence of detectable plasma salicylate was confirmed.	Aspirin	(236)
1994	Bioinequivalent formulations	Diclofenac	(269)
2008	This study concluded that the enteric coated formulations were less effective since their iron may not be released in the duodenum, where iron is absorbed.	Iron	(270)
2010	In this study there were significant differences in the bioavailability and pharmacokinetic parameters of the enteric- and film-coated tablet formulations of flurbiprofen. Thus, the 2	Flurbiprofen	(249)

formulations could not be considered bioequivalent.

2013	This study failed to identify a single case of true drug resistance. However, delayed and reduced drug absorption was observed in enteric coated formulations but not with immediate release aspirin administration.	Aspirin	(234)
2017	A high proportion of patients (52.8%) treated with EC aspirin failed to achieve the desired therapeutic effect due to incomplete absorption.	Aspirin	(230)

The majority of the clinical observations presented in Table 7.1 involved marketed EC products, pointing out that there seems to be a hidden performance problem with these products. This has been a clinically recognized but neglected problem for over 70 years, even though all the products had passed the performance tests both for registration and market release (232,235,260). Hence there is a gap between clinical observations and the quality control testing.

Considering that the human intestine is buffered by bicarbonate buffer (BCB), it is reasonable to use bicarbonate-based systems for the performance test of drug products (28,271). However, the handling of BCB is delicate and requires constant sparging of CO₂ to maintain the medium pH. This is why this buffer is not the first choice in quality control (QC) testing and phosphate buffer took its place, as seen by the wide use of compendial simulated intestinal fluid (19,28).

In addition to the traditional quality control tests for tablets, other non-invasive technologies and techniques can be used for the characterization of physical-mechanical properties of tablets. Examples are near infrared spectroscopy, Raman spectroscopy, X-ray microtomography, nuclear magnetic resonance (NMR) imaging, terahertz pulsed imaging, laser-induced breakdown spectroscopy, and various acoustic- and thermal-based techniques (272). In

the present study, computerized x-ray microtomography (micro-CT) was used as a non-invasive method to accurately measure tablet coat thickness before dissolution testing.

The current pilot study mechanistically investigated the performance of five EC products available in the Canadian market. The evaluated parameters were the buffer system (bicarbonate buffer vs. phosphate buffer), buffer capacity and medium pH.

We hypothesized that the performance of EC products in BCB would be different compared with compendial phosphate buffer, giving more physiological insight. API properties (acid vs. base) would additionally impact the dissolution behavior in BCB.

The objectives of this study were to firstly apply physiologically relevant conditions to examine the effect of the aforementioned parameters on the release pattern of commercially available EC products and compare the results with the current United States Pharmacopeia (USP) test for EC dosage forms. Secondly, we aimed to establish a first step towards making the use of bicarbonate-based systems feasible in a quality control setting.

7.2 Materials

Sodium phosphate monobasic monohydrate and sodium hydroxide were purchased from Fisher Scientific (New Jersey, USA), sodium bicarbonate was purchased from Caledon (Ontario, Canada), sulfasalazine, pantoprazole sodium, acetylsalicylic acid and esomeprazole magnesium were purchased from Sigma-Aldrich Co. (Montana, USA), diclofenac sodium was purchased from Medisca (Quebec, Canada).

EC products obtained from the market were: Teva-Pantoprazole (T) 40mg (Teva Canada Limited, LOT: 0691118), PMS-Sulfasalazine EC 500mg (Pharmascience Inc., LOT: 1037737), APO-Esomeprazole Magnesium DR 40mg (Apotex Inc., LOT: NV2183), Diclofenac sodium

(Sandoz Canada Inc., LOT: JN9884), Aspirin EC 81mg (Bayer Inc., LOT: NAA68A2 and NAA72T6).

Buffer solutions were prepared with purified water (Elgastat Maxima UF and an Elgastat Option 3B water purifier by ELGA Laboratories Ltd. (Mississauga, ON, Canada)).

7.3 Methods

7.3.1 Micro-CT analysis

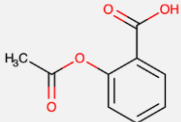
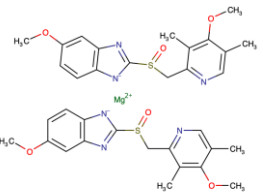
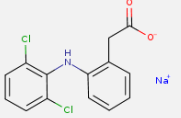
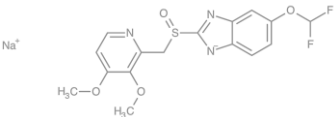
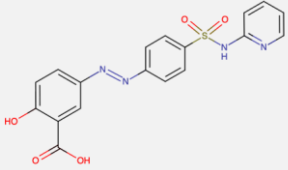
Tablet coat properties, such as coat thickness, may affect the drug release from the dosage form. Hence, all five products were micro-CT scanned prior to dissolution testing in order to measure the coat thickness and to assess the coat structure in correlation with subsequent coat failure.

Tablets were mounted on a styrofoam holder and analyzed using a Micro-CT imager (SkyScan 1076; Bruker-Skyscan, Kontich, Belgium) at 9 μm voxel image resolution with the x-ray tube set to 45 kV, 555 μA , with a 0.2 mm aluminum filter used to remove low energy photons. Tablets were scanned through 180° with a sampling rotation step of 0.5°. The scans were reconstructed using a modified Feldkamp back-projection algorithm with vendor-bundled software with a cross section to image conversion threshold of 0.0 to 0.046 (NRecon, Bruker-Skyscan, version 1.6.3.3). After reconstruction, tablet CT slices were viewed and measured. Representative slice subsets of the whole tablet were chosen by selecting an upper and lower bound slice for different regions of the tablet. The collected data was analyzed using the CT Analyzer software (CTan, Bruker-Skyscan, version 1.17.7.2 [16 bit]). In the cross-section images, the software allows to assess the coat thickness by converting pixels into μm . Measurements were done in four different regions of each tablet (mid-point of top and bottom and both sides).

7.3.2 Performance tests

All four biopharmaceutics classification system (BCS) classes were considered as well as physicochemical parameters (pKa – acid vs. base), as summarized in Table 7.2.

Table 7.2. API properties (BCS class and pKa) and coating polymer of the tested EC products

Drug product	BCS class	pKa	API structure	Coating polymer	Dissolution pH threshold [#]
Aspirin (Bayer Inc.)	I	3.41 (Acid) (273)		Methacrylic acid and ethyl acrylate copolymer	5.5 (274)
Esomeprazole magnesium (Apotex Inc.)	II	14.7 (Base) (275)		Methacrylic acid and ethyl acrylate copolymer	5.5 (274)
Diclofenac sodium (Sandoz Inc.)	II	4.15 (Base) (276)		Undisclosed	?*
Pantoprazole sodium (Teva Ltd.)	III	8.19 (Base) (277)		Methacrylic acid and ethyl acrylate copolymer	5.5 (274)
Sulfasalazine (PMS Inc.)	IV	3.23 (Acid) (278)		Acryl resin	?*

*The exact polymer used is not disclosed by the manufacturer.

[#] Value specified by the manufacturer. It is the pH value in which the polymer starts to dissolve.

All dissolution tests were performed in a VK 7020 system from Varian Inc. dissolution tester coupled to a VK 8000 autosampler. USP apparatus II with 75 rpm rotation speed was used with dissolution media temperature set at 37 °C.

In order to test the gastric resistance and coat integrity, the pharmacopeial test method for EC formulations establishes an acid stage prior to the buffer stage. Hence, for all experiments, the EC tablets were exposed to 0.1 N hydrochloric acid for 2 hours prior to the buffer stage, as specified by the USP. The drug release was determined by UV-spec at the end of the 2 hours using the appropriate wavelength for each drug. The tablets were then transferred to vessels containing 900 ml of pre-heated buffer solutions. The buffer stage was performed as described below.

7.3.2.1 Phosphate-based dissolution medium

Dissolution testing was performed according to the <USP 711> two stage procedure in acid and buffer. The recommended buffer media for enteric coated dosage forms is 50mM phosphate buffer pH 6.8, except for sulfasalazine tablets, which were tested in 50mM phosphate buffer pH 7.2, as specified in its monograph. The drug release at specific time points was determined by UV-spectroscopy using the appropriate wavelength for each drug (aspirin: 283nm, esomeprazole: 304.5nm, pantoprazole: 288nm, sulfasalazine: 359nm and diclofenac: 276nm).

7.3.2.2 Bicarbonate-based dissolution medium

Based on the reported values of BCB molarity and pH values at the human proximal intestine, the dissolution tests were performed in 5mM bicarbonate buffer pH 6.5 (44).

The bicarbonate buffer was prepared by dissolving the appropriate amount of sodium bicarbonate in deionized water to obtain a 5mM concentration. The dissolution medium was poured into the dissolution vessels allowing the temperature to equilibrate before commencing the experiments. The pH was adjusted to 6.5 by sparging the medium with CO_{2(g)} and it was

continuously monitored and maintained throughout the dissolution tests by sparging CO_{2(g)} as needed. The pH was monitored using an accumet® AB250 pH-meter from Fisher Scientific (Fair Lawn, NJ, USA). The drug release at specific time points was determined by UV-spectroscopy using the appropriate wavelength for each drug (aspirin: 283nm, esomeprazole: 304.5nm, pantoprazole: 288nm, sulfasalazine: 359nm and diclofenac: 276nm).

7.3.2.2.1 Effect of buffer molarity and pH

In order to assess the effect of buffer molarity and pH on the enteric polymer dissolution, diclofenac sodium tablets were tested in BCB in a molarity range reflective of the one found along the human GI tract (i.e. 2.5, 5, 10, 15, 20 and 30mM) (52,222,279–286). The media was not sparged, hence presenting a higher bulk pH.

The dissolution experiments were conducted with freshly prepared buffer, one day and one week old to investigate if buffer age has any impact on the dissolution, as reported in literature (1). The buffer pH was measured before and monitored during the dissolution tests. Because there was no sparging with CO_{2(g)}, the medium pH was not maintained.

7.4 Results

7.4.1 Micro-CT analysis

The coat thickness measured for each tablet is presented in Table 7.3 and the scans results for all the products are shown in Figure 7.1. The coat could be easily distinguished due to the difference in density between the coating material and the tablet core. The outer denser region in Figure 7.1B and C represent a coloured film coating that was washed off during the acid stage.

Table 7.3. Coat thickness measured prior to dissolution testing using Dataviewer Software (mean \pm SD)

Product	Coat thickness (μm)
Aspirin [#]	64.5 \pm 4.45
Diclofenac sodium [#]	100.1 \pm 4.45
Esomeprazole magnesium [*]	62.3 \pm 10.3
Pantoprazole sodium	171.4 \pm 4.45
Sulfasalazine	111.3 \pm 8.9

[#] Measurements included the film coating

^{*} The coating on the sides of the tablet was thicker than the top and bottom, hence the higher SD.

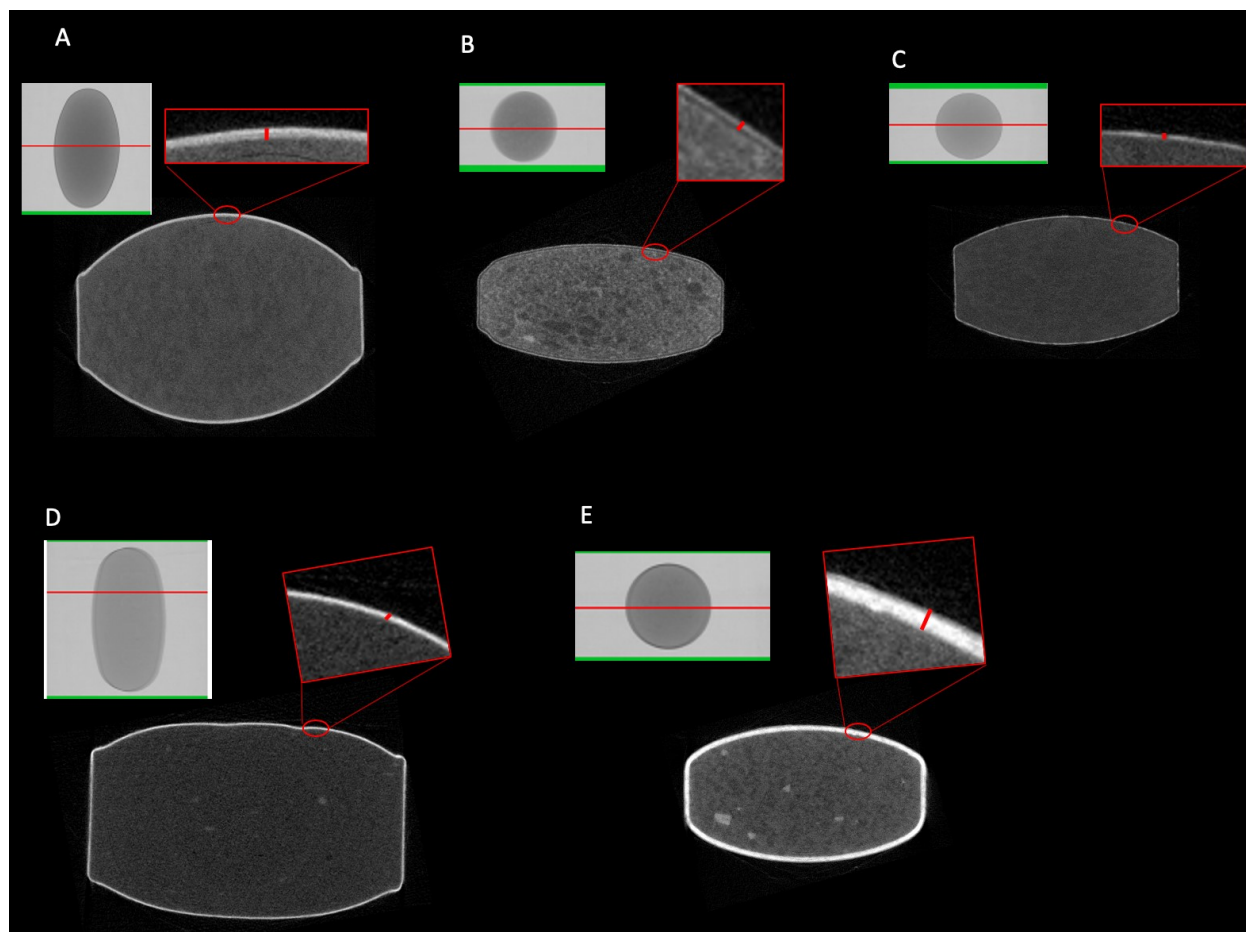


Figure 7.1. Cross-sectional micro-CT images of marketed EC tablets prior to dissolution testing. (A) Sulfasalazine (B) Diclofenac (C) Aspirin (D) Esomeprazole (E) Pantoprazole. The red line in each upper shadow projection indicates the location of each lower reconstructed micro-CT image slice (voxel resolution of 9 μm isotropic). Differences in enteric coating thickness can readily be seen, as can density differences in tablet excipient content.

7.4.2 Performance tests

The pharmacopeial tolerance specification for the acid stage is not more than 10% release after 2 hours exposure to 0.1N HCl. Esomeprazole magnesium and sulfasalazine tablets presented holes (defects) in the coat after the acid stage, however, the criteria of not more than 10% released was still met. The coatings of the other products (aspirin, pantoprazole sodium and diclofenac sodium) were intact after the acid stage (i.e., no release). Hence, all products passed the USP acid stage criteria showing no drug release or less than 10% within the 2h exposure to 0.1M HCl (data not shown).

In phosphate buffer the various EC products displayed rapid dissolution and were compliant to the USP tolerance specifications for drug release in the buffer stage (described in each drug's respective monograph) (Figure 7.2 and Table 7.4). On the contrary, the dissolution results in bicarbonate buffer failed to meet the current USP criteria for the tested EC products. An interesting visual observation was the distinct pattern of coat opening between the two media. In phosphate buffer the coat rapidly dissolved away, leaving the tablet core completely exposed to the dissolution medium. In BCB, however, the coat firstly presented ruptures through which the water could penetrate and reach the tablet core. Instead of completely dissolving, we observed parts of the coating "peeling off" of the tablet core and floating in the dissolution medium and other parts remained on the dosage form (especially the bottom side of the tablet that was in contact with the dissolution vessel). This highlights the slower dissolution rate that EC polymers present in BCB.

The comparative dissolution for each formulation in phosphate buffer 50mM vs. BCB 5mM is presented in Figure 7.2. For all formulations, the onset of drug release was delayed in

bicarbonate media compared to phosphate buffer, as well as the rate and extent of drug release (Figure 7.2 A-E).

Interestingly, there was a remarkable difference between esomeprazole magnesium and aspirin in BCB (Figure 7.3). Both tablets were coated with the same coating polymer, presented similar coat thickness, but differed in their physicochemical properties: basic API vs. acidic API, respectively (Tables 7.2 and 7.3). Acidic drugs in the tablet core can have an acidifying effect on the inner side of the coat which might prolong the coat opening. The opposite might happen with basic drugs, i.e. a basic microenvironment is created under the coat, promoting coat opening and drug release. This was clearly seen when comparing pantoprazole sodium with aspirin in BCB. Pantoprazole sodium tablets had a thicker coat (and the same polymer) compared to aspirin tablets but the release was nevertheless much faster because of its alkalinity.

Likewise, esomeprazole magnesium and pantoprazole sodium tablets were coated with the same coating polymer (Table 7.2), however the onset of drug release for esomeprazole magnesium was faster than pantoprazole sodium in BCB (Figure 7.3). Both tablets contained basic API's but differed in their coat thickness (Figure 7.1 and Table 7.3). In this case, the coat thickness seemed to play a role in drug release.

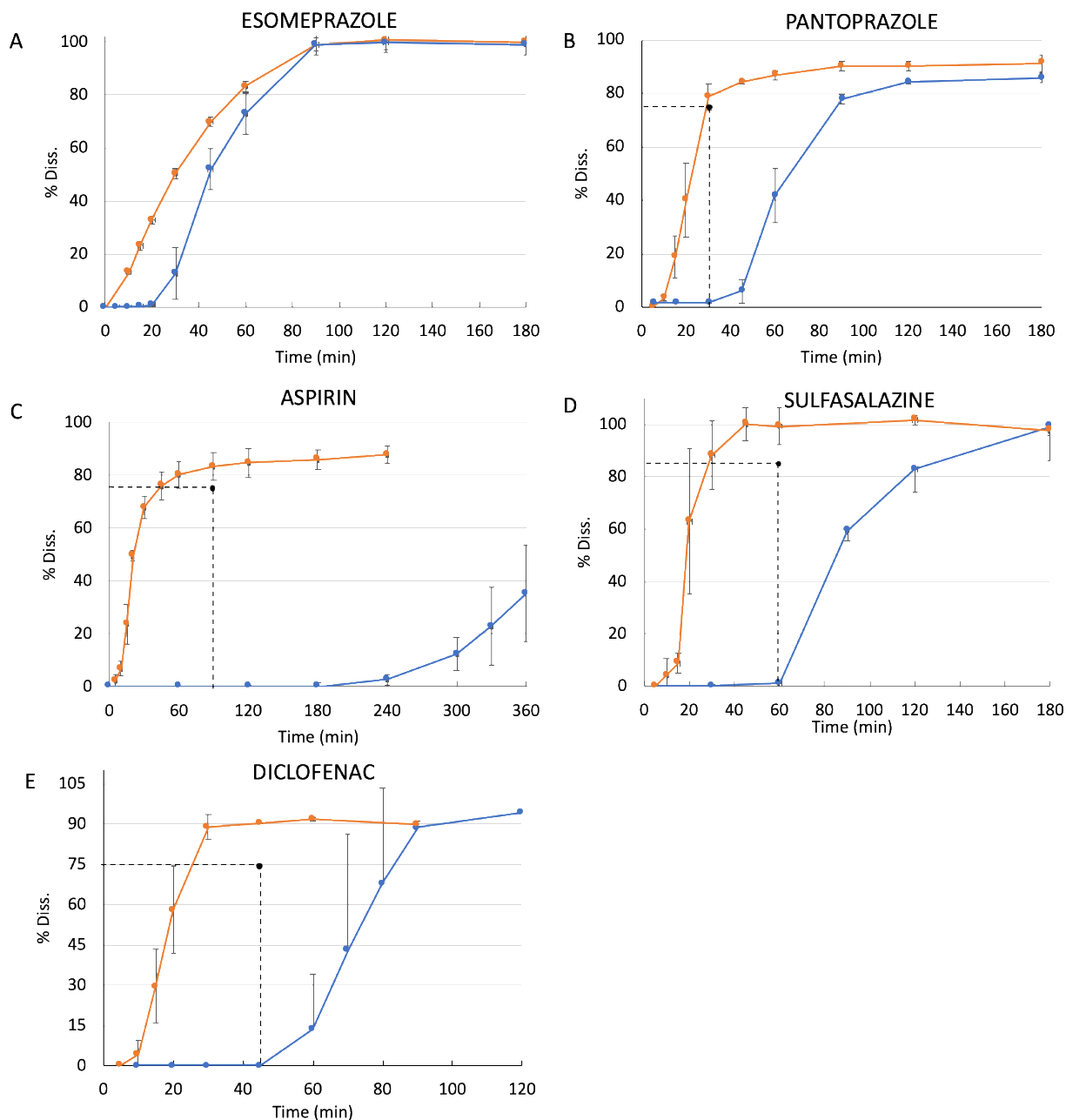


Figure 7.2. Dissolution profiles of enteric coated formulations in 50mM phosphate buffer (orange line) and 5mM bicarbonate buffer (blue line); USP dissolution specification (when available): black dashed line. Esomeprazole magnesium (A), Pantoprazole sodium (B); Aspirin (C), Sulfasalazine (D) and Diclofenac sodium (E).

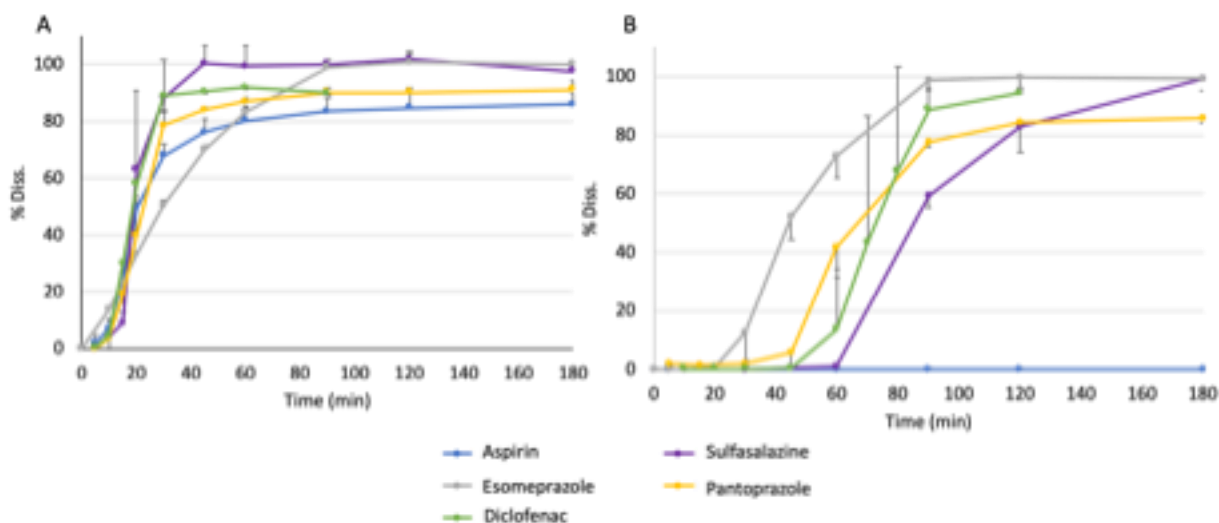


Figure 7.3. Comparison of dissolution profiles of enteric coated formulations in 50mM phosphate buffer (A) and 5mM bicarbonate buffer (B).

Table 7.4. USP tolerance specification for drug release in the buffer stage and percent released in PB and BCB

Drug	USP tolerance specification	Q (%) at the specified time	
		PB	BCB
Aspirin	NLT 75% in 90 minutes	83.4%	0.0%
Pantoprazole sodium	NLT 75% in 30 minutes	78.6%	1.80%
Sulfasalazine	NLT 85% in 60 minutes	99.3%	1.10%
Diclofenac sodium	NLT 75% in 45 minutes	90.4%	0.40%
Esomeprazole magnesium	N/A	N/A	N/A

Q: % of drug dissolved; PB: Phosphate buffer; BCB: Bicarbonate buffer; NLT: Not less than. Green: Compliant with USP specification. Red: Failed USP specification. N/A: Not available

The effect of buffer molarity was evaluated in non-sparged bicarbonate media. For all molarities tested, the medium pH (pH_{BCB}) was above the polymer's pH threshold (pH_{EC}). Even though the $pH_{BCB} > pH_{EC}$, the buffer molarity had greater influence than the bulk pH in promoting the coat opening, i.e. the higher the BCB molarity, the faster the onset of drug release (Figure 7.4). This observation is in accordance with recent findings (78,85). Within the physiological range of bicarbonate molarity values, the buffer concentration seems to be more

important than the bulk buffer pH for the opening of the enteric coat, given that $\text{pH}_{\text{BCB}} > \text{pH}_{\text{EC}}$ is established.

The higher the molarity of the BCB buffer was the higher the final pH was. However, the differences between the lowest and highest pH value was only 0.58 pH units, which is not surprising based on the inherently amphoteric nature of the bicarbonate species.

Table 7.5. Non sparged bicarbonate medium pH at time zero (mean \pm standard deviation)

	2.5mM	5mM	10mM	15mM	20mM	30mM
Fresh	7.85 \pm 0.026	7.94 \pm 0.03	8.16 \pm 0.01	8.13 \pm 0	8.29 \pm 0.01	8.27 \pm 0.01
1 day old	7.75 \pm 0.14	8.04 \pm 0.02	8.12 \pm 0.02	8.20 \pm 0.02	8.28 \pm 0.02	8.33 \pm 0.01
1 week old	7.85 \pm 0.021	7.97 \pm 0.03	8.27 \pm 0.01	8.31 \pm 0.04	8.41 \pm 0.02	8.28 \pm 0.03

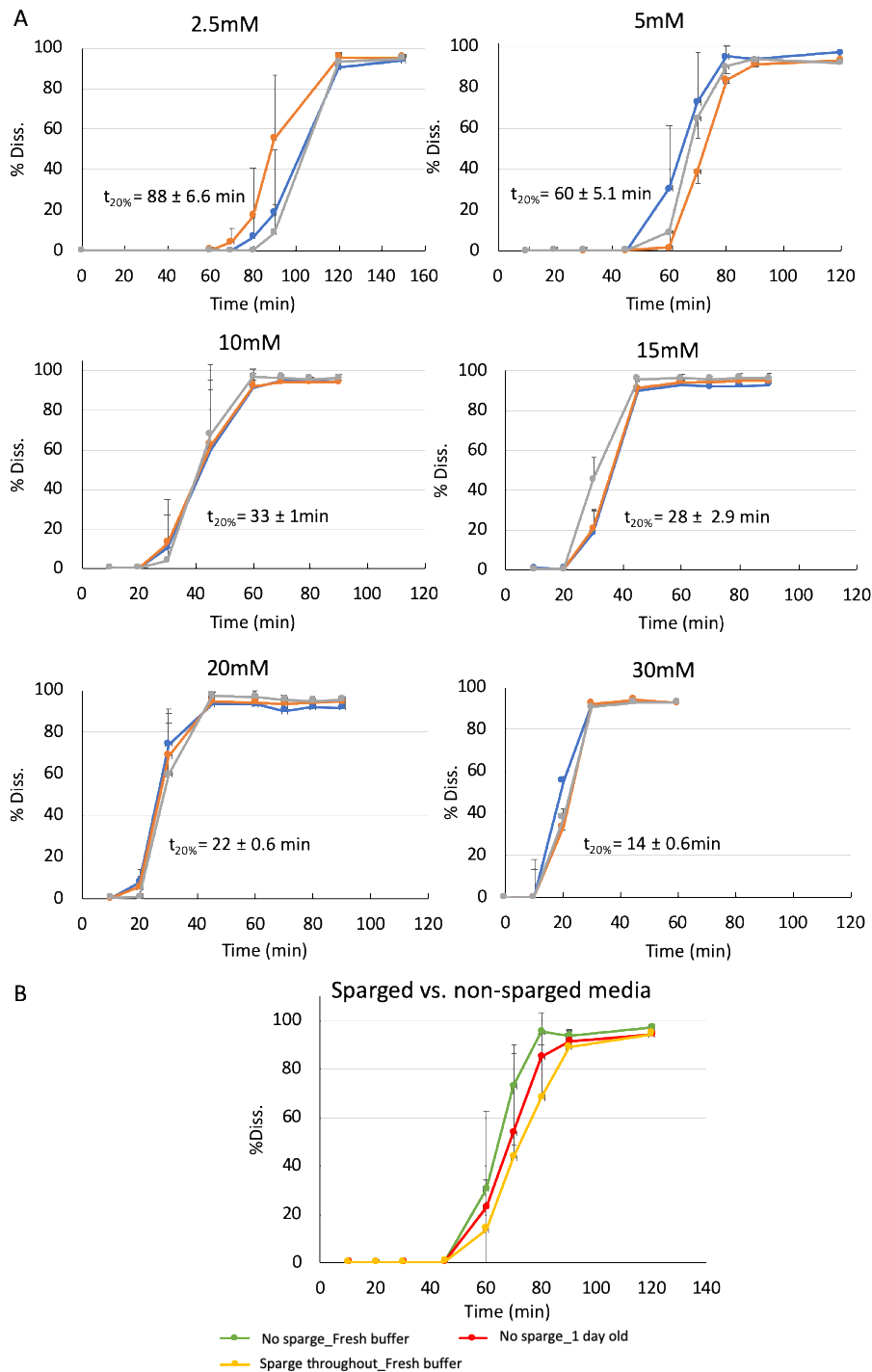


Figure 7.4. Dissolution of enteric coated diclofenac sodium tablets in various bicarbonate molarities and effect of sparging the medium. (A) Dissolution profiles of enteric coated diclofenac sodium tablets in bicarbonate buffer 2.5 – 30mM range. Blue line: fresh buffer; orange line: a day old; grey line: a week old; $t_{20\%}$: time taken for 20% release. (B) Effect of sparging the media (5mM bicarbonate buffer) on the dissolution of enteric coated diclofenac sodium tablets.

7.5 Discussion

In our mechanistic evaluation of a limited set enteric coated products, the buffer system, buffer capacity and medium pH were studied for acidic and basic drugs belonging to different BCS classes. Micro-CT was used to measure the tablet coat thickness due to its non-invasive and non-destructive capacity. This technique has been used to examine various properties of solid dosage forms such as tablet density, pore structures, deformation behavior of polymorphs, uniformity of API distribution in tablets and coating thickness (287–290). Because of the contrast between the coating polymer and the tablet core, the coat thickness can be measured. The advantage of using such technique is that it's a non-destructive and non-invasive tomographic tool that reveals the three-dimensional structure of various objects at a high spatial resolution (291).

The coat thickness seemed to matter when comparing esomeprazole magnesium and pantoprazole sodium tablets, which were coated with the same coating polymer and both are basic API's. As expected, the thicker coat on the pantoprazole sodium tablets took longer to open than esomeprazole magnesium (45 min vs. 30 min, respectively). On the other hand, the greater thickness of the coating of pantoprazole sodium tablets makes it difficult to determine to which extent the greater basicity of esomeprazole magnesium contribute to its faster release.

This was not the case when comparing pantoprazole sodium and aspirin tablets. They were also coated with the same coating material, but even though pantoprazole sodium tablets had a much thicker coat, the onset of drug release was much faster than for aspirin tablets (45 min vs. 4 hours). The major difference lies on the physicochemical properties of the APIs, i.e., base vs. acid. In this case, the physicochemical properties seem to outweigh the coat thickness.

Both esomeprazole magnesium and aspirin tablets were coated with the same coating material, presented comparable coat thickness and differed only in the API physicochemical properties. There was a significant difference in the onset of drug release between the two formulations: 30 minutes vs. 4 hours, respectively (Figure 7.2A vs 7.2C). At the end of a 2 hours period, esomeprazole magnesium tablets presented some ruptures in the coat layer, which could expedite the drug release in the buffer stage. Due to the openings in the coat, the dissolution medium can penetrate to the tablet core surface, causing it to expand and physically break the coat, which is an additional force besides the coat dissolution. In addition to that, the basicity of the API could also have played a role. As shown in Figure 7.3B, it is very noticeable that the release of the acidic APIs aspirin is further delayed in BCB. This is most likely due to an acidifying effect of such API on the inner side of the enteric coat, which can be an additional hindrance to the polymer's dissolution (150). In contrast, basic APIs such as esomeprazole magnesium and pantoprazole sodium could increase the coat dissolution process by buffering it from the inside, which was evidenced by the faster onset of drug release (Figure 7.3B). Basic APIs can accept protons formed from the carboxyl groups ionization, thus promoting faster coat opening than acidic APIs.

Liu and coworkers have reported similar observations (292). The use of an inner coating (composed of a partially neutralized anionic polymeric material) under the outer enteric coating (composed of an anionic polymeric material which is less or not at all neutralized than the inner coating) helped to disintegrate and to release the drug earlier compared to a formulation having no subcoat. Rapid disintegration upon entry into the small intestine is not the case for “conventional EC dosage forms”, the authors proposed the use of such a subcoat for promoting drug release already at the entry of the intestine (292).

After oral administration, an EC dosage form first reaches the stomach, where it resides between 0.1-3 hours depending on the presence of food and other physiological and disease states (293,294). After gastric emptying, it moves on to the small intestines where the drug release takes place. Based on this, the USP recommended dissolution test for enteric coated products is a two-stage procedure (295). In the first stage, the acid stage (2 hours), HCl 0.1N (pH ~ 1) is used as the dissolution medium, which is followed by the buffer stage in compendial phosphate buffer pH 6.8 (unless otherwise specified in the individual monograph) (7). The first stage mimics the dosage form's passage through the stomach and the latter the intestine. Even though the acid stage pH value (around 1) is at the lower range of the fasting gastric pH *in vivo*, conducting the acid stage at the upper range values (around 2.9) is not likely to result in more release because this value is still below the pH threshold for coat opening (starting from 5.5) (44).

This procedure is also based on the premise that an enteric coating is insoluble under acidic conditions, thus resisting dissolution, but would readily dissolve at more basic conditions of the intestinal tract (296).

Our investigation shows that, in compendial phosphate buffer the drug release is rapid with little discrimination for the dissolution behaviour between different EC formulations (Figure 7.3A) (72). However, phosphate buffer lacks physiological relevance in many aspects, such as buffer species and molarity (27). The main buffering system in the human intestinal fluid is bicarbonate-based and the *in vivo* molarity values are much lower than the 50mM used in compendial buffers (31,149). The bicarbonate concentration in the human intestine has been reported to range from 2-15 mM in the duodenum, 2-30 mM in the jejunum and 30-75 mM in the ileum (52,222,279–286). Hence, testing EC dosage forms in BCB can give much more

physiological insight to understand the pronounced discrepancies between the *in vitro* and *in vivo* performance of EC dosage forms, as observed in the numerous case reports (Table 7.1). Many of the *in vivo* failures of EC products were related to a lower rate and extent of drug absorption. As shown in Figure 7.2, the coat opening is promptly promoted in phosphate buffer. On the other hand, the lower rate and extent of drug absorption observed *in vivo* was reflected when applying physiologically relevant conditions using BCB with different molarities (Figures 7.2 and 7.4). Hence, there is a disconnect between the *in vitro* and *in vivo* performance of EC products.

The clinical irrelevance of phosphate buffer to predict the *in vivo* performance of EC dosage forms lies on the fact that phosphate has an equilibrium kinetics completely different from bicarbonate. Due to its pKa of 6.8 (under physiological ionic strength) (20), dihydrogen phosphate (H_2PO_4^-) is usually the species of choice in phosphate buffers. In aqueous medium H_2PO_4^- dissociates, forming monohydrogen phosphate ion (HPO_4^{2-}) and a proton (Figure 7.5 Eq. A) (297).

The pKa of the BCB system (Figure 7.5 Eq.B) reported in the literature is around 6.04 (72,84,85). This value is obtained when measuring the pKa with a potentiometric method at physiological temperature and ionic strength. Because the titration procedure used in the potentiometric determination of pKa is relatively slow, carbonic acid and carbon dioxide are at equilibrium. That is the situation in the bulk solution in a dissolution vessel, where the pKa of BCB is 6.04 (Eq. B in Figure 7.5) (78).

However, as reported by Al-Gousous *et. al.*, at the solid-liquid interface (diffusion layer) around dissolving solutes (e.g. drug or EC polymer) the situation is more complex. In contrast to the very rapid ionization reactions, the CO_2 hydration and H_2CO_3 dehydration processes are much slower, with dehydration being up to 800 times faster than hydration (Fig. 7.6 Eq. C)

(298,299). The consequence of this is that, even though the hydration/dehydration reaction ($H_2CO_{3(aq)} \rightleftharpoons H_2O_{(l)} + CO_{2(aq)}$) occurs, it does not typically reach equilibrium within the effective diffusion layer. This results in the effective pKa of bicarbonate in the diffusion layer to be lower than the bulk value of 6.04 but higher than the intrinsic pKa of 3.30 ($H_2CO_{3(aq)} \rightleftharpoons H^+_{(aq)} + HCO^-_{3(aq)}$). Therefore, the buffering capacity of bicarbonate in the boundary layer is governed by a pKa value that is lower than the interfacial pH value needed for the EC polymer's dissolution (92). This means that BCB has a limited ability to buffer the pH of the dissolving polymer's surface and cannot promote prompt dissolution, which presents a major difference between BCB and phosphate buffer and is clearly seen in the dissolution behavior shown in Figure 7.2.

Evidently, the opening of the enteric coat is very dependent on the medium properties, however factors such as the intrinsic solubilities and pKa's of both the drug and polymer also play a role (300–303). Hence, the assumption that an EC formulation rapidly disintegrates in the intestines, behaving like an immediate release is a misconception (292).

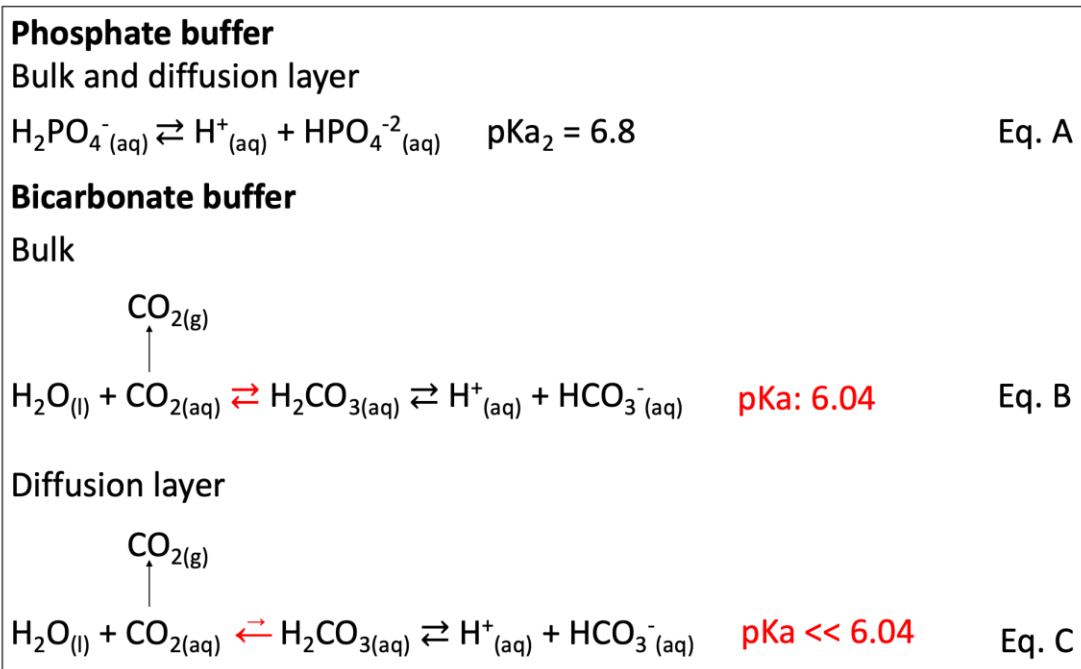


Figure 7.5. Phosphate and bicarbonate buffer equilibrium reactions and pKa values taking place in the bulk solution and diffusion layer.

The unpredictable performance of EC formulations in BCB is well acknowledged in the literature (28,76,191–193,237,239,244,293,303). As a matter of fact, the dissolution rate of enteric polymers is determined by the pH at the solid-liquid interface instead of the bulk pH (92). Because of the reaction between the polymer's carboxyl groups and the basic components of the buffer system, the surface pH is expected to be lower than the bulk pH. As the buffer capacity (i.e. resistance to change in pH) of the medium increases, the gap between the bulk pH and polymer surface pH decreases (78).

According to the derivation of the van Slyke equation, we see that an increase in the concentration of the buffer components results in a greater buffer capacity (304). Hence, more concentrated buffers tend to have a higher buffer capacity, increasing the polymer's dissolution rate with consequent faster onset of drug release. This can be clearly seen in Figure 7.4A, a higher buffer concentration results in a faster onset of drug release. For example, the time taken

to reach 20% of drug release in BCB 2.5mM was 88 ± 6.6 minutes, whereas in 5mM, double the molarity but comparable pH values (Table 7.5), the time went down to 60 ± 5.1 minutes. Here we see that the coat opening was more dependent on buffer molarity than on bulk pH. This is in accordance with Al-Gousous and coworkers who have also observed the more predominant effect of BCB molarity on the release properties of EC formulations over bulk pH (78), particularly when the bulk pH is above the polymer's dissolution pH threshold value (which is an interfacial rather than bulk pH value).

However, working with BCB can be experimentally challenging. Due to the loss of $\text{CO}_{2(\text{aq})}$ to the gas phase, the medium pH increases, hence it needs to be sparged with CO_2 to maintain the bulk pH at the desired pH value (243). Different dissolution method set-ups have been proposed in order to overcome this difficulty, all of which are focused on re-establishing the bulk pH (28). On the other hand, it is acknowledged that the enteric coating *in vivo* dissolution is primarily limited by the surface pH and buffer molarity rather than bulk pH. Hence, sparging the medium to maintain the bulk pH may not be as essential as using an adequate BCB molarity in the dissolution test. We studied the use of non-sparged medium in order to determine whether it could be an alternative to sparged medium, which would make the use of bicarbonate-based medium more feasible.

Since buffer molarity (not pH, if above the threshold pH value) seems to be the limiting factor for enteric coat opening, we tested EC diclofenac sodium formulations in BCB in a 2.5 – 30 mM range (biological range of bicarbonate concentration) without sparging the media. When the bicarbonate-based medium was not sparged with CO_2 , the bulk pH could not be maintained. Nonetheless, because the medium is not sparged, the pCO_2 is lower, which leads to a decreased

escape of CO₂ compared to the sparged medium. Consequently, the pH fluctuation in the non-sparged medium was much less noticeable.

We assessed the effect of CO₂ loss by preparing the buffer freshly and storing it for one day and a week prior to the dissolution test (Figure 7.4A). The older the BCB is the higher the CO₂ loss, however the time points for onset and total drug release in freshly prepared buffer vs. 1 day old vs. a week old were similar (Figure 7.4A). As long as the pH was above the recommended pH threshold, only buffer molarity was found to be important to meet the USP criteria (NTL 75% release in 45 minutes). Currently, USP specifies 1 time point collection, hence the variability observed in between would not be a concern.

In order to assess the influence of sparging the media, we fixed the buffer molarity at 5mM and compared the drug release in non-sparged buffer (fresh and a day old) versus freshly prepared media with sparging throughout the dissolution test to maintain the bulk pH at 6.5 (Figure 7.4B). The onset of drug release was very similar between the tested media (i.e. after 45 minutes) as well as the time for total release (80-90 minutes). Considering the overall performance, sparging the medium to maintain the bulk pH did not influence much.

Therefore, while the principle of “dissolution will happen as long as the fluid pH is greater than the polymer’s dissolution pH threshold” (256) may be true in 50 mM phosphate buffer and high molarity BCB, our results show that different BCB molarities significantly impact the performance of EC products (as a result of the larger gap between the bulk and interfacial pH values in BCB systems). These results are in line with *in vivo* observations of EC products. Considering the results presented herein and the “lessons learned” from the many case reports of *in vivo* failure of EC products, setting a molarity threshold rather than a bulk pH threshold might be a better approach in the development of enteric coated dosage forms (78).

Moreover, the use BCB may be indispensable in the performance testing of EC formulations during product development and quality control. Non sparged BCB set at an adequate molarity may be a first step towards more physiologically relevant dissolution test for many and maybe even most EC products. Further investigations need to be performed in this regard.

7.6 Conclusion

In this pilot study we demonstrated that there is a considerable delay in the onset of drug release from EC formulations in BCB compared to compendial phosphate buffer. The delay in BCB was additionally impacted by the nature of the API (acid vs base), which seems to outweigh the coat thickness. This demonstrates that the coat opening is influenced by the properties of the immersion medium (composition, pH and molarity) and the internal pH at the tablet/coat interface.

Enteric coat dissolution is prompt in compendial buffer, revealing that USP dissolution test for enteric coated tablets seems to be clinically irrelevant and it needs to be reevaluated. Using BCB to test EC formulations is, therefore, a more physiologically relevant test condition.

The reported *in vivo* failures of EC products known in the literature seem to be due to, at least in part, poor performance in the intestinal fluids, which is buffered by bicarbonate at low buffer molarity. Testing these products in a fluid that closely resembles the intestinal lumen can provide crucial insight on how the formulation would behave in the physiological environment thus bringing clinical relevance to the test since the systemic therapeutic effect can only occur after the drug has been released, dissolved, and absorbed. An *in vivo* relevant performance test for EC products needs to be developed. Special consideration should be taken for acidic drugs once its release could be further delayed.

SECTION THREE: PHYSIOLOGICALLY RELEVANT *IN VITRO* TESTING:

BICARBONATE BUFFER

CHAPTER EIGHT

Physiologically relevant dissolution conditions towards improved *in vitro* - *in vivo* relationship – A case study with enteric coated pantoprazole tablets

A version of this chapter has been accepted to be published in:

International Journal of Pharmaceutics. 2021. Manuscript number: IJPHARM-D-21-01038

8.1 Introduction

Delayed release formulations have been used for many years both for medication and nutrition supplements (e.g. iron) (305). This formulation technology is applied in cases which there is a need to protect the formulated compound from the acid in the stomach; or to protect the gastric mucosa; or to target the drug release to a particular segment in the intestines (305). The drug release is not expected to take place in the stomach, only in the intestines, hence the “delayed” terminology (306,307). The delayed release characteristic of such formulations is usually obtained through the coating of the tablet core with a pH responsive polymer, which are referred as enteric coating (EC) polymers. Such polymers are designed to dissolve when the medium pH is above its dissolution pH threshold, thus allowing drug release (305). Examples of polymers used for enteric coating are cellulose derivatives (e.g. cellulose acetate phthalate, cellulose acetate trimellitate, hydroxyl propyl methyl cellulose phthalate and hydroxyl propyl methyl cellulose acetate succinate), polyvinyl acetate phthalate and methacrylic acid copolymers, which is one of the most widely used polymers for the intended purpose.

However, concern has been raised regarding delayed release formulations due to many therapeutic failures reported over the years, including bioequivalence (BE) studies (88). A recent study from our group (88) and other groups (68,71,75,78,191,192,239) suggest that this drawback seems to be related to the poor *in vivo* performance of EC formulations. The human intestinal juice is mainly composed of pancreatic and hepatic secretions. The pancreatic secretion contains a large volume of sodium bicarbonate solution along with of various digestive enzymes. Similarly, sodium bicarbonate is also added to the hepatic secretion (bile). Furthermore, the epithelial cells of the duodenum secrete an alkaline mucus to protect the duodenal wall from the acidic content coming from the stomach. This mucus contains bicarbonate ions, which adds to

the bicarbonate ions from the pancreatic and hepatic secretions. This results in an overall effect where the luminal fluids of the small intestine are predominantly buffered by bicarbonate at low molarity values (28,149).

In contrast, during the drug product development process, formulations are tested in highly concentrated pharmacopeial phosphate-based buffers (e.g. 50mM phosphate buffer). However, the concentration of phosphates in the human gastrointestinal luminal fluids is insignificant, which makes the use of phosphate-containing media poorly representative of the human intestines. Hence, there is a disconnect between the *in vivo* environment that the product is exposed to and the *in vitro* test setting regarding buffer species (carbonate vs. phosphate) and buffer molarity (88). Using buffer systems that are not reflective of the *in vivo* environment during the pharmaceutical development phase can be misleading and cause poor selection of prototype formulations for a BE study.

Another important aspect to consider is the physicochemical properties of the active pharmaceutical ingredient (API). Acidic APIs can create a low pH microenvironment on the inner side of the coat, which can be a further hindrance to the coat dissolution (88). Since bicarbonate buffer (BCB) does not promote prompt dissolution of the enteric coating, such acidifying effect is pronounced in physiological environments.

In vitro - *in vivo* correlation/ relationship (IVIVC/R) constitute an important tool for formulation development, mainly for modified-release systems, aiming to optimize prototypes, reduce the number of BE studies during the development, supporting post-approval changes and setting dissolution limits (308,309). In this context, IVIVC/R works as a powerful mathematical model linking an *in vitro* property of a dosage form to a relevant *in vivo* response, making possible a rational development based on *in vitro* biopredictive conditions (29). Despite of its

powerful application in the development of formulations, an IVIVC/R with significant predictability power is more difficult to obtain for highly variable drug and drug products (29,310), especially when these formulations are administered with meals. In such cases *in vitro* - *in vivo* relationships can be valuable.

In this study we reassessed two pantoprazole EC formulations from a failed BE study under fed conditions. These were chosen as model formulations because they were coated with methacrylic acid - ethyl acrylate copolymer (widely used as coating materials) and pantoprazole is a basic API, hence an API acidifying effect on the inner side of the coat can be ruled out. The provided *in vivo* data presented an extremely delayed opening of the formulations together with a great variability. We hypothesized that the release profile in physiologically relevant BCB would detect possible performance differences between test and reference formulations enabling more accurate IVIVR results and predictability. Thus, the objective of this study was to establish a relationship between the *in vitro* performance of test and reference formulations (both in BCB and pharmacopeial phosphate buffer) with the *in vivo* BE study results using the IVIVC module present on GastroPlus®.

8.2 Materials

Sodium phosphate monobasic monohydrate and sodium hydroxide were purchased from Fisher Scientific (New Jersey, USA), sodium bicarbonate was purchased from Caledon (Ontario, Canada), pantoprazole sodium was purchased from Sigma-Aldrich Co. (Montana, USA). The EC pantoprazole formulations were kindly donated by a pharmaceutical industry. Both formulations were coated with the same polymer (methacrylic acid - ethyl acrylate copolymer). Buffer solutions were prepared with purified water (Elgastat Maxima UF and an Elgastat Option 3B water purifier by ELGA Laboratories Ltd. (Mississauga, ON, Canada).

The excipient compositions of the formulations as available in the drug leaflet are described below.

Reference: sodium carbonate, mannitol, povidone, calcium stearate, hypromellose, titanium dioxide, iron oxide (yellow), propylene glycol, methacrylic acid-ethyl acrylate copolymer, sodium laureth sulfate, polysorbate 80 and triethyl citrate.

Test: sodium carbonate, triethyl citrate, iron oxide (yellow), crospovidone, silicon dioxide, titanium dioxide, calcium stearate, mannitol, hypromellose, macrogol, methacrylic acid-ethyl acrylate copolymer and povidone.

8.3 Methods

8.3.1 *In vitro* dissolution testing

The EC pantoprazole formulations used in the dissolution study were from the same lot as those used in the BE studies and were still within its shelf-life period.

All dissolution tests were performed in a VK 7020 system from Varian Inc. dissolution tester coupled to a VK 8000 autosampler. USP apparatus II with 75 rpm rotation speed was used with dissolution media temperature set at 37 °C.

Dissolution testing was performed according to USP <711> two stage procedure in an acid stage followed by a buffer stage. The acid stage was carried out in 0.1N HCl for 2 hours prior to the buffer stage. The drug release was determined by UV-spec at the end of the 2 hours. The tablets were then transferred to vessels containing 900 ml of pre-heated buffer solutions. The buffer stage was composed of either pharmacopeial phosphate buffer (50mM concentration at pH 6.8) or bicarbonate buffer. The reported bicarbonate concentration in the duodenum under fed state is 10mM with a wide pH range of 3.1 - 6.7 (37,44,186). Hence, a 10mM BCB was used with pH adjusted to 6 by sparging the medium with CO_{2(g)}. The phosphate buffer system was

composed of sodium phosphate monobasic monohydrate (50mM) and sodium hydroxide to adjust the solution's pH. The bicarbonate buffer system was composed of sodium bicarbonate (10mM) dissolved in filtered water.

The pH was monitored using an accumet® AB250 pH-meter from Fisher Scientific (Fair Lawn, NJ, USA). The drug release at specific time points was determined by UV-spectroscopy (288nm wavelength).

8.3.2 Statistical analysis

The Microsoft ExcelTM add-in DDSolver was used to compare the dissolution profiles by f_2 statistics (147). The factor f_2 is a similarity factor that measures the closeness between two profiles. Similarity is indicated by a f_2 value between 50-100.

8.3.3 Bioequivalence study

The plasma concentration-time data for two pantoprazole EC formulations (test and reference) were used in order to investigate a failed BE result under fed condition. The study design was randomized, single dose, two-treatment, two-sequence, four-period (2x2x4) full replicated crossover with a 7-day washout period. Forty-four (44) adult healthy subjects of both genders were enrolled in the study and thirty-five (35) completed the study (70 individual PK data considering the replicated design). Serial blood samples were collected up to 36h post-dose. The study was approved by a Research Ethics Committee and followed the Good Clinical Practices Guidelines (311) and the ethical principles for medical research involving human subjects stated in the Declaration of Helsinki (312). The study followed standard guideline for BE study under fed conditions (313).

8.3.4 Pharmacokinetic data

Since the pharmacokinetics (PK) results were extremely scattered with some subjects peaking much later than others (refer to Figures 8.3 and 8.4 under “Results” section), the mean curve presented an “artificial” double peak. Hence, the mean curve was not reflective of the real absorption pattern of the EC pantoprazole formulations, thence not suitable to be used in the IVIVR studies.

For this reason, the subjects were divided into three cohorts of T_{max}, namely: (1) 2.0-3.5h, (2) 4.0-5.5h, and after (3) 6.0h. The cohorts were chosen based on the first observed T_{max} among all the subjects (i.e. 2 hours) and a 1.5h increment size was used as the cut off between the cohorts.

Cohort 1 represents those subjects that would have the “expected” plasma curve profile if the enteric coating would rapidly dissolve upon reaching the intestines, where the fluid’s pH is above the polymer’s dissolution pH threshold. In other words, there would be no additional delay on the drug release and absorption process once the dosage form has transitioned to the intestines (high pH environment). Hence, the mean plasma curve obtained from the subjects in cohort 1 was correlated with the release profile in phosphate buffer, including the 2 hours period in HCl (in which there was no release).

Cohort 2 represents subjects that had a further delay on the drug release and absorption process. Low buffering capacity and intestinal fluid composition could be the one of the causes for the much more delayed coat opening with further drug release. Hence, the mean plasma curve obtained from the subjects in cohort 2 was correlated with the release profile in bicarbonate buffer. Finally, cohort 3 is a miscellaneous group which includes subjects peaking at various time points, even after 12 hours.

In this way we were able to eliminate the artificial double peak and apply a mechanistic analysis to use a more representative plasma time curve for EC formulations and their corresponding *in vitro* performance. When analyzing the individual PK data no double peak was observed, hence we could conclude that the mean curve presented an artificial double peak.

8.3.5 In silico studies

The IVIVR was built using the commercially available software GastroPlus[®] (v 9.7; Simulations Plus, Lancaster, CA). The physicochemical parameters of pantoprazole (e.g., pKa, pH-solubility profile, LogP and permeability) were obtained from its chemical structure using the ADMET Predictor[®] module in GastroPlus[®]. Additionally, the dose number (D_o), absorption number (A_n) and dissolution number (D_n) were calculated.

The human pharmacokinetic parameters were obtained from the intravenous administration data reported by Simon et al, 1990 (314) fitted to a compartmental pharmacokinetic model using the PKPlus[®] module (Simulations Plus, Lancaster, CA). The developed compartmental PK model was validated using external data from an oral administration of EC pantoprazole under fasted state obtained from the literature (315).

The validated model was used to build the reference and test formulations databases. The dosage form “DR: Tablet Enteric Coat” was selected and the dose was set to 40 mg (as used in the BE study). The default absorption model ASF Opt logD Model SA/V 6.1 was selected using the human physiology in the fed state.

The experimental dissolution data in both bicarbonate and phosphate buffer for each formulation was loaded (as *.dsd files) along with the selected oral plasma curves from zero to t_{last} (as *.opd files) for both cohorts 1 and 2.

8.3.6 *In vitro* – *In vivo* Relationship

The IVIVCPlus™ module was used to develop the correlations. The pantoprazole *in vivo* fraction absorbed (absolute bioavailability rate) was calculated by numerical deconvolution of the selected oral plasma concentration- time profile (cohorts 1 and 2) from the BE study (for both test and reference) using the Loo–Riegelman (two compartment) model (Equation 8-1). After deconvoluting, the correlation was formed by comparing the fraction of drug dissolved *in vitro* with the fraction of absorbed drug at the same time points. The correlations were evaluated through regression analysis and the best fit among the functions (linear, power function, second and third order polynomial) was automatically chosen by GastroPlus (316–318).

A numeric convolution was performed using the dissolution data obtained through the compendial method for cohort 1 and the non-compendial method for cohort 2. The predicted plasma concentration–time profile for each cohort was compared to the observed data.

$$\frac{A_T}{V_c} = C_T + k_{el} \int_0^T C dt + k_{12} e^{-k_{21}T} \int_0^T C e^{k_{21}t} dt \quad (\text{Equation 8-1})$$

Where A_T is the amount of drug absorbed between time zero (time of administration) and the blood sampling time, T ($0 < T < t$), V_c is the volume of the central compartment, C_T is the plasma concentration of unchanged drug at time T and k are the rate constants.

8.4 Results

8.4.1 *In vitro* dissolution testing

The pharmacopeial tolerance specification for the acid stage is not more than 10% release after 2 hours exposure to 0.1N HCl. Both test and reference formulations complied to the specification (data not shown). In phosphate buffer the EC products displayed rapid dissolution

and were compliant to the USP tolerance specifications for drug release in the buffer stage of not less than 75% in 45 min (Figure 8.1). However, the f_2 test failed ($f_2 = 45$). Similarly, the dissolution results in bicarbonate buffer failed the f_2 test ($f_2=11$). The comparative dissolution for both formulations in phosphate buffer 50mM vs. BCB 10mM is presented in Figure 8.1. Not only was the onset of drug release much more delayed in bicarbonate media compared to phosphate buffer, but the difference in performance between test and reference products was much more evidenced in BCB, making it clear that these formulations don't have a similar *in vitro* dissolution performance. The shape of the curves also differed.

The delayed opening of the formulations in BCB can be linked to the distinct pattern of coat dissolution between the two media. In phosphate buffer the coat around the tablet rapidly dissolved and the tablet core was exposed to the dissolution medium, allowing fast disintegration and drug release. In BCB, however, the coat did not dissolve instantly, but presented ruptures through which the water could penetrate and reach the tablet core. The ruptures (“tearing” on the coating material) were detected by visual inspection of the tablets in the dissolution vessel (schematic picture is shown in Figure 8.2). This was reflected in the slower disintegration of the dosage form further delaying the drug release. This points out to the slower dissolution rate that EC polymers have in BCB.

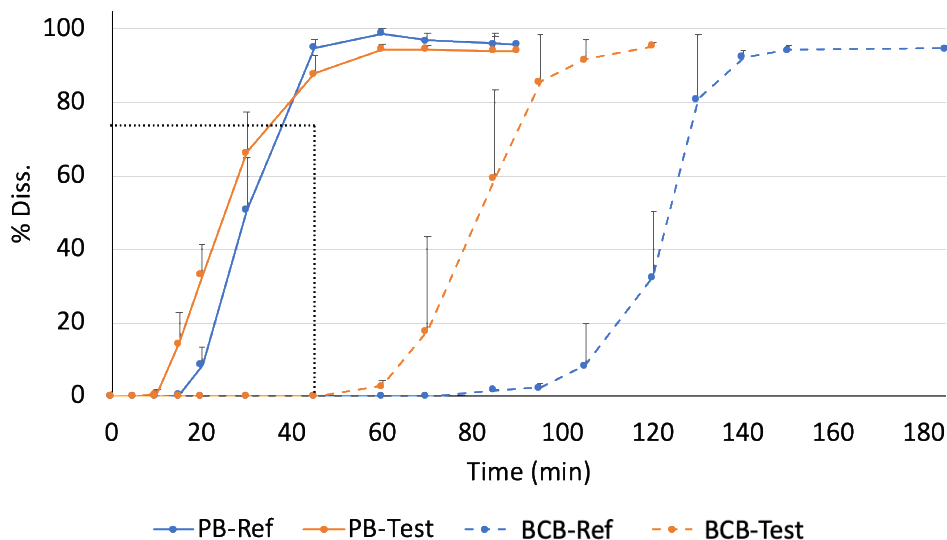


Figure 8.1. Dissolution profile of pantoprazole EC formulations in the buffer stage (mean \pm SD; n=3). Orange: test; blue: reference; solid line: phosphate buffer (PB); dashed line: bicarbonate buffer (BCB); Dotted black line: USP dissolution specification.

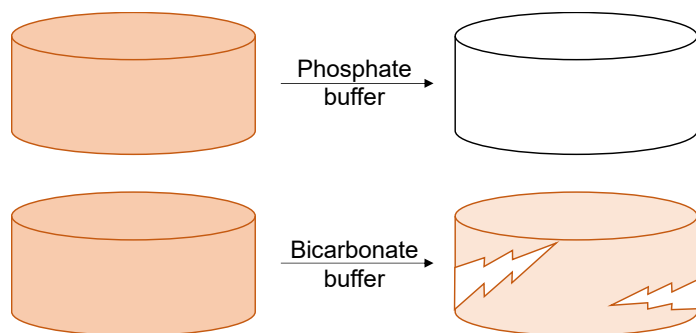


Figure 8.2. Schematic picture of the contrast between phosphate buffer and bicarbonate buffer. In phosphate buffer the coating material rapidly dissolved, leaving the tablet core exposed to the dissolution medium (Top), whereas in bicarbonate buffer the coating presented ruptures instead of completely dissolving (Bottom).

8.4.2 Pharmacokinetic data

Figures 8.3 and 8.4 show the plasma concentration data for each subject of the BE study performed under fed condition for the reference and test formulations, respectively.

The following final results have been reported by the failed BE study: geometric mean ratios between test:reference (90% confidence intervals) for C_{max} and AUC_{0-t} were 79.23 % (69.13 – 90.80 %) and 83.45 % (75.84–91.82 %), respectively.

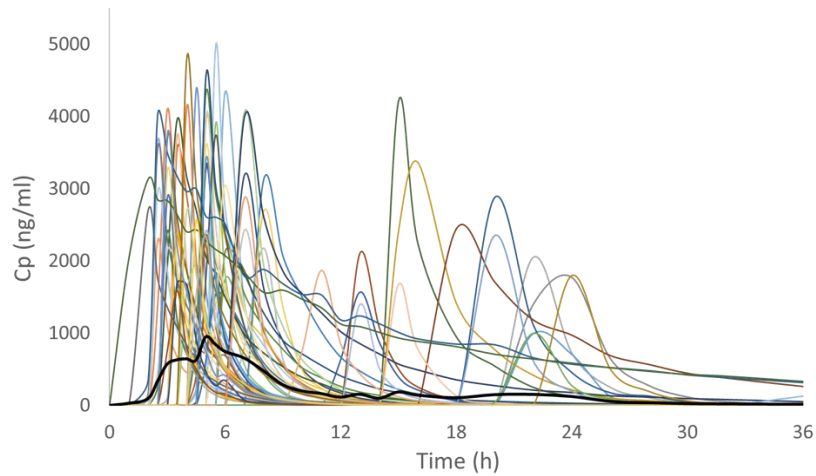


Figure 8.3. Plasma concentration-time curves of reference formulation after oral administration under fed condition (N = 70). Highlighted black line: mean curve.

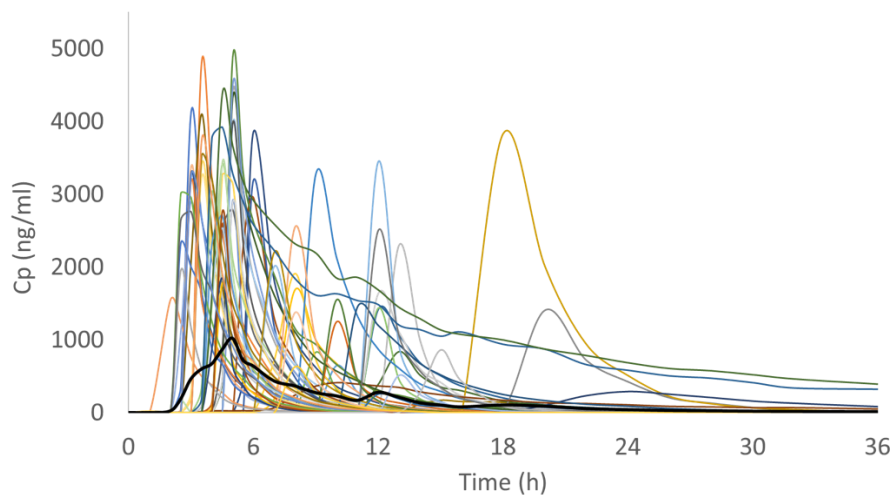


Figure 8.4. Plasma concentration-time curves of test formulation after oral administration under fed condition (N = 70). Highlighted black line: mean curve.

8.4.3 Cohorts

Table 8.1 shows the number of subjects in each Tmax cohort. Figures 8.5 and 8.6 show the mean plasma concentration profile for the subjects in cohort 1 and cohort 2, respectively. For both test and reference formulations a number of 10 same subjects fell into cohort 1 (48% and

59% of total for reference and test formulations, respectively) and 11 same subjects fell into cohort 2 (50% of total).

It's interesting to notice that in BCB the *in vitro* onset of drug release for the test formulation was at least 40 minutes earlier than the reference, and was nearly zero order. The reference formulation shows a longer lag time with a slower initial release followed by a zero-order release. Both release patterns can also be seen in the PK data presented in Figure 8.6, reinforcing how the results in BCB seems to be representative of this population set.

Table 8.1. Number of subjects per Tmax cohort for both test and reference formulations

Tmax cohort	Number of subjects	
	Reference	Test
Cohort 1 (2.0-3.5h)	21	17
Cohort 2 (4.0-5.5h)	22	22
Cohort 3 (After 6.0)	27	31
Total	70	70

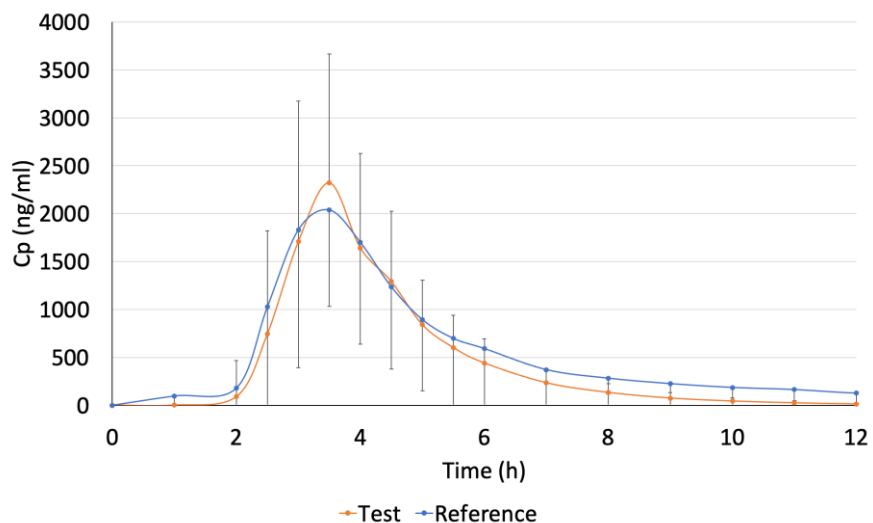


Figure 8.5. Plasma concentration-time curves of test and reference formulations for Tmax Cohort 1. Data are shown as mean \pm SD.

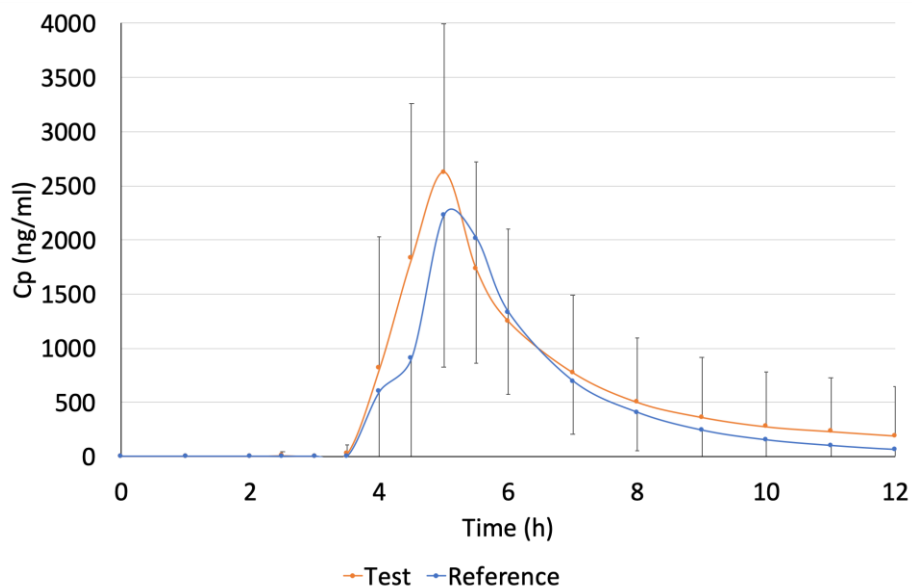


Figure 8.6. Plasma concentration-time curves of test and reference formulations for Tmax Cohort 2. Data are shown as mean \pm SD.

8.4.4 In silico studies

A 2-compartment PK model was established using the IV data in PKPlusTM. The PK parameters are as follows: Cl (L/h/Kg): 0.089; t_{1/2} (h): 1.94; K₁₂ (h⁻¹): 0.294; K₂₁(h⁻¹): 0.501. The model validation with oral administration had a correlation coefficient of 0.862.

The physicochemical parameters derived from the drug's chemical structure are as follows: pKa of 9.15 (acid) and 3.55 (base), LogP of 1.5, effective permeability of 1.41×10^4 cm/s; D_o = 0.0973; A_n = 2.823 and D_n = 54.06.

Based on this result, the 2-compartment Loo-Riegelman deconvolution method was used to generate the fraction absorbed and the best correlation fit was formed through a power function. Table 8.2 presents the IVIVR statistical information for test and reference using both bicarbonate and compendial dissolution data.

Table 8.2. Deconvolution statistical results for both Test and Reference

	Reference		Test	
	Cohort 1 (PB)	Cohort 2 (BCB)	Cohort 1 (PB)	Cohort 2 (BCB)
Power Function[#]	$y=0.941(x)^{1.892}$	$y=0.833(x)^{91.42}$	$y=1.505(x)^{12.90}$	$y=0.952(x)^{86.83}$
Rsqr	0.805	0.99	0.894	0.975
SEP	0.189	0.04	0.124	0.073
MAE	0.15	0.027	0.092	0.049
AIC	-1.333	-67.7	-19.67	-40.83

[#]where x = Fraction *in vitro* release and y = Fraction absolute bioavailability

BCB: Bicarbonate buffer 10mM; PB: Phosphate buffer 50mM

The dissolution data in both PB and BCB had a good fit to the respective *in vivo* data, as shown by the correlation coefficient (Rsqr) and Akaike information criterion (AIC) values. The *in vitro* data in BCB (for both test and reference) yielded in a superior fit than PB, which can be clearly seen in Figure 8.7.

The formed correlations were then used to convolute the data and predict the plasma concentration-time profiles. Table 8.3 presents the validation statistics of the convolution for C_{max} and AUC. The predicted vs. observed plasma concentration-time profiles for Cohorts 1 and 2 are shown in Figures 8.8 and 8.9, respectively. The simulated plasma concentration vs. time curves were generally in agreement with the observed clinical results in Cohort 2 (Figure 8.9).

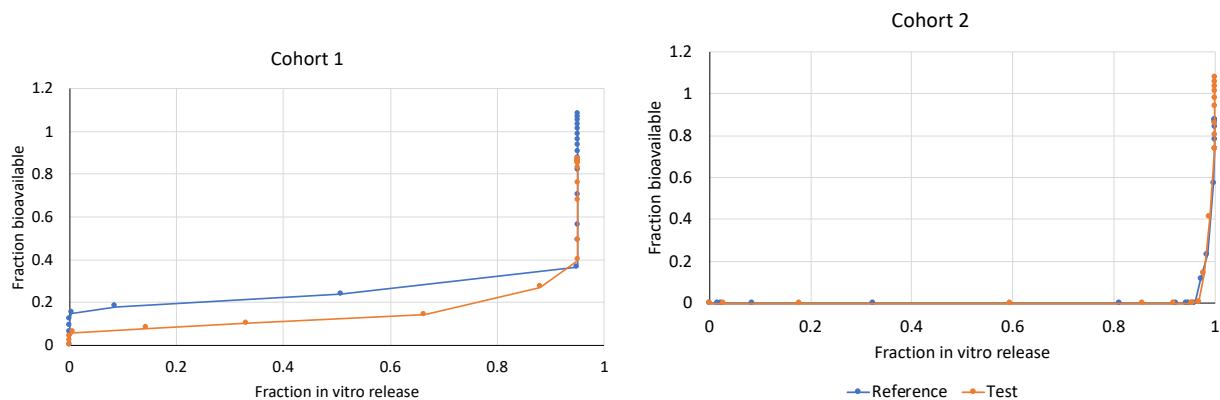


Figure 8.7. IVIVR graph. The compendial buffer *in vitro* data was correlated with the *in vivo* data from Cohort 1 and the *in vitro* data from bicarbonate buffer was correlated with the *in vivo* data from Cohort 2.

Table 8.3. Convolution validation statistics for Test and Reference

	Cmax		% Pred error	AUC		% Pred error	Rsq	SEP	MAE	AIC
	(ng/mL)			(ng/mL*h)						
	Obs.	Pred.	Obs.	Pred.						
Reference										
Cohort 1 (PB)	2037	4472	119.5	6668	5165	22.5	0.766	467.8	341	259.2
Test										
Cohort 1 (PB)	2321	4064	75.1	5388	4900	9.05	0.723	636.2	314.2	269.7
Reference										
Cohort 2 (BCB)	2227	2774	24.5	5435	5176	4.7	0.952	183.6	109.9	227.4
Test										
Cohort 2 (BCB)	2624	3538	34.8	6546	5940	9.2	0.909	294.1	204.8	243.4

BCB: Bicarbonate buffer; PB: Phosphate buffer

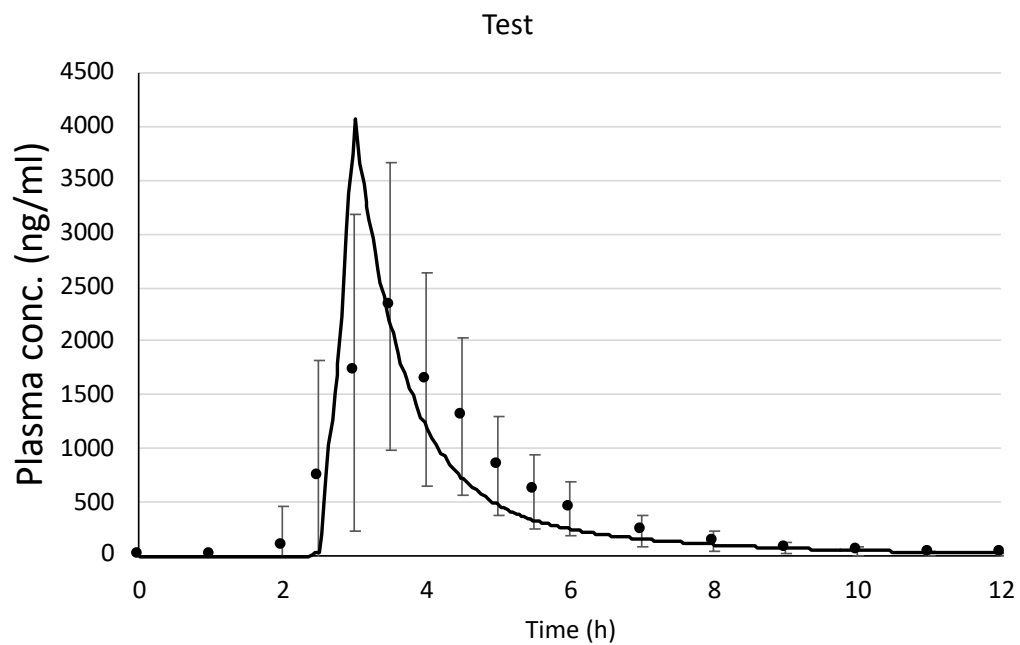
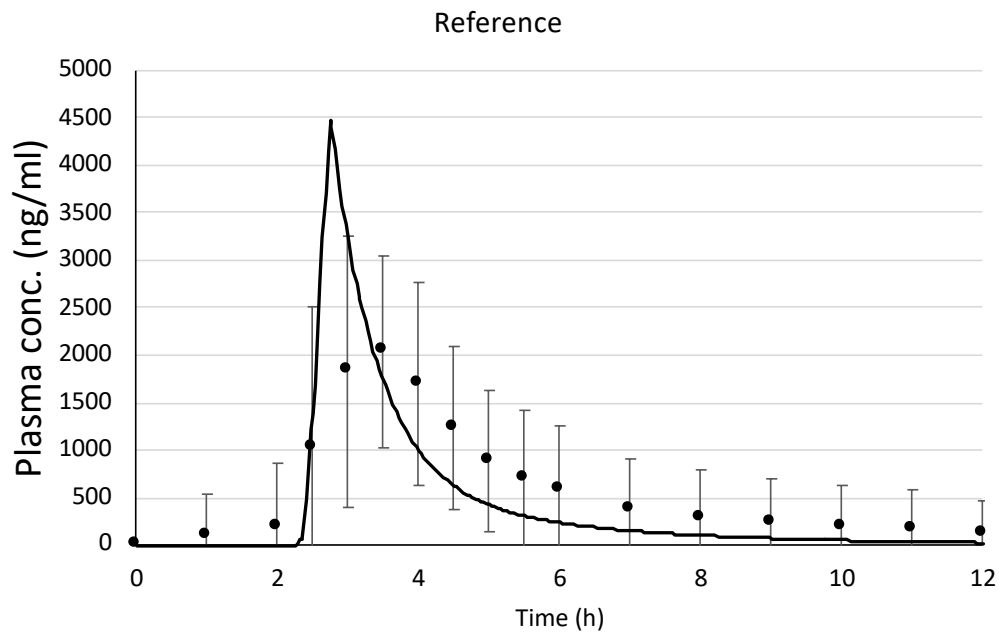


Figure 8.8. IVIVR model predicted (lines) vs. observed (circles, mean \pm SD) plasma concentration-time profiles for Cohort 1 (prediction using phosphate buffer dissolution data).

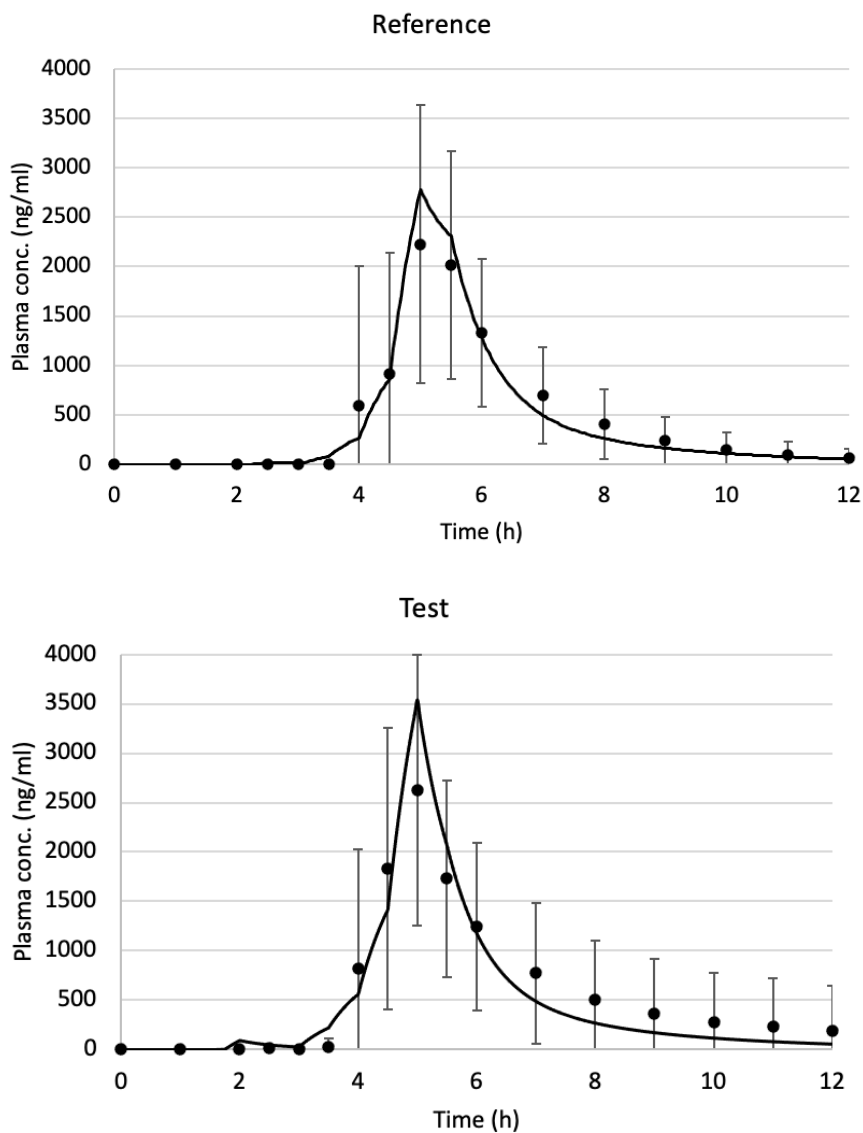


Figure 8.9. IVIVR model predicted (lines) vs. observed (circles, mean \pm SD) plasma concentration-time profiles for Cohort 2 (prediction using bicarbonate buffer dissolution data).

8.5 Discussion

Enteric coating polymers are polyacids which are insoluble at acidic pH values(305). The generally accepted concept regarding such polymers is that they will promptly dissolve once exposed to a medium with pH higher than its dissolution pH threshold. However, studies have shown that buffer molarity and species are of primary importance for the dissolution process of such polymers (88). There are many reports in the literature showing the great *in vivo*

variability related to EC formulations, both intra and inter subject (28,88) (and references cited thereby). This may be due, in part, to the intestinal buffer composition. The buffer system in the human gastrointestinal tract is mainly bicarbonate based and the performance of EC formulations in this system can be quite different compared to compendial phosphate buffer (88,239) (Figure 8.1), which is often used in the drug product development.

Considering this, using more physiologically relevant dissolution conditions can give a better mechanistic understanding of the *in vivo* performance of a given formulation (38). Physiologically relevant conditions can be defined as one that simulates the *in vivo* dissolution environment in one or more aspects beyond the typical quality control/batch release method (17). More complex formulations, such as delayed release, can be best evaluated using such conditions that incorporate the main parameters driving *in vivo* drug release and dissolution (319).

The selection of a prototype formulation to proceed to a BE study relies mostly on the similarity of the *in vitro* performance of test and reference. In most cases, the generic industry seeks for the simplest, quickest and cheapest *in vitro* methods and standards (17). Additionally, a one-time point collection at the USP specification is usually the practice in the industry instead of drawing the whole profile and, many times, meeting the specification is “good enough”. However, as this study has shown, similar *in vitro* performance using compendial conditions and compliance with USP specifications does not guarantee similar *in vivo* behavior, which may lead to failure in a BE study.

The USP specification for delayed release tablets is >75% release at 45 minutes (7). This means that the products being compared could release the API faster than the other, while satisfying the standard for drug dissolution. The results in Figure 8.1 and the f2 statistical analysis clearly show that, in spite of the fact that the test and reference formulations met the compendial

specification, they already failed f2 in phosphate buffer. This was even more pronounced in BCB, where a clear distinction between the two formulations can be seen. Based on the f2 results we can see that BCB, a physiologically relevant system, could differentiate the *in vitro* performance of test and reference products more clearly than the compendial conditions.

However, even with bicarbonate-based media, a case by case study is a more valuable approach instead of using a “one fits all” condition and specification (319,320). In the last decades, many non-compendial dissolution methods have been proposed in attempt to mimic the *in vivo* environment and the incorporation of such data into *in silico* PK models is an ongoing challenge (319).

Due to the high buffer capacity of compendial PB, the coat opening with further drug release is readily prompted. Differently, the equilibrium kinetics of BCB at the solid-liquid interface (diffusion layer) results in an effective bicarbonate pKa lower than the interfacial pH value needed for the EC polymer's dissolution (85,88). The pKa of the BCB system in the bulk solution is around 6.04. However, at the solid-liquid interface (diffusion layer) around the dissolving EC polymer the hydration/dehydration reaction ($H_2CO_{3(aq)} \rightleftharpoons H_2O_{(l)} + CO_{2(aq)}$) does not typically reach equilibrium. This results in the effective pKa of bicarbonate in the diffusion layer to be lower than the bulk value (6.04) but higher than the intrinsic pKa of 3.30 ($H_2CO_{3(aq)} \rightleftharpoons H^+_{(aq)} + HCO^-_{3(aq)}$). Therefore, BCB has a limited ability to buffer the pH of the dissolving polymer's surface and cannot promote prompt dissolution and opening of the coat. This presents a major difference between BCB and phosphate buffer and is clearly seen in Figure 8.1. Such delay in the coat opening/dissolution was captured in the physiologically relevant dissolution medium.

The main difference in the release profiles in the compendial vs. non-compendial methods was the onset of drug release, and not the API dissolution rate / extent released. Once the coating polymer starts to dissolve/ open the drug can be released from the tablet core. Pantoprazole is a BCS class III drug (high solubility/ low permeability) (315), hence the API dissolution, once release from the dosage form, is not likely to be a major issue but cannot be ruled out completely. The dose D_0 of 0.0973 indicates that pantoprazole is a drug with high solubility. The calculated dissolution number refers to the time required for drug dissolution (ratio of the intestinal residence time to the dissolution time). Hence, the higher the dissolution number the higher will be the fraction-dose absorbed. The calculated D_n of 54.06 indicates that dissolution is faster than transit.

If pantoprazole is a BCS III drug, then permeation across the GI membrane could be a rate-determining step to absorption for the formulations studied. However, according to ADMET predictor, pantoprazole has a calculated P_{eff} of 1.41×10^4 cm/s, which is roughly on the borderline of low/high effective permeation rate. Additionally, An A_n larger than 1 suggests complete absorption. The calculated A_n was 2.823, which indicates that, even though pantoprazole is a borderline BCS III drug, it is well and completely absorbed. These observations make it evident that the main issue with the tested products is the opening of the coat.

On one hand, there were a number of subjects (cohort 1) in which the *in vitro* results in phosphate buffer correlated with the *in vivo* data, as shown in Table 8.3 and Figure 8.8. Even though there was an overprediction for C_{max} , the overall behavior and AUC had a good fit. However, this would only be predictive of a small portion of the entire study group, which can be misleading and eventually culminated in the failed BE study – if decisions were taken solely based the compendial results. Such data represent the “text book” knowledge concerning EC

formulations, which is no release in the stomach (acidic media stage) followed by prompt release in the intestines (phosphate buffer stage), i.e. classic behavior of pH-responsive polymers.

The overprediction of C_{max} further reinforces the impact not only on the onset but also on the extent of absorption when EC formulations are administered. This is in line with clinical observations. There are several reports in the literature comparing the administration of a given API in an EC formulation *versus* a non-coated formulation (230,235,250,261). In all cases, EC formulations presented a later T_{max} and much lower C_{max} , and in some cases there was complete failure, hence both the rate and extent of absorption can be compromised with the poor *in vivo* performance of EC formulations.

The dissolution of the coating in phosphate buffer is very prompt, which allows complete release of the API from the tablet core because the coating is no longer preventing the release. In PB both extent and onset of release are “ideal”, i.e. complete release in a short period of time. If this were the *in vivo* situation, after the dosage form reached the intestines, rapid drug dissolution would take place, making the whole administered dose available for absorption. Based on this we can understand the overprediction of C_{max} by the *in silico* model.

On the other hand, as mentioned before, buffer molarity is also of utmost importance for EC formulations, even if the medium pH is above the polymer’s dissolution pH threshold. This was represented by cohort 2, in which the results in BCB were predictive of, as shown in Table 8.3 and Figure 8.9. The correlation using BCB was very accurate in terms of C_{max} , AUC and T_{max} , demonstrating how powerful physiologically relevant dissolution methods can be. However, similarly to phosphate buffer, this would only be representative of a portion of the entire study group. The deconvolution results presented in Table 8.2 and Figure 8.7 also point

out the superiority of BCB in relation to PB. The *in vitro* release shape obtained in BCB correlates better with the *in vivo* observed data than PB.

Considering this, we see that both tests hold their importance and shouldn't be treated as "either or" but as complementary results for a robust development process. A formulation that meets USP criteria and presents a similar behavior under both test conditions would increase the chances to establish bioequivalence between the products. Also, subjects from cohorts 1 and 2 outnumber cohort 3 (61.4% vs 38.5% for reference and 55.7% vs 44.2% for test) and would probably give enough statistical power for a successful BE study. Hence, using both *in vitro* methods would greatly benefit the industry by bringing *in vivo* studies successfully over the finish line of BE.

The pattern presented in all cohorts, especially for cohort 3 can be due to a number of factors. The great PK data variability observed both inter and intra individuals (Figures 8.3 and 8.4) is a result of the many layers of complexity when conducting a BE study with a delayed release formulation in the fed state. A major source of variability for enteric coated drug products after postprandial application is gastric emptying time. Certain variability of gastric residence time under fasted conditions is expected depending on the time relative to phase III of the interdigestive migrating complex when stomach content is cleared. Under fed conditions the gastric emptying depends on the amount, the composition (caloric density), and temperature of food culminating in higher variability. During the postprandial phase large monolithic dosage forms are generally retained by the pylorus and are only allowed to pass to the duodenum during phase III motility movements of the subsequent interdigestive phase.

Drug absorption is not only influenced by the physicochemical properties of the drug itself, but formulation effects including excipients and many physiological factors also play an

important role. Physiological factors that can affect bioavailability include, but are not limited to, gastric emptying time, intestinal motility, blood flow rate, gastrointestinal pH, first pass metabolism, circadian rhythm, presence of food and meal composition (321). Under the fed state many changes occur in the GI tract, such as secretion of gastric acid, bicarbonate, bile and pancreatic fluids as well as modification of gastric and intestinal motility patterns. All of these can greatly influence the drug absorption pattern and thus be a source of variability in BE studies (321,322).

The high *in vivo* variability of Pantoprazole observed for the BE study corroborates the findings published by De Campos et al., 2007 (315), where it was observed that, in the fed state, the intra-subject variability is much higher than in the fasted state. In addition, as observed by De Campos et al., 2007 (315), the inter-subject variability of T_{max} is also expected to be higher under fed condition.

As required by many regulatory agencies, a bioequivalence study under fed condition (in addition to a fasting study) is necessary for registering a delayed-release formulation. Thus, considering that this type of formulation shows a high variability *in vivo* when administered in the fed state, new approaches based on biopredictive dissolution conditions, as well as computational tools should be considered as part of the development routine of pharmaceutical industry and research centers. In these cases, IVIVC/R should be viewed as a multidisciplinary tool to predict *in vivo* dissolution through *in vitro* assays (317). Many compendial methods were set decades ago before biopredicability was a concern, hence they might fall short in establishing a successful IVIVC/R.

The use of biopharmaceutical tools to link *in vitro* performance to measured human exposure is therefore critical to understanding the product performance and to optimize

formulations. Its application is indispensable for better and more efficacious development of drug products with consistent quality for the patients. For this, good quality and meaningful *in vitro* input data is of primary importance for reliable predictions.

The new approach taken in this study covered the use of both *in vitro* methods (compendial and non-compendial) in establishing IVIVRs. Understanding how each method correlates to a different group within the population and then combining these results can benefit the industry in developing products that would meet the expected performance in a broader portion of the population. In the case of BE studies, developing a test product that has a similar performance to the reference in both conditions increases its likelihood to be bioequivalent. This is an innovative analysis and can be a powerful tool in the formulation development process to identify formulations for which BE can be established.

8.6 Conclusion

Using buffer systems that are not reflective of the *in vivo* environment during the pharmaceutical development phase can be misleading and cause poor selection of prototype formulations. However, solely satisfying the standard for drug dissolution does not guarantee similar *in vivo* behavior. Incorporating physiological aspects into the *in vitro* dissolution method can give a better mechanistic understanding of a formulation's *in vivo* performance.

Using physiologically relevant *in vitro* data in combination with compendial results might be a powerful approach to develop a formulation that can have an optimized performance in different population groups, increasing the likelihood for a successful BE study and for a robust formulation development process.

8.7 Shortfalls

The authors recognize that using visual assessment to select the cohorts may seem arbitrary. The cut off at 3.5h for cohort 1 and 5.5h for cohort 2 was done in order to maintain same size of 1.5h increment. The design of the clinical trial seemed to be a highly variable *in vivo* model. This could have decreased the statistical power in detecting differences in the products' biopharmaceutical qualities. The approach taken in this manuscript was done in order to have scientific insight and mechanistic understanding rather than a regulatory application.

**SECTION FOUR: OTHER ASPECTS OF *IN VIVO* DRUG PRODUCT
PERFORMANCE**

The impact of formulation composition and physiology state

CHAPTER NINE

**Are Excipients Inert? Phenytoin Pharmaceutical Investigations with New
Incompatibility Insights**

A version of this chapter is published in:

J Pharm Pharm Sci. 2018;21(1s):29745. <https://doi.org/10.18433/jpps29745>
Reprinted from reference (396).

9.1 Introduction

The U.S. Pharmacopeia defines excipients as substances other than the active pharmaceutical ingredient (API) that are added in a drug delivery system in order to aid in the manufacturing process and enhance stability, bioavailability, safety, effectiveness and delivery of the drug. These substances have been appropriately evaluated for safety (7).

Although excipients are well characterized and evaluated for safety, they can interact with the API chemically or physically (323). An incompatibility can possibly affect the drug delivery performance and bioavailability, leading to loss of quality and potency, and compromising the safety and efficacy of the medication (324,325). Thus, choosing the right excipients based on their function and compatibility with the API is of primary importance for a good quality drug product.

Phenytoin is an anti-epileptic drug related to the barbiturates in its chemical structure (326). Its therapeutic window ranges from 10 to 20 ug/ml. This narrow safety margin makes therapeutic drug monitoring of utmost importance for this drug to maintain drug efficacy and safety (327).

The 1968 phenytoin intoxication outbreak in Brisbane, Australia, is a classic example of an API – excipient interaction (328–330). According to Bochner *et. al.* (330) and the known evidence at the time, patients taking a certain brand of diphenylhydantoin (phenytoin) showed characteristic signs of intoxication related to the medication they were taking. After an extensive investigation the authors concluded that a change in excipient of the medication was the reason behind the changes in bioavailability and resultant intoxication. Studies (330) showed that when administered with CaSO₄ as an excipient the absorption of phenytoin was jeopardized due to an interaction between the API and the calcium salt. When CaSO₄ was replaced in the formulation

by lactose, the amount of phenytoin absorbed was much higher, resulting in the observed intoxication.

Bochner *et. al.* (329) investigated capsules containing CaSO₄ as an excipient taken by the patients and compared the solubility of the API in the formulation with that of phenytoin sodium. The study concluded that the solubility of phenytoin sodium had changed prior to ingestion and absorption was reduced. This finding alongside the recovery of phenytoin from the patient's feces confirmed their hypothesis of decreased alimentary absorption of phenytoin. The authors speculated that the formation of a calcium salt of phenytoin might be responsible for the much lower solubility.

The purpose of this study was to investigate further the interactions between excipients and phenytoin to mechanistically re-examine the hypothesis and interpretations of the previous studies.

9.2 Materials

Phenytoin USP grade and Calcium Sulfate NF were purchased from PCCA, USA (Houston, TX, USA; LOT: C172948 and LOT: C178073, respectively). Phenytoin sodium USP grade was obtained from Medisca® (Saint-Laurent, QC, Canada; LOT: 612840/A). Calcium chloride was purchased from Sigma-Aldrich. Lactose monohydrate was used from Meggle Wasserburg, Germany. Parteck® SI 150 (Sorbitol) was purchased from EMD Chemicals Inc. (Darmstadt, Germany; LOT: M285083). Regular milk and lactose free milk was purchased from a local grocery store and used before the expiration date. The powder mixture samples were put in glass ampoules and analyzed by thermal activity monitor III (TAM III) (TA instruments, USA). Commercial extended phenytoin sodium capsules were purchased: Dilantin (Pfizer Canada Inc, lot # T25924, exp. 05/2019), APO-Phenytoin Sodium (Apotex Inc. Toronto, Canada, lot #

NH9926, exp. 01/2019), Taro Pharmaceuticals U.S.A. Inc. (lot # 316157, exp.03/01/19), Akyma Pharmaceuticals (Amneal), U.S.A., LLC. (lot # HL16617, exp.03/01/19).

Water for the dissolution tests and high-performance liquid chromatography (HPLC) analysis was purified by Elgastat Maxima UF and an Elgastat Option 3B water purifier by ELGA Laboratories Ltd. (Mississauga, ON, Canada) and then filtered. Gelatin capsules size 0 were used for the dissolution tests.

9.3 Methods

9.3.1 Titration

A phenytoin solution was prepared by adding 1.4g of phenytoin into a 250 mL of an alkaline NaOH solution. One portion of the phenytoin solution was titrated with calcium chloride (CaCl_2) in solution and the other portion with lactose solution. ^1H NMR was performed to analyze the precipitate obtained in the titration with the CaCl_2 solution.

9.3.2 Calorimeters experiments

Samples were analyzed by thermal activity monitor III (TAM III) (TA instruments, USA) to investigate excipient-API interactions, e.g. as solid-state reactions or in solution. The microcalorimeter ampoule experiment was selected and the experiments were performed at 40°C.

Two scenarios were investigated: dry powder mixtures and water (1 ml) added to the powders mixtures, as described in Table 9.1. After adding the given compound combination into the ampoules, they were vortexed yielding a homogenous mixture, and then put into measuring position in the calorimeter. The experiments ran for a minimum of three days and ended after a flat line was obtained.

Table 9.1. Powder mixtures composition used in the calorimeter experiments

Dry powder mixtures	Powder mixtures with water
Phenytoin sodium	Phenytoin sodium
Calcium Sulfate	Calcium Sulfate
Phenytoin sodium	Phenytoin sodium
Lactose	Lactose
Phenytoin	Phenytoin
Magnesium Sulfate	Lactose
Phenytoin	Lactose*
Sodium Sulfate	
Phenytoin	Phenytoin*
Calcium Sulfate	
Phenytoin sodium*	Phenytoin sodium*
Phenytoin*	Water*
Calcium Sulfate*	Calcium Sulfate*
Lactose*	
Magnesium Sulfate*	
Sodium Sulfate*	

*Controls

Mixtures of milk with both phenytoin sodium and phenytoin were also analyzed. Furthermore, commercially available capsules from Canada and the United States of America were tested. The content of the capsules obtained from the market was transferred into the calorimeter vials with milk, water or lactose free milk as solvents.

9.3.3 Dissolution tests

Capsules were prepared by adding the powder mixture (API and excipients) one by one using a 2:1 ratio between excipient and API. The excipients used were lactose, CaSO₄ or sorbitol. For the dissolution tests a VK 7020 system (Varian Inc.) coupled with VK 8000 auto sampler (Varian Inc.) was used. All dissolution tests were performed according to the USP monograph “prompt phenytoin sodium capsules” with additional sample points. In brief: USP Apparatus 1, 900 mL dissolution media (water), 50 rpm rotation speed and temperature set at 37.0°C. Samples

were collected at 5, 10, 15, 20, 30 minutes and quantified in a VP-class Shimadzu Scientific Instruments (Kyoto, Japan) liquid chromatograph, equipped with a Lichrospher® 60 RP Select B column (5 µm, 12.5×4 mm).

9.3.4 Statistical analysis

The Microsoft Excel™ add-in DDSolver was used to analyze the dissolution data. The dissolution profiles for the lactose and CaSO₄ containing formulations were compared by f₂ statistics. The factor f₂ is a similarity factor that measures the closeness between two profiles (331). According to the FDA criteria, f₂ value between 50-100 indicates similarity between two dissolution profiles.

9.4 Results

9.4.1 Titration

The titration experiments with CaCl₂ and lactose were performed to verify the precipitation of phenytoin. A precipitate was only obtained when performing the titration with the calcium salt, confirming that, in solution, phenytoin interacted with calcium forming a product compound with low solubility (189,332). Figure 9.1 shows H¹NMR result of the precipitate with calcium chloride, confirming that the precipitate was phenytoin.

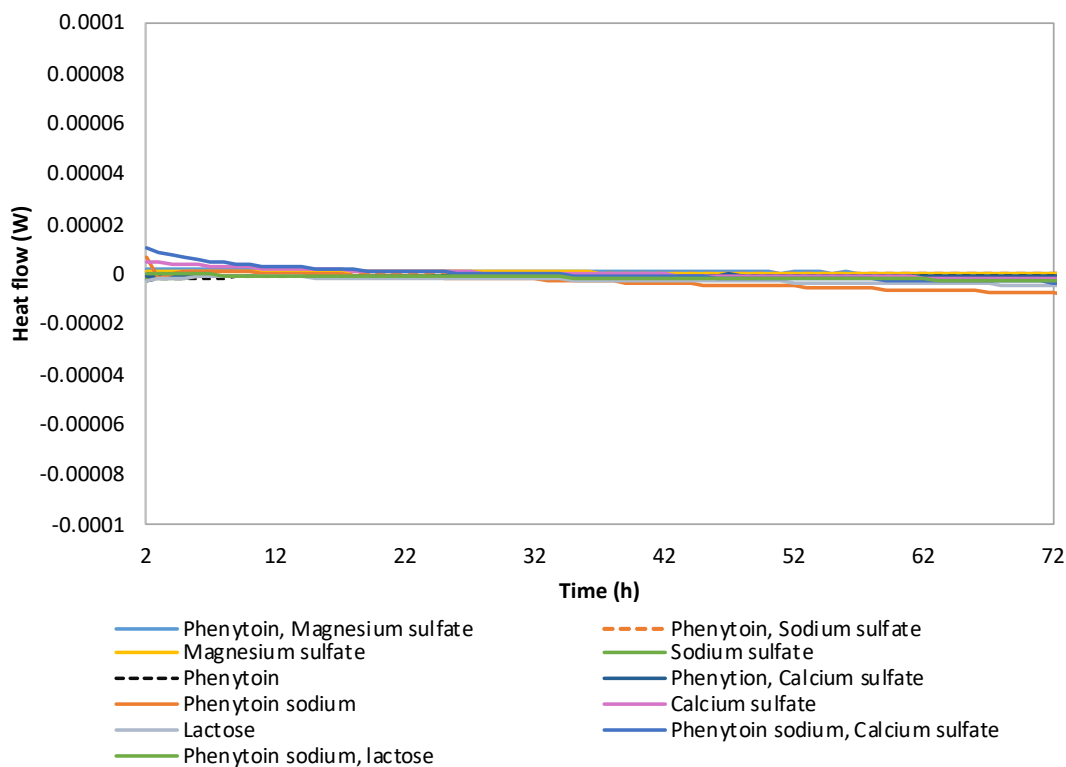


Figure 9.2. Calorimeter experiments result for the dry powder mixtures.

Considering the above, another experiment was conducted with water added to all powder mixtures (Figure 9.3). Phenytoin sodium interacts with calcium sulfate (red line) in the presence of water, and also with lactose (blue line).

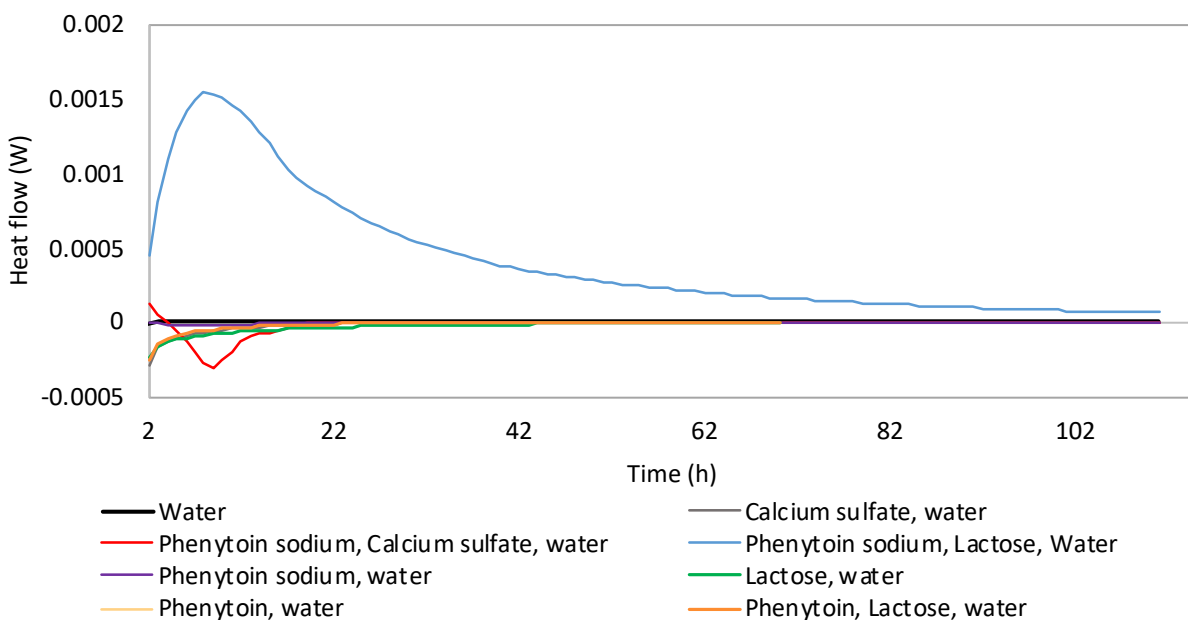


Figure 9.3. Calorimeter experiments result for the powder mixtures with water added.

The ampoule containing phenytoin sodium, calcium sulfate and water mixture formed crystals on the wall of the vial. Hence, both the heat flow (red line in Figure 9.3) and the crystals formed suggest that phenytoin sodium interacts with CaSO_4 in aqueous medium.

The increased heat flow in Figure 9.3 (blue line) corresponds to the mixture of phenytoin sodium, lactose and water. After experimental completion, the inside of the ampoule demonstrated the presence of a brown compound formed, suggesting a Maillard reaction in aqueous medium between phenytoin sodium and lactose. The heat flow (blue line in Figure 9.3) and the brown compound formed suggest that phenytoin sodium not only is incompatible with CaSO_4 and precipitates, but it is also incompatible with lactose and reacts. This was further confirmed and verified by HPLC. No phenytoin peak was detected (data not shown) when the brown compound was analyzed, suggesting that phenytoin sodium had been converted into another compound.

However, no reaction between phenytoin as free form and lactose was observed in aqueous media. This shows differential effects of a salt and the free form interacting with an excipient. This was further confirmed by the flat line (orange line) in the microcalorimeter experiment in Figure 9.3. The negative heat flow in the first 22 hours observed for the orange and green lines is suggested to be due to the solubilization of lactose in water.

To further investigate this finding, a calorimeter experiment was performed with mixtures of milk with both phenytoin and sodium phenytoin, as shown in Figure 9.4. Upon completion of the experiment, the vial with the phenytoin sodium and milk mixture yielded a yellow colour, whereas the mixture with the free base and milk did not.

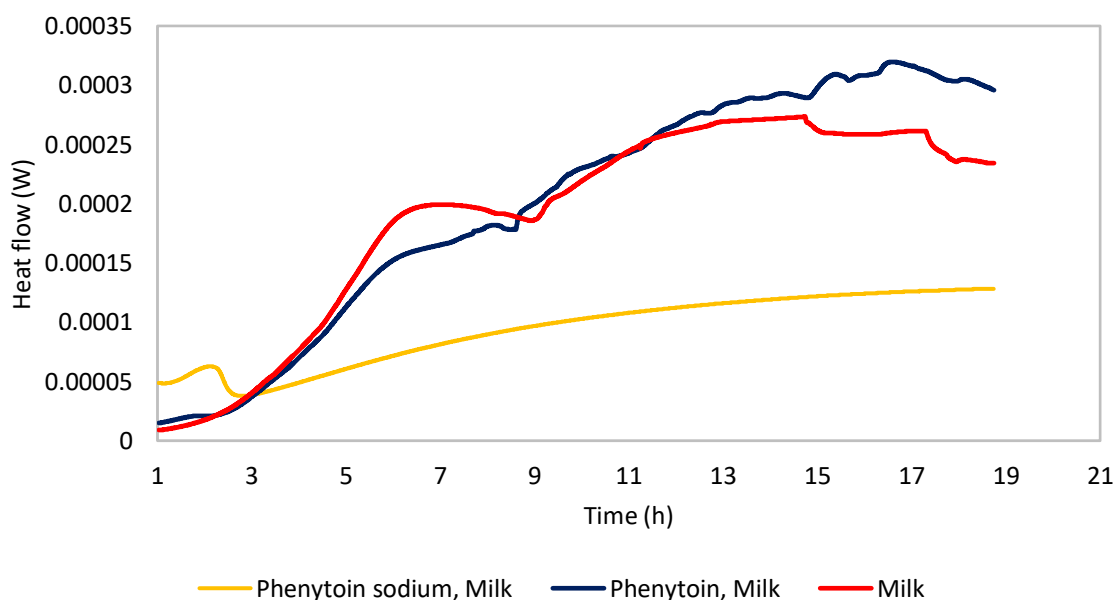


Figure 9.4. Calorimeter experiments result for the mixtures: milk and phenytoin; milk and sodium phenytoin.

Finally, commercially available products were tested with milk to assess whether such a reaction would take place (Figure 9.5). The heat flow indicated that all tested products interacted with milk. This was confirmed by the Maillard reaction which turned the samples brown.

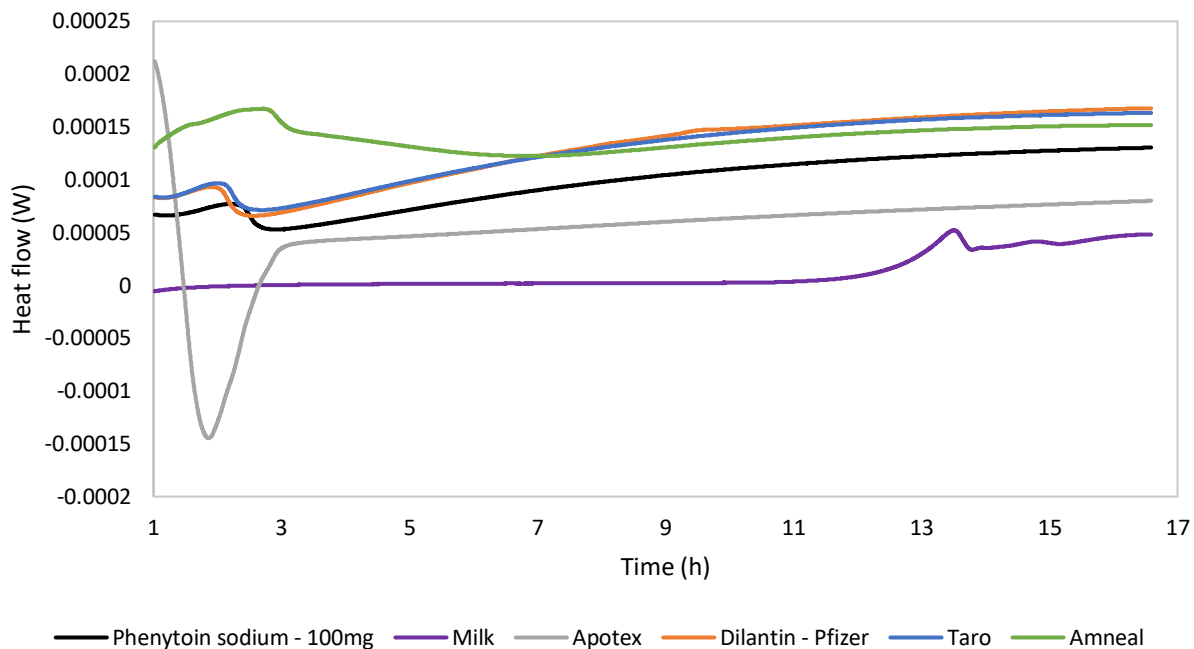


Figure 9.5. Calorimeter experiments result for commercially available extended release phenytoin sodium capsules (100 mg) in milk.

For comparison purposes the above-mentioned formulations were also tested in water and lactose free milk (Figure 9.6). In water, only lactose containing formulations (Dilantin – Pfizer Canada Inc. and Taro Pharmaceuticals U.S.A.) resulted in browning. In lactose free milk a slight tinge of yellow colour was obtained for the non-containing lactose formulations due to traces of lactose in the product.

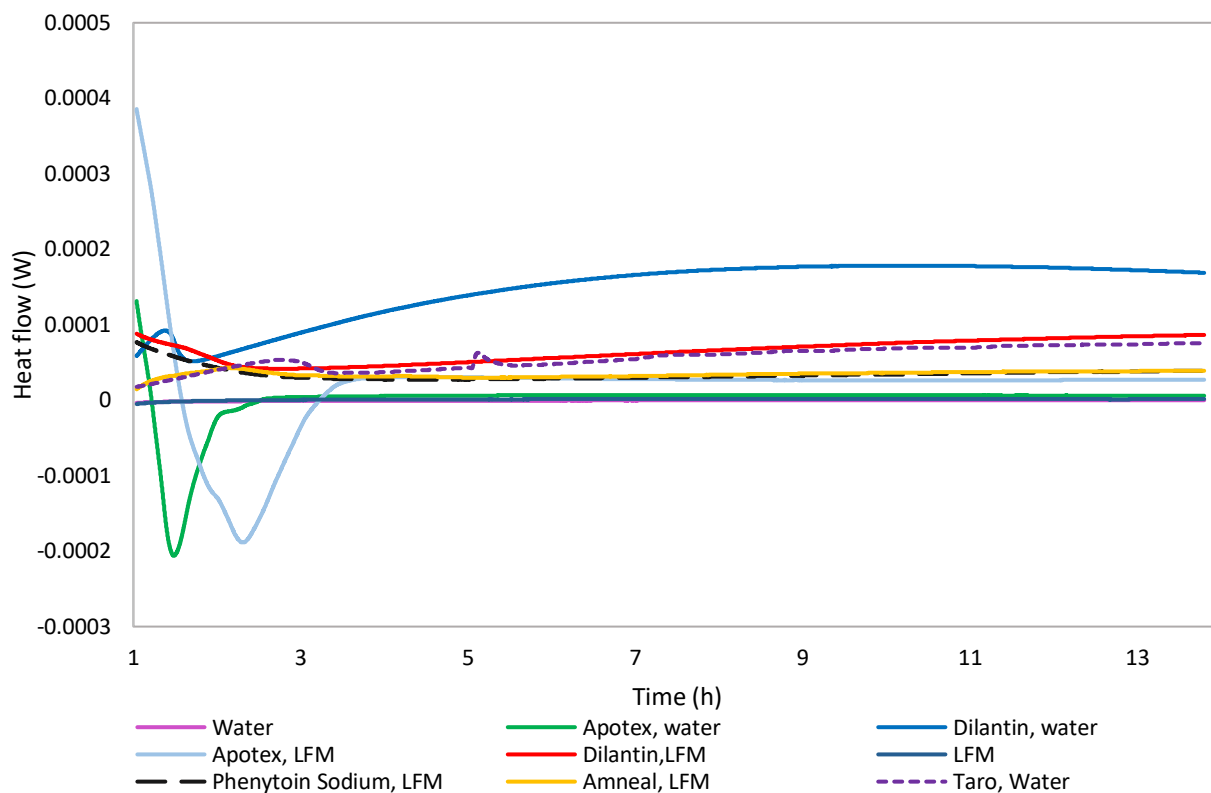


Figure 9.6. Calorimeter experiments result for commercially available extended release phenytoin sodium capsules (100 mg) in water and lactose free milk (LFM).

9.4.3 Dissolution

Dissolution tests using USP apparatus 1, 50 rpm and water 900 mL are the USP recommended parameters for “prompt release phenytoin sodium capsules” (6), this monograph was recently withdrawn from the USP because this dosage form is not used for human use in the United States. However, the capsules prepared by adding the powder mixture (API and excipients) one by one using a 2:1 ratio between excipient and API showed a suitable dissolution profile using this method (Figure 9.7) rather than the official USP method which is for extended release capsules.

As shown in Figure 9.7 and according to the f2 test performed (f2: 52) for the lactose and CaSO₄ containing formulations the dissolution profiles were similar when using water as the

dissolution medium. Since <85% release in 15 minutes was obtained for both profiles, they were compared and found as similar (f_2 test = 52).

The f_2 test was not performed for the sorbitol containing formulation because >85% release was obtained in 15 minutes, demonstrating that the release profile for this formulation is not similar to the other two. Sorbitol was chosen as an excipient because it is not a reducing sugar and it does not interact with phenytoin.

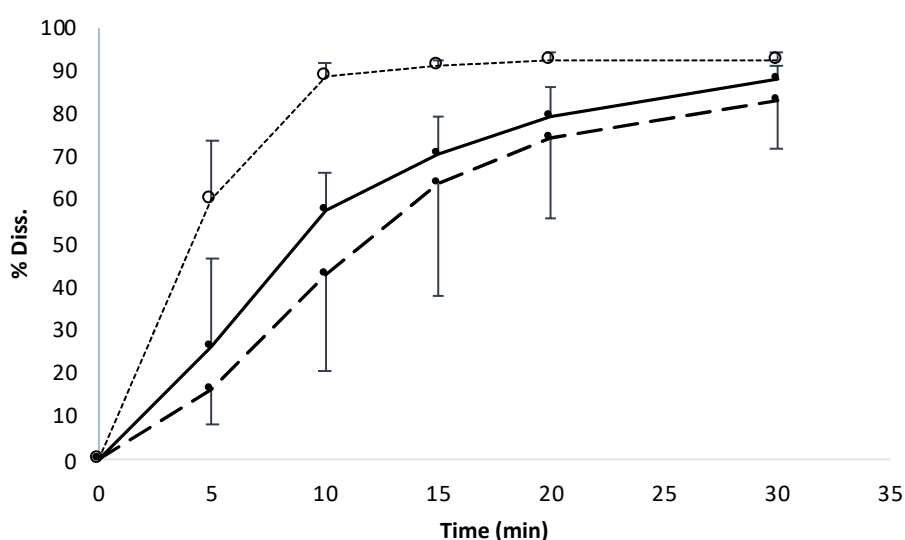


Figure 9.7. Dissolution profiles obtained for phenytoin sodium with lactose (dashed line), phenytoin sodium with CaSO₄ (solid line) and phenytoin with sorbitol (dotted line and open circles) capsules in water.

The formulation containing sorbitol had a higher and faster release rate than the other formulations. At 30 minutes the amount released was statistically different for the sorbitol containing formulation compared to the lactose containing formulation and similar to the formulation with CaSO₄. Our dissolution results demonstrate that the rate but not the extent of dissolution and not solubility was affected.

In addition, the capsules containing lactose were slightly yellow (Figure 9.8) at the end of the dissolution test, implying that a Maillard reaction was occurring at body temperature.



Figure 9.8. Phenytoin sodium and lactose capsules after the dissolution tests. After 30 minutes at body temperature (37.0°C) the capsules became yellow.

9.5 Discussion

In 1972, after studying the phenytoin excipient effect in patients, Bochner *et al* (329) concluded that CaSO_4 interacted with phenytoin sodium forming a compound with different solubility than phenytoin sodium. They reported that, prior to ingestion, the capsules containing CaSO_4 had almost 25% of phenytoin with altered solubility properties, however, the mechanism by which the conversion occurred was not experimentally delineated.

As shown in Figure 9.2, our data cannot confirm a solid-state reaction between CaSO_4 and phenytoin sodium. Our results demonstrated that a reaction occurs (red line in Figure 9.3) in the presence of water. Thus, it is suggested that the interaction between phenytoin sodium and CaSO_4 could occur *in situ* or in a manufacturing process where humidity is used, such as wet granulation. However, we know from discussions with a manufacturer that humidity in the manufacturing process is strictly controlled due to the hygroscopic properties of the API. (Dr. J. Cook, personal communication, November 28, 2017)

A possible explanation for the reduced solubility of phenytoin sodium prior to ingestion in the capsules containing CaSO_4 is the absorption of moisture and CO_2 from the atmosphere providing the needed conditions for the API-excipient interaction to occur (333). Newton DW *et al.* (333) has already reported that in bottles of phenytoin sodium powder the solubility decreased over time due to absorption of moisture and transformation of phenytoin sodium to the free form.

In the dissolution experiments (Figure 9.7) it was observed a slower dissolution rate but not a lower solubility for the CaSO₄ capsules we formulated. However, phenytoin precipitated (Figure 9.1) when titrated with a calcium salt solution. The effect of convection in a dissolution experiment may limit crystal formation. In addition, in the dissolution vessel a medium volume of 900 mL in which both the phenytoin sodium and calcium salt solubilize is much larger than the titration studies with a smaller volume of 100 mL where more concentrated solutions of phenytoin and calcium are present.

Since the 1968 phenytoin intoxication outbreak in Australia many studies have been conducted to investigate the incompatibility between phenytoin and CaSO₄ (334–337). However, our results show that phenytoin sodium is also not compatible with lactose. This incompatibility was evident due to the colouring after both dissolution and calorimeter experiments. The yellow-brown colour suggests that a Maillard reaction is occurring between the two compounds, given that phenytoin sodium has a nitrogen with a negative charge and lactose is a reducing sugar (324). On the other hand, phenytoin acid did not react with lactose in the same way that the sodium salt did (Figure 9.3). This may be due to the lack of the negative charge on the nitrogen in the free form.

The presence of an amine and a reducing sugar alone may not be enough for the Maillard reaction to happen, other factors besides ionization seem to play a role too. For example, lactose concentration in the product and the solid-state form of lactose can also impact API-excipient interactions since its crystalline form is considered to be less reactive than the amorphous one (338,339). In addition, other factors such as moisture and temperature can also play an important role in a Maillard reaction. The incompatibility between phenytoin sodium and lactose

could represent a loss of drug when patients take such formulation since this reaction can occur at body temperature (Figure 9.8).

Continuing with the investigation on how this reaction would take place, phenytoin sodium was mixed with milk and analyzed through microcalorimetry. The heat flow of milk only and phenytoin/milk mixture were similar while the phenytoin sodium/milk mixture demonstrated a reduced heat flow pattern. The vials containing milk and phenytoin with milk did not show any difference in colour. The blue and red lines in Figure 9.4 could represent bacteria growth, since the pattern is similar to the ones obtained in other milk calorimetry studies (340,341). Maillard reactions are exothermic (342–344) and this explains the higher heat flow in the first two hours in the phenytoin sodium/milk sample mixture (yellow line in Figure 9.4). The lactose readily reacted with phenytoin sodium and the heat flow is taking place at a lower rate (yellow line Figure 9.4 from 3 hours on) due to the decreased amount of lactose.

Furthermore, the calorimetry experiments performed with commercial products showed that phenytoin sodium interacted with milk regardless of the formulation composition (Figure 9.5). When tested in water, only the lactose containing products showed browning, confirming, once again, the incompatibility between API and excipient.

According to the Canadian Food Inspection Agency “lactose- free means that there is no detectable lactose in the food using an acceptable analytical method”. Therefore, lactose free milk can have some acceptable remaining amount of lactose. This explains the slight colouration observed for the Apotex and Amneal products with lactose free milk. The more evident browning for Dilantin in lactose free milk may be due to interaction with the additional lactose in the formulation, as colour change was observed in water. The negative heat flow for the Apotex

product can be attributed to the disintegration process of the minitablets. The colour change intensity for each formulation in the different tested media is summarized in Table 9.2.

In previous studies by Macheras *et al.* the authors investigated the effect of milk on the solubility of phenytoin sodium (345). They report a significant increase in solubility, but surprisingly no incompatibility between the API and milk is reported. However, in an *in vivo* study administering 200 mg phenytoin sodium capsules with water or milk a significant decrease in AUC and C_{max} were observed when milk was used. The AUC dropped from 151.2 ±72.2 µg h mL⁻¹ (control with water) to 81.9 µg h mL⁻¹ (±21.3) (control with milk) and C_{max} dropped from 3.3 (±0.7) µg mL⁻¹ to 2.6 (±0.5) µg mL⁻¹. This indicates a food effect with milk for the tested formulations due likely to the presence of both lactose and calcium.

In another study by Neuvonen *et al.* (346) patients received phenytoin as a free acid with milk or water. No differences in C_{max} were observed. The authors concluded that “a direct physicochemical interaction between phenytoin and milk constituents is unlikely” since the absorption of phenytoin was not changed. This is consistent with and corroborates our results regarding the lack of interaction between phenytoin free acid and lactose.

The change in excipients (from CaSO₄ to lactose) by Parke-Davis was undertaken in the early 1960's (329,330) and ever since the reference product Dilantin (Pfizer) contains lactose as an excipient (347). Its monograph in Canada was last revised in August, 2017 (347). Interestingly, in Canada, the generic brands Apotex Canada Inc. and Taro Pharmaceuticals Inc. of extended phenytoin sodium capsule do not contain lactose as an excipient (from package insert). It is noteworthy that the formulations with and without lactose were bioequivalent, which is different than the food effect observed with milk. The bioequivalence results might be due to

the slow release of the drug from the formulation. The USP requires an release of 45, 65 and 70 % at 30, 60, 120 min. *In vivo* the lactose and the API might dissolve at different rates.

Also, the innovator product was bioequivalence tested in a fasted / fed study (348) with milk as one of the components of the meal. No bioequivalence problems were observed. This might be due to the dilution of the milk throughout the entire meal, which could be at variance with the study (345) where only milk was utilized. In addition, according to a query to the Canada Vigilance Program no reports of lactose or milk interactions with phenytoin were found from 1965 – 2017 (349).

Moreover, the other marketed products in the USA also don't contain lactose as an excipient, with exception of Taro Pharmaceuticals (information taken from products' package insert), which is intriguing, as their approved product in Canada does not contain lactose in its formulation. In a food effect study comparing the innovator product to a particular generic product, it was found that the generic formulation was within the bioequivalence criteria of the FDA. However, the author state: "when taking phenytoin sodium with food, product switches may result in either side effects or loss of seizure control" (350). How much of this (if any) can be attributed to excipient API effects or the API dissolution is not known.

The published literature appears to be contradictory and the amount of lactose necessary to cause an interaction that results in a change in bioavailability remains unanswered. The tests may be overly discriminatory for the *in vivo* performance. Our results suggest that amounts of dissolved API and lactose at the same location within the gastrointestinal tract may facilitate a Maillard reaction. Nevertheless, the lactose amount needed for the reaction to happen *in vivo* affecting the drug's bioavailability is unknown, once it is a different milieu than the conditions of a dissolution vessel.

Table 9.2. Excipients composition of different approved products of extended release phenytoin sodium capsules 100 mg in Canada and in the USA, and colour change intensity for the tested products in Milk, lactose free milk (LFM) and water

Company	Excipients composition	Colour change
Canada		
Parke-Davis (Pfizer)* Reference	Lactose, magnesium stearate, sugar and talc.	Milk: +++ Water: +++ LFM: +++ Excipient content: 57%
Apotex*	Colloidal silicon dioxide, hydroxypropyl methylcellulose, and magnesium stearate.	Milk: +++ Water: - LFM: + Excipient content: 28%
Taro Pharmaceuticals	Lactitol monohydrate, magnesium stearate, sodium lauryl sulphate, and talc.	
USA		
Parke-Davis (Pfizer) Reference	Lactose monohydrate, magnesium stearate, sugar and talc.	
Taro Pharmaceuticals*	Lactose monohydrate, magnesium stearate, sugar, talc and hypromellose.	Milk: +++ Water: ++ Excipient content: 58%
Mylan Pharmaceuticals Inc.	Colloidal silicon dioxide, hydroxyethyl cellulose, magnesium oxide, magnesium stearate, microcrystalline cellulose, povidone and sodium lauryl sulfate.	
Sun Pharmaceutical Industries, Inc.	Lactitol monohydrate, sodium lauryl sulfate, talc and magnesium stearate.	
Anneal Pharmaceuticals*	Hydroxypropyl cellulose, mannitol, magnesium stearate, talc and titanium dioxide.	Milk: +++ LFM: + Excipient content: 43%
Aurobindo Pharma Limited	Confectioner's sugar, hypromellose, magnesium oxide, magnesium stearate, microcrystalline cellulose, and talc.	

* Tested products; +++: Dark brown; ++: Light brown; +: Yellow; -: no browning

Hence, considering the excipient concentrations in approved phenytoin products, it becomes clear that even with the most commonly used excipients, which are generally considered “pharmaceutically inert”, a chemical or physical interaction with the active pharmaceutical

ingredient could compromise the dissolution testing and potentially alter bioavailability and bioequivalence. Bioequivalence and bioavailability tests can delineate the effect of potential interactions, an awareness of the issue at the development level could save time and cost. However, despite evidence of this interaction and potential interaction *in vivo* there does not yet appear to be any definitive reduction of bioavailability for contemporary commercial Canadian and USA brands that contain lactose leading to bioinequivalence issues nor, to the best of our knowledge, any therapeutic failure due to the interaction of phenytoin products with milk/lactose has been reported.

9.6 Conclusion

Our study mechanistically investigated previous reports of excipient-API interactions with phenytoin. The calorimeter experiments results indicate that phenytoin sodium interacts with CaSO_4 in aqueous media. Furthermore, phenytoin sodium also interacts with lactose through a Maillard reaction at body temperature which could possibly lead to bioavailability variations if administered with lactose containing milk. In Canada and the USA, the reference product still has lactose as an excipient in the formulation listed since it was changed in the 1960's, whereas all Canadian and most USA generic formulations do not contain lactose.

The current bioequivalence data do not suggest that a potential lactose-phenytoin sodium interaction challenges the therapeutic equivalence between the available products. However, assuming that the commonly used excipients are so called inert could still cause potential development issues. Phenytoin was first introduced as drug product in 1938 and much has been learned about drug-excipient incompatibility with calcium, but even after of eighty years of clinical use a new incompatibility between phenytoin and lactose has been experimentally delineated .

SECTION FOUR: OTHER ASPECTS OF *IN VIVO* DRUG PRODUCT

PERFORMANCE:

The impact of formulation composition and physiology state

CHAPTER TEN

Application of in Silico Tools in Clinical Practice using Ketoconazole as a Model Drug

A version of this chapter is published in:

J Pharm Pharm Sci. 2018;21(1S):242s-253s. <https://doi.org/10.18433/jpps30227>
Reprinted from reference (397).

10.1 Introduction

Hypochlorhydria is a physiological state in which the hydrochloric acid production in the stomach is low, causing an increase in the intragastric pH. Disease state (gastric mucosal infection caused by *Helicobacter pylori* and AIDS patients), ethnicity, age and administration of antisecretory agents, such as omeprazole, a Proton Pump Inhibitor (PPI), may induce hypochlorhydria (351–353). Changes in physiological properties such as stomach pH can impact the *in vivo* drug product performance, especially from dosage forms with API controlled dissolution (120,354). Thus, antisecretory agents can affect the absorption of orally co-administered drugs, given that gastric acidity plays a major role in the process of dissolution sequentially followed by absorption of various drugs (355). This is the case for drugs that are primarily weak bases.

A clinical example of this is the administration of ketoconazole in PPI-induced hypochlorhydria states. Several studies (353,356–358) have reported its reduced absorption under such conditions. Ketoconazole is an antifungal agent with a broad-spectrum activity against various fungal infections (359). It is used to treat both mucocutaneous and systemic opportunistic fungal infections that commonly occur in immunocompromised patient (357,358,360). It is a chiral imidazole piperazine compound, which is a weak dibasic compound (358), and within the Biopharmaceutics Classification System (BCS), it is a low soluble and highly permeable drug (class II) (30). Since ketoconazole solubility is pH dependent, its absorption after oral administration is variable, achieving the highest plasma concentrations at low gastric pH (357,361). Due to its high lipophilicity, ketoconazole is readily absorbed after conversion to the water-soluble salt by gastric acid (362–364).

Under this scenario of different physiological conditions, physiologically based pharmacokinetic (PBPK) computer models are useful tools to help predict the plasma concentration–time profiles of a given drug. GastroPlus™ (Simulations Plus Inc., Lancaster, CA, USA) is an example of commercially available software that includes PBPK models (365). Using pre-determined parameters and physiology, PBPK modeling can predict *in vivo* data, improving the therapeutic outcomes by designing different disposition profiles (352,366). Much attention has been drawn to the use of such models for drug development and formulation development process (367–371), nevertheless there is a great opportunity in using simulations to investigate different clinical approaches by clinical practitioners.

In order to predict drug absorption from the gastrointestinal (GI) tract, GastroPlus™ includes the Advanced Compartmental Absorption and Transit (ACAT) model (372), which is a refinement of the Compartmental Absorption and Transit (CAT) model (373,374). This model takes into consideration factors that impact drug bioavailability and absorption, such as physicochemical attributes of the compound (e.g. solubility), physiological properties of the GI tract (e.g. pH) and formulation characteristics (e.g. particle size).

The purpose of this study was to demonstrate the use of *in silico* studies to support changes in clinical practice with a mechanistic approach in view. The selection of ketoconazole was based on *in vivo* data availability reported in the literature.

10.2 Materials

Ketoconazole USP grade was purchased from Medisca, (Saint-Laurent, QC; LOT: 613650/D. Coca Cola® and Orange juice (Minute Maid®) were bought at a local store in Edmonton, Canada. Water for the high-performance liquid chromatography (HPLC) assay was purified by Elgastat Maxima UF and an Elgastat Option 3B water purifier by ELGA Laboratories

Ltd. (Mississauga, ON, Canada) and then filtered using 0.45 μm pore size filter. Methanol and acetonitrile used were HPLC grade and were purchased from Fisher Scientific (Fair Lawn, NJ, USA).

10.3 Methods

10.3.1 Systematic search for clinical studies reporting Ketoconazole malabsorption due to increased gastric pH

Databases such as Medline, Scopus, Web of Science, Google Scholar, Sciencedirect and Scifinder were systematically searched to identify relevant studies using key-words alone and in combination with each other such as: pH, absorption, solubility, antisecretory therapy, ketoconazole, omeprazole, ranitidine, cimetidine, gastric pH and co-administration. Clinical studies performed on adult humans reporting ketoconazole malabsorption due to gastric acid secretion inhibition by the use of PPIs and/or Histamine₂-receptor antagonists were selected.

10.3.2 Chemical structure analysis

The database chemicalize (<http://www.chemicalize.org/>) was used to analyze ketoconazole chemical structure and its ionization characteristics throughout the pH range 0- 14.

10.3.3 Computer simulations using GastroPlus™

GastroPlus™ version 9.0 (Simulations Plus Inc., Lancaster, CA, USA) is a computer program that allows the prediction of drug absorption from oral administration of dosage forms when physicochemical and biopharmaceutical properties of drugs are available (214,294,317,365,366,375,376). The program is composed of different input tabs, such as Compound Tab, Gut Physiology and Pharmacokinetics. The other two tabs (Simulation and

Graph) display the results for the simulations performed. The parameters and modules used in each tab for the different sets of simulation are described in detail.

10.3.3.1 Compound Tab

In the Compound Tab, ketoconazole physicochemical properties were input as shown in Table 10.1. These parameters comprise but are not limited to: dose, dosage form, solubility, permeability, molecular weight, particle density, particle size and pKa.

Even though being a weak base, the literature reports that ketoconazole is a slow precipitating drug (377–379). Hence, the default value of precipitation time was found to be adequate for this simulation setting.

Table 10.1. Drug properties used as input data in Compound Tab in GastroPlus™

Compound Tab Inputs	Value	Reference
Molecular weight (g/mol)	531.44	ADMET Predictor™
Permeability (10 ⁻⁴ cm/s)	3.7	(380)
pKa (Dibasic compound)		(13,358,381)
pKa1	2.9	
pKa2	6.5	
LogP	3.74	ADMET Predictor™
pH for reference solubility	4.4	
Solubility (mg/ml)	0.5	(47)
Initial dose (mg)	200	
Dose volume (ml)	250	GastroPlus™ default value
Drug particle density (g/ml)	1.2	GastroPlus™ default value
Mean precipitation time (s)	900	GastroPlus™ default value
Diffusion coefficient (cm ² /s x 10 ⁵)	0.56	ADMET Predictor™

10.3.3.2 Pharmacokinetics Tab

Since no intravenous human study has been reported to date (379), published data with the administration of ketoconazole 200 mg oral suspension (382) was used to set the human pharmacokinetics of ketoconazole using the PBPK model in GastroPlus™. In the Compound Tab the Dosage Form selected was Immediate Release (IR) Suspension.

PBPKPlus™ (Simulations Plus Inc., Lancaster, CA, USA) is an additional module in GastroPlus™ that enables the prediction of the drug's distribution and clearance for all tissue compartments such as gut, lung, adipose tissue, muscle, liver, spleen, heart, brain, kidney, skin, and rest of the body that are interconnected by the systemic vasculature circulation (365,379,383).

When using PBPK simulations for small molecules a partition coefficient between tissue and plasma has to be set. This tissue/plasma partition coefficient (Kp) is a mean to measure the amount of drug in the tissue and it can be estimated from physicochemical properties such as logP, pKa, unbound fraction of drug in plasma and blood/plasma concentration ratio (383). A modified Rodgers and Rowland predictive method present in GastroPlus™ was selected to calculate the Kps .

Perfusion-limited kinetics with no concentration gradient in the tissue was used, given that ketoconazole is a highly lipophilic and highly permeable molecule and is classified as a BCS class II compound (379). Therefore it is reasonable to assume that the amount of drug that partitions into the tissue is limited by the blood flow rate through the tissue (perfusion rate) rather than permeability and surface area and partitioning is instantaneous (383).. The scheme in Figure 10.1 helps to illustrate this process.

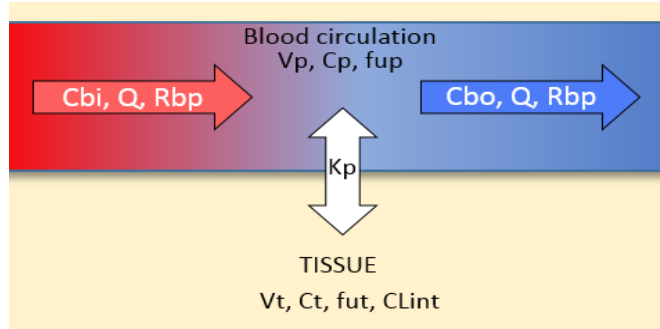


Figure 10.1. Scheme of perfusion-limited tissue. V_t : tissue volume; C_t : tissue concentration, f_{ut} : fraction unbound in tissue, CL_{int} : tissue intrinsic clearance; V_p : plasma volume; C_p : plasma concentration; f_{up} : fraction unbound in plasma; C_{bi} : blood concentration in (arterial) tissue; R_{bp} : blood/plasma concentration ratio; Q : tissue blood flow; C_{bo} : blood concentration out (venous) of tissue; K_p : tissue/plasma partition coefficient. (Image adapted from GastroPlus™ Manual, 2015).

Ketoconazole's major route of excretion is through the bile into the GI tract with more than 50% being excreted in the feces (384,385). Hence the hepatic clearance (CL_{hep}) was set equal to oral clearance (CL_{po}) of 12.5 L/h for a 200 mg dose (380,382). The default physiology (Human Physiological Fasted) was used.

10.3.3.3 Physiology Tab

Three sets of simulations were performed, and the predicted absorption was compared to the experimental data for the different physiology conditions in the stomach. The first set of simulations aimed to build a PBPK model using published data of ketoconazole 200 mg suspension administration (382). Once the model was built, the same pharmacokinetics parameters obtained were used to run further simulations. The other two sets of simulations comprised of ketoconazole 200 mg in an immediate release (IR) tablet dosage form for both normal and increased stomach pH. For those two sets of simulation, the dosage form in the compound tab was set to "IR: Tablet".

These three sets of simulations: PBPK model; human fasted – no hypochlorhydria physiology and human fasted - hypochlorhydria physiology are described below and presented in Table 10.2.

10.3.3.3.1 Physiology Based Pharmacokinetics (PBPK) model

As mentioned above, a clinical study using ketoconazole 200mg oral suspension (382) was selected to build the PBPK model. Since this study was conducted in humans in a fasted state, the default values in GastroPlus™ for human fasted physiology were used, as shown in Table 10.2. The default absorption model (Opt logD Model SA/V 6.1 model) and perfusion limited kinetics were used.

10.3.3.3.2 Human fasted - Normal intragastric pH - No hypochlorhydria

Experimental data were taken from a published study using ketoconazole tablets 200 mg (Nizoral; Janssen Pharmaceutica Inc., Mississauga, Ontario, Canada) (358). A parameter sensitivity analysis (PSA) was performed on gastric transit time since the dosage form was changed from suspension to tablet, and it was set to one hour. It is reasonable to use a longer gastric transit time given that a solid oral dosage form takes longer to be emptied out of the stomach when compared to a suspension.

10.3.3.3.3 Human fasted - Co-administration with PPI – Hypochlorhydria

Data from a study performed in subjects receiving 60 mg of omeprazole (Losec; Astra Pharma Inc.) on the night prior to receiving ketoconazole 200 mg was used (358). The experimental data were compared with the simulations performed at increased intragastric pH. Stomach pH was set to 6.9, as reported in the study (Table 10.2). Besides that, gastric retention

time was set to one hour to account for the difference between tablet and suspension dosage form and their gastric emptying rate.

The absorption scale factor (ASF) of the ACAT model was optimized. ASF is used to scale the effective permeability to account for various absorption-rate-determining effects, such as pH effects (294,383).

The improvement of ketoconazole's absorption with administration of drug with an acidic beverage (Coca Cola®) in the presence of drug-induced hypochlorhydria was also assessed. The data was taken from the aforementioned study (358). In this case, the stomach pH was decreased from 6.9 to 5.5.

Table 10.2. ACAT parameters used in Physiology Tab for human fasted – PBPK model, normal and hypochlorhydria physiologies

Physiology	Human fasted - PBPK model		Human fasted – Normal - No hypochlorhydria		Human fasted - hypochlorhydria	
	pH	Transit time (h)	pH	Transit time (h)	pH	Transit time (h)
Stomach	1.30	0.25	1.3	1	6.90	1
Duodenum	6.0	0.26	6.0	0.26	6.0	0.26
Jejunum proximal	6.2	0.93	6.2	0.93	6.2	0.93
Jejunum distal	6.4	0.74	6.4	0.74	6.4	0.74
Ileum proximal	6.6	0.58	6.6	0.58	6.6	0.58
Ileum medial	6.9	0.42	6.9	0.42	6.9	0.42
Ileum terminal	7.4	0.29	7.4	0.29	7.4	0.29
Caecum	6.4	4.31	6.4	4.31	6.4	4.31
Asc Colon ^a	6.8	12.93	6.8	12.93	6.8	12.93

^aAsc Colon = ascending colon

10.3.3.4 Simulation and Graph Tab

The temporal length for the simulations was adjusted for each study according to the corresponding available data. Once the simulation for the plasma concentration curve was

complete, the predicted curve was displayed in the Graph tab, which automatically generates the regression coefficient (R^2) between predicted and observed data, along with other statistical parameters: sum of squared errors (SSE), root mean squared error (RMSE) and mean absolute error (MAE).

Since ketoconazole is a BCS class II drug the influence of particle size on drug absorption was investigated by running a PSA. The particle size range analyzed was 2-250 μm . After running a PSA, the Graph tab displayed the results delineating the particle size statistics effect on ketoconazole's pharmacokinetics.

10.3.4 Data analysis

The data was analyzed through statistical parameters such as SSE, RMSE and MAE. The SSE measures the discrepancy between the model and data. Therefore, the smaller the value, the better the fit is. The differences between the predicted values and observed values is given by the RMSE. It combines the magnitude of the errors for the various time points into a single measure. It is a non-negative value and the closer to zero the better the fit. MAE, as the name indicates, is the average of all absolute errors.

Besides that, the pharmacokinetic parameters AUC, Tmax and Cmax were assessed in terms of the fold error between the observed and the predicted values, according to Equation 10-1. As it is widely applied within pharmaceutical industries, a two-fold error was considered to be an acceptable prediction (386,387).

$$\text{Fold Error} = \frac{\text{Predicted value}}{\text{Observed value}}$$

Equation 10-1

10.3.5 Solubility test

The solubility of ketoconazole was determined using the equilibrium solubility test (Shake flask method). Four different media were tested in triplicate: Simulated gastric fluid (SGF) pH 1.2, SGF pH 5.0, Coca-Cola® and Orange Juice (Minute Maid®), the latter two were utilized directly from the commercial products. Each medium (5ml) was saturated with ketoconazole pure drug powder and there was no mixture of media. The flasks were shaken for 24 hours at room temperature to assure equilibrium. At equilibrium, the pH in each flask was measured.

Samples from each medium (SGF pH1.2; SGF pH 5; Orange juice and Coca-Cola) were centrifuged for 10 min at 11900xg and the supernatant was diluted. The supernatant of Orange juice and Coca-Cola samples was diluted with methanol and the supernatant from SGF pH 1.2 and pH 5 was diluted with acetonitrile. The diluted supernatant from all samples was then centrifuged again for 10 min at 4400xg. The resulting supernatant was used in the HPLC assay. The mobile phase for the HPLC assay was composed of methanol, water and diethylamine 74:26:0.1 (v/v/v) and a Lichrospher® 60 RP Select B column (5 µm, 12.5×4 mm) column was used (388).

10.4 Results

10.4.1 Chemical structure analysis

The graph below (Figure 10.2), retrieved from the Chemicalize database (<http://www.chemicalize.org/>), shows the result for the ionization microspecies distribution throughout the pH range 0 to 14. The green line represents the microspecies with both basic

groups - imidazole and piperazine - protonated, the blue line is the neutral form and the orange line is the microspecies with only the imidazole group protonated (Figure 10.2).

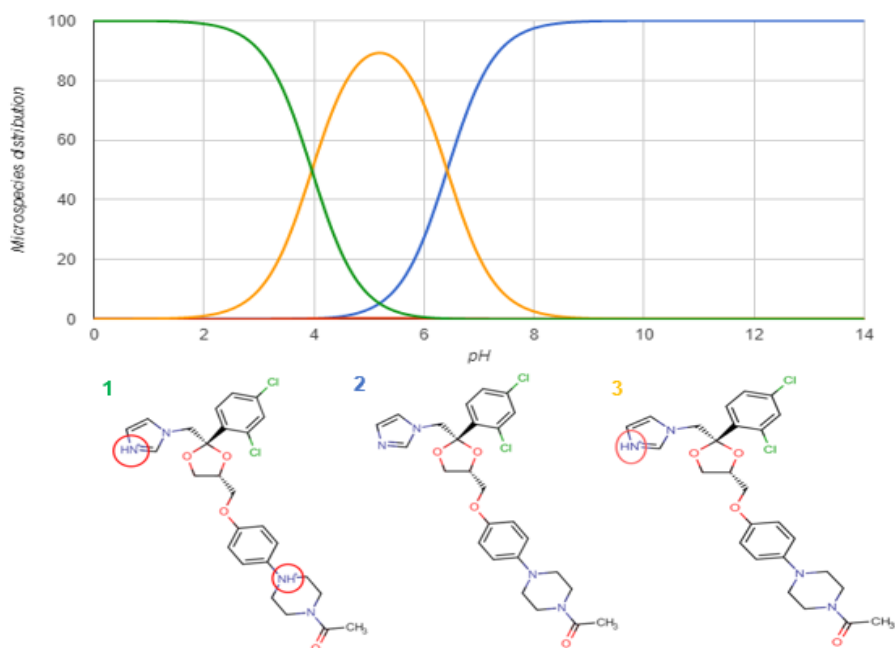


Figure 10.2. Microspecies distribution throughout pH range 0-14. Green line corresponds to microspecies 1 (both basic groups protonated - highlighted in red circles), blue line corresponds to microspecies 2 (neutral microspecies) and orange line corresponds to microspecies 3 (imidazole group protonated - highlighted in red circle). Images taken from <http://www.chemicalize.org/>.

10.4.2 PBPK model

Using the stated conditions, GastroPlus™ was able to closely predict the observed data for ketoconazole 200 mg suspension administration ($R^2 = 0.95$, SSE= 1.92, RMSE= 0.438, MAE= 0.33), as shown in Figure 10.3A. Also, the values of Area Under the Curve (AUC), C_{\max} and T_{\max} for the predicted data showed a good match to the observed parameters (Table 10.3). All the simulated parameters were within 2-fold error of the observed pharmacokinetic parameters.

Table 10.3. Area under the curve ($AUC_{0-\infty}$), C_{max} and T_{max} and after oral administration of ketoconazole 200 mg suspension

Parameter	Observed*	Predicted
$AUC_{0-\infty}$ ($\mu\text{g}\cdot\text{h}/\text{mL}$)	15.84 (\pm 7.05)	12.65
C_{max} ($\mu\text{g}/\text{mL}$)	5.04 (\pm 1.58)	4.73
T_{max} (h)	1.2 (\pm 0.5)	1.36

*Observed parameters were taken from Huang *et al.*

10.4.2.1 Human fasted - Normal intragastric pH - No hypochlorhydria

The simulated plasma concentration curve for ketoconazole in normal gastric pH state resulted in a very good prediction for the observed plasmatic concentration curve ($R^2 = 0.913$, $SSE= 2.776$; $RMSE= 0.502$; $MAE= 0.394$) (Figure 10.3B). The pharmacokinetics parameters $AUC_{0-\infty}$, C_{max} and T_{max} and are summarized in Table 10.4, showing a well-defined match between the predicted and observed data. All the simulated parameters were within 2-fold error of the observed pharmacokinetic parameters.

10.4.2.2 Human fasted - Co-administration with PPI - Hypochlorhydria

Figure 10.3C shows the observed and simulated plasma concentration time curve for ketoconazole in hypochlorhydria state and the plasma concentration time curve for the administration of the drug with Coca-Cola[®]. Both resulted in a good match ($R^2 = 0.89$; $SSE= 0.45$; $RMSE= 0.20$; $MAE= 0.156$ and $R^2 = 0.965$; $SSE= 0.26$; $RMSE= 0.161$; $MAE= 0.125$, respectively). Values of AUC , C_{max} and T_{max} for the predicted and observed data are summarized in Table 10.4. All the simulated parameters were within 2-fold error of the observed pharmacokinetic parameters.

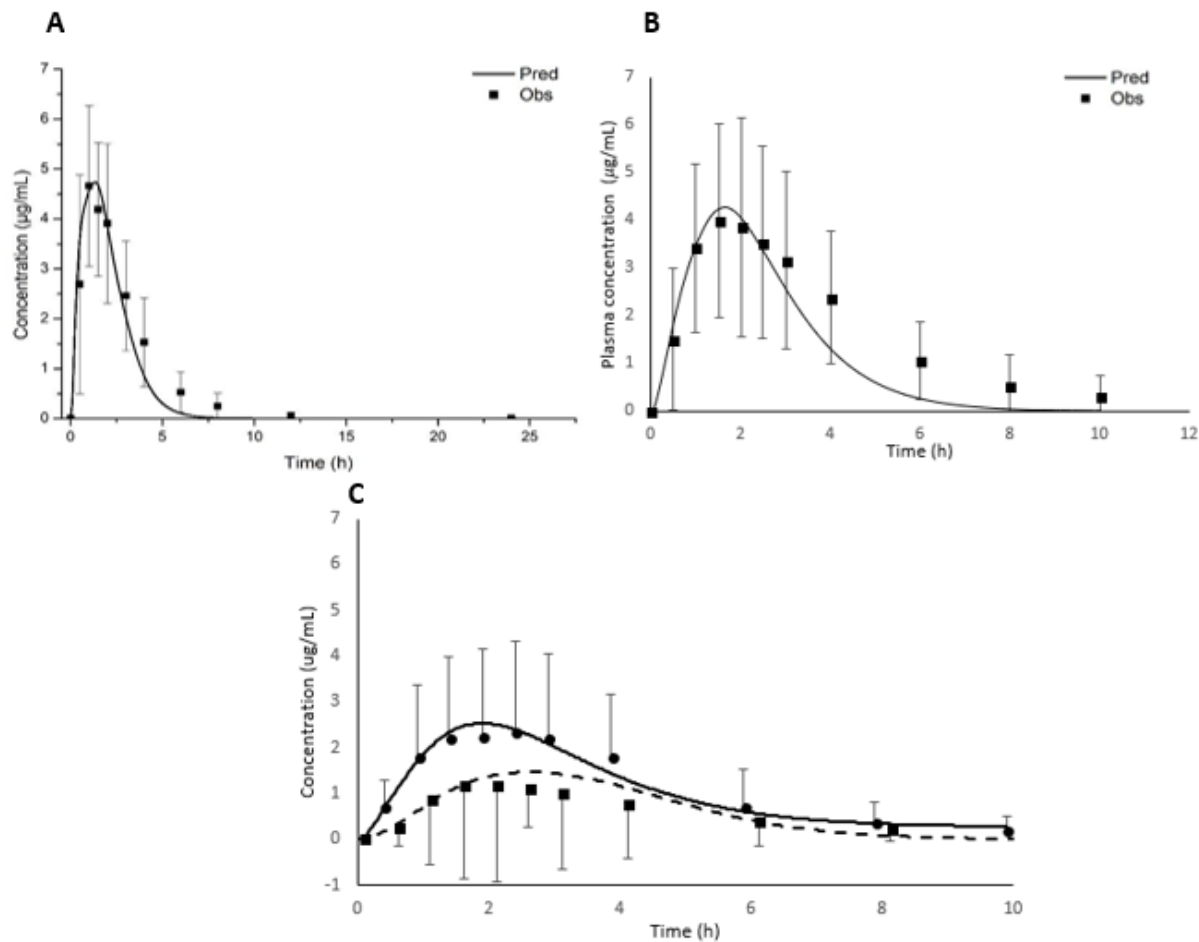


Figure 10.3. Plasma concentration-time profiles under different scenarios. (A) after administration of ketoconazole 200 mg suspension; (B) ketoconazole 200 mg tablet to subjects with normal intragastric pH under a fasted condition; (C) ketoconazole 200 mg tablet to subjects with increased intragastric pH with water (predicted: dashed line; and Observed - black squares) and with Coca-Cola[®] (predicted: solid line and observed: black circles).

10.4.3 Parameter Sensitivity Analysis

Since ketoconazole is a BCS class II compound, the effect of particle size on its absorption was investigated. The PSA showed that only in a hypochlorhydric condition was ketoconazole bioavailability sensitive to changes in drug particle size (Figure 10.4A and B).

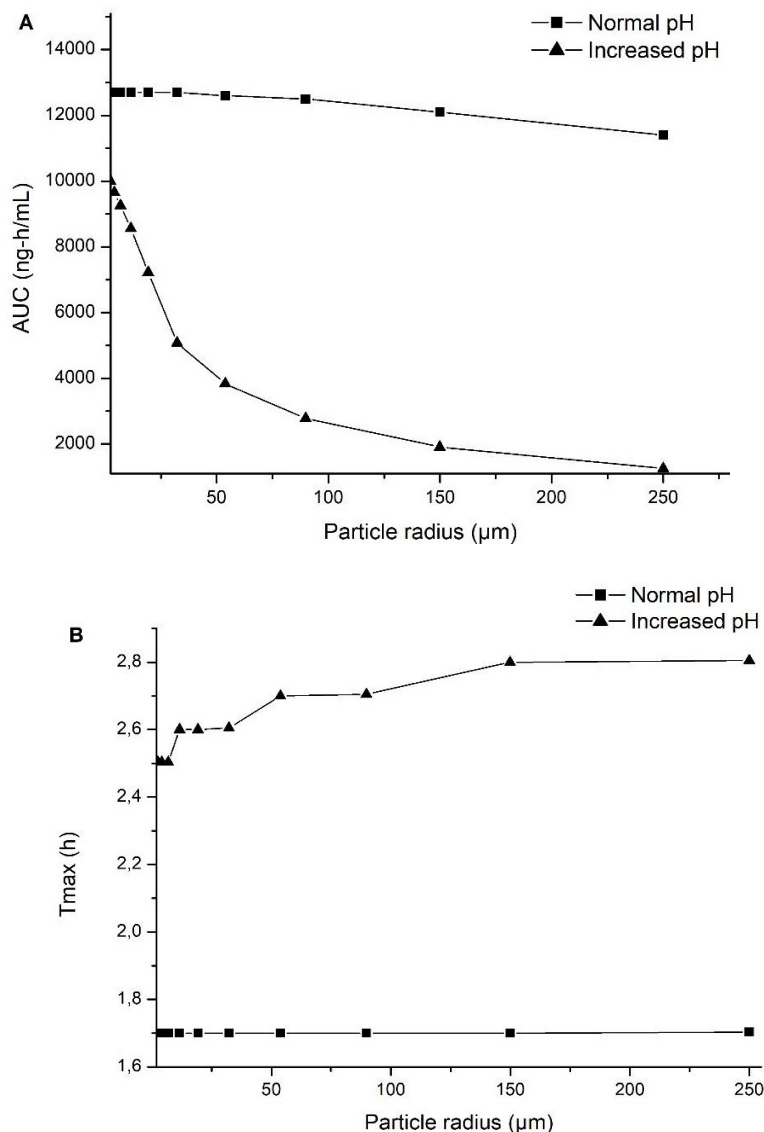


Figure 10.4. Parameters sensitivity analysis: influence of particle size on AUC_{0-∞}, (A) and T_{max} (B) of ketoconazole in normal (squares) and increased intragastric pH (triangle).

10.4.4 Solubility test

Ketoconazole had its highest solubility in SGF pH 1.2 (48 mg/mL ± 0.68); followed by Orange Juice and Coca-Cola[®] (2.6 mg/mL ± 0.027; 2.23 mg/mL ± 0.024, respectively) and finally SGF pH 5.0 (0.43 mg/mL ± 0.032) in which it presented the lowest solubility. The measured equilibrium pH for the media was 2.8; 4.3; 3.62 and 5.7, respectively. The mean solubility of ketoconazole was ~5 times higher in Coca-Cola[®] and orange juice than its solubility

in SGF at pH 5.0 and the corresponding $AUC_{0-\infty}$, reflecting extent of systemic exposure, was increased 3-fold when the drug was administered with Coca-Cola® (Table 10.4) rather than water.

Table 10.4. ($AUC_{0-\infty}$), C_{max} and T_{max} after oral administration of ketoconazole 200 mg tablet

Parameter	No hypochlorhydria		Hypochlorhydria			
	Observed*	Predicted	Observed*	Predicted	Coca-Cola® Observed*	Coca-Cola® Predicted
$(AUC_{0-\infty})$, ($\mu\text{g}\cdot\text{h}/\text{mL}$)	17.89 (± 13.11)	12.65	3.46 (± 5.08)	6.22	11.22 (± 10.57)	18.25
C_{max} ($\mu\text{g}/\text{mL}$)	4.13 (± 1.95)	4.26	0.8 (± 1.09)	1.47	2.44 (± 1.72)	2.54
T_{max} (h)	1.5 (± 0.5)	1.67	2.9 (± 1.5)	2.61	2.2 (± 1.1)	1.9

*Observed parameters were taken from Chin *et al.*

10.5 Discussion

Considering ketoconazole microspecies distribution (Figure 10.2), at normal intragastric pH (~1.5), the predominant microspecies (99%) has both basic groups (imidazole and piperazine) protonated, hence high solubility (Figure 10.2 – microspecies 1). In contrast, at pH 6.9 the predominant microspecies (75%) is neutral and poorly soluble (Figure 10.2 - microspecies 2) (Data taken from <http://www.chemicalize.org/>). Given that omeprazole (a PPI) reduces gastric acid secretion thus making the stomach pH much higher, it significantly impairs ketoconazole dissolution (358). Additionally, the solubility test results also demonstrated a pH dependent solubility of ketoconazole.

Thus, it becomes clear that sufficient gastric acidity is of utmost importance for adequate dissolution and further absorption of the drug (358,389). In altered physiological states where

gastric acidity isn't enough to solubilize BCS class II compounds, in this case, ketoconazole, the drug's bioavailability may be reduced. A central tenet of clinical pharmacology is the relationship between drug concentration and pharmacological/ toxicological effects. Hence, the therapeutic outcome of the given treatment will be altered as a consequence (381). The built *in silico* PBPK model properly predicted ketoconazole malabsorption caused by the hypochlorhydria state (Figure 10.3C), consistent with the primary role of gastric dissolution on the absorption of weak bases.

A common strategy used to circumvent the hypochlorhydric effect on the drug's bioavailability is to administer it with low pH drinks, such as Coca-Cola[®], in order to decrease the pH of the gastric fluid, thus increasing ketoconazole's dissolution and further absorption, as shown by Chin et al. The model was able to predict the increased bioavailability when administering the drug with Coca-Cola[®] (Figure 10.3C). This demonstrates the utility of *in silico* methods in further delineating different clinical strategies to avoid therapeutic failures.

As shown in Figure 10.4A, once sufficient gastric acidity is provided to facilitate complete ketoconazole dissolution, its absorption is not affected by particle size (squares), rather it depends on gastric transit time (55,359). Nevertheless, if the gastric pH is not acidic enough to completely dissolve ketoconazole in the stomach, it will depend on intestinal dissolution to be absorbed, where the particle size matters (triangles in Figure 10.4A). Due to its low solubility at intestinal pH, incomplete absorption will occur (showed by a smaller AUC) (381,390).

It is already known that particle size can influence drug absorption, mainly for BCS class II compounds (390). In API driven dissolution dosage forms, the drug's properties such as particle size and surface area will have an impact on determining drug dissolution. Thus, the drug product performance will depend on such properties in addition to the physiological

environment that the drug is exposed to. Our results corroborate that stomach and intestinal pH play a major role in ketoconazole dissolution followed by absorption process. Particle size, however, seems to play a role only under a hypochlorhydric condition.

Furthermore, both results from the PSA performed (Figure 10.4B) and predicted plasma concentration time curves (Figures 10.3B and 10.3C), show that the hypochlorhydria condition also results in a slower absorption rate, indicated by a longer T_{\max} when compared to the one in normal intragastric pH (Table 10.4).

Hence, impaired absorption can occur when weakly basic drugs are administered to patients that have reduced gastric acidity, leading to a potential therapeutic failure due to subtherapeutic plasma concentrations (61,353,358,391).

For that reason, the development of formulations that can overcome the hypochlorhydric stomach environment is of primary importance to obtain the desired therapeutic result and efficacy (391).

As demonstrated by Mitra *et al.* (391) and Kou *et al.* (352) the use of *in silico* tools, such as GastroPlus™, can help to predict the *in vivo* performance of such formulations in humans, using PBPK and ACAT models to mimic the given patient's physiology (294). On one hand, combining *in silico* results with tests can be a powerful tool to select the most promising formulation to further continue studies (e.g. bioequivalence studies), on the other hand it can also be used to design different clinical approaches in order to reduce therapeutic failures (30,366,380,391). In this study we showed that rather simple computer simulations are a useful adjunctive tool when evaluating BCS II drug absorption when co-administered with a PPI. All weak bases would potentially behave in this manner; however, this could be compensated with

the use of low pH beverages instead of water. Therefore, simulations come in handy to assess alternative clinical dosing approaches.

In the clinical environment PBPK models have gained much importance to enable personalized medicine and to assess drug-drug/ drug-disease interactions (392–395). For these purposes, its usefulness rely on its ability to determine the importance of subpopulations and to optimize the formulation to obtain the targeted drug plasma concentration profile (392). Nevertheless, not much attention has been drawn to the utility of computer models when designing alternative clinical approaches.

10. 6 Conclusion

Physiologically based pharmacokinetic computer modeling using the software GastroPlus™ was able to accurately predict the plasma concentration vs. time profiles for ketoconazole tablets under different physiological states (normal gastric acid secretion and hypochlorhydria), capturing how well the drug would be absorbed and how the pharmaceutical product would perform under each condition. As experimentally observed, the simulated profiles showed a much lower ketoconazole absorption when the gastric acid secretion was low (hypochlorhydria) compared to individuals with a normal gastric pH. The model was also able to analyze the success of a different clinical approach (use of another beverage) showing the use of in silico models to support changes in clinical practice. Thus, reliable PBPK models can be used to predict possible pharmacokinetic pitfalls, which opens up additional approaches to explore different dosing strategies in clinical practice.

**SECTION FIVE: GENERAL DISCUSSION, CONCLUSION AND
FUTURE DIRECTIONS**

CHAPTER ELEVEN
General Discussion and Conclusion

11.1 General discussion

This thesis outlines many important aspects that need to be considered when developing physiologically relevant *in vitro* conditions. Such methods usually don't apply compendial conditions such as highly concentrated buffers. Hence, its use is most meaningful during the development phase rather than for QC purposes, such as batch release, for example (17). The approach taken in this work was such that allowed a mechanistic understanding of the underlying science behind clinical observations, such as slower *in vivo* dissolution, therapeutic failures, drug-excipient interaction, and the impact of physiological state.

In this thesis, initially, we investigated the matter of buffer capacity as an *in vivo* relevant parameter, since the buffering system in the intestinal lumen operates at low molarity values. For drugs with low solubility, such as Ibuprofen (Chapter 4), the buffer capacity impacted the dissolution rate in a manner that correlated with the observed slower *in vivo* dissolution rate. On the other hand, for highly soluble drugs, such as Metronidazole (Chapter 5) buffer capacity seemed not to be as important for the *in vitro* dissolution rate. Metronidazole and ibuprofen were used as representatives of BCS classes I and II, respectively. However, future studies with other drugs should be conducted.

The dissolution of a poorly soluble drugs is mainly affected by the surface pH around the drug particle (319). In compendial conditions (highly concentrated buffers) the interfacial pH is very similar to the bulk pH, resulting in a fast dissolution rate, which is known not to be the *in vivo* situation. As the drug is being dissolved, it is also absorbed in the gut, allowing bulk pH control with further drug dissolution and absorption *in vivo*. On the other hand, for highly soluble drugs the difference of surface pH and bulk pH would not have such a prominent impact on the dissolution rate because the drug is freely soluble. Hence, the absorption would mostly depend

on gastric emptying time and, once in the intestines, the parameter of most relevance would be absorption (79).

Going a step further into building physiological relevance to the *in vitro* system, the low buffer capacity medium was paired with an organic layer (n-octanol) to mimic the concurrent drug absorption that happens with the *in vivo* dissolution. Not only did this system present improved physiological relevance, but the use of an absorptive phase also added a sink to the low buffer capacity media, which decreased pH shifts while the dissolution test was performed (27).

This mechanistic analysis of the *in vivo* processes for different BCS class drugs (I and II) was undertaken with the proposed biphasic method in Chapters 4 and 5. For a poorly soluble drug, not only was the bulk pH shift better controlled due to drug partitioning – a process which likely occurs *in vivo* – but this method was also able to capture differences in formulation that might impact *in vivo* performance. In a similar manner, for IR formulations containing BCS I drugs, we demonstrated that compendial conditions might have been overdiscriminating and that the formulations were similar in terms of partitioning. Since this process correlates to the *in vivo* absorption, the formulations might have been equivalent. *In vivo* studies are needed to confirm these findings.

With the lessons learned from the theoretical and experimental assessment of buffer capacity and IR formulations, we studied more complex delivery systems addressing both the matter of buffer capacity and buffer species on the drug product performance (Chapter 7 and 8). The intestinal buffering system is bicarbonate based, hence we used bicarbonate buffer at *in vivo* molarities values to study enteric coated formulations, due to the

overwhelming evidence of the disconnect between *in vitro* conditions and clinical observations (Chapter 6).

We demonstrated that there is a considerable delay in the onset of drug release from EC formulations in BCB compared to compendial phosphate buffer. This is a result of the poor ability of BCB in buffering the dissolution of enteric coating polymers. Our *in vitro* findings are in line with *in vivo* observations of therapeutic failures with this kind of formulation, showing that the problem lies on their poor performance in the intestinal fluids leading to lower to no absorption (78,88).

The mechanistic understanding of the performance of EC products in BCB allowed us to delineate some of the main parameters that seem to affect the coat opening. The nature of the API (acid vs. base) can have a pronounced impact due to a microenvironment pH at the tablet/coat interface. This seems to outweigh the coat thickness when comparing acidic and basic drugs. However, the coat thickness matters for EC formulations containing the same API or APIs with similar physicochemical properties. Besides that, parameters such as the composition, pH and molarity of the immersion medium have to be factored in for physiological insight (88).

To provide further evidence of these observations, we tested EC pantoprazole formulations in BCB and compendial conditions and correlated it with *in vivo* data from a failed BE study (Chapter 8). Enteric coat dissolution was prompt in compendial buffer and both test and reference formulations complied with the pharmacopeial specifications. Evidently, solely satisfying the standard for drug dissolution does not guarantee similar *in vivo* behavior. In BCB, however, test and reference products presented remarkably different

performances and the release in BCB correlated better with the *in vivo* data. This shows the importance of using buffer systems reflective of the *in vivo* environment during the pharmaceutical development phase to avoid poor selection of prototype formulations.

Finally, we report the mechanistic assessment of other important aspects of *in vivo* drug product performance, such as formulation composition and physiology state (Chapters 9 and 10). Again, taking a mechanistic approach led to a more thorough understanding of the clinical observations. In terms of formulation properties, we not only confirmed an excipient-drug interaction that culminated in an intoxication outbreak in Australia, but also delineated a new incompatibility between phenytoin and lactose, that could cause potential development issues (396).

In respect of physiology state, the understanding of the interplay between the physicochemical properties of the API and the GI tract conditions at the time of dosing is of primary importance to achieve proper therapeutic outcome (Chapter 10). As expounded in Chapter 1, a basic drug, such as ketoconazole (BCS Class IIb) is good soluble in the acidic stomach environment but may precipitate upon transit through the intestines where the pH is less favourable to its dissolution. When there is sufficient time for dissolution in the stomach, good absorption in the proximal intestinal region is expected. However, in altered physiology state, such as decreased stomach acidity, the dissolution in the gastric environment is compromised, thus compromising drug absorption. In this scenario, PBPK modeling is a valuable mechanistic approach to investigate the success of different clinical approaches and alternative dosing strategies (380,397).

11.2 Conclusion

In this thesis, we showed the importance of a mechanistic understanding of the *in vivo* drug dissolution process to set physiologically relevant conditions to the *in vitro* performance tests. The first thing addressed was the matter of buffer capacity. It is well known that the buffering system in the human intestines is bicarbonate based at low molarity values. Literature reports have shown that *in vivo* drug dissolution might occur at a slower rate for poorly soluble drugs due to the reduced buffer capacity of the intestinal luminal fluids compared to compendial conditions. In our work we have demonstrated that the high buffer concentration used in compendial methods (to maintain sink conditions) causes a prompt drug dissolution. However, when applying a physiologically relevant buffer strength, the dissolution rate was slower, which is in line with the observed *in vivo* data. Additionally, because of the slower dissolution rate, differences between the formulations (composition and manufacturing process) were captured, which was not the case for compendial buffer, thus making this method more discriminative. The organic layer, mimicking the *in vivo* absorption process, acted as an additional sink that allowed pH control throughout the test. Subsequently, using biphasic dissolution test for IR formulations containing highly soluble drugs was shown to have beneficial attributes to estimate the *in vitro* behavior and performance of formulations as an alternative BCS-based biowaiver approach.

A fundamental consideration of this dissertation has been the behaviour of drug products in bicarbonate buffer, given that this system is the most representative of the luminal fluids. Due to the inherent pragmatical difficulties with this buffer system, it is desirable to design a surrogate buffer that can give the same physiological insight as bicarbonate-based buffers. When possible, this approach was taken in our studies. However, there are cases in which the peculiarities and kinetics of BCB play an essential role in drug dissolution, making it difficult to

find a proper buffer replacement, which is the case for enteric coated formulations. We demonstrated that BCB has a limited ability to buffer the dissolution of enteric coating polymers due to a lower pKa value at the solid-liquid interface compared to the bulk. This resulted in a considerable delay in the onset of drug release from EC formulations compared to compendial phosphate buffer. Again, our findings were in line with clinical observations. Hence, the reported *in vivo* failures of EC products known in the literature seem to be due to, at least in part, poor performance in the intestinal fluids.

Using the conditions outlined in the USP dissolution method resulted in a very prompt release. Hence, the compendial method for enteric coated tablets seems to be clinically irrelevant and it needs to be reevaluated. Using buffer systems that are not reflective of the *in vivo* environment during the pharmaceutical development phase can be misleading and cause poor selection of prototype formulations. Hence, an *in vivo* relevant performance test for EC products needs to be developed.

Overall, the findings of this thesis comprehensively demonstrates that meaningful differences in *in vitro* performance and accordance to clinical reports were only obtained when physiological relevant conditions were applied. Hence, our results indicate that the central hypothesis was answered positively.

**SECTION FIVE: GENERAL DISCUSSION, CONCLUSION AND FUTURE
DIRECTIONS**

CHAPTER TWELVE
Future Directions

12.1 Bicarbonate buffer and biphasic dissolution

As mentioned previously, the need of purging bicarbonate buffer media to maintain the pH makes its use difficult and unfeasible at times. Hence, we herein suggest the use of a biphasic system with the aqueous layer composed of bicarbonate buffer. We believe that the coupling of BCB with an organic layer (octanol) would prevent the escape of CO₂, thus taking away the need to sparge the medium. This approach would also allow the assessment of the drug partitioning, correlating to the absorption process. This would be a very robust physiologically relevant approach and we suggest that future *in vitro* studies along this line be conducted.

12.2 Simplification of *in vitro* tests for Quality Control application – Delayed release and Immediate release

We have demonstrated in Chapter 7 that buffer molarity seems to play a bigger role than bulk pH for the dissolution of enteric coated products. For a QC approach, there may not be the need to sparge the medium, as long as the buffer capacity of the system is carefully controlled. Future steps into developing a QC method for delayed release formulations would involve the study of a broader range of formulations in sparged vs. non sparged BCB media to set release specifications. Furthermore, the development of surrogate buffers should be conducted to find a system that matches the pKa of BCB at the boundary layer, which is a case-by-case study, as shown in the decision tree in Figure 2.4.

As shown in Chapters 3 and 5, for immediate release formulations that present an API-controlled dissolution, disintegration is the critical quality attribute of the dosage form and determines the onset of dissolution. Since the dissolution would be determined by the API properties, disintegration testing could become a release test for such formulations. After disintegration is completed, dissolution can be linked to API properties since the dosage form has limited impact

on the product performance. In this scenario, well established mass transport models (such as Noyes-Whitney) can be used to estimate and predict dissolution behavior if parameters such as medium pH, viscosity and surfactant concentrations are known. Hence, future studies need to be conducted to establish the scientific framework for using disintegration testing as a performance test, which would result in saving time and cost. A thorough investigation should be conducted to establish the test specifications for less variable results, such as beaker specifications, medium composition, medium viscosity, surface tension, time specification, among others.

REFERENCES

1. Amaral Silva D, Webster GK, Bou-chacra N, Löbenberg R. The Significance of Disintegration Testing in Pharmaceutical Development. *Dissolution Technol.* 2018;(August):30–8.
2. Noyes AA, Whitney WR. The rate of solution of solid substances in their own solutions. *J Am Chem Soc.* 1897 Dec 1;19(12):930–4.
3. <711> Dissolution. United States Pharmacopeia and National Formulary USP43-NF38 2S; The United States Pharmacopeial Convention, Inc.: Rockville, MD, 2020.
4. Hörter D, Dressman JB. Influence of physicochemical properties on dissolution of drugs in the gastrointestinal tract. *Adv Drug Deliv Rev.* 2001 Mar;46(1–3):75–87.
5. Shiu GK. Dissolution Methodology: Apparatus and Conditions. *Drug Inf J* [Internet]. 1996 Oct 1;30(4):1045–54. Available from: <https://doi.org/10.1177/009286159603000421>
6. Issa MG, Ferraz HG. Intrinsic dissolution as a tool for evaluating drug solubility in accordance with the biopharmaceutics classification system. *Dissolution Technol.* 2011;18(3):6–13.

7. The United States Pharmacopeia and National Formulary USP43-NF38 2S; The United States Pharmacopeial Convention, Inc.: Rockville, MD, 2020.
8. Blanquet S, Zeijdner E, Beyssac E, Meunier J-P, Denis S, Havenaar R, et al. A dynamic artificial gastrointestinal system for studying the behavior of orally administered drug dosage forms under various physiological conditions. *Pharm Res.* 2004 Apr;21(4):585–91.
9. Sperry DC, Hawley M. Dynamic artificial stomach and intestine model to evaluate the bioavailability of drugs and formulations. In: ABSTRACTS OF PAPERS OF THE AMERICAN CHEMICAL SOCIETY. AMER CHEMICAL SOC 1155 16TH ST, NW, WASHINGTON, DC 20036 USA; 2000. p. U81–U81.
10. Shargel L, Yu ABC. *Applied Biopharmaceutics & Pharmacokinetics*, 7e. Chapter 1. Introduction to Biopharmaceutics and Pharmacokinetics. McGraw-Hill Education; 2016.
11. Amidon GL, Lennernäs H, Shah VP, Crison JR. A theoretical basis for a biopharmaceutic drug classification: the correlation of *in vitro* drug product dissolution and *in vivo* bioavailability. *Pharm Res.* 1995;12(3):413–20.
12. Immediate Release Solid Oral Dosage Forms Scale-Up and Postapproval Changes: Chemistry, Manufacturing, and Controls, *In Vitro* Dissolution

- Testing, and *In Vivo* Bioequivalence Documentation, Center for Drug Evaluation and Research (CDER), FDA. 1995.
13. Tsume Y, Mudie DM, Langguth P, Amidon GE, Amidon GL. The Biopharmaceutics Classification System: Subclasses for *in vivo* predictive dissolution (IPD) methodology and IVIVC. *Eur J Pharm Sci.* 2014;57:152–63.
 14. Löbenberg R, Amidon GL. Modern bioavailability, bioequivalence and biopharmaceutics classification system. New scientific approaches to international regulatory standards. *Eur J Pharm Biopharm.* 2000;50(1):3–12.
 15. Guidance for Industry: SUPAC-MR: Modified Release Solid Oral Dosage Forms, US Department of Health and Human Services, Food and Drug Administration, Center for Drug Evaluation and Research (CDER), Rockville, Md, USA, 1997.
 16. Anand O, Yu LX, Conner DP, Davit BM. Dissolution testing for generic drugs: an FDA perspective. *AAPS J.* 2011/04/09. 2011 Sep;13(3):328–35.
 17. Grady H, Elder D, Webster GK, Mao Y, Lin Y, Flanagan T, et al. Industry's View on Using Quality Control, Biorelevant, and Clinically Relevant Dissolution Tests for Pharmaceutical Development, Registration, and Commercialization. *J Pharm Sci.* 2018;107(1):34–41.

18. Marroum PJ. History and evolution of the dissolution test. *Dissolution Technol.* 2014;21(3):11–6.
19. Bou-Chacra N, Melo KJC, Morales IAC, Stippler ES, Kesisoglou F, Yazdanian M, et al. Evolution of Choice of Solubility and Dissolution Media After Two Decades of Biopharmaceutical Classification System. *AAPS J.* 2017;19(4):989–1001.
20. Sheng JJ, McNamara DP, Amidon GL. Toward an *In Vivo* dissolution methodology: A comparison of phosphate and bicarbonate buffers. *Mol Pharm.* 2009;6(1):29–39.
21. Wu C-Y, Benet LZ. Predicting Drug Disposition via Application of BCS: Transport/Absorption/Elimination Interplay and Development of a Biopharmaceutics DrugDisposition Classification System. *Pharm Res.* 2005;22(1):11–23.
22. Boetker JP, Rantanen J, Rades T, Müllertz A, Østergaard J, Jensen H. A New Approach to Dissolution Testing by UV Imaging and Finite Element Simulations. *Pharm Res.* 2013;30(5):1328–37.
23. Dorożyński PP, Kulinowski P, Mendyk A, Młynarczyk A, Jachowicz R. Novel Application of MRI Technique Combined with Flow-Through Cell Dissolution Apparatus as Supportive Discriminatory Test for Evaluation of

- Controlled Release Formulations. *AAPS PharmSciTech*. 2010;11(2):588–97.
24. Jantratid E, Janssen N, Reppas C, Dressman JB. Dissolution Media Simulating Conditions in the Proximal Human Gastrointestinal Tract: An Update. *Pharm Res*. 2008;25(7):1663.
 25. Reppas C, Friedel H-D, Barker AR, Buhse LF, Cecil TL, Keitel S, et al. Biorelevant *In Vitro* Performance Testing of Orally Administered Dosage Forms—Workshop Report. *Pharm Res*. 2014;31(7):1867–76.
 26. Azarmi S, Roa W, Löbenberg R. Current perspectives in dissolution testing of conventional and novel dosage forms. *Int J Pharm*. 2007;328:12–21.
 27. Amaral Silva D, Al-Gousous J, Davies NM, Bou Chacra N, Webster GK, Lipka E, et al. Biphasic Dissolution as an Exploratory Method during Early Drug Product Development. *Pharmaceutics*. 2020;12(5):420.
 28. Amaral Silva D, Al-Gousous J, Davies NM, Bou Chacra N, Webster GK, Lipka E, et al. Simulated, biorelevant, clinically relevant or physiologically relevant dissolution media: The hidden role of bicarbonate buffer. *Eur J Pharm Biopharm*. 2019;142(May):8–19.
 29. Fotaki N, Vertzoni M. Biorelevant dissolution methods and their applications in *in vitro in vivo* correlations for oral formulations. *Open Drug Deliv J*.

- 2010;2:2–13.
30. Galia E, Nicolaidis E, Hörter D, Löbenberg R, Reppas C, Dressman JB. Evaluation of Various Dissolution Media for Predicting *In Vivo* Performance of Class I and II Drugs. *Pharm Res.* 1998;15(5):698–705.
 31. Mudie DM, Samiei N, Marshall DJ, Amidon GE, Bergström CAS. Selection of *In Vivo* Predictive Dissolution Media Using Drug Substance and Physiological Properties. *AAPS J.* 2020 Mar 27;22(2):34.
 32. Fuchs A, Leigh M, Kloefer B, Dressman JB. Advances in the design of fasted state simulating intestinal fluids: FaSSIF-V3. *Eur J Pharm Biopharm.* 2015;94:229–40.
 33. Vertzoni M, Dressman J, Butler J, Hempenstall J, Reppas C. Simulation of fasting gastric conditions and its importance for the *in vivo* dissolution of lipophilic compounds. *Eur J Pharm Biopharm Off J Arbeitsgemeinschaft für Pharm Verfahrenstechnik eV.* 2005 Aug;60(3):413–7.
 34. Fuchs A, Dressman JB. Composition and physicochemical properties of fasted-state human duodenal and jejunal fluid: a critical evaluation of the available data. *J Pharm Sci.* 2014 Nov;103(11):3398–411.
 35. Hens B, Tsume Y, Bermejo M, Paixao P, Koenigsnecht MJ, Baker JR, et al.

- Low Buffer Capacity and Alternating Motility along the Human Gastrointestinal Tract: Implications for *in Vivo* Dissolution and Absorption of Ionizable Drugs. *Mol Pharm.* 2017;14:4281–94.
36. Koenigsknecht M, Baker J, Wen B et al. *In Vivo* Dissolution and Systemic Absorption of Immediate Release Ibuprofen in Human Gastrointestinal Tract under Fed and Fasted Conditions. *Mol Pharm.* 2017;14(12):4295–304.
37. Riethorst D, Mols R, Duchateau G, Tack J, Brouwers J, Augustijns P. Characterization of Human Duodenal Fluids in Fasted and Fed State Conditions. *J Pharm Sci.* 2016 Feb 1;105(2):673–81.
38. Markopoulos C, Andreas CJ, Vertzoni M, Dressman J, Reppas C. In-vitro simulation of luminal conditions for evaluation of performance of oral drug products: Choosing the appropriate test media. *Eur J Pharm Biopharm.* 2015;93:173–82.
39. Lambert R, Martin F, Vagne M. Relationship between hydrogen ion and pepsin concentration in human gastric secretion. *Digestion.* 1968;1(2):65–77.
40. Efentakis M, Dressman JB. Gastric juice as a dissolution medium: Surface tension and pH. *Eur J Drug Metab Pharmacokinet.* 1998;23(2):97–102.

41. Dressman JB, Berardi RR, Dermentzoglou LC, Russell TL, Schmaltz SP, Barnett JL, et al. Upper gastrointestinal (GI) pH in young, healthy men and women. *Pharm Res.* 1990 Jul;7(7):756–61.
42. Dressman JB, Amidon GL, Reppas C, Shah VP. Dissolution Testing as a Prognostic Tool for Oral Drug Absorption: Immediate Release Dosage Forms. *Pharm Res.* 1998;15(1):11–22.
43. Kalantzi L, Goumas K, Kalioras V, Abrahamsson B, Dressman JB, Reppas C. Characterization of the human upper gastrointestinal contents under conditions simulating bioavailability/bioequivalence studies. *Pharm Res.* 2006 Jan;23(1):165–76.
44. Mudie DM, Amidon GL, Amidon GE. Physiological parameters for oral delivery and *in vitro* testing. *Mol Pharm.* 2010;7(5):1388–405.
45. Gibaldi M, Feldman S. Mechanisms of surfactant effects on drug absorption. *J Pharm Sci.* 1970 May;59(5):579–89.
46. Ruby M V, Davis A, Schoof R, Eberle S, Sellstone CM. Estimation of Lead and Arsenic Bioavailability Using a Physiologically Based Extraction Test. *Environ Sci Technol.* 1996 Jan 1;30(2):422–30.
47. Vertzoni M, Pastelli E, Psachoulas D, Kalantzi L, Reppas C. Estimation of

- Intragastric Solubility of Drugs : In What Medium ? Pharm Res. 2007;24(5):909–17.
48. Macheras P, Koupparis M, Tsaprounis C. Drug dissolution studies in milk using the automated flow injection serial dynamic dialysis technique. Int J Pharm. 1986;33(1):125–36.
 49. Nicolaides E, Galia E, Efthymiopoulos C, Dressman JB, Reppas C. Forecasting the *in vivo* performance of four low solubility drugs from their *in vitro* dissolution data. Pharm Res. 1999 Dec;16(12):1876–82.
 50. Kalantzi L, Persson E, Polentarutti B, Abrahamsson B, Goumas K, Dressman JB, et al. Canine intestinal contents vs. simulated media for the assessment of solubility of two weak bases in the human small intestinal contents. Pharm Res. 2006 Jun;23(6):1373–81.
 51. U.S. Food and Drug Administration. Guidance for Industry: Dissolution testing of immediate release solid oral dosage forms. Center for Drug Evaluation and Research (CDER), 1997.
 52. McConnell EL, Fadda HM, Basit AW. Gut instincts: Explorations in intestinal physiology and drug delivery. Int J Pharm. 2008;364(2):213–26.
 53. Persson EM, Gustafsson A-S, Carlsson AS, Nilsson RG, Knutson L, Forsell

- P, et al. The effects of food on the dissolution of poorly soluble drugs in human and in model small intestinal fluids. *Pharm Res.* 2005 Dec;22(12):2141–51.
54. Wei H, Löbenberg R. Biorelevant dissolution media as a predictive tool for glyburide a class II drug. *Eur J Pharm Sci.* 2006 Sep;29(1):45–52.
55. Psachoulas D, Vertzoni M, Butler J, Busby D, Symillides M, Dressman J, et al. An *In Vitro* Methodology for Forecasting Luminal Concentrations and Precipitation of Highly Permeable Lipophilic Weak Bases in the Fasted Upper Small Intestine. *Pharm Res.* 2012;29(12):3486–98.
56. Cristofolletti R, Dressman JB. Matching phosphate and maleate buffer systems for dissolution of weak acids: Equivalence in terms of buffer capacity of bulk solution or surface pH? *Eur J Pharm Biopharm.* 2016;103:104–8.
57. Cristofolletti R, Dressman JB. FaSSIF-V3, but not compendial media, appropriately detects differences in the peak and extent of exposure between reference and test formulations of ibuprofen. *Eur J Pharm Biopharm.* 2016;105:134–40.
58. Söderlind E, Karlsson E, Carlsson A, Kong R, Lenz A, Lindborg S, et al. Simulating fasted human intestinal fluids: understanding the roles of lecithin

- and bile acids. *Mol Pharm.* 2010 Oct;7(5):1498–507.
59. Fagerberg JH, Tsinman O, Sun N, Tsinman K, Avdeef A, Bergström CAS. Dissolution rate and apparent solubility of poorly soluble drugs in biorelevant dissolution media. *Mol Pharm.* 2010 Oct;7(5):1419–30.
60. Klein S. The Use of Biorelevant Dissolution Media to Forecast the *In Vivo* Performance of a Drug. *AAPS J.* 2010;12(3):397–406.
61. Dressman JB, Reppas C. *In vitro–in vivo* correlations for lipophilic, poorly water-soluble drugs. *Eur J Pharm Sci.* 2000;11:S73–80.
62. Lue B-M, Nielsen FS, Magnussen T, Schou HM, Kristensen K, Jacobsen LO, et al. Using biorelevant dissolution to obtain IVIVC of solid dosage forms containing a poorly-soluble model compound. *Eur J Pharm Biopharm.* 2008;69(2):648–57.
63. Nicolaidis E, Symillides M, Dressman JB, Reppas C. Biorelevant Dissolution Testing to Predict the Plasma Profile of Lipophilic Drugs After Oral Administration. *Pharm Res.* 2001;18(3):380–8.
64. Khan MZI, Rausl D, Zanoski R, Zidar S, Mikulčić JH, Krizmanić L, et al. Classification of loratadine based on the biopharmaceutics drug classification concept and possible *in vitro-in vivo* correlation. *Biol Pharm Bull.* 2004

- Oct;27(10):1630–5.
65. Kossena GA, Charman WN, Boyd BJ, Dunstan DE, Porter CJH. Probing drug solubilization patterns in the gastrointestinal tract after administration of lipid-based delivery systems: A phase diagram approach. *J Pharm Sci.* 2004;93(2):332–48.
 66. Jede C, Wagner C, Kubas H, Weigandt M, Weber C, Lecomte M, et al. Improved Prediction of *in Vivo* Supersaturation and Precipitation of Poorly Soluble Weakly Basic Drugs Using a Biorelevant Bicarbonate Buffer in a Gastrointestinal Transfer Model. *Mol Pharm.* 2019 Sep 3;16(9):3938–47.
 67. Litou C, Vertzoni M, Xu W, Kesisoglou F, Reppas C. The impact of reduced gastric acid secretion on dissolution of salts of weak bases in the fasted upper gastrointestinal lumen: Data in biorelevant media and in human aspirates. *Eur J Pharm Biopharm.* 2017;115:94–101.
 68. Boni JE, Brickl RS, Dressman J. Is bicarbonate buffer suitable as a dissolution medium? *J Pharm Pharmacol.* 2007 Oct 1;59(10):1375–82.
 69. Allen A, Flemström G. Gastroduodenal mucus bicarbonate barrier: protection against acid and pepsin. *Am J Physiol - Cell Physiol.* 2005;288:C1–19.
 70. Scott N, Patel K, Sithole T, Xenofontos K, Mohylyuk V, Liu F. Regulating

- the pH of bicarbonate solutions without purging gases: Application to dissolution testing of enteric coated tablets, pellets and microparticles. *Int J Pharm.* 2020;585:119562.
71. Fadda HM, Merchant HA, Arafat BT, Basit AW. Physiological bicarbonate buffers: stabilisation and use as dissolution media for modified release systems. *Int J Pharm.* 2009;382:56–60.
 72. Liu F, Merchant HA, Kulkarni RP, Alkademi M, Basit AW. Evolution of a physiological pH6.8 bicarbonate buffer system: Application to the dissolution testing of enteric coated products. *Eur J Pharm Biopharm.* 2011;78(1):151–7.
 73. Sakamoto A, Izutsu K, Yoshida H, Abe Y, Inoue D, Sugano K. Simple bicarbonate buffer system for dissolution testing: Floating lid method and its application to colonic drug delivery system. *J Drug Deliv Sci Technol.* 2021;63:102447.
 74. McNamara DP, Whitney KM, Goss SL. Use of a Physiologic Bicarbonate Buffer System for Dissolution Characterization of Ionizable Drugs. *Pharm Res.* 2003;20(10):1641–6.
 75. Goyanes A, Hatton GB, Merchant HA, Basit AW. Gastrointestinal release behaviour of modified-release drug products: Dynamic dissolution testing of mesalazine formulations. *Int J Pharm.* 2015;484:103–8.

76. Garbacz G, Kołodziej B, Koziol M, Weitschies W, Klein S. A dynamic system for the simulation of fasting luminal pH-gradients using hydrogen carbonate buffers for dissolution testing of ionisable compounds. *Eur J Pharm Sci.* 2014;51:224–31.
77. Boni JE, Brickl RS, Dressman J. Is bicarbonate buffer suitable as a dissolution medium? *J Pharm Pharmacol.* 2007;59:1375–82.
78. Al-Gousous J, Ruan H, Blechar JA, Sun KX, Salehi N, Langguth P, et al. Mechanistic analysis and experimental verification of bicarbonate-controlled enteric coat dissolution: Potential *in vivo* implications. *Eur J Pharm Biopharm.* 2019;139:47–58.
79. Hofmann M, García MA, Al-Gousous J, Ruiz-Picazo A, Thieringer F, Nguyen MA, et al. *In vitro* prediction of *in vivo* absorption of ibuprofen from suspensions through rational choice of dissolution conditions. *Eur J Pharm Biopharm.* 2020;149:229–37.
80. Tsume Y, Langguth P, Garcia-Arietac A, Amidon GL. In silico prediction of drug dissolution and absorption with variation in intestinal pH for BCS class II weak acid drugs: ibuprofen and ketoprofen. *Biopharm Drug Dispos.* 2012;33:366–377.
81. Mooney KG, Mintun MA, Himmelstein KJ, Stella VJ. Dissolution Kinetics

- of Carboxylic Acids II: Effect of Buffers. *J Pharm Sci.* 1981;70(1):22–32.
82. Mooney KG, Mintun MA, Himmelstein KJ, Stella VJ. Dissolution kinetics of carboxylic acids I: Effect of pH under unbuffered conditions. *J Pharm Sci.* 1981;70(1):13–22.
83. Krieg BJ, Taghavi SM, Amidon GL, Amidon GE. *In Vivo* Predictive Dissolution: Comparing the Effect of Bicarbonate and Phosphate Buffer on the Dissolution of Weak Acids and Weak Bases. *J Pharm Sci.* 2015;104:2894–904.
84. Krieg BJ, Taghavi SM, Amidon GL, Amidon GE. *In vivo* predictive dissolution: Transport analysis of the CO₂, bicarbonate *in vivo* buffer system. *J Pharm Sci.* 2014;103:3473–90.
85. Al-Gousous J, Salehi N, Amidon GE, Ziff RM, Langguth P, Amidon GL. Mass Transport Analysis of Bicarbonate Buffer: Effect of the CO₂–H₂O–HCO₃⁻ Hydration–Dehydration Kinetics in the Fluid Boundary Layer and the Apparent Effective pK_a Controlling Dissolution of Acids and Bases. *Mol Pharm.* 2019 Jun 3;16(6):2626–35.
86. Salehi N, Al-Gousous J, Mudie DM, Amidon GL, Ziff RM, Amidon GE. Hierarchical Mass Transfer Analysis of Drug Particle Dissolution, Highlighting the Hydrodynamics, pH, Particle Size, and Buffer Effects for

- the Dissolution of Ionizable and Nonionizable Drugs in a Compendial Dissolution Vessel. *Mol Pharm.* 2020 Oct 5;17(10):3870–84.
87. Alvarez C, Núñez I, Torrado JJ, Gordon J, Potthast H, García-Arieta A. Investigation on the possibility of biowaivers for ibuprofen. *J Pharm Sci.* 2011 Jun;100(6):2343–9.
88. Amaral Silva D, Davies NM, Doschak MR, Al-Gousous J, Bou-Chacra N, Löbenberg R. Mechanistic understanding of underperforming enteric coated products: Opportunities to add clinical relevance to the dissolution test. *J Control Release.* 2020;325:323–34.
89. Blechar JA, Al-Gousous J, Wilhelmy C, Postina AM, Getto M, Langguth P. Toward Mechanistic Design of Surrogate Buffers for Dissolution Testing of pH-Dependent Drug Delivery Systems. Vol. 12, *Pharmaceutics* . 2020.
90. Aghabegi Moghanjoughi A, Khoshnevis D, Zarrabi A. A concise review on smart polymers for controlled drug release. *Drug Deliv Transl Res.* 2016;6(3):333–40.
91. Ibekwe VC, Fadda HM, McConnell EL, Khela MK, Evans DF, Basit AW. Interplay between intestinal pH, transit time and feed status on the *in vivo* performance of pH responsive ileo-colonic release systems. *Pharm Res.* 2008;25(8):1828–35.

92. Nguyen DA, Fogler HS. Facilitated diffusion in the dissolution of carboxylic polymers. *AIChE J.* 2005;51(2):415–25.
93. Sugano K. Theoretical comparison of hydrodynamic diffusion layer models used for dissolution simulation in drug discovery and development. *Int J Pharm.* 2008;363(1):73–7.
94. Markl D, Zeitler JA. A Review of Disintegration Mechanisms and Measurement Techniques. *Pharm Res.* 2017;34(5):890–917.
95. RUBINSTEIN MH, BODEY DM. Disaggregation of Compressed Tablets. *J Pharm Sci.* 1976;65(12):1749-1753. DOI: 10.1002/jps.2600651214.
96. Aulton ME, Taylor K. *Aulton 's Pharmaceutics. The Design and Manufacture of Medicines.* Churchill Livingstone; 2013.
97. Quodbach J, Kleinebudde P. A critical review on tablet disintegration. *Pharm Dev Technol.* 2016;21(6):763-774. DOI: 10.3109/10837450.2015.1045618.
98. Lowenthal W. Disintegration of Tablets. *J Pharm Sci.* 1972;61(11):1695-1711. DOI: 10.1002/jps.2600611102.
99. Desai PM, Liew CV, Heng PWS. Review of Disintegrants and the Disintegration Phenomena. *J Pharm Sci.* 2016;105(9):2545-2555. DOI: 10.1016/j.xphs.2015.12.019.

100. Kissa E. Wetting and wicking. *Text Res J.* 1996;66(10):660-668. DOI: 10.1177/004051759606601008.
101. Patel N, Hopponent R. Mechanism of action of starch as a disintegrating agent in aspirin tablets. *J Pharm Sci.* 1966;55(10):1065–1068. DOI: 10.1002/jps.2600551015.
102. Patel S, Kaushal A, Bansal A. Effect of particle size and compression force on compaction behavior and derived mathematical parameters of compressibility. *Pharm Res.* 2007;24(1):111–24.
103. Lowenthal W. Mechanism of action of tablet disintegrants. *Pharm Acta Helv.* 1973;48(11–12):589–609.
104. Ferrari F, Bertoni M, Bonferoni M, Rossi S, Caramella C, Nyström C. Investigation on bonding and disintegration properties of pharmaceutical materials. *Int J Pharm.* 1996;136(1–2):71-79. DOI: 10.1016/0378-5173(96)04489-4.
105. Matsumaru H. Studies on the mechanism of tablet compression and disintegration IV evolution of wetting heat and its reduction by Compressional force. *Yakugaku Zasshi.* 1959;79(1):63-64. DOI: 10.1248/yakushi1947.79.1_63.

106. Donauer N, Löbenberg R. A mini review of scientific and pharmacopeial requirements for the disintegration test. *Int J Pharm.* 2007;345(1–2):2-8.
DOI:10.1016/j.ijpharm.2007.08.045.
107. Al-Gousous J, Langguth P. Oral Solid Dosage Form Disintegration Testing - The Forgotten Test. *J Pharm Sci.* 2015;104(9):2664-2675. DOI: 10.1002/jps.24303.
108. *Pharmacopoeia Helvetica.* 1907. Bern, Switzerland: The Swiss Pharmacopoeia Commission.
109. *British Pharmacopoeia (BP).* 1948. London, United Kingdom: The General Council of Medical education and Registration of the United Kingdom.
110. Gershberg S, Stoll FD. Apparatus, for Tablet Disintegration, and for Shaking-Out Extractions. *J Am Pharm Assoc (Scientific ed).* 1946;35(9):284-287. DOI: 10.1002/jps.3030350910.
111. Almukainzi M, Salehi M, Chacra NAB, Löbenberg R. Comparison of the rupture and disintegration tests for soft-shell capsules. *Dissolution Technol.* 2011;18(1):21-25. DOI: 10.14227/DT180111P21.
112. <701> Disintegration. In *The United States Pharmacopeia and National Formulary USP43-NF38 2S*; The United States Pharmacopeial Convention,

- Inc.: Rockville, MD, 2020.
113. <2040> Disintegration and Dissolution of Dietary Supplements. In The United States Pharmacopeia and National Formulary USP43-NF38 2S; The United States Pharmacopeial Convention, Inc.: Rockville, MD, 2020.
 114. Almukainzi M, Salehi M, Araci Bou-Chacra N, Löbenberg R. Investigation of the Performance of the Disintegration Test for Dietary Supplements. *AAPS J.* 2010;12(4):602–7.
 115. Al-Gousous J, Langguth P. European versus United States Pharmacopeia disintegration testing methods for enteric-coated soft gelatin capsules. *Dissolution Technol.* 2015;22(3):6-8. DOI: 10.14227/DT220315P6.
 116. International Conference on Harmonisation. 1999. ICH Q6A Guideline: Specifications: Test procedures and acceptance criteria for new drug substances and new drug products: Chemical substances.
 117. Dissolution Testing and Specification Criteria for Immediate-Release Solid Oral Dosage Forms Containing BCS Class 1 and 3 Drugs: Guidance for Industry; U.S. Department of Health and Human Services, Food and Drug Administration, CDER, 2015.
 118. <2> ORAL DRUG PRODUCTS—PRODUCT QUALITY TESTS. In The

United States Pharmacopeia and National Formulary USP43-NF38 2S; The United States Pharmacopeial Convention, Inc.: Rockville, MD, 2020.

119. Klute AS. Disintegration Testing : Release Dosage Forms in Exploratory Development. *Am Pharm Rev.* 2009;(August):90–3.
120. Uebbing L, Klumpp L, Webster GK, Löbenberg R. Justification of disintegration testing beyond current FDA criteria using *in vitro* and *in silico* models. *Drug Des Devel Ther.* 2017;11:1163–74.
121. Stamatakis MK, Alderman JM, Meyer-Stout PJ. Influence of pH on *In Vitro* Disintegration of Phosphate Binders. *Am J Kidney Dis.* 1998;32(5):808-812. DOI: 10.1016/S0272-6386(98)70137-4.
122. Alam AS, Parrott EL. Effect of dissolution media on disintegration and dissolution of hydrochlorothiazide tablets. *J Pharm Sci.* 1971;60(5):795-797. DOI: 10.1002/jps.2600600531.
123. Zuo J, Gao Y, Almukainzi M, Löbenberg R. Investigation of the disintegration behavior of dietary supplements in different beverages. *Dissolution Technol.* 2013;20(4):6-9. DOI:10.14227/DT200413P6.
124. Schmid K, Löbenberg R. Influence of the Changed USP Test Performance. *Dissolution Technol.* 2010;17(1):6-10. DOI: 10.14227/DT170110P6.

125. Bachour G, Bou-Chacra NA, Löbenberg R. Evaluation of the rupture test for stability studies of soft-shell capsules. *Dissolution Technol.* 2017;24:16–9.
126. Radwan A, Wagner M, Amidon GL, Langguth P. Bio-predictive tablet disintegration: Effect of water diffusivity, fluid flow, food composition and test conditions. *Eur J Pharm Sci.* 2014;57(1):273-279. DOI: 10.1016/j.ejps.2013.08.038.
127. Nickerson B, Kong A, Gerst P, Kao S. Correlation of dissolution and disintegration results for an immediate-release tablet. *J Pharm Biomed Anal.* 2018;150:333-340. DOI: 10.1016/j.jpba.2017.12.017.
128. Gupta A, Hunt RL, Shah RB, Sayeed VA, Khan MA. Disintegration of Highly Soluble Immediate Release Tablets: A Surrogate for Dissolution. *AAPS PharmSciTech.* 2009;10(2):495-499. DOI: 10.1208/s12249-009-9227–0.
129. Han J, Gallery J. A risk-based approach to *in vitro* performance testing: A case study on the use of dissolution vs. disintegration for liquid-filled gelatin capsules. *Am Pharm Rev.* 2006;9:152–7.
130. Dokoumetzidis A, Macheras P. A century of dissolution research: from Noyes and Whitney to the Biopharmaceutics Classification System. *Int J Pharm.* 2006;321(1):1–11.

131. Abend A, Curran D, Kuiper J, Lu X, Li H, Hermans A, et al. Dissolution Testing in Drug Product Development: Workshop Summary Report. AAPS J. 2019;21(2):1–12.
132. Gibaldi BM, Feldman S. Establishment of Sink Conditions in Dissolution Rate Determinations. J Pharm Sci. 1967;56(10):1238–42.
133. Phillips DJ, Pygall SR, Cooper VB, Mann JC. Overcoming sink limitations in dissolution testing: A review of traditional methods and the potential utility of biphasic systems. J Pharm Pharmacol. 2012;64(11):1549–59.
134. Pestieau A, Evrard B. *In vitro* biphasic dissolution tests and their suitability for establishing *in vitro-in vivo* correlations: A historical review. Eur J Pharm Sci. 2017;102:203–19.
135. Deng J, Staufenbiel S, Hao S, Wang B, Dashevskiy A, Bodmeier R. Development of a discriminative biphasic *in vitro* dissolution test and correlation with *in vivo* pharmacokinetic studies for differently formulated racecadotril granules. J Control Release. 2017;255:202–9.
136. Tsume Y, Igawa N, Drelich AJ, Ruan H, Amidon GE, Amidon GL. The *in vivo* predictive dissolution for immediate release dosage of donepezil and danazol, BCS class IIc drugs, with the GIS and the USP II with biphasic dissolution apparatus. J Drug Deliv Sci Technol. 2019 Jan;In

- press.(<https://doi.org/10.1016/j.jddst.2019.01.035>).
137. Tsume Y, Igawa N, Drelich AJ, Amidon GE, Amidon GL. The Combination of GIS and Biphasic to Better Predict *In Vivo* Dissolution of BCS Class IIb Drugs, Ketoconazole and Raloxifene. *J Pharm Sci.* 2018;107(1):307–16.
 138. Xu H, Shi Y, Vela S, Marroum P, Gao P. Developing Quantitative *In Vitro*–*In Vivo* Correlation for Fenofibrate Immediate-Release Formulations With the Biphasic Dissolution-Partition Test Method. *J Pharm Sci.* 2018;107(1):476–87.
 139. Xu H, Krakow S, Shi Y, Rosenberg J, Gao P. *In vitro* characterization of ritonavir formulations and correlation to *in vivo* performance in dogs. *Eur J Pharm Sci.* 2018;115:286–95.
 140. Xu H, Vela S, Shi Y, Marroum P, Gao P. *In Vitro* Characterization of Ritonavir Drug Products and Correlation to Human *in Vivo* Performance. *Mol Pharm.* 2017;14:3801–14.
 141. Mudie DM, Shi Y, Ping H, Gao P, Amidon GL, Amidon GE. Mechanistic analysis of solute transport in an *in vitro* physiological two-phase dissolution apparatus. *Biopharm Drug Dispos.* 2012;33:378–402.
 142. Doluisio JT, Swintosky JV. Drug partitioning II *in vitro* model for drug

- absorption. *J Pharm Sci.* 1964;53:597 – 601.
143. Deng J, Staufenbiel S, Bodmeier R. Evaluation of a biphasic *in vitro* dissolution test for estimating the bioavailability of carbamazepine polymorphic forms. *Eur J Pharm Sci.* 2017;105:64–70.
144. Kalepu S, Nekkanti V. Insoluble drug delivery strategies: Review of recent advances and business prospects. *Acta Pharm Sin B.* 2015;5(5):442–53.
145. Mudie DM, Murray K, Hoad CL, Pritchard SE, Garnett MC, Amidon GL, et al. Quantification of Gastrointestinal Liquid Volumes and Distribution Following a 240 mL Dose of Water in the Fasted State. *Mol Pharm* [Internet]. 2014 Sep 2;11(9):3039–47. Available from: <https://pubs.acs.org/doi/10.1021/mp500210c>
146. Zuo J, Gao Y, Bou-Chacra N, Löbenberg R. Evaluation of the DDSolver software applications. *Biomed Res Int.* 2014/04/27. 2014;2014:204925.
147. Zhang Y, Huo M, Zhou J, Zou A, Li W, Yao C, et al. DDSolver: an add-in program for modeling and comparison of drug dissolution profiles. *AAPS J.* 2010/04/06. 2010 Sep;12(3):263–71.
148. Al-Gousous J, Sun KX, McNamara DP, Hens B, Salehi N, Langguth P, et al. Mass Transport Analysis of the Enhanced Buffer Capacity of the

- Bicarbonate–CO₂ Buffer in a Phase-Heterogenous System: Physiological and Pharmaceutical Significance. *Mol Pharm* [Internet]. 2018 Nov 5;15(11):5291–301. Available from:
<https://pubs.acs.org/doi/10.1021/acs.molpharmaceut.8b00783>
149. Guyton and Hall Textbook of Medical Physiology, Thirteenth Edition Chapter 65. Secretory Functions of the Alimentary Tract. 2016. Philadelphia, PA: Elsevier.
150. Valizadeh H, Nokhodchi A, Qarakhani N, Zakeri-Milani P, Azarmi S, Hassanzadeh D, et al. Physicochemical Characterization of Solid Dispersions of Indomethacin with PEG 6000, Myrj 52, Lactose, Sorbitol, Dextrin, and Eudragit® E100. *Drug Dev Ind Pharm*. 2004;30(3):303–17.
151. Rowe R, Sheskey P, Owen S. Handbook of Pharmaceutical Excipients, 5th ed. Pharmaceutical Press; 2006. 96–100 p.
152. Baradari H, Damia C, Dutreih-colas M, Laborde E, Pécout N, Champion E, et al. Calcium phosphate porous pellets as drug delivery systems : Effect of drug carrier composition on drug loading and *in vitro* release. *J Eur Ceram Soc*. 2012;32:2679–90.
153. Choi AH, Ben-Nissan B, Matinlinna JP, Conway RC. Current perspectives: Calcium phosphate nanocoatings and nanocomposite coatings in dentistry. *J*

- Dent Res. 2013;92(10):853–9.
154. Mccarthy LG, Kosiol C, Healy AM, Bradley G, Sexton JC, Corrigan I. Simulating the Hydrodynamic Conditions in the United States Pharmacopeia Paddle Dissolution Apparatus. AAPS PharmSciTech. 2003;4(2):1–16.
155. Todaro V, Persoons T, Grove G, Healy AM, D’Arcy DM. Characterization and Simulation of Hydrodynamics in the Paddle, Basket and Flow-Through Dissolution Testing Apparatuses - A Review. Dissolution Technol. 2017;August:24–36.
156. Sjögren E, Abrahamsson B, Augustijns P, Becker D, Bolger MB, Brewster M, et al. *In vivo* methods for drug absorption - Comparative physiologies, model selection, correlations with *in vitro* methods (IVIVC), and applications for formulation/API/excipient characterization including food effects. Eur J Pharm Sci. 2014;57(1):99–151.
157. Pestieau A, Lebrun S, Cahay B, Brouwers A, Streel B, Cardot J-M, et al. Evaluation of different *in vitro* dissolution tests based on level A *in vitro* – *in vivo* correlations for fenofibrate self-emulsifying lipid-based formulations. Eur J Pharm Biopharm. 2017;112:18–29.
158. Vangani S, Li X, Zhou P, Del-Barrio M-A, Chiu R, Cauchon N, et al. Dissolution of poorly water-soluble drugs in biphasic media using USP 4 and

- fiber optic system. Clin Res Regul Aff. 2009 Jun 1;26(1–2):8–19.
159. Shi Y, Gao P, Gong Y, Ping H. Application of a biphasic test for characterization of *in vitro* drug release of immediate release formulations of celecoxib and its relevance to *in vivo* absorption. Mol Pharm. 2010;7(5):1458–65.
160. Ullah I, Cadwallader DE. Dissolution of Slightly Soluble Powders under Sink Conditions II: Griseofulvin Powders. J Pharm Sci. 1971;60(2):230–3.
161. Ullah I, Cadwallader DE. Dissolution of Slightly Soluble Powders under Sink Conditions III: Transport of Drug Solution across Screens and Membrane Barriers. J Pharm Sci. 1971;60(10):1496–9.
162. Shi Y, Erickson B, Jayasankar A, Lu L, Marsh K, Menon R, et al. Assessing Supersaturation and Its Impact on *In Vivo* Bioavailability of a Low-Solubility Compound ABT-072 With a Dual pH , Two-Phase Dissolution Method. J Pharm Sci. 2016;105(9):2886–95.
163. Al Durdunji A, Alkhatib HS, Al-Ghazawi M. Development of a biphasic dissolution test for Deferasirox dispersible tablets and its application in establishing an *in vitro-in vivo* correlation. Eur J Pharm Biopharm. 2016;102:9–18.

164. Gupta E, Barends DM, Yamashita E, Lentz KA, Harmsze AM, Shah VP, et al. Review of global regulations concerning biowaivers for immediate release solid oral dosage forms. *Eur J Pharm Sci.* 2006;29(3):315–24.
165. Food and Drug Administration (FDA) Center for Drug Evaluation and Research Guidance for industry: waiver of *in vivo* bioavailability and bioequivalence studies for immediate-release solid oral dosage forms based on a biopharmaceutics classification system. 2017.
166. European Medicines Agency (EMA) Note for guidance on the investigation of bioavailability and bioequivalence. 2002.
167. WHO Expert Committee on Specifications for Pharmaceutical Preparations Technical report series 40th report: Annex 7 Multisource (generic) pharmaceutical products: guidelines on registration requirements to establish interchangeability. 2006.
168. Hofsäss MA, Dressman JB. The Discriminatory Power of the BCS-Based Biowaiver: A Retrospective With Focus on Essential Medicines. *J Pharm Sci.* 2019;108(9):2824–37.
169. European Medicines Agency (EMA) Committee for medicinal products for human use (CHMP), guideline on the investigation of bioequivalence. 2010.

170. WHO Expert Committee on Specifications for Pharmaceutical Preparations
Technical report series 51st report. 2017.
171. ICH M9 guideline on biopharmaceutics classification system-based
biowaivers. 2020.
172. Löbenberg R, Chacra NB, Stippler ES, Shah VP, DeStefano AJ, Hauck WW,
et al. Toward global standards for comparator pharmaceutical products: case
studies of amoxicillin, metronidazole, and zidovudine in the Americas.
AAPS J. 2012/04/19. 2012 Sep;14(3):462–72.
173. Rediguieri CF, Porta V, G. Nunes DS, Nunes TM, Junginger HE, Kopp S, et
al. Biowaiver monographs for immediate release solid oral dosage forms:
Metronidazole. J Pharm Sci. 2011 May 1;100(5):1618–27.
174. Steingoetter A, Fox M, Treier R, Weishaupt D, Marincek B, Boesiger P, et
al. Effects of posture on the physiology of gastric emptying: a magnetic
resonance imaging study. Scand J Gastroenterol. 2006 Oct;41(10):1155–64.
175. Pedersen BL, Brøndsted H, Lennernäs H, Christensen FN, Müllertz A,
Kristensen HG. Dissolution of Hydrocortisone in Human and Simulated
Intestinal Fluids. Pharm Res. 2000;17(2):183–9.
176. Lindahl A, Ungell A-L, Knutson L, Lennernäs H. Characterization of fluids

- from the stomach and proximal jejunum in men and women. *Pharm Res.* 1997;14(4):497–502.
177. Vertzoni M, Fotaki N, Nicolaides E, Reppas C, Kostewicz E, Stippler E, et al. Dissolution media simulating the intraluminal composition of the small intestine: physiological issues and practical aspects. *J Pharm Pharmacol.* 2004;56:453–62.
178. Schiller C, Fröhlich CP, Giessmann T, Siegmund W, Mönnikes H, Hosten N, et al. Intestinal fluid volumes and transit of dosage forms as assessed by magnetic resonance imaging. *Aliment Pharmacol Ther.* 2005;22:971–9.
179. Sheng JJ, Kasim NA, Chandrasekharan R, Amidon GL. Solubilization and dissolution of insoluble weak acid, ketoprofen: Effects of pH combined with surfactant. *Eur J Pharm Sci.* 2006;29:306–14.
180. Ozturk SS, Palsson BO DJ. Dissolution of Ionizable drugs in buffered and unbuffered solutions. *Pharm Res.* 1988;5(5):272-82.
181. Balakrishnan A, Rege BD, Amidon GL, Polli JE. Surfactant-mediated dissolution: Contributions of solubility enhancement and relatively low micelle diffusivity. *J Pharm Sci.* 2004;93(8):2064–75.
182. Jinno J, Oh DM, Crison JR, Amidon GL. Dissolution of ionizable water-

- insoluble drugs: The combined effect of pH and surfactant. *J Pharm Sci.* 2000;89(2):268–74.
183. HOGAN DL, AINSWORTH MA, ISENBERG JI. Review article: gastroduodenal bicarbonate secretion. *Aliment Pharmacol Ther.* 1994;8:475–88.
184. Isenberg, J. I.; Hogan, D. L.; Thomas FJ. Duodenal mucosal bicarbonate secretion in humans: a brief review. *Scand J Gastroenterol.* 1986;Suppl. 125:106–9.
185. Rees WDW, Botham D, Turnberg LA. A demonstration of bicarbonate production by the normal human stomach *in vivo*. *Dig Dis Sci.* 1982;27(11):961–6.
186. Rune SJ. Acid-Base Parameters of Duodenal Contents in Man. *Gastroenterology.* 1972;62(4):533–9.
187. Flemstrom, G. Gastric and duodenal mucosal secretion of bicarbonate; Raven Press: New York, 1994.
188. Rune, S. J. The duodenal PCO₂ in duodenal ulcer patients and normal subjects. *Acta Hepato-Gastroenterol.* 1972, 19, 386 – 387.
189. Bastami SM, Groves MJ. Some factors influencing the *in vitro* release of

- phenytoin from formulations. *Int J Pharm.* 1978;1(3):151–64.
190. Fadda HM, Basit AW. Dissolution of pH responsive formulations in media resembling intestinal fluids: bicarbonate versus phosphate buffers. *J Drug Deliv Sci Technol.* 2005;15(4):273–9.
191. Garbacz G, Kolodziej B, Koziol M, Weitschies W, Klein S. An automated system for monitoring and regulating the pH of bicarbonate buffers. *AAPS PharmSciTech.* 2013;14:517–22.
192. Karkossa F, Klein S. Assessing the influence of media composition and ionic strength on drug release from commercial immediate-release and enteric-coated aspirin tablets. *J Pharm Pharmacol.* 2017;69:1327–40.
193. Merchant HA, Goyanes A, Parashar N, Basit AW. Predicting the gastrointestinal behaviour of modified-release products: Utility of a novel dynamic dissolution test apparatus involving the use of bicarbonate buffers. *Int J Pharm.* 2014;475:585–91.
194. Pines D, Ditkovich J, Mukra T, Miller Y, Kiefer PM, Daschakraborty S, et al. How Acidic Is Carbonic Acid? *J Phys Chem B.* 2016;(120):2440–51.
195. Almukainzi M, Bou-chacra NA, Walker RB, Löbenberg R. Therapeutic Delivery Solutions. Chapter 12 BIORELEVANT DISSOLUTION

- TESTING. 1st ed. Chan CC, Chow K, Mckay B, Fung M, editors. John Wiley & Sons, Inc.; 2014. 335–365 p.
196. Tong C, Lozano R, Yun M, Mirza T, Löbenberg R, Nickerson B, Gray V WQ. The value of *in vitro* dissolution in drug development. *Pharm Technol.* 2009;33(4):52–64.
197. Gray V, Kelly G, Xia M, Butler C, Thomas S, Mayock S. The science of USP 1 and 2 dissolution: Present challenges and future relevance. *Pharm Res.* 2009;26(6):1289–302.
198. Stippler E, Kopp S, Dressman J. Comparison of US Pharmacopeia simulated intestinal fluid TS (without pancreatin) and phosphate standard buffer pH 6.8, TS of the International Pharmacopoeia with respect to Their Use in *In Vitro* Dissolution Testing. *Dissolution Technol.* 2004;(May):6–10.
199. Ropers MH, Czichocki G, Brezesinski G. Counterion Effect on the Thermodynamics of Micellization of Alkyl Sulfates. *J Phys Chem B.* 2003;107:5281–8.
200. Ku MS, Lu Q, Li W, Chen Y. Performance qualification of a new hypromellose capsule : Part II . Disintegration and dissolution comparison between two types of hypromellose capsules. *Int J Pharm.* 2011;416(1):16–24.

201. Tochio, S., Nagata, S., Yamashita, S., 2002. The influence of the composition of test fluids on dissolution from HPMC capsules. AAPS PharmSci. 4 (abstract W4340).
202. Honkanen, O., Seppä, H., Eerikäinen, S., Tuominen, R., Marvola, M., 2001. Bioavailability of ibuprofen from orally and rectally administered hydroxypropyl methyl cellulose capsules compared to corresponding gelatin capsules. STP Pharma Sci. 11, 181 – 185.
203. Cole, E.T., Scott, R.A., Cade, D., Connor, A.L., Wilding, I., 2004. *In vitro* and *in vivo* pharmacoscintigraphic evaluation of ibuprofen hypromellose and gelatin capsules. Pharm. Res. 21, 793 – 798.
204. Marques MRC. Enzymes in the Dissolution Testing of Gelatin Capsules. AAPS PharmSciTech. 2014;15(6):1410–6.
205. Lu X, Shah P. Dissolution of gelatin capsules: Evidence and confirmation of cross-linking. Dissolution Technol. 2017;24:6–21.
206. Marchais H, Cayzeele G, Legendre JY, Skiba M, Arnaud P. Cross-linking of hard gelatin carbamazepine capsules: Effect of dissolution conditions on *in vitro* drug release. Eur J Pharm Sci. 2003;19:129–32.
207. Khan MZI, Raušl D, Radošević S, Filić D, Danilovski A, Dumić M, et al.

- Classification of torasemide based on the Biopharmaceutics Classification System and evaluation of the FDA biowaiver provision for generic products of Class I drugs. *J Pharm Pharmacol.* 2006;58:1475–82.
208. Fang JB, Robertson VK, Rawat A, Flick T, Tang ZJ, Cauchon NS, et al. Development and application of a biorelevant dissolution method using USP apparatus 4 in early phase formulation development. *Mol Pharm.* 2010;7(5):1466–77.
209. Leigh M, Kloefer B, Schaich M. Comparison of the solubility and dissolution of drugs in fasted-state biorelevant media (FaSSIF and FaSSIF-V2). *Dissolution Technol.* 2013;20:44–50.
210. Fotaki N. Flow-Through Cell Apparatus (USP Apparatus 4): Operation and Features. *Dissolution Technol.* 2011;46–9.
211. Sunesen VH, Pedersen BL, Kristensen HG, Müllertz A. *In vivo in vitro* correlations for a poorly soluble drug, danazol, using the flow-through dissolution method with biorelevant dissolution media. *Eur J Pharm Sci.* 2005;24:305–13.
212. Alsenz J, Haenel E, Anedda A, Du Castel P, Cirelli G. Miniaturized INtrinsic DISSolution Screening (MINDISS) assay for preformulation. *Eur J Pharm Sci.* 2016;87:3–13.

213. Hammad MA, Müller BW. Increasing drug solubility by means of bile salt-phosphatidylcholine-based mixed micelles. *Eur J Pharm Biopharm.* 1998;46:361–7.
214. Okumu A, DiMaso M, Löbenberg R. Dynamic dissolution testing to establish *in vitro/in vivo* correlations for montelukast sodium, a poorly soluble drug. *Pharm Res.* 2008;25(12):2778–85.
215. Kloefer B, Hoogevest P Van, Moloney R, Kuentz M, Leigh MLS, Dressman J. Study of a Standardized Taurocholate– Lecithin Powder for Preparing the Biorelevant Media FeSSIF and FaSSIF. *Dissolution Technol.* 2010;6–13.
216. Ramtoola Z, Corrigan OI. Influence of the buffering capacity of the medium on the dissolution of drug-excipient mixtures. *Drug Dev Ind Pharm.* 1989;15(14–16):2359–74.
217. Levis KA, Lane ME, Corrigan OI. Effect of buffer media composition on the solubility and effective permeability coefficient of ibuprofen. *Int J Pharm.* 2003;253:49–59.
218. Corrigan OI, Devlin Y, Butler J. Influence of dissolution medium buffer composition on ketoprofen release from ER products and *in vitro-in vivo* correlation. *Int J Pharm.* 2003;254(2):147–54.

219. Ashford M, Fell JT, Attwood D, Sharma H, Woodhead PJ. An *in vivo* investigation into the suitability of pH dependent polymers for colonic targeting. *Int J Pharm.* 1993;91:241–5.
220. Hamed R, Awadallah A, Sunoqrot S, Tarawneh O, Nazzal S, AlBaraghtli T, et al. pH-Dependent Solubility and Dissolution Behavior of Carvedilol—Case Example of a Weakly Basic BCS Class II Drug. *AAPS PharmSciTech.* 2016;17(2):418–26.
221. Waiver of the *in vivo* bioavailability and bioequivalence studies for immediate-release solid oral dosage forms based on a biopharmaceutics classification system. Guidance for industry. U.S. Department of Health and Human Services. FDA. Available from:
<https://www.fda.gov/downloads/Drugs/Guidances/ucm070246.pdf>
222. McGee LC, Hastings AB. The carbon dioxide tension and acid-base balance of jejunal secretions in man. *J Biol Chem.* 1942;142:893–904.
223. Perez de la Cruz Moreno M, Oth M, Deferme S, Lammert F, Tack J, Dressman J AP. Characterization of fasted-state human intestinal fluids collected from duodenum and jejunum. *J Pharm Pharmacol.* 2006;58(8):1079–1089.
224. Bergstrom C, Holm R, Jorgensen SA, Andersson SBE, Artursson P, Beato S,

- Borde A, Box K, Brewster M, Dressman J, Feng K-I, Halbert G, Kostewicz E, McAllister M, Muenster U, Thinnes J, Taylor R M, A. Early pharmaceutical profiling to predict oral drug absorption: Current status and unmet needs. *Eur J Pharm Sci.* 2014;57:173–199.
225. Rudolph MW, Klein S, Beckert TE, Petereit HD. A new 5-aminosalicylic acid multi-unit dosage form for the therapy of ulcerative colitis. *Eur J Pharm Biopharm.* 2001;51:183–90.
226. Chan WA et al. Comparison of the release profiles of a water soluble drug carried by Eudragit-coated capsules in different in-vitro dissolution liquids. *Powder Technol.* 2001;119:26–32.
227. Ibekwe VC, Fadda HM, Parsons GE, Basit AW. A comparative *in vitro* assessment of the drug release performance of pH-responsive polymers for ileo-colonic delivery. *Int J Pharm.* 2006;308:52–60.
228. Jirmář R, Widimský P. Enteric-coated aspirin in cardiac patients: Is it less effective than plain aspirin? *Cor Vasa.* 2018;60:e165–8.
229. Maree AO, Curtin RJ, Dooley M, Conroy RM, Crean P, Cox D, et al. Platelet response to low-dose enteric-coated aspirin in patients with stable cardiovascular disease. *J Am Coll Cardiol.* 2005;47(7):1258–63.

230. Bhatt DL, Grosser T, Dong J, Logan D, Jeske W, Angiolillo DJ, et al. Enteric Coating and Aspirin Nonresponsiveness in Patients With Type 2 Diabetes Mellitus. *J Am Coll Cardiol.* 2017;69(6):603–12.
231. Cerit L, Duygu H. Collapse of the Aspirin Empire. *J Am Coll Cardiol.* 2017;69(23):2878–9.
232. Levy G, Hollister L. Failure of U.S.P. disintegration test to assess physiologic availability of enteric coated tablets. *N Y State J Med.* 1964;64:3002–5.
233. Cox D, Maree AO, Dooley M, Conroy R, Byrne MF, Fitzgerald DJ. Effect of enteric coating on antiplatelet activity of low-dose aspirin in healthy volunteers. *Stroke.* 2006;37:2153–8.
234. Grosser T, Fries S, Lawson JA, Kapoor SC, Grant GR, FitzGerald GA. Drug resistance and pseudoresistance: an unintended consequence of enteric coating aspirin. *Circulation.* 2012/12/04. 2013;127(3):377–85.
235. Wagner JG, Wilkinson PK, Sedman AJ, Stoll RG. Failure of USP Tablet Disintegration Test to Predict Performance in Man. *J Pharm Sci.* 1973;62(5):859–60.
236. Aihie AP, Halpern SM, Streete PJ, Crome P. Slow release aspirin in the

- elderly. *J R Soc Med.* 1994;87(3):183.
237. Varum FJO, Merchant HA, Goyanes A, Assi P, Zboranová V, Basit AW. Accelerating the dissolution of enteric coatings in the upper small intestine: Evolution of a novel PH 5.6 bicarbonate buffer system to assess drug release. *Int J Pharm.* 2014;468:172–7.
238. Cole ET, Scott RA, Connor AL, Wilding IR, Petereit HU, Schminke C, et al. Enteric coated HPMC capsules designed to achieve intestinal targeting. *Int J Pharm.* 2002;231:83–95.
239. Al-Gousous J, Amidon GL, Langguth P. Toward Biopredictive Dissolution for Enteric Coated Dosage Forms. *Mol Pharm.* 2016;13:1927–36.
240. Bochner F, Williams DB, Morris PMA, Siebert DM, Lloyd J V. Pharmacokinetics of Low-Dose Oral Modified Release , Soluble and Intravenous Aspirin in Man , and Effects on Platelet Function. *Eur J Clin Pharmacol.* 1988;35:287–94.
241. Bochner F, Somogyi AA, Wilson KM. Bioinequivalence of Four 100mg Oral Aspirin Formulations in Healthy Volunteers. *Clin Pharmacokinet.* 1991;21(5):394–9.
242. Al-Gousous J, Ruan H, Blechar JA, Sun KX, Salehi N, Langguth P, et al.

- Mechanistic analysis and experimental verification of bicarbonate-controlled enteric coat dissolution: Potential *in vivo* implications. *Eur J Pharm Biopharm.* 2019;139:47–58.
243. Shibata H, Yoshida H, Izutsu KI, Goda Y. Use of bicarbonate buffer systems for dissolution characterization of enteric-coated proton pump inhibitor tablets. *J Pharm Pharmacol.* 2016;68:467–74.
244. Karkossa F, Klein S. Individualized *in vitro* and *in silico* methods for predicting *in vivo* performance of enteric-coated tablets containing a narrow therapeutic index drug. *Eur J Pharm Biopharm.* 2019;135:13–24.
245. Gelderen M Van, Olling M, Barends D, Meulenbelt J, Salomons P, Rauws A. The bioavailability of diclofenac from enteric coated products in healthy volunteers with normal and artificially decreased gastric acidity. *Biopharm Drug Dispos.* 1994;15:775–88.
246. Elkoshi Z, Behr D, Mirimsky A, Tsvetkov I, Danon A. Multiple-Dose Studies can be a More Sensitive Assessment for Bioequivalence than Single-Dose Studies. The Case with Omeprazole. *Clin Drug Invest.* 2002;22(9):585–92.
247. Liu Z, Ding L, Zhong S, Cao X, Jiang L, Duan H. Pharmacokinetics of a New Immediate-release Compound Omeprazole Capsule and its Comparison

- with the Enteric-coated Formulation under Fasting and Fed Conditions. *Drug Res.* 2013;63:370–5.
248. Licht D, Cohen R, Spiegelstein O, Rabinovich-guilatt L, Zholkovsky M, Gilbert A, et al. Is it possible to achieve bio-equivalence between an oral solid immediate-release and an analogue enteric-coated formulation ? *J Pharm Pharmacol.* 2016;68:1278–89.
249. Ahmad M, Pervaiz F. Comparative bioavailability and pharmacokinetics of investigational enteric- and film-coated formulations of flurbiprofen 100-mg tablets: a single-dose, randomized, open-label, two-period, two-way crossover study in healthy Pakistani male volunteers. *Clin Ther.* 2010;32(3):607-13.
250. Pieniaszek HJ, Resetarits D, Wilferth W, Blumenthal H, Bates. T. Relative Systemic Availability of Sulfapyridine from Commercial Enteric-Coated and Uncoated Sulfasalazine Tablets. *J Clin Pharmacol.* 1979;19(1):39–45.
251. Schwade LJ. Enteric-coated pills as a cause of fecal impaction. *Am J Surg.* 1950;79(1):184–5.
252. Fraaces L. Selye. The absorption of enteric-coated ammonium chloride. *Canad M A J.* 1946;55:445–7.

253. Burnikel RH, Sprecher HC. The value of proctosigmoidoscopic examination in the management of intestinal obstruction. *Am J Surg.* 1953;85(1):35-42.
254. Davies N. Sustained release and enteric coated NSAIDs: are they really GI safe? *J Pharm Pharm Sci.* 1999;2(1):5-14.
255. Davies NM. Toxicity of Nonsteroidal Anti-Inflammatory Drugs in the Large Intestine. *Dis Colon Rectum.* 1995;38(12):1311-21.
256. Porter S, Sackett G, Liu L. Chapter 33 - Development, Optimization, and Scale-up of Process Parameters: Pan Coating. Qiu Y, Chen Y, Zhang GGZ, Liu L, Porter WRBT, editors. *Developing Solid Oral Dosage Forms: Pharmaceutical Theory and Practice*, Academic Press, Burlington. San Diego: Academic Press; 2009. 761-805 p.
257. Peter J. Tarcha E. *Polymers for controlled drug delivery*. CRC Press, Boca Raton, FL. CRC Press, Boca Raton, FL.; 1991. 39-64 p.
258. Yoshida T, Lai TC, Kwon GS, Sako K. pH- and ion-sensitive polymers for drug delivery. *Expert Opin Drug Deliv.* 2013;10(11):1497-513.
259. Selye FL. The absorption of enteric coated ammonium chloride. *Can Med Assoc J.* 1946;55(5):445-7.
260. Corbus HF. Enteric coated thyroid as a cause of relapse in myxedema. *Calif*

- Med. 1964;100(5):364–5.
261. Graham G, Rowland M. Application of Salivary Salicylate Data to Biopharmaceutical Studies of Salicylates. *J Pharm Sci.* 1972;61(8):1219–22.
262. Al-Habet S, Kinsella HC, Rogers HJ, Trounce JR. Malabsorption of prednisolone from enteric-coated tablets after ileostomy. *Br Med J.* 1980;281(6244):843–4.
263. Schwartz H. Lower gastrointestinal side effects of nonsteroidal antiinflammatory drugs. *J Rheumatol.* 1981;8:952–4.
264. Walker SE, Paton TW, Cowan DH, Manuel MA, Dranitsaris G. Bioavailability of iron in oral ferrous sulfate preparations in healthy volunteers. *CMAJ.* 1989;141(6):543–7.
265. Bochner F, Somogyi AA WK. Bioinequivalence of four 100 mg oral aspirin formulations in healthy volunteers. *Clin Pharmacokinet.* 1991;21:394–9.
266. Stamm C, Pearce W, Larsen B et. al. Colonic ulcerations associated with non-steroidal anti-inflammatory ingestion. *Gastrointest Endosc.* 1991;37:260.
267. Matsushashi N, Yamada A, Hiraishi M et al. Multiple Strictures of the small intestine after long-term nonsteroidal anti-inflammatory drug therapy. *Am J Gastro.* 1992;87:1183–6.

268. Ridell R, Tanaka M, Mazzoleni G. Nonsteroidal anti-inflammatory drugs as possible cause of collagenous colitis: a case control study. *Gut*. 1992;683-6.
269. Van Gelderen MEM, Olling M, Barends DM, Meulenbelt J, Salomons P, Rauws AG. The bioavailability of diclofenac from enteric coated products in healthy volunteers with normal and artificially decreased gastric acidity. *Biopharm Drug Dispos*. 1994;15(9):775–88.
270. Alleyne M, Horne MK, Miller JL. Individualized treatment for iron-deficiency anemia in adults. *Am J Med*. 2008;121(11):943–8.
271. Al-Gousous J, Tsume Y, Fu M, Salem II, Langguth P. Unpredictable Performance of pH-Dependent Coatings Accentuates the Need for Improved Predictive *in Vitro* Test Systems. *Mol Pharm*. 2017 Dec 4;14(12):4209–19.
272. Dave VS, Shahin HI, Youngren-Ortiz SR, Chougule MB, Haware R V. Emerging technologies for the non-invasive characterization of physical-mechanical properties of tablets. *Int J Pharm*. 2017;532(1):299–312.
273. Available at: <https://www.drugbank.ca/drugs/DB00945>. Accessed on February 22, 2020.
274. Available at:
<https://healthcare.evonik.com/sites/lists/NC/DocumentsHC/Evonik->

- Eudragit_brochure.pdf. Accessed on May 06, 2020.
275. Available at: <https://www.drugbank.ca/salts/DBSALT001222>. Accessed on February 22, 2020.
276. Available at: <https://www.drugbank.ca/drugs/DB00586>. Accessed on February 22, 2020.
277. European Medicines Agency_Assessment report for Pantozol Control_Procedure No. EMEA/H/C/001013_May 2009.
278. Available at: <https://www.drugbank.ca/drugs/DB00795>. Accessed on February 22, 2020.
279. Johnson, L. R. Fluid and Electrolyte Absorption. In *Gastrointestinal Physiology*, 6th ed.; Johnson, L. R., Ed.; Mosby: St. Louis, 2001; pp 143–154.
280. West, J. B. Absorption. In *Best and Taylor's Physiological Basis of Medical Practice*, 11th ed.; Williams & Wilkins: Baltimore, 1985; pp 751–790.
281. Davenport, H. W. Digestion and Absorption. In *Physiology of the Digestive Tract*; Year Book Medical Publishers, Inc.: Chicago, 1982; pp 179–235.
282. Rune SJ, Henriksen FW. Carbon Dioxide Tensions in the Proximal Part of the Canine Gastrointestinal Tract. *Gastroenterology*. 1969;56(4):758–62.

283. Banwell JG, Gorbach SL, Pierce NF, Mitra R, Mondal A. Acute undifferentiated human diarrhea in the tropics: II. Alterations in intestinal fluid and electrolyte movements. *J Clin Invest.* 1971;50(4):890–900.
284. White, A.; Handler, P.; Smith, E. L. Specialized Extracellular Fluids. In *Principles of Biochemistry*, 4th ed.; McGraw-Hill: New York, 1968; pp 806–827.
285. Bucher GR, Flynn JC, Robinson CS. The action of the human small intestine in altering the composition of physiological saline. *J Biol Chem.* 1944;155:305–13.
286. Repishti M, Hogan DL, Pratha V, Davydova L, Donowitz M, Tse CM, et al. Human duodenal mucosal brush border Na⁺/H⁺ exchangers NHE2 and NHE3 alter net bicarbonate movement. *Am J Physiol Liver Physiol.* 2001;281(1):G159–63.
287. Russe I-S, Brock D, Knop K, Kleinebudde P, Zeitler JA. Validation of Terahertz Coating Thickness Measurements Using X-ray Microtomography. *Mol Pharm.* 2012;9(12):3551–9.
288. Radtke J, Wiedey R, Kleinebudde P. Effect of coating time on inter- and intra-tablet coating uniformity. *Eur J Pharm Sci.* 2019;137:104970.

289. Novikova A, Markl D, Zeitler JA, Rades T, Leopold CS. A non-destructive method for quality control of the pellet distribution within a MUPS tablet by terahertz pulsed imaging. *Eur J Pharm Sci.* 2018;111:549–55.
290. Yin X-Z, Wu L, Li Y, Guo T, Li H-Y, Xiao T-Q, et al. Visualization and quantification of deformation behavior of clopidogrel bisulfate polymorphs during tableting. *Sci Rep.* 2016;6(1):21770.
291. Wu Y, Adeb S, Doschak M. Using Micro-CT Derived Bone Microarchitecture to Analyze Bone Stiffness - A Case Study on Osteoporosis Rat Bone. Vol. 6, *Frontiers in Endocrinology.* 2015. p. 80.
292. Liu F, Basit AW, Lizio R, Petereit H-U, Meier C, Damm M. SOLID DOSAGE FORMS COMPRISING AN ENTERIC COATING WITH ACCELERATED DRUG RELEASE. 2013. p. United StatesUS 2013/0058986 A1.
293. Chen Y, Gao Z, Duan JZ. Chapter 13 - Dissolution Testing of Solid Products. In: Qiu Y, Chen Y, Zhang GGZ, Yu L, Mantri R V, editors. *Developing Solid Oral Dosage Forms.* Second Ed. Boston: Academic Press; 2017. p. 355–80.
294. Almukainzi M, Jamali F, Aghazadeh-Habashi A, Löbenberg R. Disease specific modeling: Simulation of the pharmacokinetics of meloxicam and

- ibuprofen in disease state vs. healthy conditions. *Eur J Pharm Biopharm.* 2016;100:77–84.
295. Friedel HD, Brown CK, Barker AR, Buhse LF, Keitel S, Kraemer J, et al. FIP Guidelines for Dissolution Testing of Solid Oral Products. *J Pharm Sci.* 2018;107(12):2995–3002.
296. Chen Y, Gao Z, Duan JZ. Dissolution testing of solid products. In: *Developing Solid Oral Dosage Forms: Pharmaceutical Theory and Practice: Second Edition.* 2017. p. 355–80.
297. Popat SC, Ki D, Young MN, Rittmann BE, Torres CI. Buffer pKa and Transport Govern the Concentration Overpotential in Electrochemical Oxygen Reduction at Neutral pH. *ChemElectroChem.* 2014;1(11):1909–15.
298. Soli AL, Byrne RH. CO₂ system hydration and dehydration kinetics and the equilibrium CO₂/H₂CO₃ ratio in aqueous NaCl solution. *Mar Chem.* 2002;78(2):65–73.
299. Roughton FJW. The Kinetics and Rapid Thermochemistry of Carbonic Acid. *J Am Chem Soc.* 1941;63(11):2930–4.
300. Dukić-Ott A, De Beer T, Remon JP, Baeyens W, Foreman P, Vervaet C. In-vitro and in-vivo evaluation of enteric-coated starch-based pellets prepared

- via extrusion/spheronisation. *Eur J Pharm Biopharm.* 2008;70(1):302–12.
301. Ariyasu A, Hattori Y, Otsuka M. Non-destructive prediction of enteric coating layer thickness and drug dissolution rate by near-infrared spectroscopy and X-ray computed tomography. *Int J Pharm.* 2017;525(1):282–90.
302. Sinha VR, Kumria R. Coating polymers for colon specific drug delivery: A comparative *in vitro* evaluation. *Acta Pharm.* 2003;53(1):41–7.
303. Ozturk SS, Palsson BO, Donohoe B, Dressman JB. Kinetics of Release from Enteric-Coated Tablets. *Pharm Res.* 1988;5(9):550–65.
304. Chapter 8 - Buffered and isotonic solutions. In: Martin's physical pharmacy and pharmaceutical sciences : physical chemical and biopharmaceutical principles in the pharmaceutical sciences. 6th ed. editor, Patrick J. Sinko ; ; assistant editor, Yashveer Si. In.
305. Agyilirah GA, Banker GS. Polymers for enteric coating applications. *Polym Control drug Deliv.* 1991;3:39–66.
306. <1151> PHARMACEUTICAL DOSAGE FORMS. In *The United States Pharmacopeia and National Formulary USP42-NF37 2S*; The United States Pharmacopeial Convention, Inc.: Rockville, MD, 2019.

307. Shargel L, Wu-Pong S, Yu ABC. Chapter 17. Modified-Release Drug Products. In: Applied Biopharmaceutics & Pharmacokinetics, 6e. New York, NY: The McGraw-Hill Companies; 2012.
308. Cardot JM, Garrat G, Beyssac E. Use of IVIVC to Optimize Generic Development. *Dissolution Technol.* 2015;22:44–8.
309. Davanço MG, Campos DR, Carvalho P de O. *In vitro – In vivo* correlation in the development of oral drug formulation: A screenshot of the last two decades. *Int J Pharm.* 2020;580:119210.
310. Cardot J-M, Davit BM. *In vitro–In Vivo* Correlations: Tricks and Traps. *AAPS J.* 2012;14(3):491–9.
311. International Conference of Harmonization (ICH) of Technical Requirements for Registration of Pharmaceuticals for Human Use. ICH Harmonized Guidelines. Integrated Addendum to ICH E6(R1): Guideline for Good Clinical Practices.
312. World Medical Association. World Medical Association Declaration of Helsinki: Ethical Principles for Medical Research Involving Human Subjects. *JAMA.* 2013;310(20):2191– 2194.
313. Food and Drug Administrations – FDA. Guidance for Industry: Food-Effect

Bioavailability and Fed Bioequivalence Studies. December 2002. A.

314. SIMON B, MÜLLER P, BLIESATH H, LÜHMANN R, HARTMANN M, HUBER R, et al. Single intravenous administration of the H⁺, K⁺-ATPase inhibitor BY 1023/SK&F 96022—inhibition of pentagastrin-stimulated gastric acid secretion and pharmacokinetics in man. *Aliment Pharmacol Ther.* 1990;4(3):239–45.
315. de Campos DR, Vieira NR, Bernasconi G, Barros FAP, Meurer EC, Marchioretto MA, et al. Bioequivalence of two enteric coated formulations of pantoprazole in healthy volunteers under fasting and fed conditions. *Arzneimittelforschung.* 2007;57(6):309—314.
316. Grbic S, Parojcic J, Ibric S, Djuric Z. *In Vitro–In Vivo* Correlation for Gliclazide Immediate-Release Tablets Based on Mechanistic Absorption Simulation. *AAPS PharmSciTech.* 2011;12(1):165–71.
317. Honório T da S, Pinto EC, Rocha HVA, Esteves VSD, dos Santos TC, Castro HCR, et al. *In Vitro–In Vivo* Correlation of Efavirenz Tablets Using GastroPlus®. *AAPS PharmSciTech.* 2013;14(3):1244–54.
318. Hussain A, Shakeel F, Singh SK, Alsarra IA, Faruk A, Alanazi FK, et al. Solidified SNEDDS for the oral delivery of rifampicin: Evaluation, proof of concept, *in vivo* kinetics, and *in silico* GastroPlus™ simulation. *Int J Pharm.*

- 2019;566:203–17.
319. Pepin XJH, Dressman J, Parrott N, Delvadia P, Mitra A, Zhang X, et al. *In Vitro* Biopredictive Methods: A Workshop Summary Report. *J Pharm Sci.* 2020;
320. Pearce GA, McLachlan AJ, Ramzan I. Bioequivalence: How, Why, and What Does it Really Mean? *J Pharm Pract Res.* 2004 Sep 1;34(3):195–200.
321. Karalis V, Macheras P, Van Peer A, Shah VP. Bioavailability and Bioequivalence: Focus on Physiological Factors and Variability. *Pharm Res.* 2008;25(8):1956–62.
322. Van Peer A. Variability and Impact on Design of Bioequivalence Studies. *Basic Clin Pharmacol Toxicol.* 2010 Mar 1;106(3):146–53.
323. Fathima N, Mamatha T, Qureshi HK, Anitha N, Venkateswara Rao J. Drug-excipient interaction and its importance in dosage form development. *J Appl Pharm Sci.* 2011;1(6):66–71.
324. Hotha KK, Roychowdhury S, Subramanian V. Drug-Excipient Interactions: Case Studies and Overview of Drug Degradation Pathways. *Am J Anal Chem.* 2016;07(01):107–40.
325. Narang AS, Yamniuk A, Zhang L, Comezoglu SN, Bindra DS, Varia SA, et

- al. Chapter 2: Drug Excipient Interactions. In: Excipient Applications in Formulation Design and Drug Delivery. 2015. p. 13–23.
326. Dilantin® [package insert]. Parke-Davis, Division of Pfizer, Inc., New York, NY; 2009.
327. Neuvonen PJ. Bioavailability of Phenytoin : Clinical Pharmacokinetic and Therapeutic Implications. *Clin Pharmacokinet.* 1979;4(2):91–103.
328. Tyrer JH, Eadie MJ, Sutherland JM, Hooper WD. Outbreak of anticonvulsant intoxication in an Australian city. *Br Med J.* 1970;4(5730):271–3.
329. Bochner F, Hooper WD, Tyrer JH, Eadie MJ. Factors Involved in an Outbreak of Phenytoin Intoxication. *J Neurol Sci.* 1972;16(4):481–7.
330. Bochner F, Hooper W, Tyrer J, Eadie M. The explanation of the 1968 Australian outbreak of diphenylhydantoin intoxication. *Proc Aust Assoc Neurol.* 1973;9:165–70.
331. Shah VP, Tsong Y, Sathe P, Liu JP. *In vitro* dissolution profile comparison- Statistics and analysis of the similarity factor, f_2 . *Pharm Res.* 1998;15(6):889–96.
332. Soryal I, Richens A. Bioavailability and dissolution of proprietary and generic formulations of phenytoin. *J Neurol Neurosurg Psychiatry.*

- 1992;55(8):688–91.
333. Newton D. Phenyton injections: From compounding to Cerebyx. *Int J Pharm Compd.* 2002;6(6):410–3.
334. Besag FMC. Is generic prescribing acceptable in epilepsy? *Drug Saf.* 2000;23(3):173–82.
335. Borgherini G. The bioequivalence and therapeutic efficacy of generic versus brand-name psychoactive drugs. *Clin Ther.* 2003;25(6):1578–92.
336. LeLorier J, Duh MS, Paradis PE, Lefebvre P, Weiner J, Manjunath R, et al. Clinical consequences of generic substitution of lamotrigine for patients with epilepsy. *Health Care (Don Mills).* 2008;2179–86.
337. Richens A. Clinical Pharmacokinetics of Phenytoin. *Clin Pharmacokinet.* 1979;4(3):153–69.
338. Bharate SS, Bharate SB, Bajaj AN. Interactions and incompatibilities of pharmaceutical excipients with active pharmaceutical ingredients : a comprehensive review. *J excipients food Chem.* 2010;1(3):3–26.
339. Chowdhury DK, Sarker H, Schwartz P. Regulatory Notes on Impact of Excipients on Drug Products and the Maillard Reaction. *AAPS PharmSciTech* [Internet]. 2017; Available from:

<http://link.springer.com/10.1208/s12249-017-0878-y>

340. Berridge NJ, Cousins CM, Cliffe AJ. Microcalorimetry applied to certain species of bacteria growing in sterilized separated milk. *J Dairy Res.* 1974;41(2):203–15.
341. Stulova I, Kabanova N, Krisciunaite T, Adamberg K, Laht TM, Vilu R. Microcalorimetric study of the growth of *Streptococcus thermophilus* in renneted milk. *Front Microbiol.* 2015;6:3389.
342. Vickery RD, Maurin MB. Utility of microcalorimetry in the characterization of the browning reaction. *J Pharm Biomed Anal.* 1999;20(1–2):385–8.
343. Choma CT. *Characterization of Drug-Excipient Compatibility* _ TA Instruments, 109 Lukens Drive, New Castle, DE 19720, USA.
344. Cavatur R, Murti Vemuri N, Chrzan Z. Use of isothermal microcalorimetry in pharmaceutical preformulation studies part III. Evaluation of excipient compatibility of a new chemical entity. *J Therm Anal Calorim.* 2004;78(1):63–72.
345. Macheras P, Ismailos G, Reppas C. Bioavailability study of a freeze-dried sodium phenytoin-milk formulation. *Biopharm Drug Dispos.* 1991;12:687–95.

346. Neuvonen P, Lehtovaara R, Bardy A. Effect of Some Gastrointestinal Factors on Serum Phenytoin Concentration. *Antiepileptic Ther Adv Drug Monit.* 1980;149–59.
347. Dilantin® [Product monograph]. Pfizer Canada Inc., Licensee Kirkland, Québec; 2017.
348. Cook J, Randinitis E, Wilder BJ. Effect of food on the bioavailability of 100-mg Dilantin Kapseals. *Neurology.* 2001;57:698–700.
349. Health Canada, Canada Vigilance program – <http://www.healthcanada.gc.ca/medeffect>. Query number CV-2018-0060.
350. Wilder BJ, Leppik I, Hietpas TJ, Cloyd JC, Randinitis EJ, Cook J. Effect of food on absorption of Dilantin Kapseals and Mylan extended phenytoin sodium capsules. *Neurology.* 2001;57:582–9.
351. Garnett WR. Considerations for long-term use of proton-pump inhibitors. *Am J Heal Pharm.* 1998;55(21):2268–79.
352. Kou D, Dwaraknath S, Fischer Y, Nguyen D, Kim M, Yiu H, et al. Biorelevant Dissolution Models for a Weak Base To Facilitate Formulation Development and Overcome Reduced Bioavailability Caused by Hypochlorhydria or Achlorhydria. *Mol Pharm.* 2017;14(10):3577–87.

353. Lahner E, Annibale B, Delle Fave G. Systematic review: Impaired drug absorption related to the co-administration of antisecretory therapy. *Aliment Pharmacol Ther.* 2009;29(12):1219–29.
354. Almukainzi M, Löbenberg R, Lukacova V. Modelling the Absorption of Metformin with Patients Post Gastric Bypass Surgery. *J Diabetes Metab.* 2014;5:353.
355. Golub AL, Frost RW, Betlach CJ, Gonzalez MA. Physiologic considerations in drug absorption from the gastrointestinal tract. *J ALLERGY CLIN IMMUNOL.* 1986;78(4 Pt 2):689–94.
356. Zhou R, Moench P, Heran C, Lu X, Mathias N, Faria TN, et al. pH-Dependent dissolution *in Vitro* and absorption *in Vivo* of weakly basic drugs: Development of a canine model. *Pharm Res.* 2005;22(2):188–92.
357. Piscitelli SC, Goss TF, Wilton JH, D’Andrea DT, Goldstein H, Schentag JJ. Effects of ranitidine and sucralfate on ketoconazole bioavailability. *Antimicrob Agents Chemother.* 1991;35(9):1765–71.
358. Chin TWF, Loeb M, Fong IW. Effects of an acidic beverage (Coca-Cola) on absorption of ketoconazole. *Antimicrob Agents Chemother.* 1995;39(8):1671–5.

359. Psachoulias D, Vertzoni M, Goumas K, Kalioras V, Beato S, Butler J, et al. Precipitation in and supersaturation of contents of the upper small intestine after administration of two weak bases to fasted adults. *Pharm Res.* 2011;28(12):3145–58.
360. Como J, Dismukes W. Oral azole drugs as systemic antifungal therapy. *N Engl J Med.* 1994;330(4):263–72.
361. Daneshmend TK, Warnock DW. Clinical Pharmacokinetics of Ketoconazole. *Clin Pharmacokinet.* 1988;14(1):13–34.
362. Ingels F, Beck B, Oth M, Augustijns P. Effect of simulated intestinal fluid on drug permeability estimation across Caco-2 monolayers. *Int J Pharm.* 2004;274:221–32.
363. Harris R, Jones HE, Artis WM. Orally Administered Ketoconazole : Route of Delivery to the Human Stratum Corneum. *Antimicrob Agents Chemother.* 1983;24(6):876–82.
364. Chan ECY, Tan WL, Ho PC, Fang LJ. Modeling Caco-2 permeability of drugs using immobilized artificial membrane chromatography and physicochemical descriptors. *J Chromatogr A.* 2005;1072:159–68.
365. Kostewicz ES, Aarons L, Bergstrand M, Bolger MB, Galetin A, Hatley O, et

- al. PBPK models for the prediction of *in vivo* performance of oral dosage forms. *Eur J Pharm Sci.* 2014;57:300–21.
366. Kesisoglou F, Chung J, van Asperen J, Heimbach T. Physiologically Based Absorption Modeling to Impact Biopharmaceutics and Formulation Strategies in Drug Development—Industry Case Studies. *J Pharm Sci.* 2016;105(9):2723–34.
367. Medarevi D, Cviji S, Dobri V, Mitri M, Djuri J, Ibri S. Assessing the potential of solid dispersions to improve dissolution rate and bioavailability of valsartan : *In vitro* - in silico approach. *Eur J Pharm Sci.* 2018;124:188–98.
368. Jones HM, Chen Y, Gibson C, Heimbach T, Parrott N, Peters SA, et al. Physiologically Based Pharmacokinetic Modeling in Drug Discovery and Development : A Pharmaceutical Industry Perspective. *Clin Pharmacol Ther.* 2015;97(3):247–62.
369. Tsume Y, Patel S, Fotaki N, Bergstr C, Amidon GL, Brasseur JG, et al. Meeting Report *In Vivo* Predictive Dissolution and Simulation Workshop Report : Facilitating the Development of Oral Drug Formulation and the Prediction of Oral Bioperformance. *AAPS J.* 2018;20(100):1–8.
370. Fotaki N. Pros and cons of methods used for the prediction of oral drug absorption. *Expert Rev Clin Pharmacol.* 2009;2(2):195–208.

371. Cvijic S, Ibric S, Parojcic J, Djuris J. An *in vitro* - *in silico* approach for the formulation and characterization of ranitidine gastroretentive delivery systems. *J Drug Deliv Sci Technol.* 2018;45:1–10.
372. Agoram B, Woltosz WS, Bolger MB. Predicting the impact of physiological and biochemical processes on oral drug bioavailability. *Adv Drug Deliv Rev.* 2001;50:S41–67.
373. Yu LX, Amidon GL. A compartmental absorption and transit model for estimating oral drug absorption. *Int J Pharm.* 1999;186:119–25.
374. Yu LX, Amidon GL. Characterization of small intestinal transit time distribution in humans. *Int J Pharm.* 1998;171:157–63.
375. Okumu A, DiMaso M, Löbenberg R. Computer simulations using GastroPlus™ to justify a biowaiver for etoricoxib solid oral drug products. *Eur J Pharm Biopharm.* 2009;72(1):91–8.
376. Wei H, Dalton C, Di Maso M, Kanfer I, Löbenberg R. Physicochemical characterization of five glyburide powders: A BCS based approach to predict oral absorption. *Eur J Pharm Biopharm.* 2008;69(3):1046–56.
377. Ruff A, Fiolka T, Kostewicz ES. Prediction of Ketoconazole absorption using an updated *in vitro* transfer model coupled to physiologically based

- pharmacokinetic modelling. *Eur J Pharm Sci.* 2017;100:42–55.
378. Pathak SM, Ru A, Kostewicz ES, Patel N, Turner DB. Model-Based Analysis of Biopharmaceutic Experiments To Improve Mechanistic Oral Absorption Modeling: An Integrated *in Vitro in Vivo* Extrapolation Perspective Using Ketoconazole as a Model Drug. *Mol Pharm.* 2017;14:4305–20.
379. Cristofolletti R, Patel N, Dressman JB. Differences in Food Effects for 2 Weak Bases With Similar BCS Drug-Related Properties : What Is Happening in the Intestinal Lumen ? *J Pharm Sci.* 2016;105(9):2712–22.
380. Cristofolletti R, Patel N, Dressman JB. Assessment of Bioequivalence of Weak Base Formulations Under Various Dosing Conditions Using Physiologically Based Pharmacokinetic Simulations in Virtual Populations . Case Examples : Ketoconazole and Posaconazole. *J Pharm Sci.* 2017;106(2):560–9.
381. Adachi M, Hinatsu Y, Kusamori K, Katsumi H, Sakane T, Nakatani M, et al. Improved dissolution and absorption of ketoconazole in the presence of organic acids as pH-modifiers. *Eur J Pharm Sci.* 2015;76:225–30.
382. Huang Y, Colaizzi JL, Bierman RH, Woestenborghs R, Heykants J. Pharmacokinetics and Dose Proportionality of Ketoconazole in Normal

- Volunteers. *Antimicrob Agents Chemother.* 1986;30(2):206–10.
383. GastroPlus TM Manual, 2015. Simulations Plus Inc., Lancaster, CA, USA.
384. Medication Guide: NIZORAL, JANSSEN PHARMACEUTICALS Inc. 2013.
385. Graybill JR, Galgiani JN, Jorgensen JH, Strandberg DA. Ketoconazole therapy for fungal urinary tract infections. *J Urol.* 1983;129(1):68–70.
386. Fahmi OA, Maurer TS, Kish M, Cardenas E, Boldt S, Nettleton D. A Combined Model for Predicting CYP3A4 Clinical Net Drug-Drug Interaction Based on CYP3A4 Inhibition , Inactivation , and Induction Determined *in Vitro*. *Drug Metab Dispos.* 2008;36(8):1698–708.
387. Heikkinen AT, Baneyx G, Caruso A, Parrott N. Application of PBPK modeling to predict human intestinal metabolism of CYP3A substrates – An evaluation and case study using GastroPlus™. *Eur J Pharm Sci.* 2012;47(2):375–86.
388. Vertzoni M V., Reppas C, Archontaki HA. Optimization and validation of a high-performance liquid chromatographic method with UV detection for the determination of ketoconazole in canine plasma. *J Chromatogr B.* 2006;839(1–2):62–7.

389. Mannisto PT, Mantyla R, Nykanen S, Lamminsivu U, Ottoila P. Impairing effect of food on ketoconazole absorption. *Antimicrob Agents Chemother.* 1982;21(5):730–3.
390. Rasenack N, Müller BW. Dissolution rate enhancement by *in situ* micronization of poorly water-soluble drugs. *Pharm Res.* 2002;19(12):1894–1900.
391. Mitra A, Kesisoglou F, Beauchamp M, Zhu W, Chiti F, Wu Y. Using absorption simulation and gastric pH modulated dog model for formulation development to overcome achlorhydria effect. *Mol Pharm.* 2011;8(6):2216–23.
392. Hartmanshenn C, Scherholz M, Androulakis IP. Physiologically-based pharmacokinetic models : approaches for enabling personalized medicine. *J Pharmacokinet Pharmacodyn.* 2016;43(5):481–504.
393. Johnson TN, Rostami-hodjegan A. Resurgence in the use of physiologically based pharmacokinetic models in pediatric clinical pharmacology : parallel shift in incorporating the knowledge of biological elements and increased applicability to drug development and clinical practice. *Pediatr Anesth.* 2011;21:291–301.
394. Marsousi N, Desmeules JA, Rudaz S, Daali Y. Usefulness of PBPK

- Modeling in Incorporation of Clinical Conditions in Personalized Medicine. *J Pharm Sci.* 2017;106(9):2380–91.
395. Xu R, Ge W, Jiang Q. Application of physiologically based pharmacokinetic modeling to the prediction of drug-drug and drug-disease interactions for rivaroxaban. *Eur J Clin Pharmacol.* 2018;74:755–65.
396. Amaral Silva D, Löbenberg R, Davies N. Are Excipients Inert? Phenytoin Pharmaceutical Investigations with New Incompatibility Insights. *J Pharm Pharm Sci* [Internet]. 2018;21(1s):29745. Available from: <http://www.ncbi.nlm.nih.gov/pubmed/29702046>
397. Amaral Silva D, Duque M, Davies N, Löbenberg R, Ferraz H. Application of in silico tools in clinical practice using ketoconazole as a model drug. *J Pharm Pharm Sci.* 2018;21(1S):242s-253s.

APPENDIX 1: Formulation of inhalable nanocrystals to be used as a therapeutic strategy against breast cancer metastasis to the lungs

Background

Breast cancer is a significant problem worldwide, being the number one diagnosed cancer in American women and number two cause of cancer-related death (A1.1). The majority of these deaths is a result of metastasis. Recent studies (A1.2- A1.3) show that patients with more aggressive types of breast cancer present an enhanced propensity for lung metastasis, negatively impacting the patient's morbidity and mortality. Advanced lung metastases are difficult to treat, highlighting the need to better understand the molecular drivers of this process and the need for effective new therapies, especially in the area of nanotechnology applied to pharmaceuticals

Recent research (A1.4- A1.5) has shown the importance of lung-derived factors on breast cancer metastatic behavior. These lung microenvironment factors, such as soluble proteins (particularly selectins), seem to contribute to the breast cancer cells spreading. Hence, targeting the metastatic microenvironment is an attractive alternative to prevent cancer cells spreading to the lungs. Direct delivery to the secondary metastatic organ (i.e., the lungs) can greatly reduce systemic toxicities with increased organ-specificity. In this context, the lung has the unique advantage of being targetable through inhalable drug delivery. Even though inhaled drugs have been used in the treatment of airway diseases (A1.6), this route of administration remains nearly underexplored in cancer treatment. Additionally, the use of nanoparticles for cancer treatment has been extensively studied, however the application of nanotechnology for inhalable drug delivery in cancer is seldom explored. Hence, in this project we aim to develop and characterize an inhalable system containing bimosiamose (a selectin inhibitor) nanoparticles as a novel anti-metastatic strategy.

Chemotherapeutics are often poorly water-soluble compounds and such molecules are difficult to formulate using conventional approaches (A1.7). Formulating these compounds as pure drug nanoparticles is one of the newer drug-delivery strategies applied to this class of molecules (A1.7). Nanoparticles are an interesting approach for cancer treatment because they present enhanced permeability and retention, allowing accumulation in the target tissue rather than systemic diffusion (A1.8). In this research project, bimosiamose nanoparticles are used in crystalline form, known as nanocrystals. Due to increased surface area to volume ratio, nanocrystals can improve solubility and increase cellular uptake due to their size (A1.8- A1.11).

On the other hand, due to their reduced size, inhaled nanocrystals would not reach the deep lung where the drug needs to be deposited. Thus, the nanocrystals are loaded into an inhalable carrier using spray-freeze drying technique to maintain the drug activity and ensure uniform distribution throughout the carrier particles (A1.12). These carriers are bigger in size (micro range) and such an approach can be used for the local delivery of nanoparticles to the lungs (A1.13- A1.14).

To the best of our knowledge a preventive approach against lung metastasis using inhalable bimosiamose nanocrystals has never been used before. This innovative research will greatly contribute to the knowledge in the field of nanotechnology applied to pharmaceuticals.

Methods and Results

Preparation of nanosuspension by miniaturized wet bead milling method.

The nanocrystals were obtained through a modified wet bead milling process which consists of an aqueous media in which the drug is insoluble, a stabilizer, the drug powder,

milling pearls (zirconia beads) and high speed magnetic stirring (A1.9). In this method, the particle size reduction is caused by mechanical forces, i.e. by physically breaking down coarse particles to finer ones. The system was stirred for a length of time and the particle size reduction was monitored through laser diffraction scattering method. Since bimosiamose is extremely poorly water soluble, this would be the most adequate method for particle size reduction (A1.10-A1.11).

The system contained bimosiamose (10 mg), zirconia beads (0.5 g) and a stabilizer aqueous solution (0.5 mL) (HPC, PVA, PVP, Poloxamer 188 or Povacoat). The milling chamber consisted of a 2 mL glass vial containing two magnetic stir bars, polygon-shaped (8x2 mm). The system was stirred at 800 rpm at room temperature up to 48hrs depending on the stabilizer used.

For HPC, PVA, PVP and Povacoat, the proportion between stabilizer and drug was 4:1 and for Poloxamer 3:1.

Particle size distribution and stabilizer screening.

The particle size distribution (PSD) as well as the polydispersity index (PDI) were measured by dynamic light scattering using a photon correlation spectrometer (Zetasizer HAS 3000) from Malvern instruments. Samples were diluted to a suitable concentration, indicated by the best attenuation coefficient. The PSD results are indicated as size distribution by volume.

Povacoat

For Povacoat, the samples were collected for analysis at 1h, 24hrs, 36hrs and 48 hrs. Table 1 shows the Z-average for the PSD of the nanosuspension system (done in triplicate) at the different collection time points. Different populations could be identified during the first hour of stirring.

Table 1. Particle size distribution (diameter, nm) and PDI of bimosiamose nanocrystals prepared with Povacoat.

Time	Z-avg (nm)	PdI	Number of peaks
1 hour	127.7	0.234	2 (150.3 and 4779 nm)
24 hours	130.9	0.108	1
36 hours	120.5	0.104	1
48 hours	108.1	0.106	1

Povacoat was initially developed as a film-coating agent, wet granulation binder and solid dispersion matrix, but recent studies revealed its use as a stabilizer to prevent aggregation of nanocrystals. Because it formed a dispersion when added to water, we investigated the particle size of Povacoat alone in water (Figure 1).

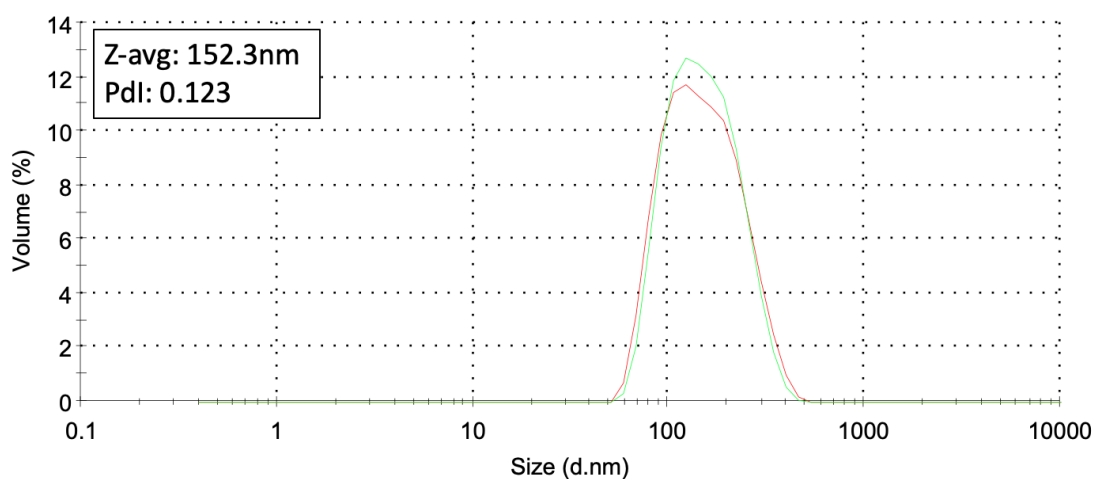


Figure 1. Particle size distribution (diameter, nm) and PDI of Povacoat alone in water.

Notably, Povacoat dispersion is also in a nano scale. Hence, in order to minimize confounding factors in the PSD measurements, other stabilizers were screened: HPC, PVA, PVP and Poloxamer 188. These were completely dissolved in water, resulting in a stabilizer solution instead of a suspension.

Povacoat, HPC, PVA, PVP and Poloxamer 188

Based on the results using Povacoat, the stirring time was set to 24 hours. Table 2 shows the Z-average for the PSD of the nanosuspension system for the different stabilizers, including a second trial using Povacoat (for comparison purposes and repeatability assessment).

Table 2. Particle size distribution (diameter, nm) and PDI of bimosiamose nanocrystals prepared with different stabilizers.

Stabilizer	Z-avg (nm)	PdI
Povacoat	91.43	0.110
HPC	123.9	0.159
Poloxamer 188	83.72	0.102
PVP	83.76	0.102

Based on the Z-average and PDI results, and considering its wide use in inhalable systems, Poloxamer 188 was the stabilizer of choice.

Poloxamer 188

In order to obtain particles with bigger particle size the stirring time was reduced to 2hrs (Table 3).

Table 3. PSD (diameter, nm) and PDI of bimosiamose nanocrystals prepared with Poloxamer 188.

Time	Z-avg (nm)	PdI
2hrs	115.70	0.140
4.5hrs	99.61	0.124
5.5hrs	92.00	0.116

To assess the repeatability of the selected system, other batches were prepared using the 2hrs stirring time and the result was consistent (Z-avg: 117.8nm; PDI: 0.120).

Microcarrier preparation

The optimized nanosuspension formulation was spray-freeze dried using a carrier agent. The agents investigated were lactose and mannitol. Lactose was not a feasible agent; hence mannitol was used in this study.

The following parameters were used for the spraying process: atomized air pressure: 1bar; spray rate: 0.49 ml/min; liquid nitrogen volume kept constant at 700 ml, spray nozzle positioned 10cm above the liquid nitrogen level. Once sprayed, the samples were lyophilized overnight.

The mass median aerodynamic diameter (MMAD) of the powder was measured using the Penn-Century dispersing device coupled to an aerosol diluter and an aerodynamic particle sizer (APS). A small scale powder disperser (SSPD) coupled to the APS was also test to compare the MMAD results using different dispersing setups (Figure 2).

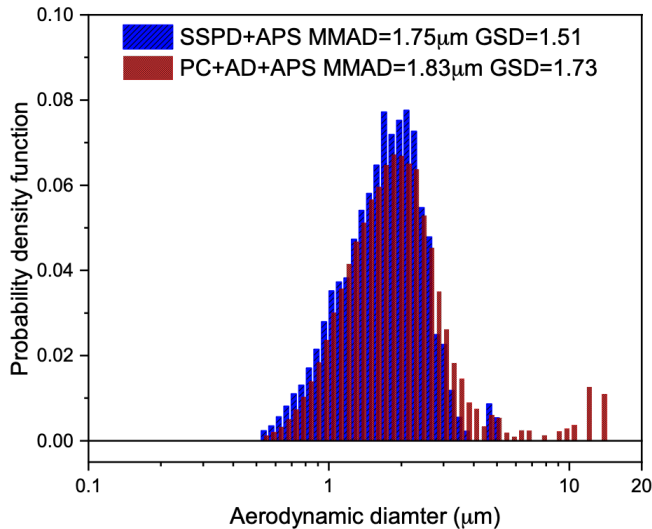


Figure 2. MMAD of mannitol carrier particles loaded with bimosiamose nanocrystals

The MMAD determines the deposition location of particles within the lungs. A size between 2-5μm is usually desired to reach the deep lung. However, the obtained value is borderline and may potentially still reach the alveolar system.

After characterization of inhalable powder and loading into the delivery device through the optimized method, the samples were sent for preclinical animal study, which are being conducted in our collaborator's facility in Western University where animal ethics approval has been granted.

References

A1.1. Retrived from National Breast Cancer Foundation, Inc. Available at:

<https://www.nationalbreastcancer.org/breast-cancer-facts>

A1.2. Kennecke, H., Yerushalmi, R., Woods, R., Cheang, M. C. U., Voduc, D., Speers, C. H., ... & Gelmon, K. (2010). Metastatic behavior of breast cancer subtypes. *Journal of clinical oncology*, 28(20), 3271-3277.

A1.3. Minn, A. J., Gupta, G. P., Padua, D., Bos, P., Nguyen, D. X., Nuyten, D., ... & Foekens, J. A. (2007). Lung metastasis genes couple breast tumor size and metastatic spread. *Proceedings of the National Academy of Sciences*, 104(16), 6740-6745.

A1.4. Chambers, A. F., Groom, A. C., & MacDonald, I. C. (2002). Dissemination and growth of cancer cells in metastatic sites. *Nature Reviews Cancer*, 2(8), 563-572.

A1.5. Chu, J. E., Xia, Y., Chin-Yee, B., Goodale, D., Croker, A. K., & Allan, A. L. (2014). Lung-derived factors mediate breast cancer cell migration through CD44 receptor-ligand interactions in a novel ex vivo system for analysis of organ-specific soluble proteins. *Neoplasia* (New York, N.Y.), 16(2), 180–191.

A1.6. Trapani, A., Di Gioia, S., Castellani, S., Carbone, A., Cavallaro, G., Trapani, G., & Conese, M. (2014). Nanocarriers for respiratory diseases treatment: recent advances and current challenges. *Current topics in medicinal chemistry*, 14(9), 1133-1147.

A1.7. Merisko-Liversidge, E. M., & Liversidge, G. G. (2008). Drug nanoparticles: formulating poorly water- soluble compounds. *Toxicologic pathology*, 36(1), 43-48.

A1.8. Roa, W. H., Azarmi, S., Al-Hallak, M. K., Finlay, W. H., Magliocco, A. M., & Löbenberg, R. (2011). Inhalable nanoparticles, a non-invasive approach to treat lung cancer in a mouse model. *Journal of controlled release*, 150(1), 49-55.

- A1.9. Azarmi, S., Tao, X., Chen, H., Wang, Z., Finlay, W. H., Löbenberg, R., & Roa, W. H. (2006). Formulation and cytotoxicity of doxorubicin nanoparticles carried by dry powder aerosol particles. *International journal of pharmaceutics*, 319(1-2), 155-161.
- A1.10. Wang, G. D., Mallet, F. P., Ricard, F., & Heng, J. Y. (2012). Pharmaceutical nanocrystals. *Current Opinion in Chemical Engineering*, 1(2), 102-107.
- A1.11. Gupta, M., Sharma, V., Chauhan, D. N., Chauhan, N. S., Shah, K., & Goyal, R. K. (2019). Nanotechnological-Based Drug Delivery System for Magical Molecule Curcumin: Delivery, Possibilities and Challenges. *Novel Drug Delivery Systems for Phytoconstituents*, 313.
- A1.12. Sweeney, L. G., Wang, Z., Loebenberg, R., Wong, J. P., Lange, C. F., & Finlay, W. H. (2005). Spray- freeze-dried liposomal ciprofloxacin powder for inhaled aerosol drug delivery. *International journal of pharmaceutics*, 305(1-2), 180-185.
- A1.13. Ely, L., Roa, W., Finlay, W. H., & Löbenberg, R. (2007). Effervescent dry powder for respiratory drug delivery. *European Journal of Pharmaceutics and Biopharmaceutics*, 65(3), 346-353.
- A1.14. Sham, J. O. H., Zhang, Y., Finlay, W. H., Roa, W. H., & Löbenberg, R. (2004). Formulation and characterization of spray-dried powders containing nanoparticles for aerosol delivery to the lung. *International Journal of Pharmaceutics*, 269(2), 457-467.

**APPENDIX 2: Design of nanostructured lipid carriers for lymphatic
delivery of Terbinafine**

Background

After oral administration of a given medication, the active pharmaceutical ingredient (API) is released from the dosage form, dissolved in the gut lumen and absorbed through the gut wall by the enterocytes. After that, it goes to the portal vein, passing through the liver (where pre systemic metabolism may occur) to finally reach the systemic circulation. When pre systemic metabolism happens, the amount of drug reaching the systemic circulations is decreased, hence the therapeutic compound will have a lower bioavailability. Highly lipophilic molecules are more prone to undergo such pre systemic metabolism (A2.1). In the current drug development pipeline, many of the lead compounds are highly lipophilic molecules, which pose a major development challenge to the pharmaceutical industry.

Selecting a lead compound which may undergo extensive pre systemic metabolism is not attractive to the industry, even if they present high potency, because the low bioavailability will require high doses, which can be toxic. Additionally, many drug-drug interactions (DDI) at the metabolizing enzymes level may occur. These molecules also present low aqueous solubility, which is a challenge for the formulation development process. Therefore, the great need to address this matter affords an opportunity to explore alternative pathways of absorption with innovative drug delivery systems.

In the intestines the lymphatic system plays an essential role in the absorption of long-chain fatty acids, triglycerides, cholesterol esters, lipid soluble vitamins, and highly lipophilic xenobiotics (A2.2). Consequently, targeting the drug delivery to the lymphatic system is advantageous in terms of increasing bioavailability (bypass of first-pass metabolism in the liver) thus reducing the dose, decreasing potential DDIs, and the ability to target diseases that spread

through this system, such as certain types of cancer and human immunodeficiency virus (A2.3-A2.9).

The absorption of highly lipophilic compounds through the lymphatics is very likely to occur similarly to the intestinal lipid transport system. Briefly, lipids are hydrolysed in the stomach and small intestine to the corresponding monoglyceride and fatty acid, which are absorbed into the enterocyte and re-esterified into triglyceride. These are then ‘packaged’ into intestinal lipoproteins, known as chylomicrons (CM), which are finally secreted into the lymph and then to the blood (A2.10).

In order to target this route, lipid-based formulations can be applied. Due to their lipidic content, such formulations stimulate the production of CM in the enterocytes. During this process, lipophilic drugs enter the lymphatic system in association with the triglyceride core of the formed CM and eventually reach the systemic circulation. Alternatively, the delivery system itself can mimic a CM, and hence be transported through the lymphatic system (A2.11). In light of the increasing trend towards highly potent, lipophilic drug candidates, exploring the lymphatic route is becoming more and more attractive, which is evidenced by the exponential increase in the number of studies on lipid-based delivery systems. Hence, the aim of this study is to develop an oral nanostructured lipid carrier for Terbinafine with lymphotropic ingredients to increase the lymphatic uptake of Terbinafine.

Methods and results

Selection of Liquid and Solid Lipids

The solubility of Terbinafine HCl was assessed in various liquid lipids using the shake flask method. Briefly: Each medium (5ml) was saturated with the pure drug powder and there

was no mixture of media. The flasks were shaken for 72 hours at room temperature to assure equilibrium. Samples from each medium (Labrasol, Oleic Acid, Castor Oil, Peceol and Maisine) were centrifuged and the supernatant was diluted, and the saturation solubility was assessed through UV-Spectroscopy (Table 1).

Table 1. Solubility of Terbinafine HCl in liquid lipids

	Labrasol	Oleic Acid	Castor Oil	Peceol	Maisine
Solubility (mg/g)	9.698	5.963	5.668	14.165	18.275
SD	0.030	0.074	0.308	3.637	2.377

Drug solubility in solid lipids was carried out by using Differential Scanning Calorimeter. Terbinafine HCl thermal behavior and solid lipids and 1:1 physical mixtures (PM) were characterized in a DSC (Perkin Elmer) cell (Perkin Elmer Corp., Norwalk, CT, USA), under a dynamic N₂ atmosphere (50 mL·min⁻¹), using sealed aluminum capsules with about 2 mg of samples. DSC curves were obtained at a heating rate of 10°C min⁻¹ in the temperature range from 25 to 290°C. An empty sealed pan was used as a reference.

The crystallinity indexes (CI) were calculated in percentage according to the following equation and are presented in Table 2:

$$CI (\%) = \frac{\Delta H_{\text{Terb PM}} * D}{\Delta H_{\text{Terb 100\%}}} * 100$$

where $\Delta H_{\text{Terb PM}}$ is the enthalpy of fusion (J·g⁻¹) of Terbinafine HCl in the binary physical mixture of the drug and solid lipid. $\Delta H_{\text{Terb 100\%}}$ is the enthalpy of fusion (J·g⁻¹) of pure drug. D is the dilution of Terbinafine in the PM, for example, 1:1: dilution of 2.

Table 2. Terbinafine in solid lipids

	Enthalpy (J/g)	D	CI
Terbinafine	157	2	
Gelucire 50/13	41.33	2	52.64
Gelucire 48/16	31.45	2	40.06
Glycerol monostearate	11.62	2	14.80

Based on the results, Maisine was chosen as the liquid lipid and GMS (lowest CI was chosen as the SL to be used.

Preparation of nanostructured lipid carriers (NLC)

Currently, NLC formulations are being developed at the University of Sao Paulo, Brazil. The method used to prepare the carriers is the high pressure homogenization. A response surface statistical design was used to evaluate the lipids and surfactant concentration effects on NLC z-average using Minitab® 18 software (State College PA, USA).

Based on the preliminary results, the ratio between SL:LL was set to 1:1, the oil phase will range from 5-8% and the surfactant concentration 1-3% (Table 3).

Table 3. Response surface design

StdOrder	ExpOrder	TypePt	Blocks	Oil Phase	TA
7	1	0	1	6.5	2.0
4	2	1	1	8	3.0
5	3	0	1	6.5	2.0
2	4	1	1	8	1.0
6	5	0	1	6.5	2.0
1	6	1	1	5	1.0
3	7	1	1	5	3.0
9	8	-1	2	8	2.0
8	9	-1	2	5	2.0
12	10	0	2	6.5	2.0
14	11	0	2	6.5	2.0
11	12	-1	2	6.5	3.0
13	13	0	2	6.5	2.0
10	14	-1	2	6.5	1.0

References

- A2.1. Porter, C. J. H. & Charman, W. N. Uptake of drugs into the intestinal lymphatics after oral administration. *Adv. Drug Deliv. Rev.* **25**, 71–89 (1997).
- A2.2. Khan, A. A., Mudassir, J., Mohtar, N. & Darwis, Y. Advanced drug delivery to the lymphatic system: Lipid-based nanoformulations. *Int. J. Nanomedicine* **8**, 2733–2744 (2013).
- A2.3. Zgair, A. *et al.* Oral administration of cannabis with lipids leads to high levels of cannabinoids in the intestinal lymphatic system and prominent immunomodulation. *Sci. Rep.* **7**, 1–12 (2017).
- A2.4. Attili-Qadri, S. *et al.* Oral delivery system prolongs blood circulation of docetaxel nanocapsules via lymphatic absorption. *Proc. Natl. Acad. Sci. U. S. A.* **110**, 17498–17503 (2013).
- A2.5. Bhalekar, M. R. *et al.* In-vivo bioavailability and lymphatic uptake evaluation of lipid nanoparticulates of darunavir. *Drug Deliv.* **23**, 2581–2586 (2016).
- A2.6. Gao, F. *et al.* Nanoemulsion improves the oral absorption of candesartan cilexetil in rats: Performance and mechanism. *J. Control. Release* **149**, 168–174 (2011).
- A2.7. Makwana, V., Jain, R., Patel, K., Nivsarkar, M. & Joshi, A. Solid lipid nanoparticles (SLN) of Efavirenz as lymph targeting drug delivery system: Elucidation of mechanism of uptake using chylomicron flow blocking approach. *Int. J. Pharm.* **495**, 439–446 (2015).
- A2.8. Mishra, A., Vuddanda, P. R. & Singh, S. Intestinal lymphatic delivery of praziquantel by solid lipid nanoparticles: Formulation design, *in vitro* and *in vivo* studies. *J. Nanotechnol.* **2014**, (2014).
- A2.9. Sitrin, M. D., Pollack, K. L., Bolt, M. J. G. & Rosenberg, I. H. Comparison of vitamin D and 25-hydroxyvitamin D absorption in the rat. *Am. J. Physiol. - Gastrointest. Liver Physiol.* **5**, (1982).
- A2.10. O’Driscoll, C. M. Lipid-based formulations for intestinal lymphatic delivery. *Eur. J. Pharm. Sci.* **15**, 405–415 (2002).
- A2.11. Hussain, M. M. A proposed model for the assembly of chylomicrons. *Atherosclerosis* **148**, 1–15 (2000).

**APPENDIX 3: Phytocannabinoid drug-drug interactions and their
clinical implications**

A version of this chapter is published in:

Pharmacology & Therapeutics. 2020 Jun 30:107621.
<https://doi.org/10.1016/j.pharmthera.2020.107621>

1. INTRODUCTION

Cannabis is a plant with a long history of human pharmacological use, both for recreational purposes and as a medicinal remedy (Balabanova, Parsche, & Pirsig, 1992; ElSohly & Slade, 2005; Grotenhermen, 2007; Hazekamp & Grotenhermen, 2010; Liskow, 1973; Raharjo & Verpoorte, 2004; Sharma, Murthy, & Bharath, 2012). Its two major chemical constituents are cannabidiol (CBD), the definitive structure of which was reported in 1963 (Mechoulam & Shvo, 1963) and Δ -9-trans-tetrahydrocannabinol (THC) which was elucidated in the following year (Gaoni & Mechoulam, 1964). These early discoveries opened the way for exploration of many similar plant-specific compounds which were ultimately termed collectively as “phytocannabinoids” (Pate, 1999), to differentiate them from the endogenous “endocannabinoids” discovered during the 1990s (Mechoulam, Hanus, Pertwee, & Howlett, 2014). The most important psychoactive phytocannabinoid is THC, usually accompanied by varying amounts of CBD, a relatively non-psychoactive compound which is able to modulate some of the psychotropic effects of THC (Eichler et al., 2012). THC is useful for several clinical indications, such as pain management, and as an antiemetic, antispasmodic and appetite stimulant (Clark, Ware, Yazer, Murray, & Lynch, 2004; Eichler et al., 2012; ElSohly, 2002; ElSohly & Slade, 2005; Furler, Einarson, Millson, Walmsley, & Bendayan, 2004; Russo, 2001, 2002; Tramer et al., 2001; Ware, Adams, & Guy, 2005; Wood, 2004). The use of high-THC content cannabis for glaucoma and asthma has been suggested (Appendino, Chianese, & Tagliatela-Scafati, 2011; Sharma et al., 2012) and the whole plant extract (as Epidiolex®) of a high-CBD Cannabis variety has recently been approved (FDANewsRelease, 2018; Gaston & Friedman, 2017; Koltai, Poulin, & Namdar, 2019) by the United States Food and Drug Administration (U.S. FDA) for application to certain forms of epilepsy.

Currently, there exist several cannabis inspired or based commercial pharmaceutical products for a range of medical indications. Dronabinol is synthetic THC and has been sold for decades as the pharmaceutical product Marinol®. It is indicated to ameliorate anorexia in patients with AIDS, and for the treatment of nausea and vomiting in cancer chemotherapy patients not responding to conventional antiemetic treatments (Dronabinol, 2019; Rong et al., 2018). Nabilone is a synthetic analog of THC which is marketed as the pharmaceutical product Cesamet®. Although distinct in molecular structure from THC, nabilone mimics THC pharmacological activity and is approved by the U.S. FDA for treatment of the same indications (Nabilone, 2019). Sativex® (generically known as “nabiximols”) is a whole plant extract derived from Cannabis which is used for the treatment of neuropathic pain originating from multiple sclerosis, and for intractable cancer pain. It is marketed as an oro-mucosal pump spray having a 1:1 ratio of THC:CBD (Nabiximols, 2019; Rong et al., 2018). Many other potential applications for cannabis have been proposed, and are currently under investigation (Medical Cannabis, 2019; Sharma et al., 2012; Zou & Kumar, 2018).

The rich chemical content of the Cannabis plant (more than 400 compounds) illustrates the possibility of a wide range of pharmacological applications (Sharma et al., 2012), as well as many possible interactions. The most well-known and most specific class of these compounds is the C₂₁/C₂₂ terpenophenolic phytocannabinoids (ElSohly & Slade, 2005; Mechoulam & Gaoni, 1967). These compounds are classified according to their molecular structure into several types, for which THC, CBD, cannabichromene (CBC), cannabigerol (CBG) and their homologues are representative.

Interestingly, in fresh Cannabis plant extracts, these terpenophenolic phytocannabinoids per se are not abundantly present, but rather found mostly as their 2-carboxy form (Figure A.1),

which are the only demonstrated biogenetic compounds. Of these, Δ -9-trans-tetrahydrocannabinolic acid (THCA) represents the majority of the collective total phytocannabinoids contained within tropically derived plants, which accumulate mainly on the flowers (exceeding a dry weight content of 20% in some recreational varieties) and leaves, and apparently serve plant protective functions (Moreno-Sanz, 2016; Pate, 1994). Cannabidiolic acid (CBDA) is predominant (at more than 10% by dry weight in a few medical strains) in plants from temperate regions. Neither compound is psychoactive per se, but both of these carboxylated compounds can be transformed into THC and CBD, respectively, through a degradative process which occurs slowly upon storage, but rapidly upon heating (Grotenhermen, 2003; Moreno-Sanz, 2016). Under field conditions, and with mild processing and cold storage, the extent of this decarboxylation is only nominal (~2–5%), which means that more carboxylic acid than phenolic forms are to be found in the oral fluid, serum, and urine of raw cannabis medical consumers (Dussy, Hamberg, Luginbühl, Schwerzmann, & Briellmann, 2005; Jung, Kempf, Mahler, & Weinmann, 2007; Moore, Rana, & Coulter, 2007; Moreno-Sanz, 2016). However, substantial to complete *in situ* decarboxylation occurs under the conditions of smoking or in baked goods.

Additionally, THC can be oxidized to cannabinol (CBN) via prolonged exposure to heat, oxygen and light (Russo, 2011). Hence, the presence of CBN indicates that a specimen is old, although most THC loss is due to the formation of polymers. The reported (Russo, 2011) pharmacological effect of CBN is mainly sedative, but this compound may also have application as an antibacterial, and may possibly decrease keratinocytes in cases of psoriasis.

Cannabichromenic acid (CBCA) is usually the third most abundant biogenetic phytocannabinoid in the Cannabis plant (McPartland & Russo, 2001), but that rank varies according to plant latitudinal origin, often being more abundant than CBDA in tropical

specimens. As its decarboxylated form, CBC appears to potentiate some THC effects *in vivo* and has modest anti-nociceptive and anti-inflammatory effects (Hatoum, Davis, Elsohly, & Turner, 1981). Even though very little is known about its pharmacology, CBC has been shown to have the potential to stimulate the growth of brain cells and the ability to normalize gastrointestinal hypermotility (Aizpurua-Olaizola et al., 2016).

Least observed in the Cannabis plant is cannabigerolic acid (CBGA), the original biogenetic phytocannabinoid which metabolically yields CBDA, CBCA and THCA via their respective synthases (De Meijer & Hammond, 2005). Decarboxylation of the acid form (Wang et al., 2016) yields CBG, which has been shown to have anti-inflammatory, antibiotic and antifungal properties (Moreno-Sanz, 2016) and inhibits the growth of human oral epithelioid carcinoma cells (Baek et al., 1998). CBG has also been shown to have promising potential for the treatment of glaucoma, prostate carcinoma and inflammatory bowel disease (Aizpurua-Olaizola et al., 2016).

The aforementioned phytocannabinoids have a pentyl side-chain, but traces of methyl (Vree, Breimer, van Ginneken, & van Rossum, 1972) and minor amounts of propyl (De Meijer & Hammond, 2005) homologues also occur. The propyl homologues of CBD and THC, named cannabidivarin (CBDV) and Δ -9-trans-tetrahydrocannabivarin (THCV) respectively, are present in the plant at various ratios, depending on the specific Cannabis variety (Deiana et al., 2012). These compounds have not yet been studied as extensively as the other phytocannabinoids, but research shows that both THCV and CBDV may have therapeutic potential for reducing nausea (Rock, Sticht, Duncan, Stott, & Parker, 2013). Additionally, CBDV may have potential for the treatment of neuronal hyperexcitability, whereas THCV improves insulin sensitivity in obesity mouse models (Iannotti et al., 2014; Wargent et al., 2013). As little is known about these

compounds, further studies regarding their pharmacological action and metabolic pathways are needed.

Recently, trace amounts of a novel seven-carbon THC homologue was isolated from Cannabis (Citti et al., 2019) and designated Δ^9 -trans-tetrahydrocannabiphorol (THCP). Reported to be much more potent than the usual five-carbon THC, its similar pharmacological actions include hypomotility, analgesia, catalepsy and decreased rectal temperature.

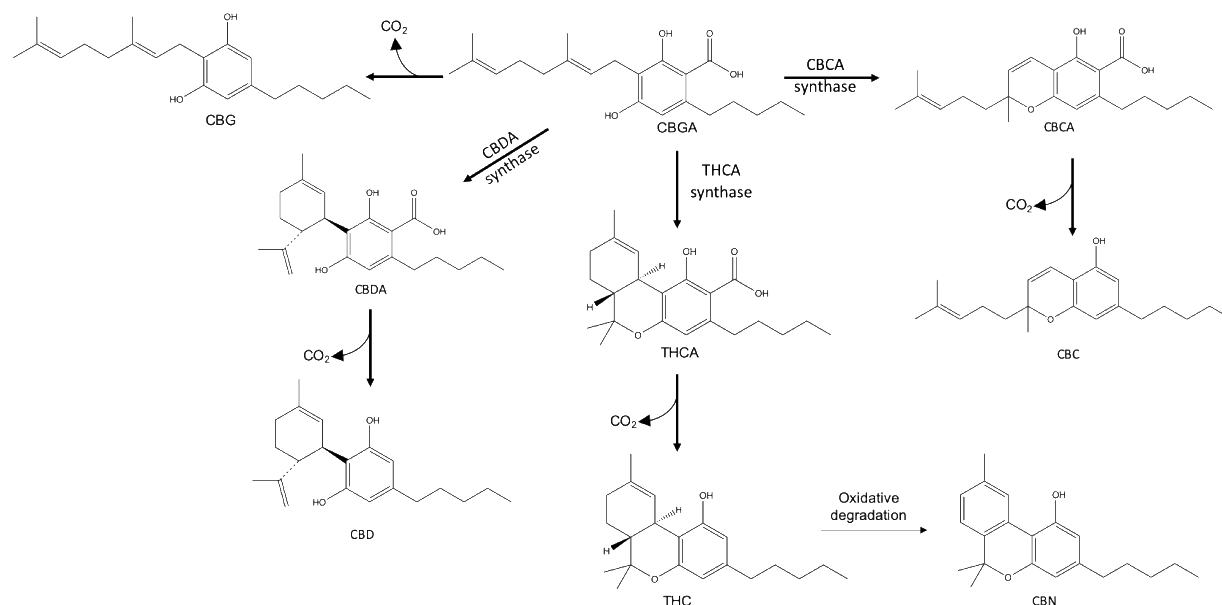


Figure 1. Biogenesis of phytocannabinoids and some of their degradation products. (CBGA: cannabigerolic acid; CBG: cannabigerol; CBDA: cannabidiolic acid; CBD: cannabidiol; THCA: tetrahydrocannabinolic acid; THC: tetrahydrocannabinol; CBCA: cannabichromenic acid; CBC: cannabichromene; CBN: cannabinol)

Oral ingestion of baked goods, or inhalation of smoke/vapor, are the most common ways in which cannabis products are consumed (Grotenhermen, 2003; Moreno-Sanz, 2016). Compared to inhalation, the oral bioavailability of phytocannabinoids is relatively low (6–20%)

due to a high first-pass metabolism within the liver (Ohlsson et al., 1980; Wall, Sadler, Brine, Taylor, & Perez-Reyes, 1983). Unlike inhaled phytocannabinoids, onset of psychoactive effects via oral ingestion is slow and varies from 30 minutes to occasionally over 2 hours (Eichler et al., 2012), with the duration of action being more prolonged. This is due to the usually larger dose administered, slow gastro-intestinal absorption, and continued gut reabsorption (Eichler et al., 2012; Garrett & Hunt, 1977; Hollister et al., 1981; Lemberger et al., 1972; Ohlsson et al., 1980).

As mainstream use of cannabis grows, it is increasingly important to understand phytocannabinoid disposition within the human body, and especially its metabolic pathways. In a generic sense, the metabolic pathways operate under two broad categories: Phase I and Phase II. Phase I reactions include oxidation, reduction and hydrolysis, which increase the molecule's hydrophilicity. Phase II metabolism involves conjugation reactions with endogenous hydrophilic compounds to either increase water solubility or inhibit pharmacological activity (Kirchmair et al., 2015, 2013; Tyzack & Glen, 2014; Tyzack & Kirchmair, 2019). These reactions include glucuronidation, sulfation, amino acid conjugation, acetylation, methylation and glutathione conjugation. Even though the complex metabolism of phytocannabinoids poses many challenges, a more thorough understanding generates many opportunities, especially with regard to the investigation (Testa, Pedretti, & Vistoli, 2012) of possible drug-drug interactions (DDIs).

DDIs can lead to adverse drug reactions, with loss of, or increase in, efficacy due to altered systemic exposure. Therefore, as variations in drug response of the co-administered drugs can occur, it is important to evaluate potential drug interactions prior to market approval, as well as during the post-approval marketing period (Izzo et al., 2012). Consideration of these factors, combined with an increasing frequency of polypharmacy, has led regulatory agencies such as the U.S. FDA and the European Medicines Agency (EMA) to issue guidelines for industry to

investigate the potential DDIs of new molecular entities. Guidance for studies of clinical drug interactions, *in vitro* metabolism, and transporter-mediated DDIs, as well as *in silico* analyses of DDIs, have been published (Prueksaritanont et al., 2013).

The application of *in silico* modelling and simulation within drug development is rapidly increasing in the R&D sector of the pharmaceutical industry (Duque et al., 2018; Silva, Duque, Davies, Löbenberg, & Ferraz, 2018). It has been suggested (Rostami-Hodjegan & Tucker, 2007) that such an approach could potentially represent up to 15% of R&D expenditures in the next 5–10 years. The *in silico* approach can be applied to all stages of the drug discovery and development process, from predicting the molecular properties of lead compounds to simulating clinical trials (Rostami-Hodjegan & Tucker, 2007). Within the context of metabolism prediction, *in silico* tools are most commonly used for predicting substrates and inhibitors of metabolic enzymes, sites of metabolism, and the structures of probable metabolites. These predictions can assist optimizations during the drug discovery process, helping to identify metabolic stability issues, *in vivo* half-lives and potentially toxic metabolites (Tyzack & Kirchmair, 2019). Furthermore, understanding the individual cytochrome P450 (CYP) isoform specificities of a given molecule can help to predict enzyme inhibitions and DDIs.

Phase I and Phase II enzymes are located in the endoplasmic reticulum of hepatocytes, hence that is where metabolic reactions such as Phase I hydroxylation by CYPs and Phase II glucuronidation occur (Elmes et al., 2019). Since phytocannabinoids are highly lipophilic molecules, a mechanism to facilitate their cytoplasmic transport from the cell membrane to the intracellular metabolic enzymes is needed (Morales, Hurst, & Reggio, 2017). It has been postulated that such trafficking is accomplished through soluble carrier proteins that cross the aqueous environments of the cytosol (Elmes et al., 2015, 2019; Huang et al., 2016).

A recent report (Elmes et al., 2019) demonstrated that the candidates which are most likely to facilitate such transport in hepatocytes are fatty acid-binding proteins (FABPs), specifically FABP1, which has high expression levels in hepatocytes. Hence, based on this, it was concluded that FABP1 plays a major role in governing phytocannabinoid metabolism by transporting it to hepatic CYP enzymes. However, more studies are needed to understand the intracellular transport of phytocannabinoids. Studies with FABP1 knock-out mice (Elmes et al., 2015) revealed only a reduced effect on cannabinoid metabolism, suggesting that other cytoplasmic lipid-binding proteins may also be involved. In addition, sterol carrier protein-2, FABP2 and heat shock protein 70 have emerged as both endocannabinoid and phytocannabinoid transport proteins within cells (Elmes et al., 2015).

FABP1 may also serve as a previously unrecognized site of drug-drug-interactions. Numerous xenobiotics such as fibrates, warfarin, diazepam, flurbiprofen, and diclofenac have been shown (Elmes et al., 2019) to bind to FABP1 with comparable affinities to THC. Hence, these compounds may compete with phytocannabinoids for cellular uptake, leading to unpredictable pharmacological responses. Further studies are required to determine the clinical significance of competition for cellular uptake between phytocannabinoids and other drugs (Elmes et al., 2015, 2019; Huang et al., 2016).

The reported *in vivo* Phase I and Phase II metabolisms of various phytocannabinoids is herein reviewed, accompanied by a parallel analysis of their predicted metabolisms *in silico*, highlighting the clinical importance of such understanding in terms of DDIs. A brief overview on the physiological mechanisms of action for phytocannabinoids is also presented.

2. METHODS

2.1 Literature search

Databases such as Medline, Scopus, Google Scholar, Science Direct and SciFinder were systematically searched to identify relevant studies using key-words alone and in combination with each other, such as: THCA, THC, CBD, CBDA, CBC, CBCA, CBG, CBGA, THCV, CBDV, cannabinoids, metabolism, CYP isoforms, drug-drug interaction, oral administration, cannabis, *in silico* prediction, mechanism of action, cannabinoid receptors and endocannabinoid system. Priority was given to papers reporting human metabolism following oral administration of phytocannabinoids. Animal metabolism and *in vitro* studies were considered in cases where human data from the scientific literature was scarce. Relevant research papers and reviews on phytocannabinoid metabolism and *in silico* prediction were then selected.

2.2 *In silico* metabolism prediction

Predictions of CYP isoforms potentially involved in phytocannabinoid metabolism were carried out using ADMET Predictor™ 9.5 (Simulations Plus, Lancaster, CA, USA). The Metabolism Module in ADMET Predictor™ classifies compounds as substrates and/or inhibitors of the major CYP isoforms (Figure A.2) using data acquired from the BIOVIA Metabolite database, the DrugBank database (Tyzack & Kirchmair, 2019; Wishart et al., 2018), and other public resources.

Chemical structures were drawn in a Mol file format using ChemDraw Prime (PerkinElmer Informatics, Inc.) and imported into ADMET Predictor™. Metabolism Module default settings were used to classify the phytocannabinoids as substrates and/ or inhibitors of various human CYP isoforms, and to predict possible metabolites.

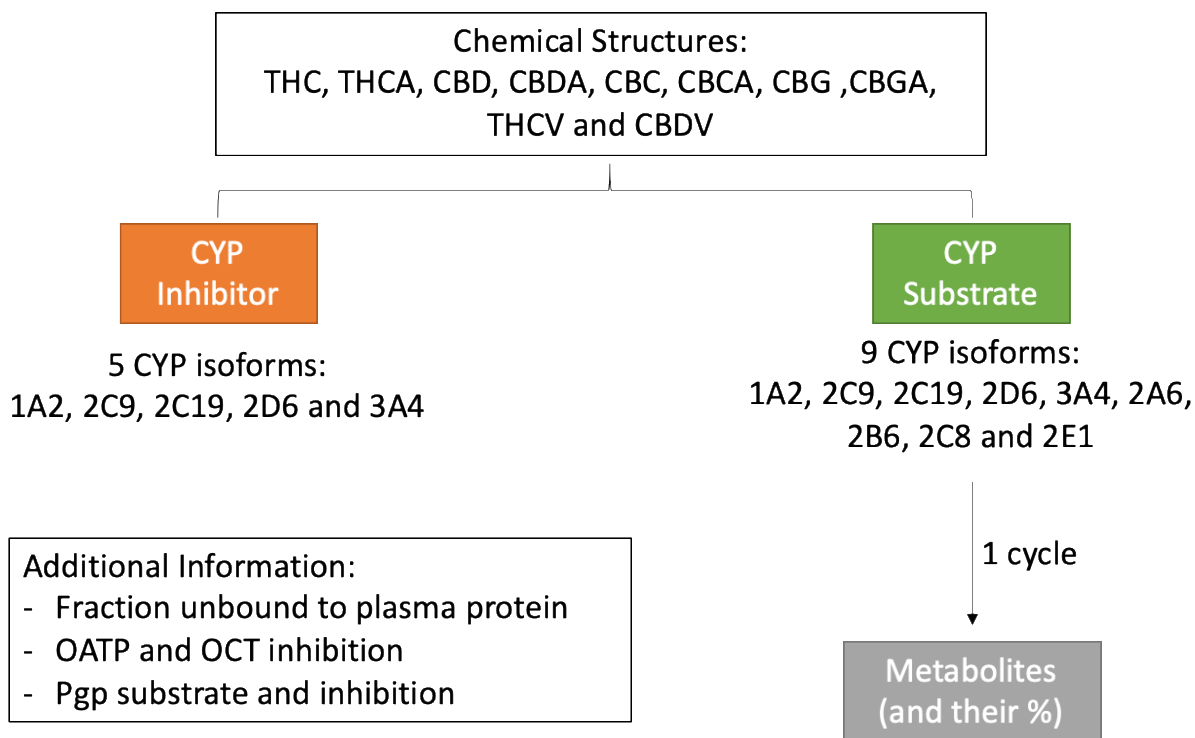


Figure 2. Simplified scheme of simulations using default settings in ADMET Predictor™ (Metabolism Module). OATP: Organic-anion-transporting polypeptides; OCT: Organic cation transporter, P-gp: P-glycoprotein.

3. RESULTS & DISCUSSION

3.1 Mechanisms of action

The first breakthrough for understanding the THC mechanism of action was in the late 1980s, with the discovery of a cannabinoid receptor in rat brain (Devane, Dysarz, Johnson, Melvin, & Howlett, 1988), now known as the cannabinoid receptor 1 (CB1). Receptors are generally activated by endogenous molecules, hence, there was a strong motivation to identify endogenous cannabinoids. The isolation and molecular structure determination of “anandamide” (an endogenous natural ligand of cannabinoid receptors) was this second ground-breaking discovery (Devane, Hanus, et al., 1992), followed by the description of SR141716A as the first CB1-specific antagonist (Rinaldi-Carmona et al., 1994). Shortly thereafter, 2-arachidonoyl

glycerol was identified as a second endocannabinoid (Mechoulam et al., 1995; Sugiura et al., 1995), eventually followed by several others. In 1993, a second cannabinoid receptor (CB2) was discovered, not in the central nervous system, but in the periphery (Munro, Thomas, & Abu-Shaar, 1993). Its receptor antagonist, SR144528, was discovered by the same group which had discovered the first CB1 receptor antagonist (Rinaldi-Carmona et al., 1998). The endocannabinoid receptors (CB1 and CB2), the endocannabinoids, and their biosynthetic and biodegrading enzymes, constitute the endocannabinoid system.

The distinction between CB1 and CB2 is based on differences in their amino acid sequence, signaling mechanisms, tissue distribution, and sensitivity to certain agonists and antagonists. Both are G protein-coupled receptors, and their agonist stimulation leads to signal transduction pathways via the Gi/o family of G proteins. Briefly, the free $G_{i\alpha}$ protein regulates adenylyl cyclase by inhibiting the production of cyclic AMP, decreasing the activation of protein kinase A. This may modulate signaling pathways, such as that of ion channels. The free $\beta\gamma$ dimers mediate the regulation of ion channels, mitogen-activated protein kinase, and phosphatidylinositol-3-kinase (Howlett et al., 2002; Schurman, Lu, Kendall, Howlett, & Lichtman, 2020).

CB1 receptors also regulate several types of calcium and potassium channels through G proteins. These receptors exist predominantly on central and peripheral neurons and their primary function is to inhibit neurotransmitter release. CB2 receptors are present mainly on immune cells, which also express CB1 receptors to a lesser extent. Their activation leads to a broad spectrum of immune effects regarding modulation of cytokine release (Howlett et al., 2002). Recent studies report the identification of functional CB2 receptors throughout the central nervous system, and their neuronal function is still being debated (Wu, 2019). The location of

these brain receptors appear to be mainly postsynaptic, while CB1 receptors are predominantly found in neuronal presynaptic terminals (Ligresti, De Petrocellis, & Di Marzo, 2016; Wu, 2019).

Phytocannabinoids show differential affinities for CB1 and CB2 receptors (Morales et al., 2017). THC is a moderate partial agonist of CB1 and CB2 receptors, which results in the well-known effects of smoking cannabis, such as increased appetite, reduced pain and inflammation, and changes to emotional and cognitive processes (Dronabinol, 2019; Morales et al., 2017). Synthetic modifications of the alkyl side-chain can influence phytocannabinoid binding to their receptors. THC analogues with longer and/or branched side chains have been shown (Devane, Breuer, et al., 1992) to have more potent cannabimimetic properties than THC itself. For example, *in vitro* studies of the natural seven-carbon THCP revealed a binding activity to the human CB1 receptor similar to that of a potent full CB1 agonist, resulting in an enhancement of the usual cannabimimetic activity (Citti et al., 2019).

Shortening the pentyl chain can also change some of its qualitative receptor behaviors. The natural three-carbon THCV molecule acts as a CB1 antagonist as well as a partial agonist of the CB2 receptor (Pertwee, 2008). It has been reported (Cascio, Zamberletti, Marini, Parolaro, & Pertwee, 2015; De Petrocellis et al., 2011) to also activate the serotonin 1A (5HT1A) receptor and to interact with the transient receptor potential cation channel, subfamily V member 2 (TRPV2).

CBD appears to have a lack of affinity for the CB1 and CB2 receptors (Russo, 2011). Nevertheless, *in vitro* studies (Laprairie, Bagher, Kelly, & Denovan-Wright, 2015) demonstrate that CBD displays weak CB1 and CB2 antagonistic effects. It was reported (Laprairie et al., 2015) that CBD behaves as a negative allosteric modulator of the CB1 receptor. Allosteric regulation is achieved through modulation of receptor activity on a site distinct from the

agonist/antagonist binding site (Laprairie et al., 2015). Additionally, there is evidence that CBD activates 5-HT_{1A} and TRPV1–2 vanilloid receptors, antagonizes alpha-1 adrenergic and μ -opioid receptors, and inhibits the uptake of various neurotransmitters (e.g., noradrenaline, dopamine, and serotonin) at the synaptic cleft. CBD has also been shown (Zhornitsky & Potvin, 2012) to inhibit the cellular uptake of anandamide and to inhibit the activity of fatty acid amide hydrolase, the anandamide degrading enzyme.

CBDV is thought to modulate TRPV1, conferring its anti-epileptic activity (Iannotti et al., 2014). It has also been shown to inhibit the activity of diacylglycerol lipase- α , which is involved in the synthesis of the endocannabinoid 2-arachidonoylglycerol (Amada, Yamasaki, Williams, & Whalley, 2013; Bisogno et al., 2003). The clinical implications of these actions are unclear. Other phytocannabinoids under current investigation for anticonvulsant action include CBD, THCV and THCA. Their anti-epileptic activity appears to be at sites other than endocannabinoid receptors, such as modulation of TRPV receptors.

Although the cannabis-related fields of study have greatly expanded since the initial discovery of the endocannabinoid receptor system and its ligands, there remains a great need to enhance our understanding of the biochemistry and pharmacology of phytocannabinoids, particularly as relevant to clinical applications.

3.2 Metabolic routes

3.2.1 Tetrahydrocannabinolic acid and tetrahydrocannabinol

THCA has no psychoactive effects in humans and does not seem to be converted substantially to THC *in vivo* (Jung et al., 2009). Both THC and THCA undergo similar major metabolic pathways: first, the 11-hydroxyl intermediate is formed, which is then oxidized to the 11-carboxylic metabolite (Moreno-Sanz, 2016) via a transient aldehyde. The parent compound

and metabolites are further conjugated with glucuronic acid and excreted into feces (65%) and urine (20%) (Eichler et al., 2012; Huestis & Cone, 1998; Lemberger, Axelrod, & Kopin, 1971; Sharma et al., 2012; Wall et al., 1983).

The metabolism of THCA in rats after oral administration has been examined (Jung et al., 2009). Hydroxylation in position 11 to 11-hydroxy- Δ -9-tetrahydrocannabinolic acid (11-OH-THCA) was identified, which was further oxidized to 11-nor-9-carboxy- Δ -9-tetrahydrocannabinolic acid (THCA-COOH). Glucuronic acid conjugation was observed with the parent compound and both main metabolites. THCA also undergoes a hydroxylation at position 8 to yield 8 α -OH-THCA and 8 β -OH-THCA, followed by dehydration (Figure A.3a).

The metabolism of THCA within human liver microsomes and via isolated CYP isoenzymes has been investigated *in vitro* (Wohlfarth, 2013). In that study, THCA was incubated with pooled human liver microsomes and with CYP isozymes 1A2, 2A6, 2B6, 2C8, 2C9, 2C19, 2D6, 2E1, 3A4 and 3A5. Mono- and di-hydroxylated metabolites were identified. A total of five out of the ten isozymes showed no catalytic activity, namely CYP 1A2, 2A6, 2B6, 2D6, and 2E1. The main enzymes involved in the metabolism of THCA were CYP2C9 and 3A4, while CYP2C8, 2C19 and 3A5 only played a minor role. It was reported that CYP2C8 generated 8 β -OH-THCA and 8 α -OH-THCA metabolites; CYP2C19 generated 8 α -OH-THCA; CYP3A5 generated 8 β -OH-THCA; CYP2C9 generated 11-OH-THCA and 8 α -OH-THCA metabolites and CYP3A4 generated both mono- and di-hydroxylated metabolites. The mono-hydroxylated metabolites included 8 β -OH-THCA and 11-OH-THCA. The di-hydroxylated metabolites included 9,10-bis-OH-THCA (9,10-bis-hydroxy-hexahydrocannabinolic acid) and 8,x-bis-OH-THCA (one hydroxylation was not identified). The metabolites detected when incubating THCA with human liver microsomes were 8 β -OH-THCA, 8 α -OH-THCA and unknown metabolites.

Interestingly, no 11-OH-THCA was found using the human liver microsome approach. The study speculated that this may be due to a difference in enzyme density of the media, which is higher in the heterologous expressed microsomes.

The metabolism of THC also takes place in the liver and potentially in the gut wall (Eichler et al., 2012) and involves liver enzymes of the CYP complex (Bland, Haining, Tracy, & Callery, 2005; Bornheim, Lasker, & Raucy, 1992; Halldin, Widman, Bahr, Lindgren, & Martin, 1982; Jung et al., 2009; Maurer, Sauer, & Theobald, 2006; Wall & Perez-Reyes, 1981; Watanabe, Matsunaga, Yamamoto, Funae, & Yoshimura, 1995). 11-hydroxy- Δ -9-tetrahydrocannabinol (11-OH-THC) is formed primarily by the CYP isoenzyme CYP2C9, and this metabolite is further oxidized via a transient aldehyde to 11-nor-9-carboxy- Δ -9-tetrahydrocannabinol (THC-COOH). After enzymatic glucuronidation of the carboxy function, the conjugate (THC-COOH glucuronide) is excreted (Jung et al., 2009; Williams & Moffat, 1980) in the urine (Figure A.3b). Approximately 80-90% of the phytocannabinoid is excreted within 5 days as hydroxylated and carboxylated metabolites (Gouille, Saussereau, & Lacroix, 2008; Sharma et al., 2012). Several other metabolites have been reported, such as those having hydroxylation at C'1 to C'5 of the side-chain, hydroxylation in position eight (followed by dehydration), and formation of an epoxide at C9–10 followed by hydrolysis or glutathione conjugation. The formation of 8-hydroxy metabolites and the C9-10 epoxide have been reported to be catalyzed by CYP3A4 (Bornheim et al., 1992; Halldin et al., 1982; Jung et al., 2009) (Figure A.3b).

Most of these metabolites are conjugated with glucuronic acid, increasing their water solubility. Among the major metabolites, THC-COOH (which has no psychotropic effects in humans) is the primary glucuronide conjugate in urine, whereas its metabolic precursor 11-OH-

THC (a very psychoactive metabolite) is the predominant form in feces (Eichler et al., 2012; Moreno-Sanz, 2016; Sharma et al., 2012). Very low excretion of unchanged drug is found in the urine due to the high lipophilicity of THC, resulting in its reabsorption by the kidney (Eichler et al., 2012).

Because of its high lipophilicity, THC is preferentially taken up by fatty tissues, and peak concentrations are reached in 4–5 days (Ashton, 2001; Eichler et al., 2012). Due to this accumulation, terminal elimination half-life of THC can be as long as 7 days, and complete elimination of a single dose can take up to 30 days (Eichler et al., 2012; Maykut, 1985). Metabolites have a much shorter half-life and therefore might serve as biomarkers for current exposure.

Another factor influencing phytocannabinoid pharmacokinetics is the route of administration. After smoking, a maximum THC plasma concentration was observed (Sharma et al., 2012) at approximately 8 minutes, whereas 11-OH-THC peaked at 15 minutes and THC-COOH at 81 minutes. THC concentrations rapidly decreased within 3-4 hours, and a slow redistribution occurred from the deep fat deposits back into the blood stream (Haggerty, Deskin, Kurtz, Fentiman, & Leighty, 1986; Hollister et al., 1981; Huestis, 2005; Sharma et al., 2012). In contrast to inhalation, THC systemic absorption after oral ingestion is fairly slow, with maximum plasma concentration being reached within 1-2 hours, but in rare cases may be delayed by a few hours (Hollister et al., 1981; Lemberger et al., 1971; Sharma et al., 2012). Even though THC oral bioavailability is reduced compared to the pulmonary route, due to extensive first-pass liver metabolism, a much higher concentration of the more psychoactive 11-OH-THC is produced after oral ingestion than by inhalation (Owens, McBay, Reisner, & Perez-Reyes, 1981; Sharma et al., 2012).

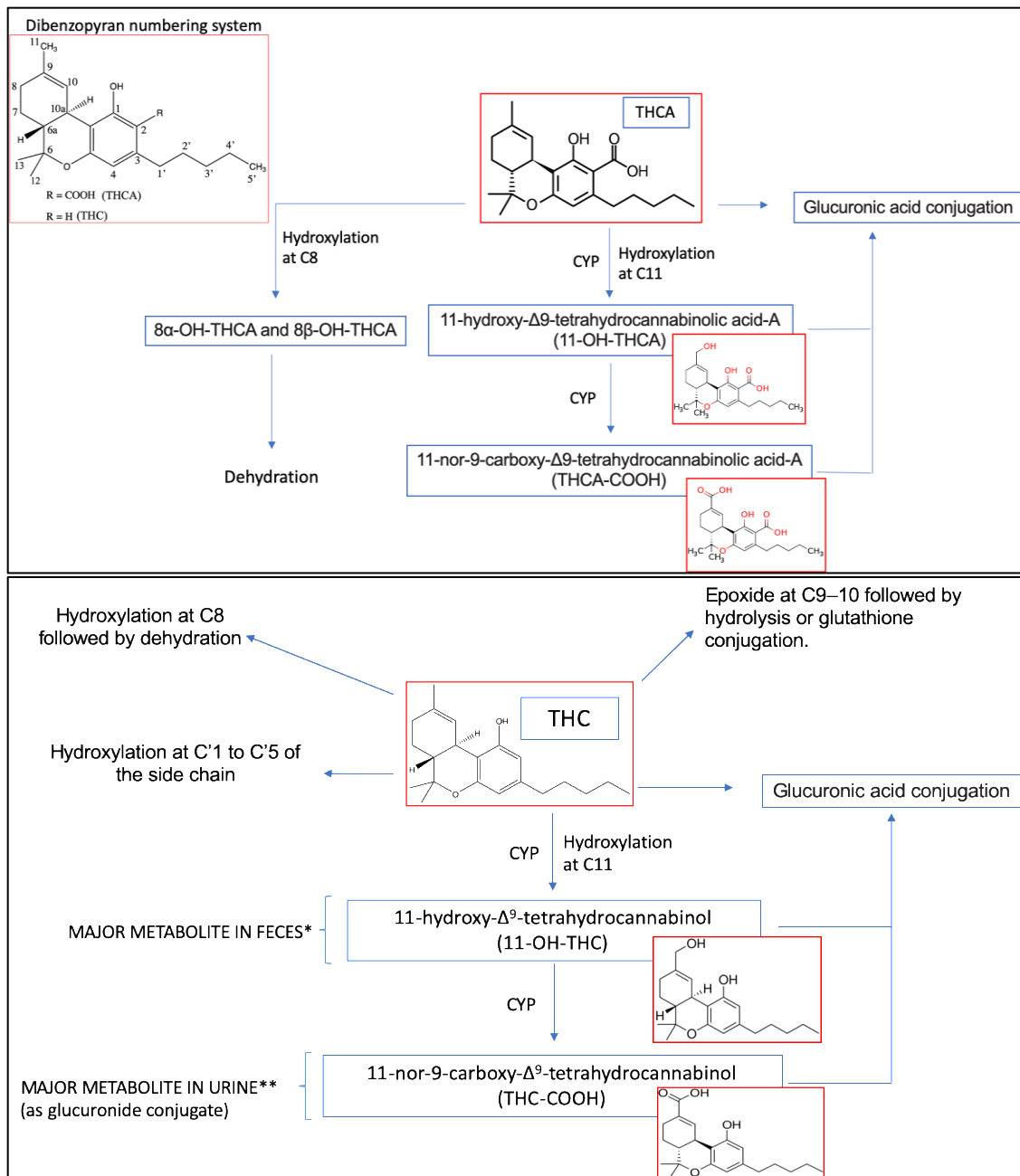


Figure 3. THCA (top) and THC (bottom) Phase I and Phase II metabolisms summary.

* Metabolite that is found in feces via biliary excretion, and not necessarily the major metabolite formed in the liver.

** Urine metabolite excreted by the kidney, and not necessarily the major metabolite formed in the liver. Glucuronides tend to make good substrates for excretion into the bile, but are often broken down in the gut by glycosidases or, in the case of acyl glucuronides, spontaneously.

Data on animal or human THCV metabolism is very scarce. It has been suggested (Elsohly, DeWit, Wachtel, Feng, & Murphy, 2001) that THCV would be metabolized in a similar manner as THC, resulting in 11-carboxy-THCV. Nevertheless, it is controversial as to whether or not its concentrations in urine would be enough to confirm cannabis consumption (Elsohly et al. , 1999, 2001; Sedgwick, 2000).

3.2.2 Cannabidiol

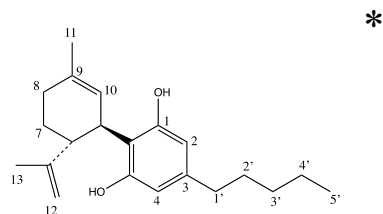
Although CBD is not significantly psychoactive, a wide range of other pharmacological effects have been reported for both the sole compound and for its combination with other drugs. Similarly to THC, CBD is also the spontaneous degradation product of its biogenetic precursor CBDA, which is decarboxylated upon heating (Ujváry & Hanuš, 2016) to form CBD (Figure A.1).

CBD undergoes extensive Phase I metabolism, which results in low bioavailability across species, and a complex pharmacokinetic disposition pattern. Studies in animals (i.e., rodents and dog), indicate that a large portion of the administered CBD is excreted intact or as its glucuronide (Harvey, 1991; Hawksworth & McArdle, 2004; Huestis, 2007; Huestis & Smith, 2014; Ujváry & Hanuš, 2016). Overall, the most abundant metabolites are hydroxylated 11-COOH derivatives which are excreted either intact or as glucuronide conjugates (Ujváry & Hanuš, 2016). As it is a good CYP substrate, CBD undergoes hydroxylation at multiple sites followed by further oxidations, resulting in a complex metabolic pattern of multiple metabolites

(Harvey, 1991; Ujváry & Hanuš, 2016). Besides the CYP oxidases, glucuronyl transferases and sulfotransferases are also involved within the enzymatic processes of metabolite formation.

Experiments reveal that 8 α -OH, 8 β -OH, 11-OH, and 4'-OH CBD are the main monohydroxylated metabolites of CBD recovered *in vitro* (Jiang, Yamaori, Takeda, Yamamoto, & Watanabe, 2011; Ujváry & Hanuš, 2016). The specific enzymes likely to be involved in the formation of the various metabolites are listed in Table 1.

Table 1. CYP isoforms involved in the metabolism of CBD in humans (Ujváry & Hanuš, 2016).



ENZYME	METABOLITE
CYP1A1	8 α / β -OH-, 11-OH-, and 1'-OH-CBD
CYP1A2	8 α / β -OH-CBD, 1'-, 2'-, 3'-, and 4'-OH-CBD
CYP2C19	8 α -OH-, 11-OH-, and 4'-OH-CBD
CYP2D6	8 α / β -OH-CBD, 11-OH-, 4'-OH-, and 5'-OH-CBD
CYP3A4	8 α / β -OH-CBD, 11-OH-, 2'-OH-, 4'-OH-, and 5'-OH-CBD
CYP3A5	8 α / β -OH-CBD, 11-OH-, 2'-OH-, 3'-OH-, and 4'-OH-CBD
CYP2A9 (Minor)	8 α / β -OH-, 11-OH-, 4'-OH-, and 5'-OH-CBD

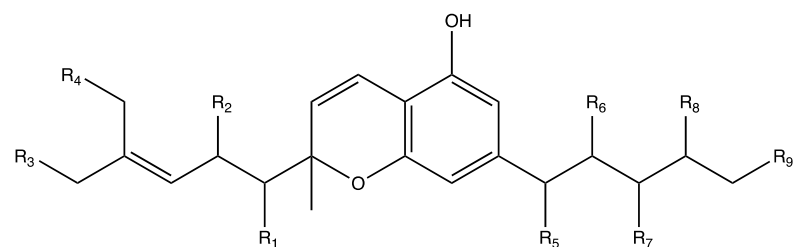
*Dibenzopyran numbering system.

In humans, the major Phase II metabolism involves glucuronidation of CBD at the phenolic oxygen, but hydroxylated metabolites of CBD could also act as substrates. Sulfonation of CBD species may also occur (Harvey & Mechoulam, 1990; Massi, Solinas, Cinquina, & Parolaro, 2013; Mazur et al., 2009; Stout & Cimino, 2014; Ujváry & Hanuš, 2016).

3.2.3 Cannabichromene

The metabolism of CBC has not been studied as extensively as the aforementioned two major phytocannabinoids and little is known about its metabolic pathways in humans. Some CBC metabolism studies have been conducted in various animals (i.e., mouse, rat, rabbit, guinea pig, cat, hamster and gerbil) and a range of metabolites have been characterized (Brown & Harvey, 1990; Kapeghian, Jones, Murphy, Elsohly, & Turner, 1983) across these different species (Table 2). The major metabolites identified were monohydroxy compounds hydroxylated at all positions of both carbon chains. No mention was made as to which CYP isoform was involved (Harvey & Brown, 1991b).

Table 2. *In vitro* CBC metabolites identified in mouse and rabbit microsomes (Brown & Harvey, 1990; Harvey & Brown, 1991b).



METABOLITE	R1	R2	R3	R4	R5	R6	R7	R8	R9	MOUSE*	RABBIT*
1'-OH	OH	H	H	H	H	H	H	H	H	8	-
2'-OH	H	OH	H	H	H	H	H	H	H	4	-

5'-OH	H	H	OH	H	H	H	H	H	H	1	1
6'-OH	H	H	H	OH	H	H	H	H	H	2	4
1''-OH	H	H	H	H	OH	H	H	H	H	5	6
2''-OH	H	H	H	H	H	OH	H	H	H	7	10
3''-OH	H	H	H	H	H	H	OH	H	H	6	3
4''-OH	H	H	H	H	H	H	H	OH	H	3	2
5''-OH	H	H	H	H	H	H	H	H	OH	5	5
1'',5'-Di-OH	H	H	OH	H	OH	H	H	H	H	-	12
1'',6'-Di-OH	H	H	H	OH	OH	H	H	H	H	-	13
3'',5'-Di-OH	H	H	OH	H	H	H	OH	H	H	-	9
3'',6'-Di-OH	H	H	H	OH	H	H	OH	H	H	-	8
4'',5'-Di-OH	H	H	OH	H	H	H	H	OH	H	-	7
4'',6'-Di-OH	H	H	H	OH	H	H	H	OH	H	-	6
5'',5'-Di-OH	H	H	OH	H	H	H	H	H	OH	-	11
5'',6'-Di-OH	H	H	H	OH	H	H	H	H	OH	-	6

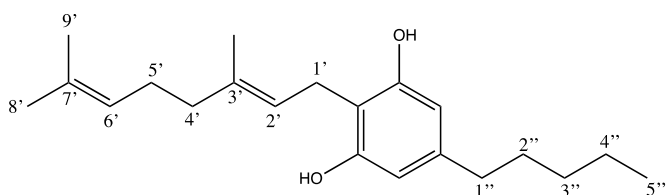
* Metabolite rank order (1 being most abundant).

3.2.4 Cannabigerol

An *in vitro* study (Harvey & Brown, 1990, 1991a) reported the metabolic pathways found for CBG using microsomes from various animals (i.e., mice, rats, cats, guinea-pigs, and rabbits). The metabolites were very similar to those found for other cannabinoids (especially CBC), in which hydroxylation and epoxidation were the major *in vitro* pathways. The preferred hydroxylation site varied considerably among the different species (Table 3). Except for mice,

allylic hydroxylation at the terminal double bond of the C-10 side-chain produced the major metabolites among the different species. The major metabolite in mice was an epoxide at this terminal double bond. Hydroxylation at the penultimate carbon of the pentyl side-chain was reported (Harvey & Brown, 1991a) as the major biotransformation route in mouse, rat and rabbit.

Table 3. *In vitro* CBG metabolites identified in liver microsomes from different animals.



METABOLITE	MOUSE*	RAT*	GUINEA	RABBIT*	CAT*
			PIG*		
1''-OH	4	7	T	4	7
2''-OH	-	-	6	-	-
3''-OH	7	6	2	5	6
4''-OH	2	4	5	3	3
5''-OH	4	7	T	4	7
4'-OH	3	3	3	5	5
8'-OH	5	1	1	1	1
9'-OH	7	5	6	5	2
6',7'-Epoxide	1	2	4	2	4
6',7'-Di-OH	6	-	6	-	T
6',7'-H2	-	5	-	-	1

*Metabolite rank order (1 being most abundant). T: Trace amount.

Cannabigerol metabolites (presumed to be the 4"-hydroxy-CBG or 5"-hydroxy-CBG) have been detected (Hidvegi & Somogyi, 2010) in human urine after cannabis consumption. Because of an absence of the corresponding phenolic peak in non-hydrolyzed urine samples, it was suggested that CBG was excreted in the glucuronated form.

3.3 In silico prediction of xenobiotic metabolism

Although a number of studies have been carried out to characterize the metabolites of THC and CBD, and to understand their metabolic pathways, data is relatively sparse on the metabolism of their acid forms (THCA and CBDA, respectively) and more so for other phytocannabinoids, such as THCV and CBDV. Within this scenario, in silico predictions can be useful to suggest the role of CYP isoforms in phytocannabinoid metabolism, which can serve as guidance for *in vitro* metabolism studies with recombinant human enzymes (Uwimana, Ruiz, Li, & Lehmler, 2019). The predicted metabolic pathways for THC/A, CBD/A, CBC/A, CBG/A, THCV and CBDV are summarized in Table 4, classifying each phytocannabinoid as a substrate and/or inhibitor of the major CYP isoforms (Figure A.2, Top).

Table 4. - Predicted phytocannabinoid substrates (top section) and inhibitors (bottom section) of CYP isoforms by ADMET Predictor™. The percentages shown within parentheses represent the degree of confidence.

CYP isoform	THCA	THC	CBDA	CBD	CBCA	CBC	CBGA	CBG	THCV	CBDV
	CYP SUBSTRATE									
CYP1A2	No (97%)	Yes (54%)	No (97%)	No (89%)	No (66%)	Yes (73%)	No (89%)	Yes (88%)	Yes (67%)	No (84%)

CYP2A6	No (60%)	Yes (69%)	No (98%)	No (88%)	No (86%)	Yes (61%)	No (98%)	No (98%)	Yes (69%)	No (79%)
CYP2B6	No (98%)	No (89%) (Stout & Cimino, 2014)	No (98%)	No (98%)	No (98%)	No (98%)	No (98%)	No (98%)	Yes (60%)	No (98%)
CYP2C8	Yes (77%)	No (71%) (Bornheim et al., 1992)	Yes (77%)	No (71%)	Yes (77%)	No (76%)	Yes (64%)	No (83%)	No (67%)	No (71%)
CYP2C9	Yes (73%)	Yes (73%) (Jung et al., 2009)	Yes (73%)	Yes (73%) (Ujváry & Hanuš, 2016)	Yes (73%)	Yes (73%)	Yes (73%)	Yes (55%)	Yes (73%)	Yes (73%)
CYP2C19	No (80%)	Yes (71%) (Stout & Cimino, 2014)	No (82%)	Yes (71%) (Jiang et al., 2011)	No (71%)	Yes (71%)	Yes (31%)	Yes (71%)	Yes (71%)	Yes (71%)
CYP2D6	No (82%)	Yes (41%)	No (86%)	Yes (42%) (Jiang et al., 2011)	No (86%)	Yes (42%)	No (95%)	Yes (45%)	Yes (48%)	Yes (42%)
CYP2E1	No (89%)	No (97%)	No (81%)	No (81%)	No (85%)	No (97%)	No (70%)	No (59%)	No (97%)	No (79%)

CYP3A4	No (41%)	Yes (83%) (Jung et al., 2009)	No (59%)	No (43%) (Jiang et al., 2011)	No (52%)	No (47%)	No (84%)	No (84%)	Yes (85%)	No (43%)
--------	-------------	-------------------------------------	-------------	-------------------------------------	-------------	-------------	-------------	-------------	--------------	-------------

CYP INHIBITOR

CYP1A2	Yes (55%)	No (59%) (Stout & Cimino, 2014)	No (86%)	No (97%) (Yamaori, Kushihara, Yamamoto, & Watanabe, 2010)	No (51%)	No (73%)	No (90%)	No (97%)	No (73%)	No (97%)
--------	--------------	--	-------------	---	-------------	-------------	-------------	-------------	-------------	-------------

CYP2C9	Yes (63%)	Yes (34%) (Yamaori, Ebisawa, Okushima, Yamamoto, & Watanabe, 2011)	Yes (43%)	Yes (64%) (Yamaori et al., 2012)	Yes (57%)	Yes (39%)	Yes (63%)	Yes (43%)	Yes (61%)	No (62%)
--------	--------------	---	--------------	---	--------------	--------------	--------------	--------------	--------------	-------------

CYP2C19	No (99%)	No (82%)	No (58%)	Yes (18%) (Jiang, Yamaori,	No (99%)	No (81%)	No (99%)	Yes (78%)	No (86%)	No (82%)
---------	-------------	----------	-------------	----------------------------------	-------------	-------------	-------------	--------------	-------------	-------------

				Okamoto, Yamamoto, & Watanabe, 2013)						
				Yes (70%) (Yamaori, Maeda, Yamamoto, & Watanabe, 2011)						
CYP2D6	No (95%)	No (65%)	No (86%)	No (84%)	Yes (44%)	No (80%)	Yes (45%)	No (72%)	Yes (55%)	
				No (71%) (Fugh- Berman et al., 2015)	No (68%)	No (81%)	No (68%)	No (78%)	No (90%)	No (81%)

(Boldface indicates prediction in agreement with literature data.)

As described in Section 3.2.1, the major CYP isoforms that metabolize THC are CYP2C9 and CYP3A4. The involvement of such enzymes in the metabolism of THC was accurately predicted by ADMET Predictor™, which also indicated the likely contributions of CYP 2C19, 2B6 and 2C8 (Table 4).

Many CYP isoforms have also been identified as CBD metabolizing enzymes. The activity of CYP isoforms 2C9, 2C19 and 2D6 were predicted accurately (shown boldface in Table 4), whereas CBD was mis-predicted as not being a substrate for CYP3A4 or CYP1A2. Both represent false positives, but the low confidence for CYP3A4 (43%) makes this merely a “soft” false positive (i.e., in a prospective application, this marginal result would indicate the need for experimental investigation). The complex metabolic pattern exhibited by CBD makes predictions of its metabolites challenging.

The inhibitory power of THC and CBD upon CYP enzymes has been more thoroughly studied than other cannabinoids (Yamaori, Ebisawa, et al., 2011; Yamaori et al., 2012, 2010; Yamaori, Maeda, et al., 2011; Yamaori, Okamoto, Yamamoto, & Watanabe, 2011). It was reported (Yamaori et al., 2010) that THC, CBD and CBN inhibited the 7-ethoxyresorufin O-deethylase catalytic activity of recombinant human CYP1A1, CYP1A2, and CYP1B1 in a competitive manner. CBD most potently inhibited CYP1A1 activity, whereas CBN decreased the activity of CYP1A2 and CYP1B1 more effectively than CYP1A1. THC inhibited CYP1 activity less potently than CBD and CBN, and also exhibited a lower selectivity.

The inactivation of recombinant CYP1A1 by CBD was characterized (Yamaori et al., 2010) as a potent mechanism-based inhibition. For human liver microsomes, this inhibition was also indicated as competitive. Their inhibition by THC and CBN indicated a mixed action, contrasting to isolated recombinant CYP1A2, which was competitively inhibited. It was speculated that these cannabinoids may interact with certain CYPs other than CYP1A2 in human liver microsomes, thus indicating various simultaneous mechanisms. CBD and CBN exhibited CYP1 isoform-selective direct inhibition and among the phytocannabinoids examined, CBD had the highest ability to inactivate human CYP1 enzymes.

CYP3A isoforms are potently inhibited by CBD in a competitive manner, especially CYP3A4 and CYP3A5 (Yamaori, Ebisawa, et al., 2011). CYP2A6 was noncompetitively inhibited by THC and CBD, whereas CYP2B6 was inhibited in a mixed fashion. THC and CBD displayed differences in their inhibition of CYP2A6 and CYP2B6, but inhibition of the latter enzyme by CBD was the most effective (Yamaori, Maeda, et al., 2011). Other studies (Yamaori, Okamoto, et al., 2011) indicated that CBD also potently inhibited CYP2C19.

CYP2D6 is responsible for the metabolism of a wide variety of clinically used drugs, such as dextromethorphan, debrisoquine, promethazine, and codeine. Specifically, dextromethorphan, an over-the-counter cough suppressant agent, is metabolized to dextrorphan by CYP2D6 through O-demethylation, which has been shown (Yamaori, Okamoto, et al., 2011) to be competitively inhibited by CBD in a concentration dependent manner. The apparent CBD K_i values for dextromethorphan O-demethylation in recombinant CYP2D6 were $2.69\mu\text{M}$ and $2.42\mu\text{M}$ for human liver microsomes. These results indicate that CBD is a potent inhibitor for CYP2D6 which could conceivably have clinical implications, as the reported plasma levels of CBD after smoking a placebo cannabis cigarette spiked with 20 mg of CBD was reported (Yamaori, Okamoto, et al., 2011) to be $0.363\ \mu\text{M}$ (114 ng/ml). However, a previous study (Yamaori et al., 2010) had found that the C_{max} for CBD after four buccal sprays of Sativex® totalling 10 mg of CBD (and 10.8 mg of THC) was only 9.62 nM (3.02 ng/ml). Notably, these plasma levels are below the K_i values, and thus, low oral doses of CBD are not anticipated to exhibit *in vivo* inhibition of CYP2D6. Further investigations are needed to elucidate *in vivo* CYP2D6-targeted drug interactions with increased doses of CBD via various routes of administration.

The predictions for CBD and THC inhibitory effects on CYP isoforms are summarized in Table 4. The same rationale for use of *in silico* predictions as guidance for *in vitro* inhibition studies can be applied. Due to the structural similarity between CBN and THC (Figure A.1) the metabolic pathways and metabolite structures were similar. The major difference was that CBN was predicted to be a CYP2C8 substrate and a CYP2D6 inhibitor, whereas THC was not.

None of the phytocannabinoids evaluated were predicted to be a substrate for BCRP or to inhibit OCT2 using models from a development version of ADMET Predictor 10.0 (Simulations Plus, Lancaster, CA, USA). All of the cannabinoids other than THC were predicted to inhibit P-gp, and its prediction was a marginally negative one (52% degree of confidence). The acidic cannabinoids - THCA, CBCA, CBGA and CBDA - were predicted to be substrates for P-gp efflux, but their relatively high passive permeability makes that unlikely to affect intestinal absorption. They were also confidently predicted to be OATP1B1 and OATP1B3 inhibitors, however, whereas THC, CBC, CBG and CBD yielded somewhat equivocal predictions, i.e., positive or negative with $\leq 60\%$ confidence.

Considering the *in silico* results of CYP inhibition, possible DDIs with prototypical drugs for each CYP can be anticipated (Table 5).

Table 5. Probable consequence of CYP inhibition based on *in silico* results

Cytochrome	Prototypical substrates#	Inhibited by*	Probable consequence/ Recommendation
CYP1A2	Acetaminophen, haloperidol, theophylline, warfarin	THCA	Increased drug plasma

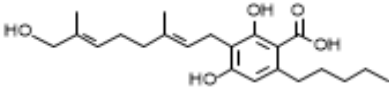
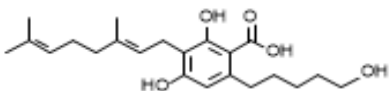
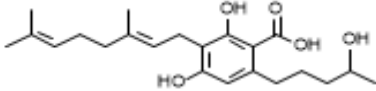
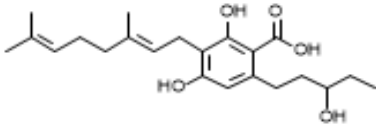
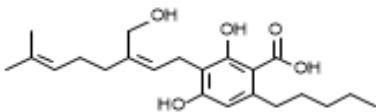
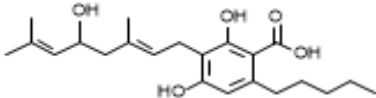
		THCA, THC,	concentration/
	Amitriptyline, celecoxib,	CBDA, CBD,	Drug dose
CYP2C9	clopidogrel, fluoxetine, losartan,	CBCA, CBC,	adjustment
	piroxicam, valproate	CBGA, CBG,	(Reduce)
		THCV	
CYP2C19	Amitriptyline, citalopram, esomeprazole, indomethacin, phenytoin	CBD, CBG	
CYP2D6	Amphetamine, carvedilol, codeine, duloxetine, lidocaine, propranolol	CBD, CBC, CBG, CBDV	
CYP3A4	Alprazolam, fentanyl, omeprazole, ritonavir, simvastatin, tamoxifen, verapamil	-	No interaction/ Maintain dose

* Based on in silico predictions; #Taken from (FlockhartTable, n.d.)

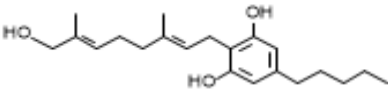
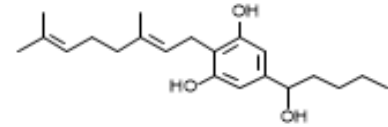
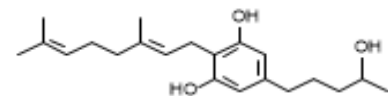
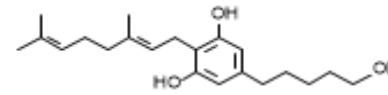
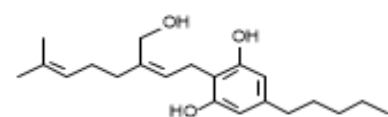
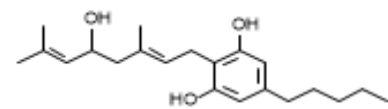
3.3.1 In silico metabolite structure prediction

Primary CYP metabolites predicted by ADMET Predictor™ indicated susceptibility to hydroxylation at several different positions on each phytocannabinoid structure (Table 6), just as was observed experimentally. Two subsequent oxidation cycles, which were run to assess further oxidation, indicated that the predicted metabolites were likely to undergo double hydroxylation, as well as further oxidation (e.g., to allylic aldehydes). These were predicted to be further oxidized to the corresponding carboxylic acids, generally at predicted clearance rates higher than that of their formation from the alcohol (details not shown).

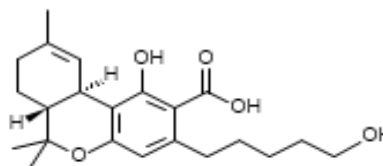
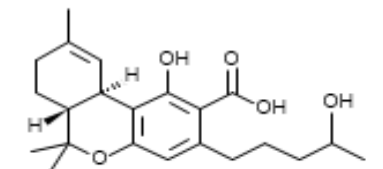
Table 6. Detectable human metabolites predicted by ADMET Predictor™ 9.5 and responsible metabolizing enzymes for the phytocannabinoids CBGA, CBG, THCA, THC, CBDA, CBD, CBCA, CBC, CBDV and THCV. Quantitative kinetic models are not available for isoforms set-off in parentheses, so any contribution they make to the estimated yield at very low substrate concentrations (intrinsic clearance) is not accounted.

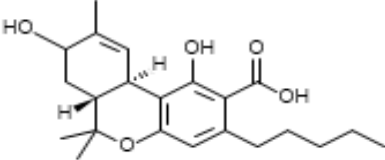
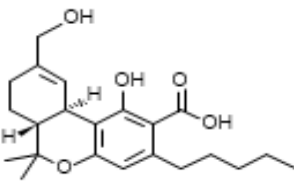
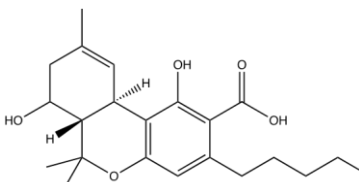
Estimated		
Metabolite structure	metabolite yield	Metabolizing enzymes
CBGA		
	26	(CYP2C8);CYP2C9; CYP2C19
	22	(CYP2C8);CYP2C9
	16	(CYP2C8);CYP2C9; CYP2C19
	13	CYP2C9
	13	(CYP2C8);CYP2C9
	11	(CYP2C8);CYP2C9

CBG

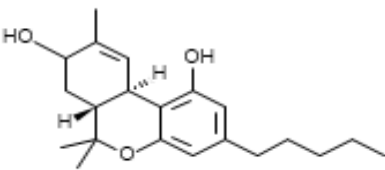
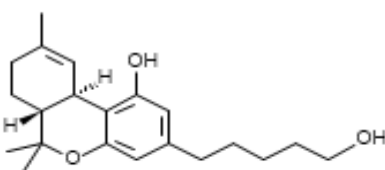
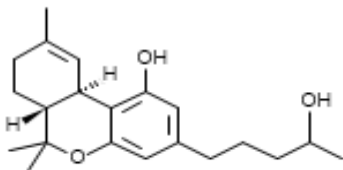
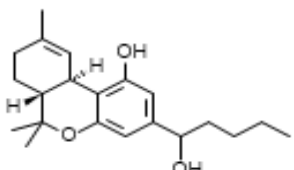
	24	CYP1A2;CYP2C9;CYP2C19;CYP2D6
	20	CYP1A2;CYP2C9;CYP2C19
	18	CYP1A2;CYP2C9;CYP2C19;CYP2D6
	18	CYP1A2;CYP2C9
	12	CYP2C9
	9	CYP2C9

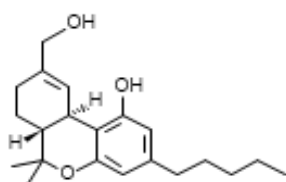
THCA

	38	(CYP2C8);CYP2C9
	22	(CYP2C8);CYP2C9

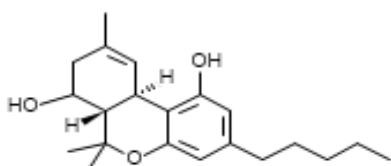
	21	(CYP2C8);CYP2C9
	19*	(CYP2C8);CYP2C9
	---	(CYP2C8)

THC

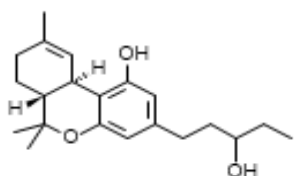
	25	CYP1A2;(CYP2A6);CYP2C9;CYP2C19;CYP2D6;CYP3A4
	21	CYP1A2;CYP2C9
	20	CYP1A2;CYP2C9;CYP2D6
	11	CYP1A2;(CYP2A6);CYP2C19;CYP3A4



9* CYP2C9;CYP2C19;CYP2D6;CYP3A4

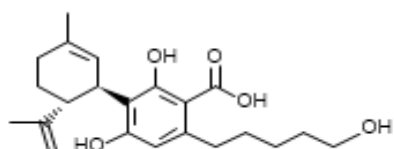


8 CYP3A4

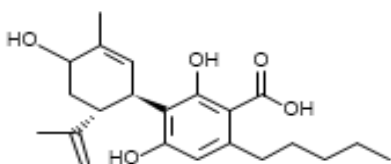


5 CYP1A2;(CYP2A6)

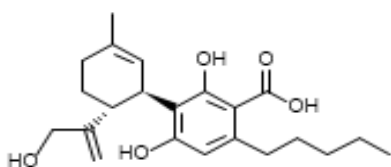
CBDA



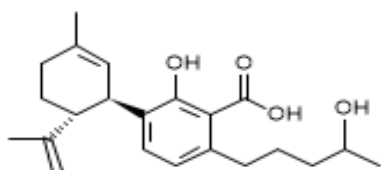
31 (CYP2C8);CYP2C9



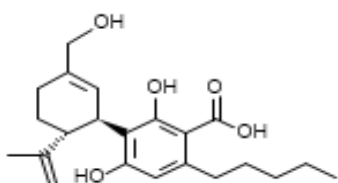
18 (CYP2C8);CYP2C9



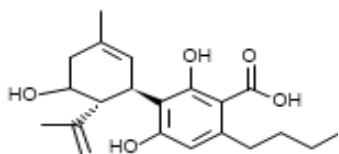
18 (CYP2C8);CYP2C9



18 (CYP2C8);CYP2C9

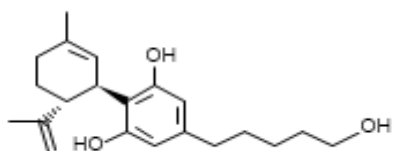


16 (CYP2C8);CYP2C9

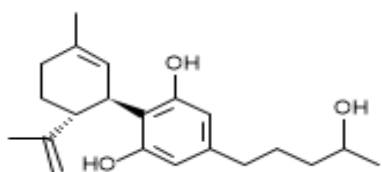


--- (CYP2C8)

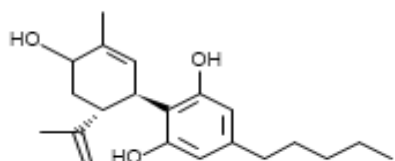
CBD



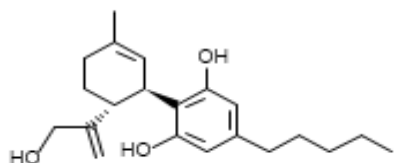
23 CYP2C9; CYP2D6



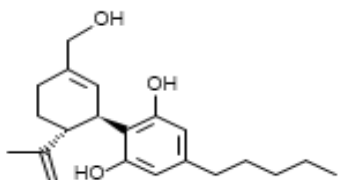
20 CYP2C9;CYP2C19;CYP2D6



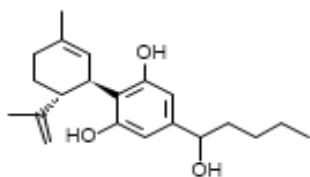
18 CYP2C9;CYP2C19;CYP2D6



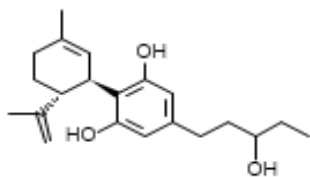
13 CYP2C9;CYP2D6



13 CYP2C9;CYP2C19;CYP2D6

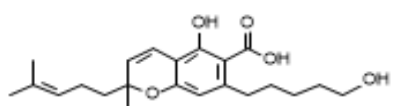


12 CYP2C9;CYP2C19

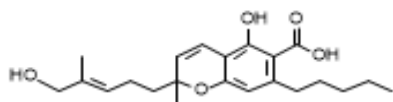


1 CYP2C19

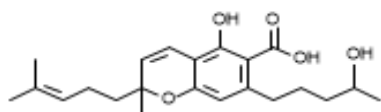
CBCA



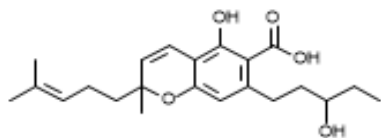
33 (CYP2C8);CYP2C9



31 (CYP2C8);CYP2C9

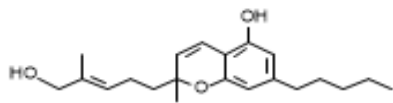


20 (CYP2C8);CYP2C9



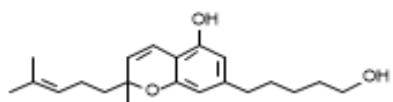
15 CYP2C9

CBC



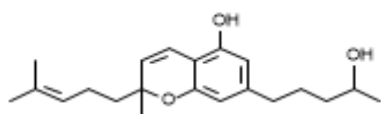
37*

CYP1A2;(CYP2A6);
CYP2C9;CYP2C19;CYP2D6



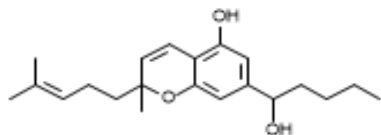
31

CYP1A2;(CYP2A6);CYP2C9



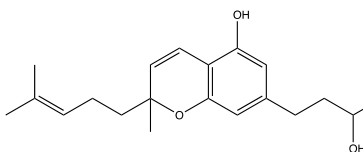
29

CYP1A2;(CYP2A6);CYP2C9;CYP2D6



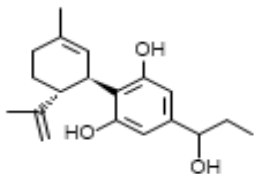
3

CYP1A2;(CYP2A6);CYP2C19



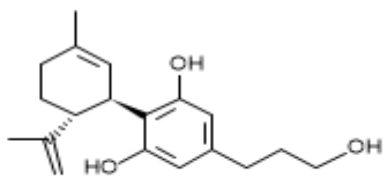
(CYP2A6)

CBDV

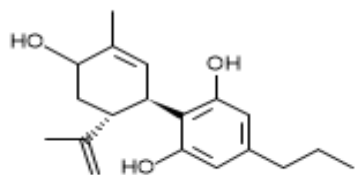


43

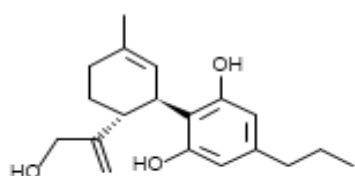
CYP2C9;CYP2C19;CYP2D6



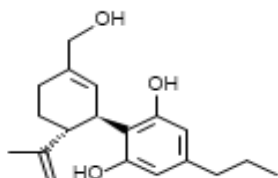
18 CYP2C9



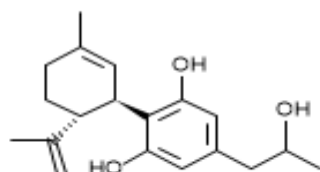
16 CYP2C9;CYP2C19;CYP2D6



11 CYP2C9;CYP2D6

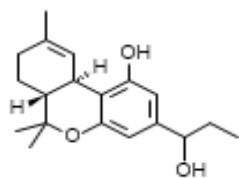


11 CYP2C9;CYP2C19;CYP2D6

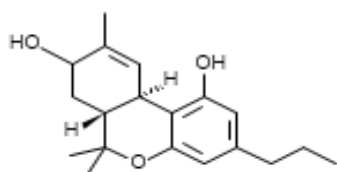


1 CYP2D6

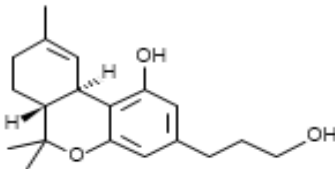
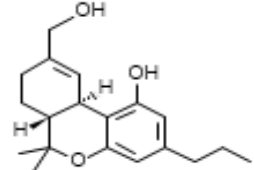
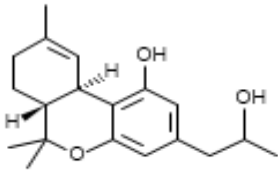
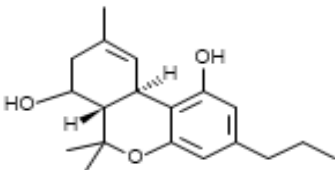
THCV



32 CYP1A2;(CYP2A6);CYP2B6;CYP2C9;CYP2C19;CYP2D6;
CYP3A4



31 CYP1A2;(CYP2A6);CYP2B6;CYP2C9;CYP2C19;CYP2D6;
CYP3A4

	11	CYP2C9
	10	CYP2C9;CYP2C19;CYP2D6;CYP3A4
	8	CYP2B6;CYP3A4
	8	CYP3A4

The software correctly predicted several of the many metabolites reported in the literature for the main phytocannabinoids, i.e., THC, CBD and CBC (Tables 4 and 6). The estimated uncertainty for the CYP clearance predictions ranged from 2.8-fold for CYP1A2 to 4.7-fold for CYP3A4. This, taken together with the complexity of CYP kinetics and the potential for auto-inhibition makes the estimated metabolite yields for ADMET Predictor™ semi-quantitative, at best, for these compounds (Table 6). In particular, the yields predicted for the major primary metabolites of THC and THCA hydroxylated at C11 (Huestis, Mazzoni, & Rabin, 2011; Jung et al., 2009) are not significantly different from those predicted for other major metabolic products. The same holds true with regard to the tertiary oxidation products THC-COOH (i.e., the main THC metabolite found in human urine) and THCA-COOH.

It should also be noted that only metabolites and labile glucuronides excreted into the bile are expected to appear in the feces, just as urinary metabolites are restricted to those eliminated through the kidneys. Hence, the distribution of metabolites in the excreta are not expected to directly reflect the distribution of primary oxidation products formed in the liver, which is what the models in ADMET Predictor™ estimate.

Hydroxylation at the 5' carbon position was predicted to be the major CBC metabolite in humans, which has been shown to be the case in microsomal preparations from laboratory animals (Brown & Harvey, 1990; Kapeghian et al., 1983).

Uridine-5'-diphospho-glucuronosyl-transferase (UGT) 1A8 and UGT1A10 were predicted to glucuronidate the phenolic groups of each phytocannabinoid considered, whereas UGT1A6 was not predicted to glucuronidate any of them. Other UGTs for which models are available (1A1, 1A3, 1A4, 1A9, 2B7 and 2B15) were predicted to glucuronidate some phytocannabinoids, but not others. Aliphatic and allylic hydroxyl groups introduced by CYP oxidation were also predicted to be glucuronidation sites. No acyl glucuronide products were predicted for the carboxylic acid groups in the compounds themselves, or in their oxidation products.

3.4 Drug-drug interactions

DDIs can result in alterations of either drug pharmacodynamics (PD), pharmacokinetics (PK), or both (Prueksaritanont et al., 2013). PK interactions are characterized by alterations of plasma concentration–time profiles resulting from influences on absorption, distribution, metabolism, excretion and toxicity (ADMET) of a drug substance by another compound, when they are given concomitantly.

Important PK drug-interactions are CYP-based, and can occur when a compound inhibits or induces a CYP isoform that metabolizes the other concomitantly administered drug. Various

studies have demonstrated that CBD is not only a substrate, but also an inhibitor of CYP enzymes. Hence, it can interfere with the metabolism of other xenobiotics, such as THC and other medicinal products (Hawksworth & McArdle, 2004; Jiang et al., 2013; Nadulski et al., 2005; Pertwee, 2004; Stout & Cimino, 2014; Ujváry & Hanuš, 2016). For example, a large oral CBD dose of 600 mg/day for 5 to 12 days inhibited hexobarbital metabolism in ten subjects leading to a significant increase in its the bioavailability and prolonged elimination half-time (Benowitz, Nguyen, Jones, Hering, & Bachman, 1980; Ujváry & Hanuš, 2016). Another study (Geffrey, Pollack, Bruno, & Thiele, 2015) investigated the effect of CBD on clobazam pharmacokinetics using a dose regimen of 5 mg/kg/day, titrating up by 5 mg/kg/day each week to the goal of a very large 25 mg/kg/day. CBD increased clobazam (anticonvulsant) plasma level by $60\% \pm 80\%$ (mean \pm SD), and the level of its active metabolite (norclobazam) increased by $500\% \pm 300\%$ (mean \pm SD). The authors concluded that there is a drug–drug interaction between clobazam and CBD. However, reduction of the clobazam dose reduces consequential side-effects, which should allow normal doses of CBD to be a safe and effective treatment of refractory epilepsy in patients receiving clobazam treatment. The primary CYP isoforms involved were CYP3A4 and CYP2C19 (Geffrey et al., 2015; Ujváry & Hanuš, 2016).

Indeed, it has been reported (Fugh-Berman et al., 2015) that CBD is a potent inhibitor of not only CYP3A4, but also CYP2D6. As CYP3A4 metabolizes about a quarter of all drugs, CBD may increase serum concentrations of macrolides, calcium channel blockers, benzodiazepines, cyclosporine, sildenafil (and other PDE5 inhibitors), antihistamines, haloperidol, anti-retrovirals, and some statins (e.g., atorvastatin and simvastatin), among many others. In addition, CYP2D6 metabolizes many antidepressants, which means that CBD could increase serum concentrations

of SSRIs, tricyclic antidepressants, antipsychotics, beta blockers, and opioids (including codeine and oxycodone).

A case report (Stott, White, Wright, Wilbraham, & Guy, 2013) of a 44-year-old Caucasian male taking pharmaceutical grade CBD (as Epidiolex®) and warfarin showed a clinically significant interaction between these two drugs. The patient's International Normalized Ratio (INR) had been stable for at least 6 months before taking CBD concomitantly with warfarin. He was placed on the starting dose of CBD at 5 mg/kg/day divided twice daily, which was increased in 5 mg/kg/day increments every two weeks. With up-titration of CBD, a non-linear increase in the INR was noted and warfarin dosage adjustments were made, and the patient was followed clinically without bleeding complications. Warfarin is metabolized by CYP2C9 and CYP3A4, which are known to be inhibited by CBD in a competitive manner. This could further impair the metabolism of warfarin leading to the observed INR increase (Grayson, Vines, Nichol, & Szaflarski, 2018).

However, given that CBD is also metabolized by CYP450 isoforms, other CYP inhibitors/inducers can also affect CBD pharmacokinetics. A Phase I study (Stott et al., 2013) assessed the potential for drug-drug interactions between a THC/CBD oromucosal spray (Sativex®) and a CYP450 inducer (rifampicin) or inhibitors (ketoconazole or omeprazole). Rifampicin significantly reduced the peak plasma concentration of CBD, while the antifungal ketoconazole almost doubled the peak plasma concentration of CBD, whereas omeprazole (a moderate CYP2C19 inhibitor) did not seem to alter the pharmacokinetics of CBD (Stott et al., 2013; Ujváry & Hanuš, 2016). The authors concluded that the THC/CBD spray was well tolerated both alone and in combination with rifampicin, ketoconazole and omeprazole, but potential effects should be taken into consideration when co-administering the THC/CBD spray

with compounds which are also metabolized by CYP3A4 (Stott et al., 2013). Generally speaking, CYP3A4 inhibitors can potentially cause a slight increase in THC and CBD levels, whereas CYP3A4 inducers can cause a slight decrease. Table 7 summarizes other PD and PK drug interactions involving THC and clinical practice recommendations.

Table 7. Possible PD and PK drug interactions involving THC

PHARMACODYNAMIC INTERACTIONS			
Concomitant Drug	Clinical Effect(s)	Recommendation	Ref
Amitriptyline, amoxapine, desipramine, other tricyclic antidepressants	Additive tachycardia, hypertension, drowsiness	Dose adjustment	(NHS, 2018; Wilens, Biederman, & Spencer, 1997)
Amphetamines, cocaine, other sympathomimetic agents	Additive hypertension, tachycardia, possibly cardiotoxicity	Discontinue in cases of serious cardiac events	(Arellano, Papaseit, Romaguera, Torrens, & Farré., 2017; Lucas, Galettis, & Schneider, 2018)
Atropine, scopolamine, antihistamines,	Additive tachycardia, drowsiness	Dose adjustment	(Horn & Hansten, 2014)

other

anticholinergic

agents

Disulfiram	A reversible hypomanic reaction was reported after smoking marijuana	Avoid smoking; Dose adjustment when taking medicinal cannabis	(Unimed Pharmaceuticals, 2006)
------------	--	--	--------------------------------

Fluoxetine	Hypomanic reaction after smoking marijuana; symptoms resolved after 4 days. Possible biochemical mechanism: enhanced inhibition of 5-hydroxytryptamine reuptake	Avoid smoking; Dose adjustment when taking medicinal cannabis	(Stoll, Cole, & Lukas, 1991)
------------	---	--	------------------------------

PHARMACOKINETIC INTERACTIONS

Concomitant Drug	(Metabolic Mechanism) Clinical Effect(s)	Recommendation	Ref
Antipyrine, barbiturates	Decreased clearance of these agents, presumably via competitive inhibition of metabolism.	Dose adjustment, therapeutic drug monitoring	(Benowitz & Jones, 1977)

	(CYP1A2)		
Theophylline	Increased theophylline metabolism reported with smoking of marijuana; effect similar to that following smoking tobacco	Avoid smoking	(Jusko, Schentag, Clark, Gardner, & Yurchak, 1978)
	(CYP2C9)		
Valproate	Can theoretically potentiate the psychotropic effects of THC by decreasing plasma clearance.	Dose adjustment	(Gaston & Friedman, 2017)
	(CYP2C9)		
Phenytoin	THC increased the <i>in vitro</i> metabolism of phenytoin	Therapeutic drug monitoring	(Gaston & Friedman, 2017)
	Gut motility	Avoid alcohol consumption when taking medicinal cannabis	(Benowitz & Jones, 1977)
Ethanol	THC may delay alcohol absorption		

Even though phytocannabinoids may present many potential DDIs, studies of THC and CBD inhibition and/or induction of major human CYP isoforms generally present low clinical risk, although more specific human data is needed (Stout & Cimino, 2014). Another important factor to take into account is the dose at which phytocannabinoids are used in the clinic and their inhibitory constants and/or half maximal inhibitory concentration values. Generally, THC and

CBD K_i and/or IC_{50} values for studied CYP isoforms are below the expected systemic concentrations of these phytocannabinoids. Nevertheless, clinically significant inhibitory effects cannot be ruled out entirely.

There is still much room for investigation of DDIs involving phytocannabinoids. Not only must CYP-mediated DDIs be considered, but other aspects such as plasma protein binding and gastrointestinal motility should be taken into account, as they may impact the absorption and other ADMET properties of concomitantly administered drugs (Izzo et al., 2012; Schwilke et al., 2009).

4. CONCLUSIONS

Understanding phytocannabinoid metabolism is developing into a key factor within the drug development process, as a strategy to reduce the risk of costly late-stage project failure due to adverse ADMET properties. DDI knowledge is also of growing practical importance in order to avoid potential clinical complications arising from the increasingly widespread use of legal marijuana, both medically and recreationally. Alternatively, possible beneficial effects, including the opportunity to exploit multiple therapeutic mechanisms and the avoidance of deleterious side-effects in concomitant drugs, may be delineated because of such interactions at a pharmacokinetic or pharmacodynamic level. Hence, more investigational efforts are required in this field. Many computer modeling methods of metabolic pathways have already been developed, but they are not perfect. More metabolism data is needed, as well as more efficient and reliable *in silico* methods. Those needs should motivate more studies along this line in the near future.

References

- Aizpurua-Olaizola, O., Soydaner, U., Öztürk, E., Schibano, D., Simsir, Y., Navarro, P., ... Usobiaga, A. (2016). Evolution of the cannabinoid and terpene content during the growth of *Cannabis sativa* plants from different chemotypes. *Journal of Natural Products*, 79(2), 324–331. <https://doi.org/10.1021/acs.jnatprod.5b00949>
- Amada, N., Yamasaki, Y., Williams, C. M., & Whalley, B. J. (2013). Cannabidivarin (CBDV) suppresses pentylenetetrazole (PTZ)-induced increases in epilepsy-related gene expression. *PeerJ*, 1, e214–e214. <https://doi.org/10.7717/peerj.214>
- Appendino, G., Chianese, G., & Tagliatalata-Scafati, O. (2011). Cannabinoids: Occurrence and medicinal chemistry. *Current Medicinal Chemistry*, 18(7), 1085–1099.
- Arellano, A. L., Papaseit, E., Romaguera, A., Torrens, M., & Farré, M. (2017). Neuropsychiatric and general interactions of natural and synthetic cannabinoids with drugs of abuse and medicines. *CNS & Neurological Disorders - Drug Targets*, 16(5). <https://doi.org/10.2174/1871527316666170413104516>
- Ashton, C. (2001). Pharmacology and effects of cannabis: A brief review. *British Journal of Psychiatry*, 178(Feb), 101–106.
- Baek, S., Kim, Y., Kwag, J., Choi, K., Jung, W., & Han, D. (1998). Boron trifluoride etherate on silica-A modified Lewis acid reagent (VII). Antitumor activity of cannabigerol against human oral epitheloid carcinoma cells. *Archives of Pharmacal Research*, 21(3), 353–356. <https://doi.org/10.1007/BF02975301>
- Balabanova, S., Parsche, F., & Pirsig, W. (1992). First identification of drugs in Egyptian mummies. *Naturwissenschaften*, 79(8), 358. <https://doi.org/10.1007/bf01140178>

Benowitz, N., & Jones, R. T. (1977). Effects of delta-9-tetrahydrocannabinol on drug distribution and metabolism. Antipyrine, pentobarbital, and ethanol. *Clinical Pharmacology and Therapeutics*, 22(3), 259–268. <https://doi.org/10.1002/cpt1977223259>

Benowitz, N., Nguyen, T., Jones, R., Herning, R., & Bachman, J. (1980). Metabolic and psychophysiologic studies of cannabidiol-hexobarbital interaction. *Clinical Pharmacology & Therapeutics*, 28(1), 115–120. <https://doi.org/10.1038/clpt.1980.139>

Bisogno, T., Howell, F., Williams, G., Minassi, A., Cascio, M. G., Ligresti, A., ... Doherty, P. (2003). Cloning of the first sn1-DAG lipases points to the spatial and temporal regulation of endocannabinoid signaling in the brain. *Journal of Cell Biology*, 163(3), 463–468. <https://doi.org/10.1083/jcb.200305129>

Bland, T., Haining, R., Tracy, T., & Callery, P. (2005). CYP2C-catalyzed delta(9)-tetrahydrocannabinol metabolism: Kinetics, pharmacogenetics and interaction with phenytoin. *Biochemical Pharmacology*, 70(7), 1096–1103.

Bornheim, L., Lasker, J., & Raucy, J. (1992). Human hepatic microsomal metabolism of delta-1-tetrahydrocannabinol. *Drug Metabolism and Disposition*, 20(2), 241–246.

Brown, N. K., & Harvey, D. J. (1990). *In vitro* metabolism of cannabichromene in seven common laboratory animals. *Drug Metabolism and Disposition*, 18(6), 1065–1070.

Cascio, M. G., Zamberletti, E., Marini, P., Parolaro, D., & Pertwee, R. G. (2015). The phytocannabinoid, Δ9-tetrahydrocannabivarin, can act through 5-HT_{1A} receptors to produce antipsychotic effects. *British Journal of Pharmacology*, 172(5), 1305–1318. <https://doi.org/10.1111/bph.13000>

Citti, C., Linciano, P., Russo, F., Luongo, L., Iannotta, M., Maione, S., ... Cannazza, G. (2019). A novel phytocannabinoid isolated from *Cannabis sativa* L. with an *in vivo* cannabimimetic

activity higher than Δ^9 -tetrahydrocannabinol: Δ^9 -Tetrahydrocannabiphorol. *Scientific Reports*, 9(1), 20335. <https://doi.org/10.1038/s41598-019-56785-1>

Clark, A., Ware, M., Yazer, E., Murray, T., & Lynch, M. (2004). Patterns of cannabis use among patients with multiple sclerosis. *Neurology*, 62(11), 2098–2100.

De Meijer, E. P. M., & Hammond, K. M. (2005). The inheritance of chemical phenotype in *Cannabis sativa* L. (II): Cannabigerol predominant plants. *Euphytica*, 145(1–2), 189–198. <https://doi.org/10.1007/s10681-005-1164-8>

De Petrocellis, L., Ligresti, A., Moriello, A. S., Allarà, M., Bisogno, T., Petrosino, S., ... Di Marzo, V. (2011). Effects of cannabinoids and cannabinoid-enriched *Cannabis* extracts on TRP channels and endocannabinoid metabolic enzymes. *British Journal of Pharmacology*, 163(7), 1479–1494. <https://doi.org/10.1111/j.1476-5381.2010.01166.x>

Deiana, S., Watanabe, A., Yamasaki, Y., Amada, N., Arthur, M., Fleming, S., ... Riedel, G. (2012). Plasma and brain pharmacokinetic profile of cannabidiol (CBD), cannabidivarin (CBDV), Δ^9 -tetrahydrocannabivarin (THCV) and cannabigerol (CBG) in rats and mice following oral and intraperitoneal administration and CBD action on obsessive-compulsive behavi. *Psychopharmacology*, 219(3), 859–873. <https://doi.org/10.1007/s00213-011-2415-0>

Devane, W. A., Breuer, A., Sheshkin, T., Jarbe, T. U. C., Eisen, M. S., & Mechoulam, R. (1992). A novel probe for the cannabinoid receptor. *Journal of Medicinal Chemistry*, 35, 2065–2069.

Devane, W. A., Dysarz, F. A. 3rd, Johnson, M. R., Melvin, L. S., & Howlett, A. C. (1988). Determination and characterization of a cannabinoid receptor in rat brain. *Molecular Pharmacology*, 34, 605–613.

Devane, W. A., Hanus, L., Breuer, A., Pertwee, R. G., Stevenson, L. A., Griffin, G., ... Mechoulam, R. (1992). Isolation and structure of a brain constituent that binds to the cannabinoid receptor. *Science*, 258, 1946–1949.

Dronabinol. (2019). Drugbank, Canada. Retrieved from <https://www.drugbank.ca/drugs/DB00470>

Duque, M. D., Issa, M. G., Silva, D. A., Barbosa, E. J., Löbenberg, R., & Ferraz, H. G. (2018). In silico simulation of dissolution profiles for development of extended-release doxazosin tablets. *Dissolution Technologies*, 25(4), 14–21. <https://doi.org/10.14227/dt250418p14>

Dussy, F., Hamberg, C., Luginbühl, M., Schwerzmann, T., & Briellmann, T. (2005). Isolation of delta9-THCA-A from hemp and analytical aspects concerning the determination of delta9-THC in cannabis products. *Forensic Science International*, 149(1), 3–10.

Eichler, M., Spinedi, L., Unfer-Grauwiler, S., Bodmer, M., Surber, C., Luedi, M., & Drewe, J. (2012). Heat exposure of Cannabis sativa extracts affects the pharmacokinetic and metabolic profile in healthy male subjects. *Planta Medica*, 78(7), 686–691. <https://doi.org/10.1055/s-0031-1298334>

Elmes, M. W., Kaczocha, M., Berger, W. T., Leung, K. N., Ralph, B. P., Wang, L., ... Deutsch, D. G. (2015). Fatty acid-binding proteins (FABPs) are intracellular carriers for Δ 9-tetrahydrocannabinol (THC) and cannabidiol (CBD). *Journal of Biological Chemistry*, 290(14), 8711–8721. <https://doi.org/10.1074/jbc.M114.618447>

Elmes, M. W., Prentis, L. E., McGoldrick, L. L., Giuliano, C. J., Sweeney, J. M., Joseph, O. M., ... Kaczocha, M. (2019). FABP1 controls hepatic transport and biotransformation of Δ 9-THC. *Scientific Reports*, 9, 7588. <https://doi.org/10.1038/s41598-019-44108-3>

ElSohly, M. (2002). Chemical constituents of Cannabis. In F. Grotenhermen & E. Russo (Eds.), *Cannabis and Cannabinoids. Pharmacology, Toxicology, and Therapeutic Potential* (pp. 27–36). Binghamton, New York, USA: The Haworth Press, Inc.

Elsohly, M., DeWit, H., Wachtel, S., Feng, S., & Murphy, T. (2001). Δ^9 -Tetrahydrocannabivarin as a marker for the ingestion of marijuana versus Marinol®: Results of a clinical study. *Journal of Analytical Toxicology*, 25(7), 565–571. <https://doi.org/10.1093/jat/25.7.565>

Elsohly, M., Feng, S., Murphy, T., Ross, S., Nimrod, A., Mehmedic, Z., & Fortner, N. (1999). Δ^9 -Tetrahydrocannabivarin (Δ^9 -THCV) as a marker for the ingestion of cannabis versus Marinol®. *Journal of Analytical Toxicology*, 23(3), 222–224.

<https://doi.org/10.1093/jat/23.3.222>

ElSohly, M., & Slade, D. (2005). Chemical constituents of marijuana: The complex mixture of natural cannabinoids. *Life Sciences*, 78(5), 539–548. <https://doi.org/10.1016/j.lfs.2005.09.011>

FDANewsRelease. (2018). FDA approves first drug comprised of an active ingredient derived from marijuana to treat rare, severe forms of epilepsy. Retrieved from

<https://www.fda.gov/news-events/press-announcements/fda-approves-first-drug-comprised-active-ingredient-derived-marijuana-treat-rare-severe-forms>

FlockhartTable. (n.d.). Available at: <https://drug-interactions.medicine.iu.edu/MainTable.aspx>.

Accessed on May 19, 2020.

Fugh-Berman, A., Wood, S., Kogan, M., Abrams, D., Mathre, M. L., Robie, A., ... Kasimu-Graham, J. (2015). Medical cannabis: Adverse effects & drug interactions. Retrieved from

<https://dchealth.dc.gov/publication/medical-cannabis-adverse-effects-and-drug-interactions>

Furler, M., Einarson, T., Millson, M., Walmsley, S., & Bendayan, R. (2004). Medicinal and recreational marijuana use by patients infected with HIV. *AIDS Patient Care and STDs*, 18(4), 215–228.

Gaoni, Y., & Mechoulam, R. (1964). Isolation, structure and partial synthesis of an active constituent of hashish. *Journal of the American Chemical Society*, 86, 1646–1647.

Garrett, E., & Hunt, C. (1977). Pharmacokinetics of delta9-tetrahydrocannabinol in dogs. *Journal of Pharmaceutical Sciences*, 66(3), 395–407.

Gaston, T. E., & Friedman, D. (2017). Pharmacology of cannabinoids in the treatment of epilepsy. *Epilepsy and Behavior*, 70, 313–318. <https://doi.org/10.1016/j.yebeh.2016.11.016>

Geffrey, A., Pollack, S., Bruno, P., & Thiele, E. (2015). Drug–drug interaction between clobazepam and cannabidiol in children with refractory epilepsy. *Epilepsia*, 56(8), 1246–1251.

Gouille, J., Saussereau, E., & Lacroix, C. (2008). Delta-9-tetrahydrocannabinol pharmacokinetics. *Annales pharmaceutiques françaises*, 66(4), 232–244.

Grayson, L., Vines, B., Nichol, K., & Szaflarski, J. P. (2018). An interaction between warfarin and cannabidiol, a case report. *Epilepsy & Behavior Case Reports Journal*, 9, 10–11. <https://doi.org/10.1016/j.ebcr.2017.10.001>

Grotenhermen, F. (2003). Pharmacokinetics and pharmacodynamics of cannabinoids. *Clin Pharmacokinet.*, 42(4), 327–360.

Grotenhermen, F. (2007). The toxicology of cannabis and cannabis prohibition. *Chemistry and Biodiversity*, 4(8), 1744–1769. <https://doi.org/doi:10.1002/cbdv.200790151>.

Haggerty, G., Deskin, R., Kurtz, P., Fentiman, A., & Leighty, E. (1986). The pharmacological activity of the fatty acid conjugate 11-palmitoyloxy-delta 9-tetrahydrocannabinol. *Toxicol Appl Pharmacol*, 84(3), 599–606.

- Halldin, M., Widman, M., Bahr, C., Lindgren, J., & Martin, B. (1982). Identification of *in vitro* metabolites of delta1-tetrahydrocannabinol formed by human livers. *Drug Metabolism and Disposition*, 10(4), 297–301.
- Harvey, D. (1991). Metabolism and pharmacokinetics of the cannabinoids. In R.R. Watson (Ed.), *Biochemistry and physiology of substance abuse* (pp. 279–365). Boca Raton, Florida, USA: CRC Press.
- Harvey, D., & Brown, N. (1990). *In vitro* metabolism of cannabigerol in several mammalian species. *Biomedical & Environmental Mass Spectrometry*, 19(9), 545–553.
- Harvey, D., & Brown, N. (1991a). Comparative *in vitro* metabolism of the cannabinoids. *Pharmacology, Biochemistry and Behavior*, 40(3), 533–540. [https://doi.org/10.1016/0091-3057\(91\)90359-A](https://doi.org/10.1016/0091-3057(91)90359-A)
- Harvey, D., & Brown, N. (1991b). Identification of cannabichromene metabolites by mass spectrometry: Identification of eight new dihydroxy metabolites in the rabbit. *Biological Mass Spectrometry*, 20, 275–285. <https://doi.org/10.1002/bms.1200200507>
- Harvey, D., & Mechoulam, R. (1990). Metabolites of cannabidiol identified in human urine. *Xenobiotica*, 20(3), 303–320.
- Hatoum, N. S., Davis, W. M., Elsohly, M. A., & Turner, C. E. (1981). Cannabichromene and Δ^9 -tetrahydrocannabinol: Interactions relative to lethality, hypothermia and hexobarbital hypnosis. *General Pharmacology*, 12(5), 357–362. [https://doi.org/10.1016/0306-3623\(81\)90090-2](https://doi.org/10.1016/0306-3623(81)90090-2)
- Hawksworth, G., & McArdle, K. (2004). Metabolism and pharmacokinetics of cannabinoids. In G.W. Guy, B.A. Whittle & P.J. Robson (Eds.), *The Medicinal Uses of Cannabis and Cannabinoids* (pp. 205–228). London, England: Pharmaceutical Press.

- Hazekamp, A., & Grotenhermen, F. (2010). Review on clinical studies with cannabis and cannabinoids 2005-2009. *Cannabinoids*, 5(special issue), 1–21.
- Hidvegi, E., & Somogyi, G. (2010). Detection of cannabigerol and its presumptive metabolite in human urine after Cannabis consumption. *Die Pharmazie*, 65(6), 408–411.
- Hollister, L., Gillespie, H., Ohlsson, A., Lindgren, J., Wahlen, A., & Agurell, S. (1981). Do plasma concentrations of delta 9-tetrahydrocannabinol reflect the degree of intoxication? *The Journal of Clinical Pharmacology*, 21(S1), 171S-177S.
- Horn, J. R., & Hansten, P. D. (2014). Drug interactions with marijuana. Retrieved from Pharmacy Times website:
<https://www.pharmacytimes.com/publications/issue/2014/december2014/drug-interactions-with-marijuana>
- Howlett, A. C., Barth, F., Bonner, T. I., Cabral, G., Casellas, P., Devane, W. A., ... Pertwee, R. G. (2002). International Union of Pharmacology. XXVII. Classification of cannabinoid receptors. *Pharmacological Reviews*, 54(2), 161–202. <https://doi.org/10.1124/pr.54.2.161>
- Huang, H., McIntosh, A. L., Martin, G. G., Landrock, D., Chung, S., Landrock, K. K., ... Schroeder, F. (2016). FABP1: A novel hepatic endocannabinoid and cannabinoid binding protein. *Biochemistry*, 55(37), 5243–5255. <https://doi.org/10.1021/acs.biochem.6b00446>
- Huestis, M. (2005). Pharmacokinetics and metabolism of the plant cannabinoids, delta9-tetrahydrocannabinol, cannabidiol and cannabinol. *Handbook of Experimental Pharmacology*, 168, 657–690.
- Huestis, M. (2007). Human cannabinoid pharmacokinetics. *Chemistry and Biodiversity*, 4(8), 1770–1804.

- Huestis, M., & Cone, E. (1998). Urinary excretion half-life of 11-nor-9-carboxy-delta9-tetrahydrocannabinol in humans. *Therapeutic Drug Monitoring*, 20(5), 570–576.
- Huestis, M., Mazzoni, I., & Rabin, O. (2011). Cannabis in sport: Anti-doping perspective. *Sports Medicine*, 41(11), 949–966. <https://doi.org/10.2165/11591430-000000000-00000>
- Huestis, M., & Smith, M. L. (2014). Cannabinoid pharmacokinetics and disposition in alternative matrices. In R.G. Pertwee (Ed.), *Handbook of Cannabis* (pp. 296–316). Oxford, England: Oxford University Press.
- Iannotti, F. A., Hill, C. L., Leo, A., Alhusaini, A., Soubrane, C., Mazzarella, E., ... Stephens, G. J. (2014). Nonpsychotropic plant cannabinoids, cannabidivarin (CBDV) and cannabidiol (CBD), activate and desensitize transient receptor potential vanilloid 1 (TRPV1) channels *in vitro*: Potential for the treatment of neuronal hyperexcitability. *ACS Chemical Neuroscience*, 5(11), 1131–1141. <https://doi.org/10.1021/cn5000524>
- Izzo, A. A., Capasso, R., Aviello, G., Borrelli, F., Romano, B., Piscitelli, F., ... Di Marzo, V. (2012). Inhibitory effect of cannabichromene, a major non-psychotropic cannabinoid extracted from *Cannabis sativa*, on inflammation-induced hypermotility in mice. *British Journal of Pharmacology*, 166(4), 1444–1460. <https://doi.org/10.1111/j.1476-5381.2012.01879.x>
- Jiang, R., Yamaori, S., Okamoto, Y., Yamamoto, I., & Watanabe, K. (2013). Cannabidiol is a potent inhibitor of the catalytic activity of cytochrome P450 2C19. *Drug Metabolism and Pharmacokinetics*, 28(4), 332–338.
- Jiang, R., Yamaori, S., Takeda, S., Yamamoto, I., & Watanabe, K. (2011). Identification of cytochrome P450 enzymes responsible for metabolism of cannabidiol by human liver microsomes. *Life Sciences*, 89(5–6), 165–170.

- Jung, J., Kempf, J., Mahler, H., & Weinmann, W. (2007). Detection of Delta9-tetrahydrocannabinolic acid A in human urine and blood serum by LC-MS/MS. *Journal of Mass Spectrometry*, 42(3), 354–360.
- Jung, J., Meyer, M., Maurer, H., Neusüß, C., Weinmann, W., & Auwärter, V. (2009). Studies on the metabolism of the Δ^9 -tetrahydrocannabinol precursor Δ^9 -tetrahydrocannabinolic acid A (Δ^9 -THCA-A) in rat using LC-MS/MS, LC-QTOFMS and GC-MS techniques. *Journal of Mass Spectrometry*, 44(10), 1423–1433. <https://doi.org/10.1002/jms.1624>
- Jusko, W. J., Schentag, J. J., Clark, J. H., Gardner, M., & Yurchak, A. M. (1978). Enhanced biotransformation of theophylline in marijuana and tobacco smokers. *Clinical Pharmacology & Therapeutics*, 24, 405–410.
- Kapeghian, J. C., Jones, A. B., Murphy, J. C., Elsohly, M. A., & Turner, C. E. (1983). Effect of cannabichromene on hepatic microsomal enzyme activity in the mouse. *General Pharmacology*, 14(3), 361–363. [https://doi.org/10.1016/0306-3623\(83\)90044-7](https://doi.org/10.1016/0306-3623(83)90044-7)
- Kirchmair, J., Göller, A. H., Lang, D., Kunze, J., Testa, B., Wilson, I. D., ... Schneider, G. (2015). Predicting drug metabolism: Experiment and/or computation? *Nature Reviews Drug Discovery*, 14(6), 387–404. <https://doi.org/10.1038/nrd4581>
- Kirchmair, J., Howlett, A., Peironcely, J., Murrell, D., Williamson, M., Adams, S., ... Glen, R. (2013). How do metabolites differ from their parent molecules and how are they excreted? *Journal of Chemical Information and Modeling*, 53(2), 354–367. <https://doi.org/10.1021/ci300487z>
- Koltai, H., Poulin, P., & Namdar, D. (2019). Promoting cannabis products to pharmaceutical drugs. *European Journal of Pharmaceutical Sciences*, 132, 118–120. <https://doi.org/10.1016/j.ejps.2019.02.027>

Laprairie, R. B., Bagher, A. M., Kelly, M. E. M., & Denovan-Wright, E. M. (2015). Cannabidiol is a negative allosteric modulator of the cannabinoid CB1 receptor. *British Journal of Pharmacology*, 172(20), 4790–4805. <https://doi.org/10.1111/bph.13250>

Lemberger, L., Axelrod, J., & Kopin, I. (1971). Metabolism and disposition of delta-9-tetrahydrocannabinol in man. *Pharmacological Reviews*, 23(4), 371–380.

Lemberger, L., Weiss, J., Watanabe, A., Galanter, I., Wyatt, R., & Cardon, P. (1972). Delta-9-tetrahydrocannabinol. Temporal correlation of the psychologic effects and blood levels after various routes of administration. *New England Journal of Medicine*, 286(13), 685–688.

Ligresti, A., De Petrocellis, L., & Di Marzo, V. (2016). From phytocannabinoids to cannabinoid receptors and endocannabinoids: Pleiotropic physiological and pathological roles through complex pharmacology. *Physiological Reviews*, 96(4), 1593–1659. <https://doi.org/10.1152/physrev.00002.2016>

Liskow, B. I. (1973). Licit and illicit drugs: The Consumers' Union report on narcotics, stimulants, depressants, inhalants, hallucinogens, and marijuana—Including caffeine, nicotine, and alcohol. *Journal of the American Medical Association*, 224(8), 1192.

Lucas, C. J., Galettis, P., & Schneider, J. (2018). The pharmacokinetics and the pharmacodynamics of cannabinoids. *British Journal of Clinical Pharmacology*, 84(11), 2477–2482. <https://doi.org/10.1111/bcp.13710>

Massi, M., Solinas, M., Cincina, V., & Parolaro, D. (2013). Cannabidiol as potential anticancer drug. *British Journal of Clinical Pharmacology*, 75(2), 303–312.

Maurer, H., Sauer, C., & Theobald, D. (2006). Toxicokinetics of drugs of abuse: Current knowledge of the isoenzymes involved in the human metabolism of tetrahydrocannabinol, cocaine, heroin, morphine and codein. *Therapeutic Drug Monitoring*, 28(3), 447–453.

Maykut, M. (1985). Health consequences of acute and chronic marijuana use. *Progress in Neuro-Psychopharmacology & Biological Psychiatry*, 9(3), 209–238.

Mazur, A., Lichti, C., Prather, P., Zielinska, A., Bratton, S., Gallus-Zawada, A., ... Moran, J. (2009). Characterization of human hepatic and extrahepatic UDP-glucuronosyltransferase enzymes involved in the metabolism of classic cannabinoids. *Drug Metabolism and Disposition*, 37(7), 1496–1504.

McPartland, J. M., & Russo, E. B. (2001). Cannabis and cannabis extracts: Greater than the sum of their parts? *Journal of Cannabis Therapeutics*, (3–4), 103–132.
<https://doi.org/10.1300/J175v01n03>

Mechoulam, R., Ben-Shabat, S., Hanus, L., Ligumsky, M., Kaminski, N. E., Schatz, A. R., ... Vogel, Z. (1995). Identification of an endogenous 2-monoglyceride, present in canine gut, that binds to cannabinoid receptors. *Biochemical Pharmacology*, 50(1), 83–90.
[https://doi.org/https://doi.org/10.1016/0006-2952\(95\)00109-D](https://doi.org/https://doi.org/10.1016/0006-2952(95)00109-D)

Mechoulam, R., & Gaoni, Y. (1967). Recent advances in the chemistry of hashish. *Progress in the Chemistry of Organic Natural Products.*, 25, 175–213.

Mechoulam, R., Hanus, L., Pertwee, R. G., & Howlett, A. (2014). Early phytocannabinoid chemistry to endocannabinoids and beyond. *Nature Reviews Neuroscience*, 15(11), 757-764.

Mechoulam, R., & Shvo, Y. (1963). The structure of cannabidiol. *Tetrahedron*, 19, 2073–2078.

Medical Cannabis. (2019). Drugbank, Canada. Retrieved from
<https://www.drugbank.ca/drugs/DB14009#reference-A32585>

Moore, C., Rana, S., & Coulter, C. (2007). Simultaneous identification of 2-carboxy-tetrahydrocannabinol, tetrahydrocannabinol, cannabinol and cannabidiol in oral fluid. *Journal of*

Chromatography B: Analytical Technologies in the Biomedical and Life Sciences, 852(1–2), 459–464.

Morales, P., Hurst, D. P., & Reggio, P. H. (2017). Molecular Targets of the Phytocannabinoids: A complex picture. In A.D. Kinghorn, H. Falk, S. Gibbons, & J. Kobayashi (Eds.), *Phytocannabinoids: Unraveling the complex chemistry and pharmacology of Cannabis sativa* (pp. 103–131), Progress in the chemistry of organic natural products book series, Volume 103. Cham, Switzerland: Springer International Publishing. https://doi.org/10.1007/978-3-319-45541-9_4

Moreno-Sanz, G. (2016). Can you pass the acid test? Critical review and novel therapeutic perspectives of Δ^9 -Tetrahydrocannabinolic acid A. *Cannabis and Cannabinoid Research*, 1(1), 124–130. <https://doi.org/10.1089/can.2016.0008>

Munro, S., Thomas, K. L., & Abu-Shaar, M. (1993). Molecular characterization of a peripheral receptor for cannabinoids. *Nature*, 365, 61–65.

Nabilone. (2019). Drugbank, Canada. Retrieved from <https://www.drugbank.ca/drugs/DB00486>

Nabiximols. (2019). Drugbank, Canada. Retrieved from <https://www.drugbank.ca/drugs/DB14011>

Nadulski, T., Pragst, F., Weinberg, G., Roser, P., Schnelle, M., Fronk, E., & Stadelmann, A. (2005). Randomized, double-blind, placebo-controlled study about the effects of cannabidiol (CBD) on the pharmacokinetics of D9-tetrahydrocannabinol (THC) after oral application of THC verses standardized cannabis extract. *Therapeutic Drug Monitoring*, 27(6), 799–810. <https://doi.org/10.1097/01.ftd.0000177223.19294.5c>

NHS. (2018). Does cannabis interact with antidepressants or lithium? Retrieved from <https://www.nhs.uk/common-health-questions/medicines/does-cannabis-interact-with-antidepressants-or-lithium/#>

Ohlsson, A., Lindgren, J., Wahlen, A., Agurell, S., Hollister, L., & Gillespi, H. (1980). Plasma delta-9 tetrahydrocannabinol concentrations and clinical effects after oral and intravenous administration and smoking. *Clinical Pharmacology & Therapeutics*, 28(3), 409–416.

Owens, S., McBay, A., Reisner, H., & Perez-Reyes, M. (1981). 125I radioimmunoassay of delta-9-tetrahydrocannabinol in blood and plasma with a solid-phase second-antibody separation method. *Clinical Chemistry*, 27(4), :619-624.

Pate, D. W. (1994). Chemical ecology of Cannabis. *Journal of the International Hemp Association*, 1(2), 29, 32-37. <http://www.internationalhempassociation.org/jiha/iha01201.html>

Pate, D. W. (1999). Cannabinoid taxonomy. In J. Mönkkönen (Ed.), *Anandamide structure-activity relationships and mechanisms of action on intraocular pressure in the normotensive rabbit model* (pp.15-21). Pharmaceutical sciences dissertation 37. Kuopio, Finland: Kuopio University Publications A. <https://www.elibrary.ru/item.asp?id=5313464>.

Pertwee, R. G. (2004). The pharmacology and therapeutic potential of cannabidiol. In V. Di Marzo (Ed.), *Cannabinoids* (pp. 32-83). New York, New York, USA: Kluwer Academic / Plenum Publishers.

Pertwee, R. G. (2008). The diverse CB1 and CB2 receptor pharmacology of three plant cannabinoids: Delta9-tetrahydrocannabinol, cannabidiol and delta9-tetrahydrocannabivarin. *British Journal of Pharmacology*, 153(2), 199–215. <https://doi.org/10.1038/sj.bjp.0707442>

Prueksaritanont, T., Chu, X., Gibson, C., Cui, D., Yee, K. L., Ballard, J., ... Hochman, J. (2013). Drug–drug interaction studies: Regulatory guidance and an industry perspective. *The American*

Association of Pharmaceutical Scientists Journal, 15(3), 629–645.

<https://doi.org/10.1208/s12248-013-9470-x>

Raharjo, T., & Verpoorte, R. (2004). Methods for the analysis of cannabinoids in biological materials: A review. *Phytochemical Analysis*, 15(2), 79–94.

Rinaldi-Carmona, M., Barth, F., Héaulme, M., Shire, D., Calandra, B., Congy, C., ... Caput, D. (1994). SR141716A, a potent and selective antagonist of the brain cannabinoid receptor.

Federation of European Biochemical Societies Letters, 350(2–3), 240–244.

[https://doi.org/10.1016/0014-5793\(94\)00773-x](https://doi.org/10.1016/0014-5793(94)00773-x)

Rinaldi-Carmona, M., Barth, F., Millan, J., Derocq, J. M., Casellas, P., Congy, C., ... Le Fur, G. L. (1998). SR 144528, the first potent and selective antagonist of the CB2 cannabinoid receptor.

Journal of Pharmacology and Experimental Therapeutics, 284(2), 644–650.

Rock, E. M., Sticht, M. A., Duncan, M., Stott, C., & Parker, L. A. (2013). Evaluation of the potential of the phytocannabinoids, cannabidivarin (CBDV) and Δ^9 -tetrahydrocannabivarin (THCV), to produce CB 1 receptor inverse agonism symptoms of nausea in rats. *British Journal of Pharmacology*, 170, 671–678. <https://doi.org/10.1111/bph.12322>

Rong, C., Carmona, N. E., Lee, Y. L., Ragugett, R.-M., Pan, Z., Rosenblat, J. D., ... McIntyre, R. S. (2018). Drug-drug interactions as a result of co-administering Δ^9 -THC and CBD with

other psychotropic agents. *Expert Opinion on Drug Safety*, 17(1), 51–54.

<https://doi.org/10.1080/14740338.2017.1397128>

Rostami-Hodjegan, A., & Tucker, G. T. (2007). Simulation and prediction of *in vivo* drug metabolism in human populations from *in vitro* data. *Nature Reviews Drug Discovery*, 6(2),

140–148. <https://doi.org/10.1038/nrd2173>

Russo, E. (2001). Hemp for headache: An in-depth historical and scientific review of cannabis in migraine treatment. *Journal of Cannabis Therapeutics*, 1(2), 21–92.

Russo, E. (2002). Cannabis treatments in obstetrics and gynecology: A historical review. *Journal of Cannabis Therapeutics*, 2(3–4), 5–35.

Russo, E. (2011). Taming THC: Potential cannabis synergy and phytocannabinoid-terpenoid entourage effects. *British Journal of Pharmacology*, 163(7), 1344–1364.

<https://doi.org/10.1111/j.1476-5381.2011.01238.x>

Schurman, L. D., Lu, D., Kendall, D. A., Howlett, A. C., & Lichtman, A. H. (2020). Molecular mechanism and cannabinoid pharmacology. In M. A. Nader & Y. L. Hurd (Eds.), *Substance Use Disorders. Handbook of Experimental Pharmacology* (pp. 323–353). Springer International Publishing.

Schwilke, E. W., Karschner, E. L., Lowe, R. H., Gordon, A. M., Cadet, J. L., Herning, R. I., & Huestis, M. A. (2009). Intra- and intersubject whole blood/plasma cannabinoid ratios determined by 2-dimensional, electron impact GC-MS with cryofocusing. *Clinical Chemistry*, 55(6), 1188–1195. <https://doi.org/10.1371/journal.pone.0178059>

Sedgwick, B. (2000). Δ^9 -Tetrahydrocannabivarin (THCV) as a marker of cannabis use: Is the methodology forensically acceptable? *Journal of Analytical Toxicology*, 24(1), 73–74.

<https://doi.org/10.1093/jat/24.1.74>

Sharma, P., Murthy, P., & Bharath, M. M. S. (2012). Chemistry, metabolism, and toxicology of cannabis: Clinical implications. *Iranian Journal of Psychiatry*, 7(4), 149–156.

Silva, D., Duque, M., Davies, N., Löbenberg, R., & Ferraz, H. (2018). Application of in silico tools in clinical practice using ketoconazole as a model drug. *Journal of Pharmacy and Pharmaceutical Sciences*, 21(1S), 242s-253s. <https://doi.org/10.18433/jpps30227>

Stoll, A. L., Cole, J. O., & Lukas, S. E. (1991). A case of mania as a result of fluoxetine marijuana interaction. *The Journal of Clinical Psychiatry*, 52(6), 280–281.

Stott, C., White, L., Wright, S., Wilbraham, D., & Guy, G. (2013). A Phase I, open-label, randomized, crossover study in three parallel groups to evaluate the effect of rifampicin, ketoconazole, and omeprazole on the pharmacokinetics of THC/CBD oromucosal spray in healthy volunteers. *SpringerPlus*, 2(1), 236. <https://doi.org/10.1186/2193-1801-2-236>

Stout, S., & Cimino, N. (2014). Exogenous cannabinoids as substrates, inhibitors, and inducers of human drug metabolizing enzymes: A systematic review. *Drug Metabolism Reviews*, 46(1), 86–95.

Sugiura, T., Kondo, S., Sukagawa, A., Nakane, S., Shinoda, A., Itoh, K., ... Waku, K. (1995). 2-Arachidonoylglycerol: A possible endogenous cannabinoid receptor ligand in brain. *Biochemical and Biophysical Research Communications*, 215(1), 89–97.
<https://doi.org/https://doi.org/10.1006/bbrc.1995.2437>

Testa, B., Pedretti, A., & Vistoli, G. (2012). Reactions and enzymes in the metabolism of drugs and other xenobiotics. *Drug Discovery Today*, 17(11–12), 549–560.

Tramer, M., Carroll, D., Campbell, F., Reynolds, D., Moore, R., & McQuay, H. (2001). Cannabinoids for control of chemotherapy induced nausea and vomiting: Quantitative systematic review. *The British Medical Journal*, 323(7303), 16-21.

Tyzack, J., & Glen, R. C. (2014). Investigating and predicting how biology changes molecules and their properties. *Molecular Informatics*, 33((6–7)), 443–445.

Tyzack, J., & Kirchmair, J. (2019). Computational methods and tools to predict cytochrome P450 metabolism for drug discovery. *Chemical Biology and Drug Design*, (93), 377–386.
<https://doi.org/10.1111/cbdd.13445>

- Ujváry, I., & Hanuš, L. (2016). Human metabolites of cannabidiol: A review on their formation, biological activity, and relevance in therapy. *Cannabis and Cannabinoid Research*, 1(1), 90–101. <https://doi.org/10.1089/can.2015.0012>
- Unimed Pharmaceuticals, I. (2006). MARINOL: Dronabinol. [Package insert]. Retrieved from https://www.accessdata.fda.gov/drugsatfda_docs/label/2006/018651s025s026lbl.pdf
- Uwimana, E., Ruiz, P., Li, X., & Lehmler, H. J. (2019). Human CYP2A6, CYP2B6, and CYP2E1 atropselectively metabolize polychlorinated biphenyls to hydroxylated metabolites. *Environmental Science and Technology*, 53, 2114–2123. <https://doi.org/10.1021/acs.est.8b05250>
- Vree, T., Breimer, D., van Ginneken, C., & van Rossum, J. (1972). Identification in hashish of tetrahydrocannabinol, cannabidiol and cannabinol analogs with methyl side-chain. *Journal of Pharmacy and Pharmacology*, 24, 7–12.
- Wall, M., & Perez-Reyes, M. (1981). The metabolism of delta9-tetrahydrocannabinol and related cannabinoids in man. *Journal of Clinical Pharmacology*, 21(S1), 178S-189S.
- Wall, M., Sadler, B., Brine, D., Taylor, H., & Perez-Reyes, M. (1983). Metabolism, disposition, and kinetics of delta-9-tetrahydrocannabinol in men and women. *Clinical Pharmacology & Therapeutics*, 34(3), 352–363.
- Wang, M., Wang, Y. H., Avula, B., Radwan, M. M., Wanas, A. S., Van Antwerp, J., ... Khan, I. A. (2016). Decarboxylation study of acidic cannabinoids: A novel approach using ultra-high-performance supercritical fluid chromatography/photodiode array-mass spectrometry. *Cannabis and Cannabinoid Research*, 1(1), 262–271. <https://doi.org/10.1089/can.2016.0020>
- Ware, M., Adams, H., & Guy, G. (2005). The medicinal use of cannabis in the UK: Results of a nationwide survey. *International Journal of Clinical Practice*, 59(3), 291–295.

Wargent, E. T., Zaibi, M. S., Silvestri, C., Hislop, D. C., Stocker, C. J., Stott, C. G., ...
Cawthorne, M. A. (2013). The cannabinoid Δ^9 -tetrahydrocannabivarin (THCV) ameliorates insulin sensitivity in two mouse models of obesity. *Nutrition and Diabetes*, 3(e68), 1–10. <https://doi.org/10.1038/nutd.2013.9>

Watanabe, K., Matsunaga, T., Yamamoto, I., Funae, Y., & Yoshimura, H. (1995). Involvement of CYP2C in the metabolism of cannabinoids by human hepatic microsomes from an old woman. *Biological and Pharmaceutical Bulletin*, 18(8), 1138–1141.

Wilens, T. E., Biederman, J., & Spencer, T. J. (1997). Case study: Adverse effects of smoking marijuana while receiving tricyclic antidepressants. *Journal of the American Academy of Child and Adolescent Psychiatry*, 36(1), 45–48. <https://doi.org/10.1097/00004583-199701000-00016>

Williams, P. L., & Moffat, A. C. (1980). Identification in human urine of delta9-tetrahydrocannabinol-11-oic acid glucuronide: A tetrahydrocannabinol metabolite. *Journal of Pharmacy and Pharmacology*, 32(7), 445-8.

Wishart, D. S., Feunang, Y. D., Guo, A. C., Lo, E. J., Marcu, A., Grant, J. R., ... Wilson, M. (2018). DrugBank 5.0: A major update to the DrugBank database for 2018. *Nucleic Acids Research*, 46(D1), D1074–D1082.

Wohlfarth, A. (2013). Pharmakokinetik und metabolismus von Δ^9 -tetrahydrocannabinolsäure A im menschen. *Toxichem Krimtech* 80(1), 60-65. https://www.gtfch.org/cms/images/stories/media/tk/tk80_1/Wohlfarth.pdf

Wood, S. (2004). Evidence for using cannabis and cannabinoids to manage pain. *Nursing Times*, 100(49), 38–40.

Wu, J. (2019). Cannabis, cannabinoid receptors, and endocannabinoid system: Yesterday, today, and tomorrow. *Acta Pharmacologica Sinica*, 40(3), 297–299. <https://doi.org/10.1038/s41401-019-0210-3>

Yamaori, S., Ebisawa, J., Okushima, Y., Yamamoto, I., & Watanabe, K. (2011). Potent inhibition of human cytochrome P450 3A isoforms by cannabidiol: Role of phenolic hydroxyl groups in the resorcinol moiety. *Life Sciences*, 88, 730–736. <https://doi.org/10.1016/j.lfs.2011.02.017>

Yamaori, S., Koeda, K., Kushihara, M., Hada, Y., Yamamoto, I., & Watanabe, K. (2012). Comparison in the *in vitro* inhibitory effects of major phytocannabinoids and polycyclic aromatic hydrocarbons contained in marijuana smoke on cytochrome P450 2C9 activity. *Drug Metabolism and Pharmacokinetics*, 27(3), 294–300. <https://doi.org/10.2133/dmpk.dmpk-11-rg-107>

Yamaori, S., Kushihara, M., Yamamoto, I., & Watanabe, K. (2010). Characterization of major phytocannabinoids, cannabidiol and cannabitol, as isoform-selective and potent inhibitors of human CYP1 enzymes. *Biochemical Pharmacology*, 79(11), 1691–1698. <https://doi.org/10.1016/j.bcp.2010.01.028>

Yamaori, S., Maeda, C., Yamamoto, I., & Watanabe, K. (2011). Differential inhibition of human cytochrome P450 2A6 and 2B6 by major phytocannabinoids. *Forensic Toxicology*, 29(2), 117–124. <https://doi.org/10.1007/s11419-011-0112-7>

Yamaori, S., Okamoto, Y., Yamamoto, I., & Watanabe, K. (2011). Cannabidiol, a major phytocannabinoid, as a potent atypical inhibitor for CYP2D6. *Drug Metabolism and Disposition*, 39(11), 2049–2056. <https://doi.org/10.1124/dmd.111.041384>

Zhornitsky, S., & Potvin, S. (2012). Cannabidiol in humans — The quest for therapeutic targets. *Pharmaceuticals (Basel, Switzerland)*, 5(5), 529–552. <https://doi.org/10.3390/ph5050529>

Zou, S., & Kumar, U. (2018). Cannabinoid receptors and the endocannabinoid system: Signaling and function in the central nervous system. *International Journal of Molecular Sciences*, 19(3), pii:E833.